

An Assessment of Aquifer Intercommunication in the B Pond-Gable Mountain Pond Area of the Hanford Site

Date Published March 1984

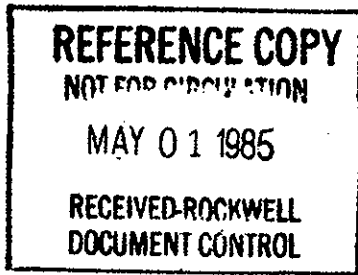
Michael J. Graham
George V. Last
Karl R. Fecht
Rockwell Hanford Operations

Prepared for the U.S. Department of Energy
under Contract DE-AC06-77RL01030



Rockwell International

Rockwell Hanford Operations
Energy Systems Group
P.O. Box 800
Richland, Washington 99352



-201

REFERENCE COPY

DISCLAIMER

This report was prepared as an account of work sponsored by an agency of the United States Government. Neither the United States Government nor any agency thereof, nor any of their employees, makes any warranty, express or implied, or assumes any legal liability or responsibility for the accuracy, completeness, or usefulness of any information, apparatus, product, or process disclosed, or represents that its use would not infringe privately owned rights. Reference herein to any specific commercial product, process, or service by trade name, trademark, manufacturer, or otherwise, does not necessarily constitute or imply its endorsement, recommendation, or favoring by the United States Government or any agency thereof. The views and opinions of authors expressed herein do not necessarily state or reflect those of the United States Government or any agency thereof.

Printed in the United States of America

Available from
National Technical Information Service
U. S. Department of Commerce
5285 Port Royal Road
Springfield, VA 22161

NTIS Price Codes
Microfiche Copy: A01

Printed Copy:

Pages	Price Codes
001-025	A02
026-050	A03
051-075	A04
076-100	A05
101-125	A06
126-150	A07
151-175	A08
176-200	A09
201-225	A10
226-250	A11
251-275	A12
276-300	A13

START
 Rockwell Hanford Operations
 Richland, WA 99352

DOCUMENT CLEARANCE REQUEST

(Do Not Use For Speeches And Articles)
 AUTHOR COMPLETES PART 1 AND SUBMITS WITH (2) COPIES
 OF DOCUMENT TO TECHNICAL INFORMATION SERVICES.

Date: 9/9/83
 Identification No: RHO-RE-ST-12 P
 Bldg: MO-028
 Phone No: 3-2981

Assessment of Aquifer Intercommunication
 in the B Pond-Gable Mountain Pond Area of
 the Hanford Site
 Author(s): G. V. Last
 M. J. Graham
 K. R. Fecht

Description of Document: Quarterly Monthly Manual Other
 Progress Topical Other
 Final Preparation: Originating Organization Other
 Tech. Info Services

Distribution: TID - 4500 Category (Unclassified Reports) Other (Specify)

DOES THIS DOCUMENT CONTAIN OR DISCLOSE ANY OF THE FOLLOWING? (If yes, identify the information and location of document)

- (A) Copyrighted Material? No Yes - Identify (B) Has permission to use been granted? No Yes
- (A) New or Novel (Patentable) subject matter? No Yes - Identify (B) Has disclosure been submitted by Rockwell or other company? No Yes - Identify
- Information received from a foreign country under an exchange agreement? No Yes - Identify
- Information received from others in confidence, such as proprietary data, trade secrets and/or inventions? No Yes - Identify
- Is any further Technical/Policy review required? No Yes - Identify

CERTIFICATION

I have reviewed the attached document and certify the information contained therein is appropriate for release and distribution as specified above.

Author: G. V. Last Supervisor: M. J. Graham Manager: L. E. Kusler Date: 9/12/83

Program Office: Approved Disapproved Classification: Unclassified Classified
 Date: [Signature] Date: 9/13/83

LEGAL APPROVALS ROCKWELL HANFORD OPERATIONS REVIEW APPROVALS DOE-RL
 Legal (Including Patent and Copyright) Patents: B. CONSTANT

D. L. Sander Approved Disapproved Signed: D. L. Sander 9/12/83 For Rockwell Hanford Operations
 Patents: B. CONSTANT Approved Disapproved Signed: [Signature] 9/15/83 For DOE

PUBLIC RELATIONS POLICY AND PROGRAM J. White
 H. B. Lindberg Approved Disapproved Signed: H. B. Lindberg (MEB) 9-12-83 For Rockwell Hanford Operations
 Approved Disapproved Signed: J. White 10/6/83 For DOE

OTHER (Specify) OTHER (Specify)
 W. F. Heine Approved Disapproved Signed: W. F. Heine 9/2/83 For Rockwell Hanford Operations
 Approved Disapproved Signed: _____ For DOE

REMARKS

Approved By Technical Information Services: V.C. Crossman Date: 10-7-83

FOR DOCUMENT CONTROL USE ONLY

Date Approval Received: 11-7-83 Date Received From Printing: 4-25-85 Date Distributed: 5-1-85 Onsite Offsite
 Date Report And 426 Form To TIC: _____

U.S. DEPARTMENT OF ENERGY

DOE AND MAJOR CONTRACTOR RECOMMENDATIONS FOR
ANNOUNCEMENT AND DISTRIBUTION OF DOCUMENTS

See Instructions on Reverse Side

1. DOE Report No. RHO-RE-ST-12 P	2. Contract No. DE-AC06-77RL01030	3. Subject Category No.
-------------------------------------	--------------------------------------	-------------------------

4. Title ASSESSMENT OF AQUIFER INTERCOMMUNICATION IN THE B POND-GABLE MOUNTAIN POND AREA OF THE HANFORD SITE

5. Type of Document ("x" one)

a. Scientific and technical report

b. Conference paper: Title of conference _____

_____ Date of conference _____

Exact location of conference _____ Sponsoring organization _____

c. Other (specify planning, educational, impact, market, social, economic, thesis, translations, journal article manuscript, etc.)

6. Copies Transmitted ("x" one or more)

a. Copies being transmitted for standard distribution by DOE-TIC.

b. Copies being transmitted for special distribution per attached complete address list.

c. Two completely legible, reproducible copies being transmitted to DOE-TIC. (Classified documents, see instructions)

d. ~~Twenty-seven~~ copies being transmitted to DOE-TIC for TIC processing and NTIS sales.

7. Recommended Distribution ("x" one)

a. Normal handling (after patent clearance): no restraints on distribution except as may be required by the security classification: Make available only

b. To U.S. Government agencies and their contractors. c. within DOE and to DOE contractors.

d. within DOE. e. to those listed in item 13 below.

f. Other (Specify)

8. Recommended Announcement ("x" one)

a. Normal procedure may be followed. b. Recommend the following announcement limitations:

9. Reason for Restrictions Recommended in 7 or 8 above.

a. Preliminary information. b. Prepared primarily for internal use. c. Other (Explain)

10. Patent, Copyright and Proprietary Information

Does this information product disclose any new equipment, process or material? No Yes If so, identify page nos. _____

Has an invention disclosure been submitted to DOE covering any aspect of this information product? No Yes

If so, identify the DOE (or other) disclosure number and to whom the disclosure was submitted.

Are there any patent-related objections to the release of this information product? No Yes If so, state these objections:

Does this information product contain copyrighted material? No Yes

If so, identify the page number _____ and attach the license or other authority for the government to reproduce.

Does this information product contain proprietary information? No Yes If so, identify the page numbers _____

("x" one) a. DOE patent clearance has been granted by responsible DOE patent group.

b. Document has been sent to responsible DOE patent group for clearance.

11. National Security Information (For classified document only; "x" one)

Document a. does b. does not contain national security information

12. Copy Reproduction and Distribution

Total number of copies reproduced _____ Number of copies distributed outside originating organization _____

13. Additional Information or Remarks (Continue on separate sheet, if necessary)

14. Submitted by (Name and Position) (Please print or type)

Organization LP UNAPP, MANAGER, DOCUMENT CONTROL

Signature ROBERT L. PERFORO OPERATIONS, RICHLAND, WA 98352 Date 4 30 85

0 9 1 1 3 4 9 1 3 2 9

EXECUTIVE SUMMARY

Aquifer intercommunication refers to the migration of ground water from the unconfined aquifer to the underlying confined aquifer through areas where the rock unit (confining bed) separating the two aquifers does not act as a complete barrier to flow. The potential for this intercommunication exists at the Hanford Site because postglacial flood waters and the ancestral Columbia River eroded portions of the basaltic rock that separate the unconfined from the confined aquifer. The discharge of large volumes of cooling water from various chemical process plants to surface disposal facilities has raised hydraulic head values in the unconfined aquifer to exceed those in the upper confined aquifer (Rattlesnake Ridge) and thus has created a driving force for transporting contamination present in the unconfined aquifer to the Rattlesnake Ridge aquifer.

This report describes a hydrogeologic investigation of aquifer intercommunication in the area surrounding two of the waste disposal ponds, B Pond and Gable Mountain Pond, and encompassing the 200-East Area where subsurface liquid-waste disposal facilities are located. The investigation was focused in this area because previous work indicated areas of erosion of the confining bed and the presence of contamination in the confined aquifer. Also, large increases in waste disposal activities are planned for the near future in this area.

The objectives of this investigation were: 1) to establish the geologic framework controlling ground-water flow in the aquifers, 2) to determine the ground-water flow characteristics of the Rattlesnake Ridge aquifer, 3) to quantify the mixing of unconfined aquifer waters in the Rattlesnake Ridge aquifer resulting from aquifer intercommunication, 4) to delineate the area where aquifer intercommunication has occurred, and 5) to determine the levels of contamination in the Rattlesnake Ridge aquifer.

Erosional "windows" through the confining bed (Elephant Mountain basalt) provide direct interconnections between the unconfined and Rattlesnake Ridge aquifers. Two areas of complete erosion of the Elephant Mountain basalt were identified in the study area. Two other areas of erosion were inferred from

geological and hydrological evidence. Downward gradients from the unconfined aquifer to the Rattlesnake Ridge aquifer were identified in the immediate vicinities of Gable Mountain Pond and B Pond. These downward gradients presently do not extend to the known or suspected areas of erosion of the Elephant Mountain basalt.

From the ground-water chemical data, an area where aquifer intercommunication has occurred was identified south and east of Gable Mountain Pond extending to 200-East Area. This intercommunication probably occurred in the late 1960s and early 1970s when the water table was at a higher elevation. As a result of the aquifer intercommunication, low levels of tritium and iodine-129 contamination (below drinking water standards) have been identified in the Rattlesnake Ridge aquifer. Contamination of the Rattlesnake Ridge aquifer also resulted from the migration of wastes by density flow down an existing borehole which had been open to the two aquifers for several years. This borehole was renovated to isolate the unconfined aquifer and was used as a test well in the investigation. The contamination in the Rattlesnake Ridge aquifer will eventually discharge back to the unconfined aquifer in the vicinity of West Lake. Surveillance of the Rattlesnake Ridge aquifer will continue through use of the wells constructed for this investigation.

CONTENTS

EXECUTIVE SUMMARY.....	iii
1.0 INTRODUCTION	1
2.0 SITE DESCRIPTION	5
2.1 CLIMATE	5
2.2 GEOLOGY	5
2.3 HYDROLOGY	9
3.0 PREVIOUS STUDIES	13
4.0 PRESENT INVESTIGATION	15
4.1 WELL CONSTRUCTION	15
4.2 BOREHOLE GEOPHYSICAL LOGGING	18
4.3 AQUIFER TESTS AND WATER-LEVEL MEASUREMENTS	18
4.4 GROUND-WATER SAMPLING	21
4.5 SINGLE-BOREHOLE TRACER TESTS	22
4.6 LABORATORY ANALYSES	22
4.6.1 Granulometric Analysis	27
4.6.2 Calcium Carbonate Analysis	27
4.6.3 X-Ray Fluorescence Analysis	28
4.6.4 Cations and Anions	28
4.6.5 Trace Metals	28
4.6.6 Stable Isotopes	28
4.6.7 Radionuclides	29
5.0 DATA ANALYSES	31
5.1 MATHEMATICAL ANALYSES	31
5.1.1 Barometric Efficiency	31

5.1.2	Transmissivity	32
5.1.3	Ground-Water Velocity	33
5.2	HYDROGEOCHEMICAL ANALYSES	36
5.2.1	Major Cations and Anions	36
5.2.2	Stable Isotopes	38
5.2.3	Hydrogen and Oxygen	38
5.2.4	Sulfur	39
6.0	DATA INTERPRETATION: A CONCEPTUAL MODEL	43
6.1	GEOLOGIC FRAMEWORK	43
6.1.1	Stratigraphy	43
6.1.2	Structure	54
6.1.3	Geomorphology	57
6.2	GROUND-WATER FLOW	57
6.2.1	Unconfined Aquifer	58
6.2.2	Rattlesnake Ridge Aquifer	60
6.2.3	Elephant Mountain Aquifer	66
6.3	AQUIFER INTERCOMMUNICATION	67
6.4	GROUND-WATER CHEMISTRY	70
6.4.1	Major Cations and Anions and Trace Metals	70
6.4.2	Stable Isotopes	75
6.4.3	Radioactive Isotopes	80
7.0	DISCUSSION	87
8.0	CONCLUSIONS	91
9.0	REFERENCES	93
APPENDIX A - WELL CONSTRUCTION DIAGRAMS		A.1
APPENDIX B - BOREHOLE GEOPHYSICAL LOGS		B.1

APPENDIX C - CONSTANT DISCHARGE AND RECOVERY TEST DATA AND ANALYSES	C.1
APPENDIX D - SLUG INJECTION AND WITHDRAWAL TEST DATA AND ANALYSES	D.1
APPENDIX E - AQUIFER WATER-LEVEL MEASUREMENTS AND WELL ELEVATIONS	E.1
APPENDIX F - BAROMETRIC EFFICIENCY DATA AND ANALYSES	F.1
APPENDIX G - SINGLE-BOREHOLE TRACER TEST DATA	G.1
APPENDIX H - X-RAY FLUORESCENCE ANALYSIS OF BASALT CHIPS FROM TEST WELLS	H.1
APPENDIX I - GROUND-WATER ANALYTICAL DATA	I.1
APPENDIX J - VELOCITY PROFILES	J.1
APPENDIX K - GEOLOGIC CROSS SECTIONS OF STUDY AREA	K.1

FIGURES

1	Hanford Site and Separations Area	2
2	Topographic Map of the Study Area	4
3	Location of Topographic Ridges Defining the Structural Boundary of the Pasco Basin	7
4	Stratigraphic Column of the Geologic Units Within the Study Area (Modified after Diediker and Ledgerwood 1980)	8
5	Water Table Map of the Hanford Site	11
6	Location of the 14 Confined Aquifer Test Wells in the Study Area	16
7	Location of Ground-Water Sample Wells in the Study Area	23
8	Comparison of Electrical Conductivity Readings of 1-Meter and 125-Meter Cables Used in Single-Borehole Tracer Tests	25
9	Tracer Injection System Used in Single-Borehole Tracer Tests	26
10	Comparison of Velocity Profiles from Tracer Tests Performed in Well 699-49-55B	35
11	Plot of ^2H and ^{18}O Values for Ground-Water Samples Collected in the Study Area Compared to Local and Global Meteoric Lines	40
12	Plot of SO_4 Concentration and ^{34}S Values for Ground-Water Samples Collected in the Study Area	42
13	Isopach Map of the Pomona Member Within the Study Area (from Myers and Price 1981)	45
14	Isopach Map of the Rattlesnake Ridge Interbed	46
15	Isopach Map of the Elephant Mountain Member	48
16	Geologic Map of the Bedrock Surface	50
17	Map of the Surface of the Ringold Formation (Modified from Tallman et al. 1979; Brown 1959; Fecht 1979)	51
18	Location Map of Faults and Folds Within the Study Area	56
19	Water Table Map of the Study Area	59

20	Hydrography of Well 699-45-42	61
21	Potentiometric Surface Map in Meters Above Sea Level of the Rattlesnake Ridge Aquifer Within the Study Area	62
22	Potentiometric Surface Map of the Rattlesnake Ridge Aquifer Within the Hanford Site	63
23	Ground-Water Flow Regimes and Relative Velocity Vectors in the Rattlesnake Ridge Aquifer Within the Study Area (Transmissivities (m ² /day) given for comparison)	65
24	Comparison of Areas of Erosion of the Elephant Mountain Basalt and the Barometric Efficiencies of the Test Wells	68
25	Areas of Present-Day Downward Gradient from the Unconfined Aquifer to the Rattlesnake Ridge Aquifer Within the Study Area	69
26	Stiff Diagrams for the Unconfined Aquifer Samples Within the Study Area	71
27	Stiff Diagrams for the Rattlesnake Ridge Aquifer Samples Within the Study Area	73
28	Distribution and Concentrations of Barium, µg/L, in the Rattlesnake Ridge Aquifer Within the Study Area	74
29	Inflow of Ground Water to the Study Area Within the Rattlesnake Ridge Aquifer and Aquifer Intercommunication Inferred from the δ ² H and δ ¹⁸ O Values	76
30	Area of Deuterium Values Less than -145, Indicating Aquifer Intercommunication Within the Study Area	78
31	Inflow of Ground Water to the Study Area Within the Rattlesnake Ridge Aquifer and Aquifer Intercommunication Inferred from the Sulfate Concentrations of δ ³⁴ S Values	79
32	Distribution and Concentrations of Tritium, pCi/mL in the Unconfined Aquifer Within the Study Area (from Wilbur et al. 1983)	81
33	Distribution and Concentrations of Tritium, pCi/L, in the Rattlesnake Ridge Aquifer	82
34	Distribution and Concentrations of Iodine-129, pCi/L, in the Rattlesnake Ridge Aquifer	84

TABLES

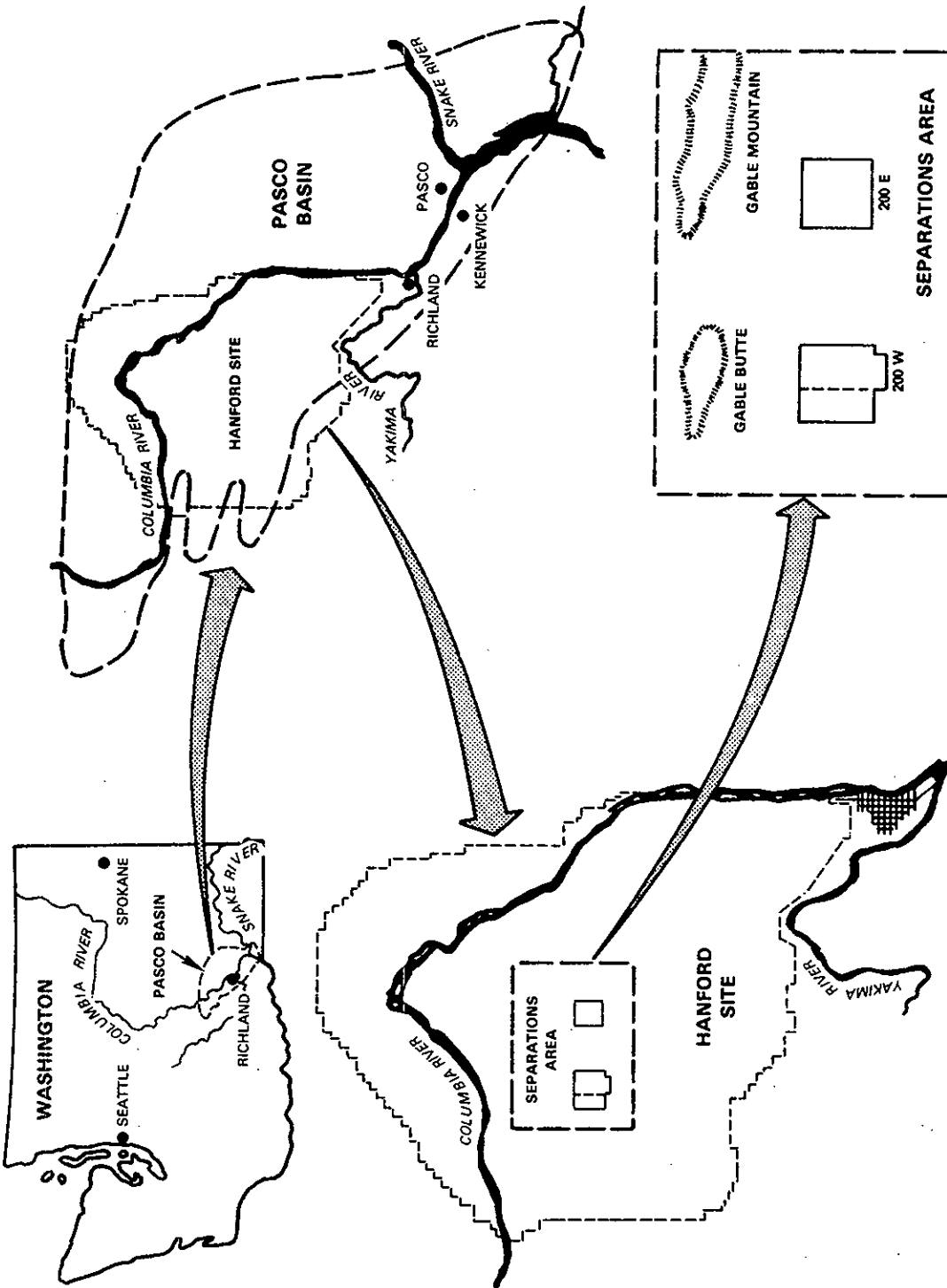
1	Borehole Logging Methods and Applications	19
2	Summary of Aquifer Tests Conducted in the Unconfined and Confined Aquifers	20
3	Details of Pumping Tests (Conducted in the Seven Test Wells)	24
4	Grain Size Nomenclature	27
5	Laboratory Analyses Performed on Ground-Water Samples	29
6	Barometric Efficiencies of the 14 Confined Test Wells	33
7	Summary of Aquifer Test Results	34
8	Equivalent Parts per Million of the Major Cations and Anions in Ground-Water Samples from the Unconfined and Rattlesnake Ridge Aquifers	37
9	Vertical Distribution of Heads in the Unconfined Aquifer from Wells 699-42-40A, B, and C near B Pond	58

1.0 INTRODUCTION

In 1943, the Manhattan District of the U.S. Army Corps of Engineers chose an unpopulated semiarid region of the Pasco Basin in Washington State as the location for the Hanford Engineering Works. The site (Figure 1) was selected because of the need to isolate the first nuclear plants for national security reasons and to have a large area for isolating nuclear wastes from the public. Today, the Hanford Site is a U.S. Department of Energy (DOE) facility, and Rockwell Hanford Operations (Rockwell), a prime contractor to DOE, is responsible for nuclear waste management at Hanford.

Nuclear waste management at Hanford includes disposing of large volumes of liquid wastes to the ground (via ditches, ponds and underground cribs) and storing highly radioactive solutions in large underground steel lined reinforced concrete tanks. The waste management (disposal and storage) facilities are located near the chemical processing facilities in the Separations Area near the center of the Hanford Site. Normally, the radionuclide concentrations of the waste discharged to the ground average below maximum permissible concentration guidelines; however, occasional, nonroutine, releases of higher concentrations have occurred. As a result of these disposal practices, the unconfined aquifer underlying the Hanford Site has become contaminated (below applicable guidelines) and the water table has increased in elevation.

There is a series of confined aquifers in the interflow zones and interbeds between the dense basalt flows that underlie the sediments containing the unconfined aquifer. When postglacial flood waters and the ancestral Columbia River flowed between Gable Mountain and Gable Butte (Figure 1), portions of the basalt flows separating the unconfined and confined aquifers were eroded. Later the water table rose to levels exceeding the potentiometric surface of the upper confined aquifer, i.e., the Rattlesnake Ridge aquifer. This action created the driving force for the transport of contamination downward to the Rattlesnake Ridge aquifer through these areas of erosion, a phenomenon known as aquifer intercommunication.



RCP8205-36

FIGURE 1. Hanford Site and Separations Area

This document is a report of a hydrogeologic investigation of aquifer intercommunication in the eastern half of the Separations Area (Figure 2). The investigation is focused in this area because previous work indicated the erosion of the confining bed and the presence of limited contamination in the Rattlesnake Ridge aquifer. Also, large increases in waste disposal activities are planned for the near future in this area, which could increase the contamination of this confined aquifer.

The objectives of this investigation are: 1) to determine the geologic framework of the study area; 2) to determine the flow characteristics of the Rattlesnake Ridge aquifer in the study area; 3) to quantify the mixing of unconfined aquifer waters in the Rattlesnake Ridge aquifer as a result of aquifer intercommunication; 4) to delineate the area where aquifer intercommunication has occurred, and 5) to determine the levels of contamination in the Rattlesnake Ridge aquifer.

Wells were drilled, deepened or modified for this investigation. The wells were designed and constructed to assure that the unconfined aquifer would be isolated from the confined system and that contamination would not be carried down into the confined aquifer during drilling. Aquifer tests were performed on wells in the area. Barometric efficiencies were determined for the confined aquifer test wells.

Ground-water samples from the unconfined and upper confined aquifers were collected from the wells drilled for this study and from existing wells in the study area. These samples were analyzed for major cations and anions, trace metals, tritium, iodine-129, other gamma emitters, oxygen-18/16, hydrogen-2/1, and sulfur-34/32.

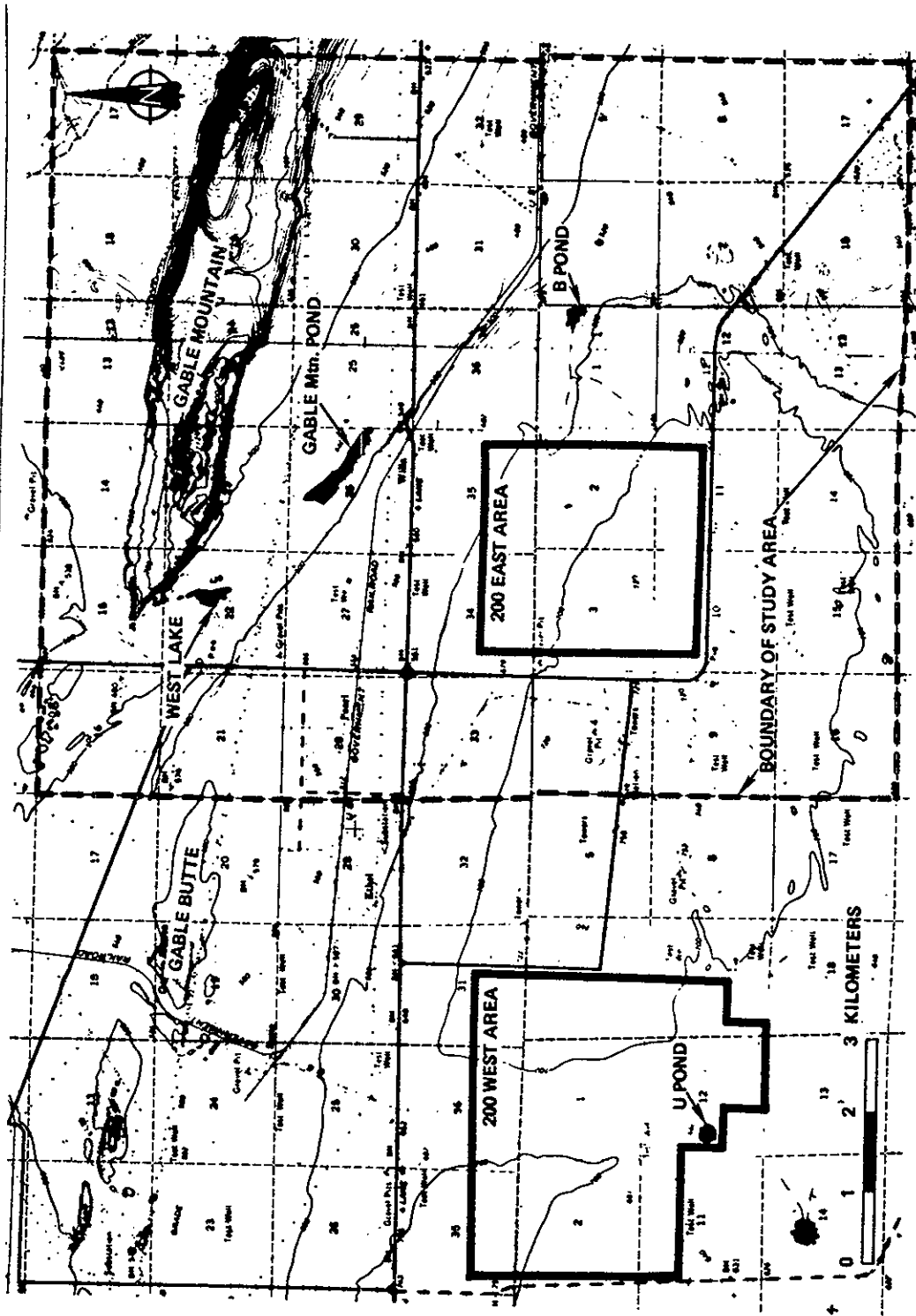


FIGURE 2. Topographic Map of the Study Area

2.0 SITE DESCRIPTION

The description of the Hanford Site and the study area includes sections on the climate, the geologic setting, and the stratigraphy beneath the study area. The hydrology section covers the unconfined aquifer and the confined aquifers within the thick basalt flows.

2.1 CLIMATE

The climate at Hanford (Stone et al. 1972) is greatly influenced by the movement of air masses from the Pacific Ocean eastward over the Cascade Range. The site, which is located in the rain shadow of the Cascades, receives an average annual precipitation of 16 centimeters. November, December, and January contribute 42% to this total; July, August, and September contribute only 10%.

The summers are sunny and warm. In July the average maximum temperature is 33.2°C; the average minimum is 16.1°C. The lowest humidities are during the summer months with a July average of 31.8%. A diurnal fluctuation of wind speeds occurs in the summer due to gravity drainage off the Cascades. June has the highest average wind speed. Although channeling results in a prevailing west-northwest wind the year round, the strongest winds are from the southwest.

The winters are relatively mild, with a range of average temperatures for January of -5.5 to 2.6 °C. The relative humidity averages 75.7% in January. December has an average wind speed of 10 kph, the lowest of the year.

2.2 GEOLOGY

The Hanford Site is located within the Pasco Basin, a structural and topographic depression in the Columbia Plateau Province (Myers and Price et al. 1979). Tholeiitic flood basalts comprising the Columbia Plateau cover approximately 200,000 km², attain a thickness of more than 3250 m, and are collectively referred to as the Columbia River Basalt Group. The boundaries of the Pasco Basin are defined by anticlinal structures of basaltic rock. These structures are the Saddle Mountains to the north; the Umtanum Ridge, Yakima

Ridge, and Rattlesnake Hills to the west; and the Rattlesnake Hills and a series of doubly plunging anticlines merging with the Horse Heaven Hills to the south (Figure 3).

Within the Pasco Basin, the Columbia River Basalt Group is covered by late Miocene- to Pleistocene-aged fluvial, lacustrine, and glaciofluvial sediments. During the late Miocene to mid-Pliocene, intercalated fluvial and lacustrine sediments, known as the Ringold Formation, partially filled the subsiding Pasco Basin (Myers and Price et al. 1979). Pleistocene-aged glaciofluvial sediments, informally known as the Hanford formation, overlie the Ringold. These coarser deposits were laid down as a result of catastrophic postglacial flood events.

The stratigraphy beneath the study area consists of the Yakima Basalt Subgroup, composed of the Grande Ronde, Wanapum, and Saddle Mountains basalts (Myers and Price 1981). The Saddle Mountains Basalt (Figure 4) within the area consists of four basalt members separated by interbedded sediments. The basalt members are, in ascending order: the Umatilla, Esquatzel, Pomona, and Elephant Mountain (Myers and Price 1981). In the northern and eastern part of the area, a fifth member, the Asotin, is present. The major fluvial sedimentary interbeds between basalt flows are the Mabton, Cold Creek, Selah, and Rattlesnake Ridge interbeds, which are part of the Ellensburg Formation (Myers and Price 1981). These interbeds and basalt interflow zones form an extensive confined aquifer system.

In most of the study area, the Ringold Formation overlies the Elephant Mountain Member. The Ringold Formation can be divided into four units on the basis of texture: the sand and gravel of the basal Ringold unit; the clay, silt, and fine sand with lenses of gravel of the lower Ringold unit; the sand and gravel of the middle Ringold unit; and the silt and fine sand of the upper Ringold unit (Tallman et al. 1979).

The early Palouse soil is a buried eolian deposit overlying the Ringold Formation in some areas (Brown 1960). This loess is up to 15 meters thick (Tallman et al. 1979).

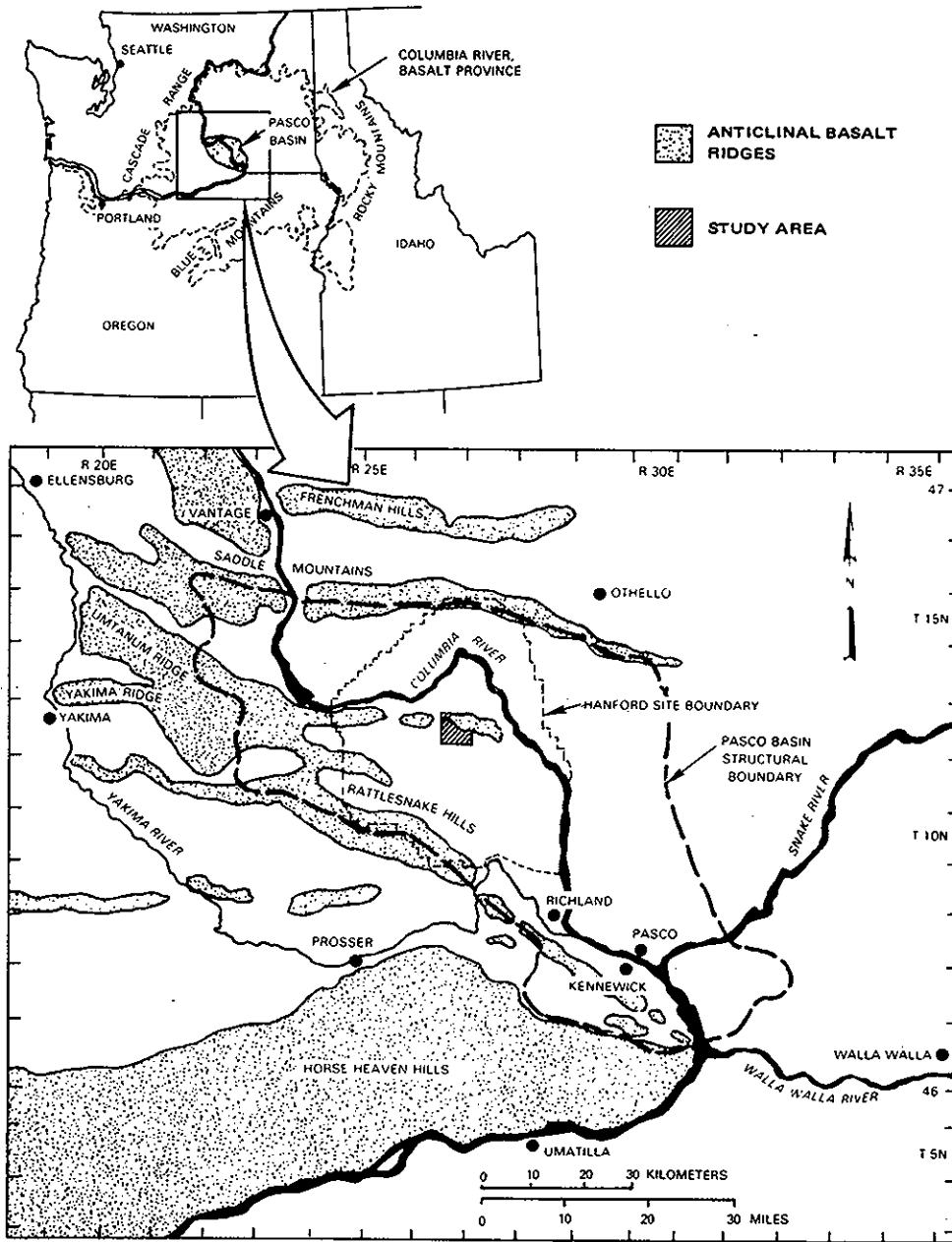


FIGURE 3. Location of Topographic Ridges Defining the Structural Boundary of the Pasco Basin

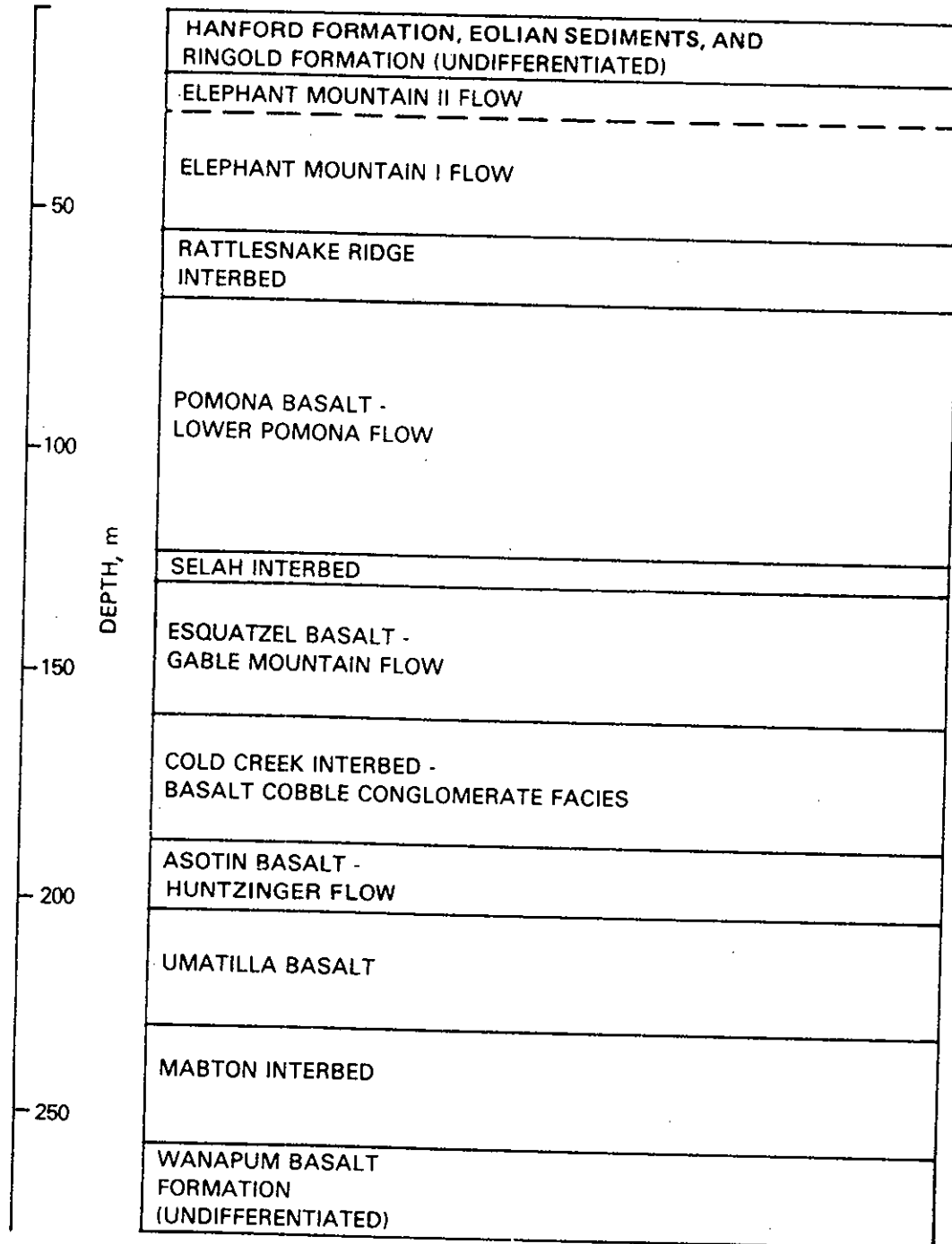


FIGURE 4. Stratigraphic Column of the Geologic Units Within the Study Area [Modified after Diediker and Ledgerwood (1980)]

The glaciofluvial sediments, known as the Hanford formation, are deposited on the Columbia River Basalt Group, Ringold Formation, and early Palouse soil. These sediments can be divided into the coarser sands and gravel, which are referred to as the Pasco Gravels (Brown 1975), and the finer sand and silt units called the Touchet Beds (Flint 1938).

Dune sands form a veneer over much of the Separations Area but are more extensive in the southern portion of the area. The eolian deposits are primarily composed of reworked Hanford formation sediments (Tallman et al. 1979).

The study area covers portions of three first-order folds; the Umtanum Ridge-Gable Mountain structure, the Wahluke syncline, and the Cold Creek syncline. The Umtanum Ridge-Gable Mountain structure is complexly deformed. The topographic expression of this structure is Gable Mountain. North and south of the Umtanum Ridge-Gable Mountain structure are the Wahluke and Cold Creek synclines, respectively. These structural lows are relatively undeformed compared to the anticlinal ridge and are broad, relatively flat, open lows. Faults have been mapped in the study area and are apparently limited in extent to less than about 3.2 km and have minor offsets. These faults are interpreted to be in response to folding, in a north-south compressional, regional stress regime (BWIP Staff 1982).

2.3 HYDROLOGY

An unconfined aquifer occurs within the Ringold Formation and the Hanford formation. The bottom of the aquifer is the basalt surface or, in some areas, the clay zones of the lower Ringold unit. Sources of natural recharge to the unconfined aquifer are rainfall and runoff from the higher bordering elevations and river water along influent reaches of the Yakima and Columbia Rivers (Gephart et al. 1979). Artificial recharge to the Separations Area, which is the result of the disposal of liquid wastes from the chemical processing plants to the ground, is estimated to be approximately ten times the natural recharge flowing into the area (Graham et al. 1981). West Lake, a natural depression located approximately 1.7 km north of Gable Mountain Pond (Figure 2), contained water intermittently before the liquid waste disposal operations began. Ground-water flow within the unconfined aquifer is predominantly west to east

(Figure 5). The unconfined aquifer discharges to the Columbia River. The artificial recharge has raised the water table, and West Lake now contains water perennially.

Large differences in aquifer properties are evident between the Hanford formation and the Ringold Formation. Hydraulic conductivities range from 3 to 3,000 meters/day; storage coefficients range from 0.02 to 0.07. The lower values are associated with the Ringold Formation; the higher values with the Hanford formation (Graham et al. 1981).

The confined aquifers consist of sedimentary interbeds and/or interflow zones between the basalt flows. The main water-bearing portion of the interflow zone occurs within a network of interconnecting vesicles and fractures of the flow tops and flow bottoms. The confining layers are the dense interiors of the basalt flows. The confined aquifer of importance for this study is the Rattlesnake Ridge aquifer. This aquifer consists of the flow bottom of the Elephant Mountain basalt, the flow top of the Pomona basalt, and the Rattlesnake Ridge interbed. In the eastern portion of the study area, an interflow zone within the Elephant Mountain basalt is present. However this interflow zone is not regionally extensive. The confined aquifers are recharged in the surrounding higher elevations.

Ground-water flow in the Saddle Mountains Basalt aquifers under the Hanford Site is predominantly west to east (Gephart et al. 1979). However, in the vicinity of Gable Mountain Pond, the ground water flows to the west in the Rattlesnake Ridge aquifer (Strait and Moore 1982). The Elephant Mountain interflow zone exhibits a much higher hydraulic conductivity than the Rattlesnake Ridge aquifer. The hydraulic conductivity in the aquifer generally ranges from 0.03 to 7.7 m/day (Gephart et al. 1979; Strait and Moore 1982).

3.0 PREVIOUS STUDIES

The Separations Area has been the subject of numerous geologic, geophysical, and hydrologic studies. Fecht (1978a and b), Myers and Price (1981), and Puget Sound Power and Light Company (1982) have performed the most detailed geologic studies of the study area, which include descriptions of local rock units, structure, and geomorphology. The sediments overlying the basalts in the Separations Area are mapped and characterized in Tallman et al. (1979). Regional geologic investigations of the Pasco Basin are presented in Myers and Price et al. (1979).

A paleochannel cut into the basalt surface beneath West Lake was identified from a gravity survey (Richard 1976). The Gable Gap area has recently been surveyed with magnetic, gravity, and seismic methods to ascertain the structural relationship between Gable Mountain, Gable Butte, and the Cold Creek Syncline (Myers and Price 1981). A multigeophysical approach was applied in the Gable Mountain Pond Area to define the top of the basalt and areas of erosion (Moore 1982).

Gephart et al. (1979) present an overview of the hydrology of the Pasco Basin, whereas earlier studies (Bierschenk 1957, 1959a and b; Parker and Piper 1949; and Newcomb and Strand 1953) focus on the characterization of the hydrology and geology of the Hanford Site. More recent works (Newcomb, Strand and Frank 1972; LaSala and Doty 1975) build on these earlier efforts. Graham et al. (1981) present a detailed analysis of the unconfined aquifer in the Separations Area.

Radionuclide contamination of the unconfined aquifer was first reported in Brown and Rupert (1950). Pacific Northwest Laboratory (operated for DOE by Battelle Memorial Institute) and Rockwell are currently responsible for monitoring and reporting radionuclide distributions within the unconfined aquifer (Eddy, Prater and Rieger 1983; Wilbur, Graham and Lu 1983). Contamination in the lower Ringold Formation near the southeast corner of 200 East Area was first noted in Eliason (1967). Ledgerwood and Deju (1976) investigated the confined aquifer within the Saddle Mountains Basalt and found that a potential zone of aquifer leakage may exist under West Lake between the uppermost

confined aquifers and the overlying unconfined aquifer. Gephart et al. (1976) notes the possibility of aquifer leakage in their study of radiochemical data taken from the surface waters and the confined and unconfined aquifers near West Lake. When Strait and Moore (1982) drilled wells around Gable Mountain Pond to define the geohydrology of the Rattlesnake Ridge aquifer interbed, they found evidence that this aquifer was contaminated from aquifer intercommunication to the south of Gable Mountain Pond.

4.0 PRESENT INVESTIGATION

The design of the well network and the field methods employed in this study are described in the following sections. The methodologies are included for well construction, borehole geophysical logging, aquifer tests and water-level measurements, ground-water sampling, single-borehole tracer tests, and laboratory analyses. The study area for the present investigation encompassed the suspected area of erosion of the Elephant Mountain basalt and the major waste disposal facilities surrounding the 200-East Area.

4.1 WELL CONSTRUCTION

The wells were constructed to isolate the unconfined aquifer from the confined system and to assure that contamination was not induced during construction. The drilling procedure for the new wells drilled for this study, 299-E26-8, 699-42-40C, 699-49-55B, and 699-56-53, (Figure 6) is described in the following paragraphs.

First, a 30-cm surface casing was set to a depth of approximately 6 meters using cable tool methods (bit and bailer). A 25.4-cm cased hole was continued through the sediments and into competent Elephant Mountain basalt. The well was then geophysically logged and a bottom section of the casing (approximately 6 m) was then perforated. The lower zone was hydrologically tested and ground-water samples were collected. The bottom of the hole was then cemented to above the zone of perforation.

Second, a 25.4-cm uncased hole was drilled through the Elephant Mountain basalt using air rotary drilling methods. If water was encountered after breaking through the cement plug, the bottom of the hole was grouted again to assure the complete isolation of the unconfined aquifer. If an interflow zone was encountered, drilling was stopped, and the zone tested and sampled. An interflow zone was encountered in Well 699-42-40C. When the flow bottom of the Elephant Mountain basalt was encountered, geophysical logs were run on the basalt. Casing (20.3 cm) was installed from the ground surface to approximately 2 meters above the bottom of the hole. Using an inflatable packer and

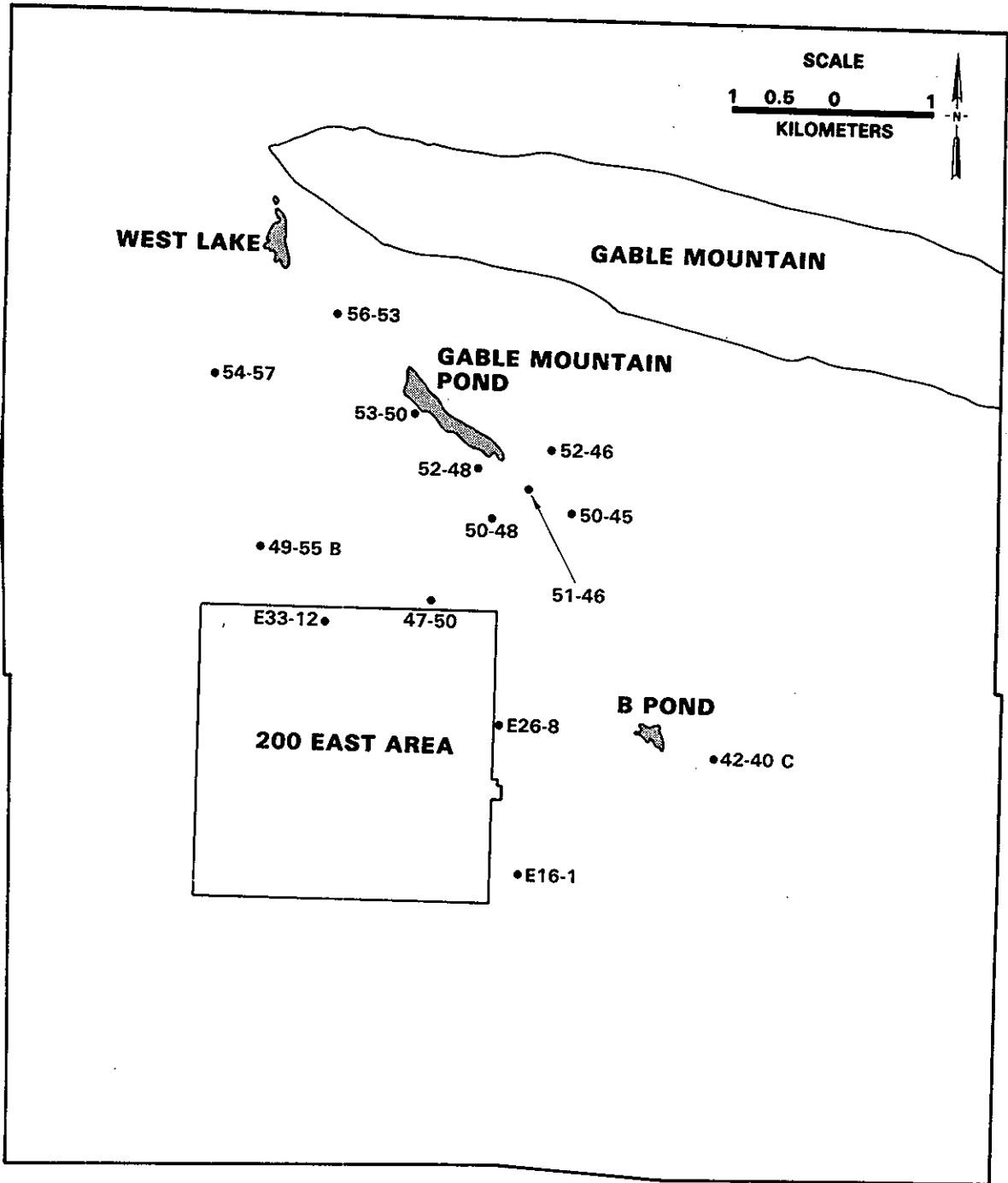


FIGURE 6. Location of the 14 Confined Aquifer Test Wells in the Study Area

grout pump, the annular space between the inner casing and the basalt and the inner casing and the 25.4-cm casing was grouted from the bottom of the hole to the top.

Finally, the well was deepened through the Rattlesnake Ridge aquifer and into competent basalt of the Pomona flow using cable tool methods. Stainless steel 20.3-cm screen was installed with a metal plate on the bottom and a self-sealing packer on the top. The well was developed by bailing or air-lifting and geophysically logged.

Well 299-E33-12 (Figure 6) was drilled in 1953 through the Rattlesnake Ridge aquifer and into the Pomona flow. The well was left uncased from approximately 0.8 meters above the Elephant Mountain flow to the bottom of the hole. This well was modified by placing a cement plug in the Elephant Mountain basalt. The unconfined aquifer was then tested and sampled. An inner casing (15.2 cm) was run from the cement plug to ground surface and the annular space grouted. The well was then completed in the same fashion as the other wells.

Wells 299-E16-1 and 699-54-57 (Figure 6) were existing wells that tagged the Elephant Mountain basalt. In deepening these wells, the same general procedure was followed. A fracture zone in the Elephant Mountain basalt was identified in Well 299-E16-1. This zone was assumed to be the interflow zone between two Elephant Mountain flows and was hydrologically tested and sampled. The well was deepened further and completed in a water-bearing zone containing sediments, which was assumed to be the Rattlesnake Ridge aquifer. Subsequent analysis revealed that this zone is the Elephant Mountain interflow zone. The well could not be deepened further due to scheduling and budgeting constraints.

Two 0.5-liter sediment samples were collected at 1.5-meter intervals throughout the drilling operations. All the wells were surveyed to a U.S. Coastal and Geodetic Survey benchmark by Kaiser Engineering. The specific as-built design and a lithologic description of the geologic units penetrated for each well are given in Appendix A.

4.2 BOREHOLE GEOPHYSICAL LOGGING

Borehole geophysical logging was conducted by Pacific Northwest Laboratory. Eight borehole sondes were used to geophysically log the test wells, both during and after construction. The resulting geophysical logs were used to assist in interpreting geologic and geohydrologic parameters such as: lithology, formation resistivity, porosity, and relative bulk density. These logs provide useful information on the source, movement, and fluid temperature of the ground water (Keys and MacCary 1971). Well construction details such as the bonding and location of cement were also interpreted from these logs. Table 1 lists the various logging methods used in this investigation and their general applications.

The geophysical logs were taken at various periods throughout the construction of the wells to minimize dampening of the responses due to cement grout and multiple thicknesses of the well casing. These logs were then normalized such that the background responses of the older logs matched those of the younger logs. The normalized logs were then combined to form one composite log for each geophysical technique. These composite geophysical logs for each well are presented in Appendix B.

4.3 AQUIFER TESTS AND WATER-LEVEL MEASUREMENTS

For the wells drilled in this investigation, pumping tests were conducted on the lower unconfined aquifer, the Elephant Mountain interflow zone, and the Rattlesnake Ridge aquifer. Including the Rattlesnake Ridge wells drilled in 1980 around Gable Mountain Pond (Strait and Moore 1982) and the wells drilled for this investigation, there were 14 confined test wells in the study area (Figure 6). Slug injection and withdrawal tests were conducted on all 14 test wells. The zones tested and the types of aquifer tests performed on each zone are listed by well in Table 2. Data for the aquifer tests are given in Appendices C and D.

For the pumping tests, a submersible or turbine pump was set in the well. The pumping rate was determined from bailing, air lifting, or step testing the well. For the unconfined aquifer or the interflow zone, the pump tests were of short duration to minimize drill rig stand-by time. After final completion of

TABLE 1. Borehole Logging Methods and Applications^(a)

<u>Geophysical Log</u>	<u>General Applications</u>
Spontaneous potential	Identify lithologic characteristics; determine zone thickness and depths
Resistivity	Make stratigraphic correlations; determine zone thickness and depths; determine mud infiltrate zones
Fluid temperature	Locate sources of ground-water contribution into borehole; identify direction of ground-water circulation in borehole; pressure corrections for head measurements; geothermal gradient
Caliper	Locate borehole breakouts and changes in borehole diameter; identify liner sections; locate large rock fractures
Natural gamma	Indicators of lithology; make stratigraphic correlations
Neutron-neutron	Determine moisture content and bulk porosity; perform stratigraphic correlations
Gamma-gamma	Determine bulk density
Sonic/cement bond log	Cement bonding between rock and casing; determine bulk porosity

(a) Information is taken from Strait and Moore (1982).

the wells, long-term (48-hour) pumping tests were conducted to permit ground-water sampling over time. Equipment malfunctions resulted in the premature termination of some tests. Water-level measurements were made with a steel tape or a Parascientific Model 8130 D.S. Digiquartz pressure transducer. The pressure transducer has a range of 0 to 130 meters of water. The pressure transducer was connected to a Parascientific Model 600 Digiquartz Pressure computer which in turn was connected with a Hewlett-Packard Model 5051A thermal printer, data logger, and timer. The height of water above the pressure transducer with time were printed out by the data logger.

TABLE 2. Summary of Aquifer Tests Conducted in the Unconfined and Confined Aquifers

<u>Well Number</u>	<u>Interval Tested</u>	<u>Type of Test</u>
299-E16-1	Elephant Mountain II fracture zone	Recovery
299-E16-1	Elephant Mountain interflow zone	Constant discharge, recovery, slug
299-E26-8	Lower unconfined	Constant discharge
299-E26-8	Rattlesnake Ridge	Constant discharge, recovery, slug
299-E33-12	Lower unconfined	Constant discharge
299-E33-12	Rattlesnake Ridge	Constant discharge, recovery, slug
699-42-40C	Unconfined	Constant discharge
699-42-40C	Elephant Mountain interflow zone	Constant discharge
699-42-40C	Rattlesnake Ridge	Constant discharge, recovery, slug
699-47-50	Rattlesnake Ridge	Slug
699-49-55B	Rattlesnake Ridge	Constant discharge
699-50-45	Rattlesnake Ridge	Slug
699-50-48	Rattlesnake Ridge	Slug
699-51-46	Rattlesnake Ridge	Slug
699-52-46	Rattlesnake Ridge	Slug
699-52-48	Rattlesnake Ridge	Slug
699-53-50	Rattlesnake Ridge	Slug
699-54-57	Rattlesnake Ridge	Constant discharge, recovery, slug
699-56-53	Lower unconfined	Constant discharge
699-56-53	Rattlesnake Ridge	Constant discharge, recovery, slug

A slug injection test and a slug withdrawal test were conducted on each well. For the slug injection test, a displacement rod (0.2127 m long, 0.0889 m in diameter, and displacing 0.00132 m³ of water) was quickly lowered into the water. This created a rise in the water level in the well. The water-level decay was monitored with the pressure transducer system described above. After the water level returned to static conditions, the displacement tool was quickly removed from the water. The displacement and subsequent rise of water in the well were again measured with the pressure transducer system. The same procedure was followed for all the wells.

Water-level measurements were monitored periodically using a steel tape in order to define seasonal changes in flow. These data are contained in Appendix E. Water-level recorders were placed on each of the 14 confined test wells in the study area for a period of 3 to 5 weeks. This provided a continuous water-level record from which barometric effects could be determined. These data are given in Appendix F.

4.4 GROUND-WATER SAMPLING

Ground-water samples were collected periodically from the pumping tests conducted during and after the drilling of the seven test wells. The pH, temperature, and electrical conductivity of the sample were determined in the field. The sample containers were prepared by rinsing out new bottles several times with deionized water. The bottles were then thoroughly flushed three times with a portion of the water to be sampled.

Various types of sampling containers were used depending upon the type of analysis to be performed:

- 1-liter polyethelene--filtered for cations and anions;
- 1-liter amber glass--filtered for tritium;
- 0.25-liter glass--filtered for deuterium and oxygen isotopes;
- 20-liter polyethelene--unfiltered for sulfur isotopes, iodine-129, and gamma scan.

In addition, samples were collected from other wells in the study area (Figure 7) after the wells had been developed and then pumped for a minimum of four hours. Duplicate samples were collected for each set of samples. The details of the sampling activities are given in Table 3.

The filtered samples were obtained by using a 45-micron filter over argon. All the samples were capped with an argon blanket over the sample. The samples for cation analyses were acidified with 2 mL of Ultrex nitric acid and then taken or shipped to the various laboratories for analysis. The duplicate samples were stored and cataloged for future reference.

4.5 SINGLE-BOREHOLE TRACER TESTS

Single-borehole tracer tests were conducted on 11 test wells in the study area to determine the ground-water velocities in the upper confined aquifer. Wells 299-E16-1, 699-51-46, and 699-52-48 could not be tested due to technical problems of accessing the wells. A Markson Model 10 electrical conductivity meter was fitted with a 125-m cable to the probe. This modification did not significantly alter the readings of the instrument (Figure 8).

The tracer tests were performed by taking electrical conductivity readings at 1-meter intervals in the wells to determine the initial electrical conductivity profiles. A concentrated solution of NaCl was injected and mixed in the well with a recirculating submersible pump system (Figure 9). The electrical conductivity profile was determined immediately after mixing and again at two selected time intervals. The data from these tests are contained in Appendix G.

4.6 LABORATORY ANALYSES

Several types of laboratory analyses were used in the present investigation to aid geologic correlation and determine the chemistry of the ground water.

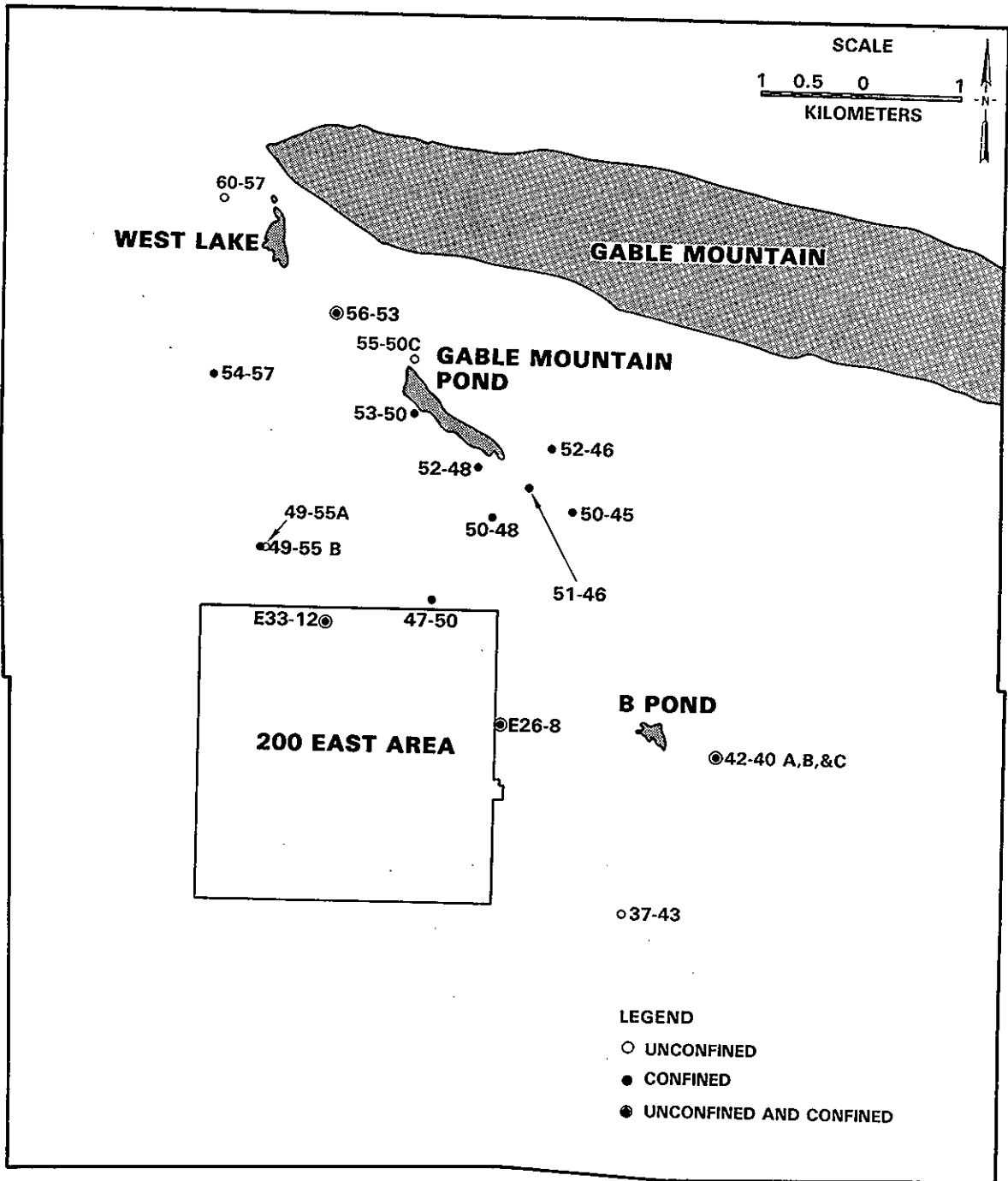


FIGURE 7. Location of Ground-Water Sample Wells in the Study Area

TABLE 3. Details of Ground-Water Sample Collection

Well Number	Zone Sampled	Date	Time	Elapsed Pumping Time, hrs	Initial Well Volume, L	Volume Removed, L	Well Volumes Removed		1-Liter Glass	0.25-Liter Glass	20-Liter Poly
							1-Liter Poly	1-Liter Glass			
299-E16-1	Elephant Mountain II fracture zone Elephant Mountain interflow zone	5/15/82	12:00	20.75	1996.4	20763.0	10.4	4	2	4	1
		7/13/82	06:00	16.00	1220.6	36404.1	29.8	4	2	4	-
		7/13/82	22:00	32.00	1220.6	72231.1	59.2	4	2	4	-
		7/14/82	14:00	48.00	1220.6	108065.5	88.5	6	3	6	1
		8/13/82	16:30	4.67	1220.6	5299.0	4.3	-	-	-	1
299-E26-8	Unconfined Rattlesnake Ridge	3/23/82		0.73	874.6	770.0	0.9	4	2	4	1
		5/18/82	11:45	15.57	1971.5	17966.5	9.1	4	2	4	-
		5/19/82	04:20	32.10	1971.5	24410.6	12.4	4	2	4	-
		5/19/82	19:45	47.58	1971.5	54919.1	27.9	4	2	4	1
		8/12/82	08:30	19.00	1971.5	20033.0	10.0	-	-	-	1
299-E33-12	Unconfined Rattlesnake Ridge	5/11/82		4.20	1082.6	8856.9	8.2	4	2	4	1
		5/21/82	08:00	15.92	1083.6	20189.2	18.6	4	2	4	-
		5/22/82	00:00	31.92	1083.6	40041.5	37.0	4	2	4	-
		5/22/82	15:45	45.67	1083.6	58412.0	53.9	4	2	4	1
		8/14/82	10:00	3.00	1083.6	3406.5	3.1	-	-	-	1
699-42-40C	Elephant Mountain interflow zone Rattlesnake Ridge	4/16/82	08:00	22.92	1795.9	9739.6	5.4	4	2	4	1
		5/20/82	14:00	16.00	2502.2	21691.8	8.7	4	2	4	-
		5/21/82	06:00	32.00	2502.2	51404.1	20.5	4	2	4	-
		5/21/82	18:15	44.15	2502.2	74890.0	29.9	4	2	4	1
		8/13/82	17:00	5.50	2502.2	9314.1	3.7	-	-	-	1
699-49-55B	Rattlesnake Ridge	5/27/82	01:30	16.50	960.3	107584.8	112.0	4	2	4	-
		5/27/82	17:40	32.67	960.3	219730.6	228.8	4	2	4	-
		5/28/82	09:00	48.00	960.3	328190.0	314.7	4	2	4	1
		8/11/82	19:00	3.00	960.3	4528.0	4.7	-	-	-	1
699-54-57	Rattlesnake Ridge	5/17/82	16:15	16.25	833.2	35105.9	42.1	4	2	4	-
		8/14/82	15:00	3.50	833.2	3212.4	3.9	-	-	-	2
699-56-53	Rattlesnake Ridge	6/03/82	01:00	16.17	2351.8	94817.7	40.3	4	2	4	-
		6/03/82	17:00	32.17	2351.8	186933.6	79.5	4	2	4	1
		8/14/82	17:15	4.00	2351.8	5865.6	2.5	-	-	-	1

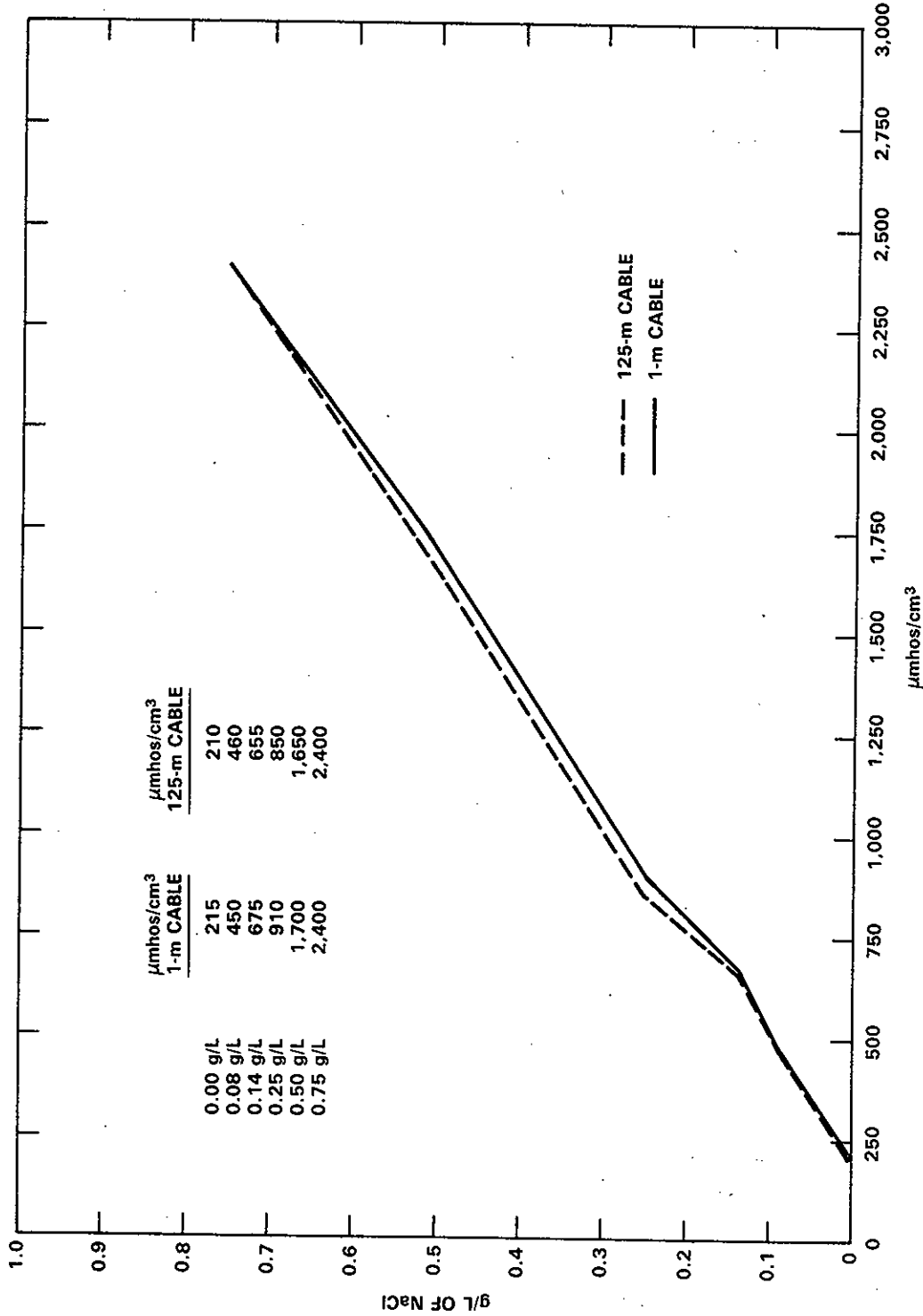


FIGURE 8. Comparison of Electrical Conductivity Readings of 1-Meter and 125-meter Cables Used in Single-Borehole Tracer Tests

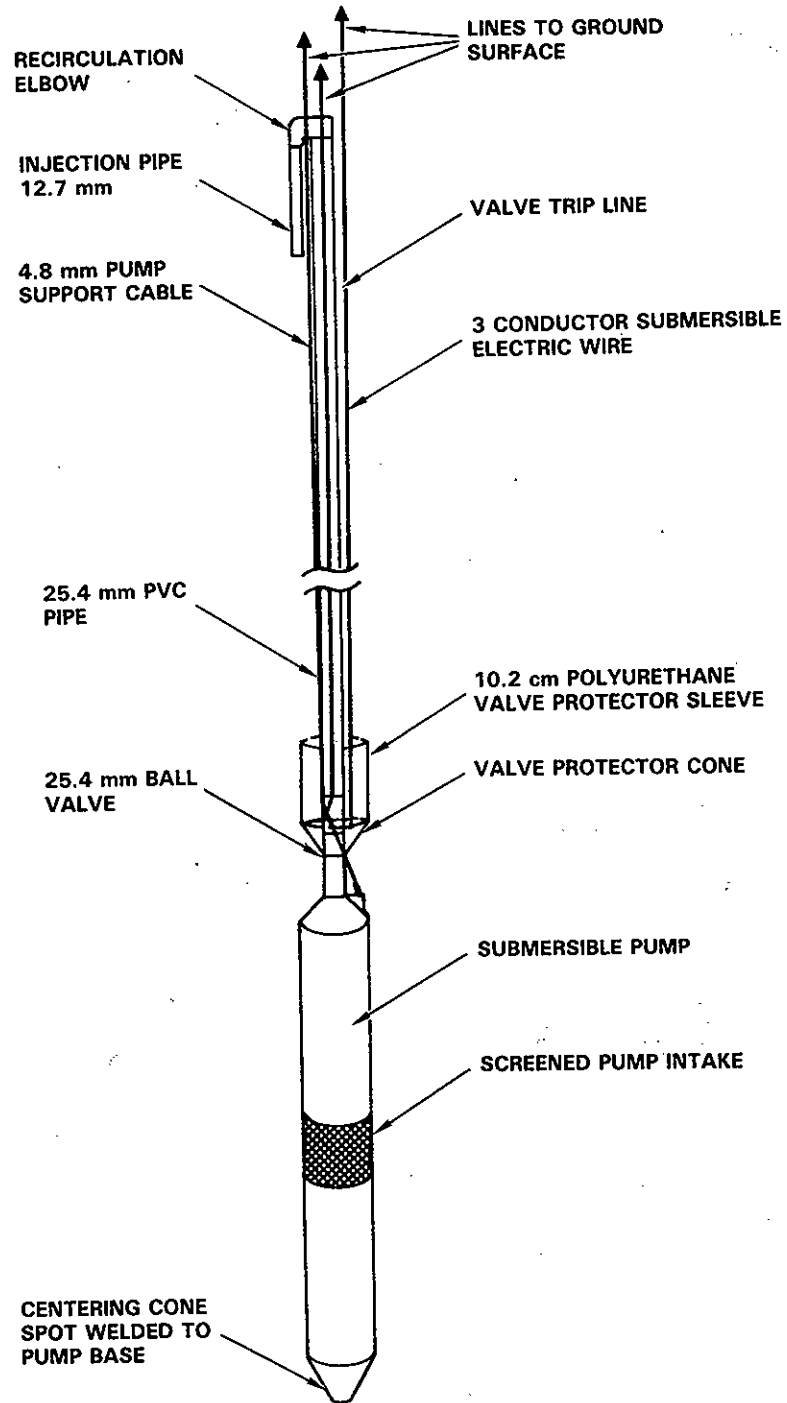


FIGURE 9. Tracer Injection System Used in Single-Borehole Tracer Tests

4.6.1 Granulometric Analysis

Borehole sediment samples were dry sieved using a Rotap shaker. A weighed aliquot was shaken for 15 minutes through a nest of nine 20.3-cm-diameter wire mesh sieves, and the disaggregate retained by each sieve was weighed and recorded. The size fractions thus separated (see Table 4) ranged from 0.037 to 4.0 mm and corresponded to Wentworth grade scale divisions (Wentworth 1922). The relative gravimetric proportions of these size fractions were used to categorize the sediment samples and to provide input to lithologic descriptions. The granulometric data are discussed in Section 6.

4.6.2 Calcium Carbonate Analysis

The calcium carbonate content of sediment samples reflects, in part, the amount of calcium carbonate cement present. The calcium carbonate

TABLE 4. Grain Size Nomenclature

<u>Particle Designation</u>	<u>Particle Diameter, mm</u>
Boulder	>256
Cobble	
large	256 - 128
small	128 - 64
Pebble	
very coarse	64 - 32
coarse	32 - 16
medium	16 - 8
fine	8 - 4
very fine	4 - 2
Sand	
very coarse	2 - 1
coarse	1 - 0.5
medium	0.5 - 0.25
fine	0.25 - 0.125
very fine	0.125 - 0.0625
Silt & Clay	<0.0625

determinations were made by reacting sediment carbonates with acid to stoichiometrically produce carbon dioxide and measure the volume of carbon dioxide gas produced (Horwitz 1970). Calcium carbonate data are discussed in Section 6.

4.6.3 X-Ray Fluorescence Analysis

Chemical analyses for major elements in selected basalt samples were conducted by Washington State University, using the X-ray fluorescence method explained in Hooper and Atkins (1969). In this procedure, a small aliquot of the powdered basalt sample was mixed one part to two parts with lithium tetraborate and fused in graphite crucibles at 1000°C to form glass wafers. The glass wafers were then analyzed using a Philips P. W. 1410 manual spectrometer for the following elements: Si, Al, total Fe, Ca, Mg, Ti, K, P, Na, and Mn. The raw data were then corrected for absorption and normalized on a volatile-free basis with Fe₂O₃ assumed to be 2.00 weight percent (Hooper et al. 1976). Eight basalt standards from the U.S. Geological Survey (USGS) (Brock and Grolier 1973) were used for calibration. Data from these analyses were used primarily for stratigraphic control. The major oxide composition of the basalt samples from this study is given in Appendix H.

4.6.4 Cations and Anions

The analyses for cations and anions were performed by the Hanford Environmental Health Foundation (HEHF) following procedures given in Standard Methods for the Examination of Water and Wastewater (Gilcreas, Taras, and Ingols 1980). The HEHF also analyzed the samples for pH, silica, total alkalinity, and total dissolved solids.

4.6.5 Trace Metals

Selected samples were analyzed for the 10 trace metals listed in Table 5. These analyses were performed by Pacific Northwest Laboratory using plasma emission spectroscopy methods.

4.6.6 Stable Isotopes

The stable isotope analyses were performed by Geochron Laboratories Division of Kreuger Enterprises Inc. The samples for deuterium (hydrogen-2/1) and

TABLE 5. Laboratory Analyses Performed on Ground-Water Samples.

<u>Analytical Category</u>	<u>Specific Analyses</u>
Cations	calcium, magnesium, sodium potassium, iron
Anions	bicarbonate, chloride, sulfate, nitrate
Trace metals	barium, silver, cadmium, zinc, copper, cobalt, nickel, chromium, lead, manganese
Stable isotopes	deuterium, oxygen-18/16, sulfur-34/32, (SO ₄ =)
Radionuclides	tritium, iodine-129, gamma scan
Other	pH, silica, total alkalinity, total dissolved solids

oxygen-18/16 required no treatment before shipment to the laboratory. The sulfur-34/32 samples were acidified with 20 mL of nitric acid to remove any carbonates. The sulfate in the samples was then precipitated with 75 g of BaCl₂. The precipitate was allowed to settle and the excess water was siphoned off the precipitate. The remaining BaSO₄ precipitate slurry was collected in a 1-liter polyethelene bottle and shipped to the laboratory. Attempts to collect sulfide in the samples by precipitation with Cd were unsuccessful. Therefore, all sulfur-34/32 analyses were performed on the sulfate species.

4.6.7 Radionuclides

The tritium analyses were performed by the University of Miami. The samples were purified by distillation before the tritium was enriched by electrolysis. The samples were then converted to gas and counted in an internal gas proportional counter.

The tritium values reported in Appendix I are given in the internationally adopted scale of U.S. National Bureau of Standards, based on their tritium water standard #4926. The stated errors are one standard deviation (1 σ). In some cases, negative tritium values are listed. Such numbers can occur because the net tritium count rate is, in principle, a difference between count rate of the sample and that of a tritium-free sample (background count or blank sample).

The iodine-129 and gamma scan analyses were performed by Pacific Northwest Laboratory. The results in Appendix I are for radionuclide anions. The errors are one standard deviation errors based on counting statistics.

5.0 DATA ANALYSES

In this section, the physical and chemical ground-water data are analyzed. Several techniques were employed to derive parameters related to ground-water flow in the unconfined and Rattlesnake Ridge aquifers. The hydrogeochemical data on the cations and anions and the stable isotopes are also analyzed. From these analyses, a conceptual model of the flow system in the unconfined and Rattlesnake Ridge aquifers was developed.

5.1 MATHEMATICAL ANALYSES

Mathematical techniques were used to derive parameters from the field data that were related to flow and transport in the aquifers. The barometric efficiencies of the confined aquifer test wells were determined from the response of water levels to changes in barometric pressure. These efficiencies were then used to correct for barometrically induced water-level changes during pumping tests and to infer areas where the confining bed has been eroded. The aquifer test data were analyzed to estimate transmissivities in the aquifers. Data from the single-borehole tracer tests were analyzed to determine the ground-water velocity profiles in the Rattlesnake Ridge aquifer.

5.1.1 Barometric Efficiency

The response of water levels in wells tapping confined aquifers to barometric pressure changes has long been recognized (Robinson 1939). The relationship is inverse; as barometric pressure increases, the water levels decrease. This phenomenon can be explained by the principle of effective stress (Jacob 1940). Any change in atmospheric pressure will be offset by a corresponding change in hydrostatic pressure at the top of the confined aquifer and a change of effective stress on the aquifer:

$$dp_a = d\sigma_e + dp_w \quad (1)$$

where: p_a = atmospheric pressure
 σ_e = effective stress acting on the aquifer skeleton
 p_w = fluid pressure.

The fluid pressure gives rise to a pressure head for a horizontal confined aquifer, any change in the pressure head is equivalent to the change in hydraulic head, h . From Equation (1), if an increase in barometric pressure is taken up largely by an increase in hydrostatic pressure, the corresponding increase in effective stress will be small. The atmospheric pressure increase pushing down on the water in the well will be offset largely by the increase in hydrostatic pressure in the aquifer. Therefore, the resultant water-level decrease in the well will be smaller than if the inverse were the case.

The barometric efficiency (B) of a well is defined as:

$$B = \frac{-dh}{dp_a}, \quad (2)$$

and is expressed conventionally as a percent. The higher the barometric efficiency, the more rigid the aquifer structure and the less the system is supported by hydrostatic pressure.

The barometric efficiencies were calculated by linear regression of the barometric changes, in centimeters of water, against the corresponding water-level changes, also in centimeters of water (Appendix F). The slopes of the regression lines represent the barometric efficiencies (Table 6).

5.1.2 Transmissivity

Transmissivity is defined as the rate at which water of the prevailing kinematic viscosity is transmitted through a unit width of aquifer under a unit hydraulic gradient (Lohman et al. 1972). Estimates of transmissivity were made by employing the Cooper-Jacob method of analysis on the field data for drawdown (Cooper and Jacob 1946), the Theis method for recovery (Jacob 1963), and the Cooper method for slug tests (Cooper, Bredehoeft and Papadopoulos 1967) (Appendices C and D). The calculated barometric efficiencies were used to correct for barometrically induced water-level fluctuations during the aquifer tests. The results are summarized in Table 7.

TABLE 6. Barometric Efficiencies of the 14 Confined Test Wells

<u>Well</u>	<u>Barometric Efficiency, %</u>	<u>Well</u>	<u>Barometric Efficiency, %</u>
299-E16-1	35.3	699-50-48	42.5
299-E26-8	24.5	699-51-46	28.5
299-E33-12	38.3	699-52-46	40.7
699-42-40C	44.4	699-52-48	42.5
699-47-50	17.3	699-53-50	39.2
699-49-55B	41.4	699-54-57	13.3
699-50-45	38.5	699-56-53	25.4

In general there is good agreement between the results of the various types of analyses for a given zone. A simple mean of all the test results was taken to describe the best estimate for transmissivity for each zone.

5.1.3 Ground-Water Velocity

Estimates of ground-water velocities were obtained from the single-borehole tracer tests. In Drost et al. (1968), the relationship is developed between ground-water velocity and the change in concentration over time of a tracer in a single borehole:

$$V = \frac{r \ln (C_0/C)}{4tn} \quad (3)$$

where:

V = ground-water velocity

r = radius of the borehole

C_0/C = ratio of the initial tracer concentration to the concentration after some time t

n = porosity.

A nondistributed porosity of 0.25 was used for these calculations. The relationship between ionic concentration and specific conductance is fairly

TABLE 7. Summary of Transmissivities Determined From the Aquifer Test

Well Number	Zone Tested	Drawdown, m ² /d	Recovery, m ² /d	Slug Injection, m ² /d	Slug Withdrawal, m ² /d	Mean, m ² /d
299-E16-1	Elephant Mountain II fracture zone	---	66	---	---	66
	Elephant Mountain interflow zone	46	109	100	52	77
299-E26-8	Unconfined	0.6	---	---	---	0.6
	Rattlesnake Ridge	3	22	19	17	15
299-E33-12	Unconfined	12	---	---	---	12
	Rattlesnake Ridge	3	4	12	12	8
699-42-40C	Unconfined	31	---	---	---	31
	Elephant Mountain interflow zone	0.7	---	---	---	0.7
699-47-50	Rattlesnake Ridge	28(a)	20(a)	85	78	44
699-49-55B	Rattlesnake Ridge	43(a)	93(a)	33	31	50
699-50-45	Rattlesnake Ridge	70	73	182	106	108
699-50-48	Rattlesnake Ridge	12(a)	16(b)	5	10	
699-51-46	Rattlesnake Ridge	34(b)	26(b)	18	11	22
699-52-46	Rattlesnake Ridge	3(b)	10(b)	2	0.3	4
699-52-48	Rattlesnake Ridge	17(b)	13(b)	21	18	17
699-53-50	Rattlesnake Ridge	3(b)	3(b)	11	5	6
699-54-57	Rattlesnake Ridge	50(b)	60(b)	74	85	67
699-56-53	Unconfined	12	13	19	12	14
699-56-53	Rattlesnake Ridge	22	---	---	---	22
	Rattlesnake Ridge	85	64	36	27	53

(a) = Average of two tests.
 (b) = From Strait and Moore, 1982.

simple and direct in dilute solutions of single salts (Hem 1970). The electrical conductivity readings, therefore, were used as concentrations in the velocity calculations.

Velocity profiles were calculated for each of the tested wells (Appendix J). The velocity profile on Well 699-49-55B was calculated after two time intervals, each following two separate injections. These four velocity profiles are in general agreement (Figure 10).

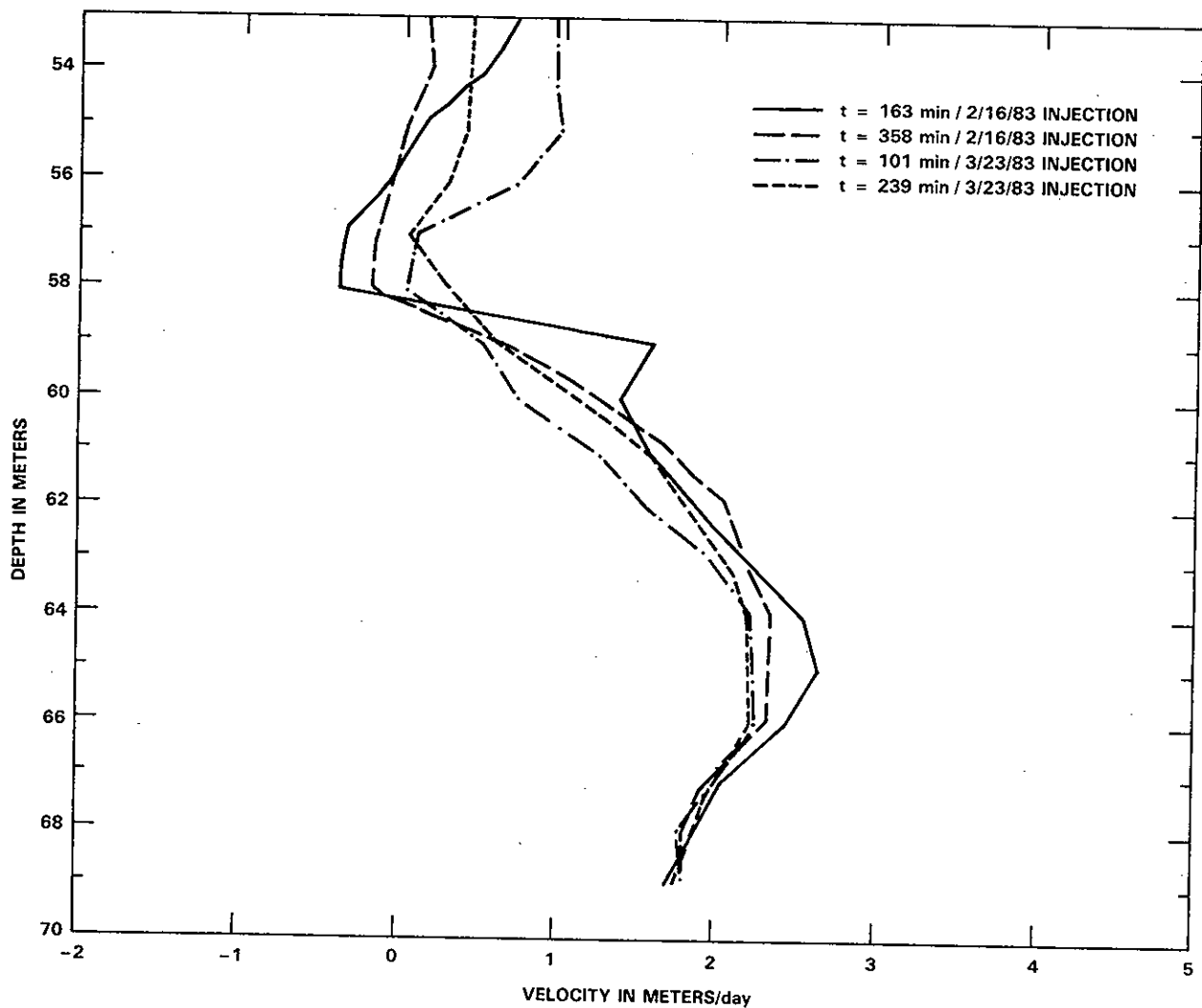


FIGURE 10. Comparison of Velocity Profiles from Tracer Tests Performed in Well 699-49-55B

5.2 HYDROGEOCHEMICAL ANALYSES

In the following sections, the data on the major cations and anions and the stable isotopes in the ground-water samples collected from the unconfined and Rattlesnake Ridge aquifers were analyzed; the equivalent parts per million (EPM) of the major cations and anions were calculated; and an EPM balance was performed. The oxygen-18 and deuterium relationship for the ground-water samples were compared with the global and local meteoric lines. The sulfate ion concentrations and the sulfur-34 values for the ground-water samples were compared.

The samples collected in the Elephant Mountain interflow zone in Wells 299-E16-1 and 699-42-40C may not be representative of the aquifer water. Both wells are located near the flow front of the upper unit of the Elephant Mountain basalt, where the Elephant Mountain aquifer is in contact with the unconfined aquifer. Drawdown induced by pumping the wells may have drawn unconfined aquifer water into the wells. Therefore, these data were not analyzed or interpreted, but included in Appendix I for reference.

5.2.1 Major Cations and Anions

The EPM for a charged ion is calculated by multiplying the molality of the species by its valence ($\times 10^{-3}$). An EPM balance is calculated as follows:

$$\text{EPM balance} = \frac{\sum \text{EPM cations} - \sum \text{EPM anions}}{\sum \text{EPM cations} + \sum \text{EPM anions}}$$

The EPM balance is commonly expressed as a percent. A positive imbalance indicates an excess of cations; a negative imbalance indicates an excess of anions. The principal sources of imbalance or error are incomplete analyses, laboratory error, or improper sampling or sample preservation procedures.

The EPM for the major cations and anions in the ground-water samples are given by well in Table 8. In the case of multiple samples collected from one well, the analyses from the last set of samples is used. An EPM balance for the analyses is also given in the table.

Five of the analyses had EPM balances greater than 10%: unconfined aquifer and Rattlesnake Ridge samples from Well 299-E33-12 and Rattlesnake

TABLE 8. Equivalent Parts Per Million of the Major Cations and Anions in Ground-Water Samples from the Unconfined and Rattlesnake Ridge Aquifers

Well	CONSTITUENT, EPM											EPM Balance, %
	CA ⁺⁺	MG ⁺⁺	NA ⁺	K ⁺	Cl ⁻	HCO ₃ ⁻	SO ₄ ⁼	NO ₃ ⁻				
E26-8, unconfined	1.29	0.88	0.68	0.14	0.27	1.64	0.60	0.01				-6
E26-8, Rattlesnake Ridge	0.95	0.76	0.83	0.25	0.23	2.08	0.77	0.03				9
E33-12, unconfined	1.70	1.08	3.22	0.18	0.16	2.00	1.46	0.58				19
E33-12, Rattlesnake Ridge	0.95	0.70	0.74	0.20	0.17	1.12	0.52	0.10				16
37-43, unconfined	4.09	2.39	2.48	0.22	0.54	1.80	6.35	0.05				3
42-40A, unconfined	0.95	1.15	1.22	0.10	0.20	1.90	0.77	0.08				8
42-40C, unconfined	1.10	1.02	1.09	0.11	0.19	1.98	0.06	0.06				8
42-40C, Rattlesnake Ridge	0.50	0.38	1.52	0.35	0.11	2.30	0.33	---				0
47-50, Rattlesnake Ridge	2.30	1.52	0.96	0.18	0.87	1.68	2.08	0.04				3
49-55A, unconfined	3.49	1.65	1.52	0.26	0.59	1.70	4.35	0.05				2
49-55B, Rattlesnake Ridge	1.90	1.02	0.52	0.17	0.30	2.18	0.35	0.01				12
50-45, Rattlesnake Ridge	4.59	1.29	0.74	0.15	0.62	2.10	0.37	0.01				38
50-48, Rattlesnake Ridge	0.95	0.51	1.44	0.28	0.73	2.00	0.65	---				-3
51-46, Rattlesnake Ridge	0.95	0.18	0.91	0.24	0.45	1.40	0.58	0.01				-4
52-46, Rattlesnake Ridge	1.20	0.86	0.70	0.19	0.71	2.00	0.40	0.01				-3
52-48, Rattlesnake Ridge	0.31	0.16	2.17	0.16	0.11	2.60	0.50	---				-7
53-50, Rattlesnake Ridge	1.50	0.90	0.91	0.19	0.59	2.10	0.60	0.01				3
54-57, Rattlesnake Ridge	1.25	0.95	1.00	0.18	0.36	2.26	0.42	0.01				5
55-50C, unconfined	0.95	0.76	0.20	0.10	0.06	1.90	0.37	---				-7
56-53, unconfined	1.25	0.86	0.37	0.14	0.10	2.12	0.17	---				4
56-53, Rattlesnake Ridge	1.90	1.11	0.91	0.17	0.76	2.44	0.04	---				12
60-57, unconfined	0.80	0.70	1.65	0.20	0.37	2.70	0.04	0.01				4

Ridge samples from Wells 699-49-55B, 699-50-45, and 699-56-53. These analyses were rerun by the laboratory with essentially the same results. Well 299-E33-12, which is located in an area where dense, high salt wastes are present in the bottom of the unconfined aquifer (Smith 1980), had an EPM balance of 19%. As stated earlier, this borehole was open from the unconfined aquifer to the Rattlesnake Ridge aquifer from 1953 until 1982. There is evidence from the geophysical logs (natural gamma, Appendix B) and the electrical conductivity profile (Appendix G) that these wastes migrated into the bottom of the borehole. The chemistry of these wastes may cause interferences that would account for the imbalance. The analyses from Wells 699-49-55B and 699-56-53 had EPM balances of 12%. Replicate sets of samples were collected from these wells (three from Well 699-49-55B and two from Well 699-56-53). While the analyses for these sets show good internal consistency (Appendix I), the source of the imbalance is not known. A review of the analytical results for the sample from Well 699-50-45 indicates that the calcium concentration is high in comparison to the other samples from the Rattlesnake Ridge aquifer; however, there was only one sample collected from this well. The most likely source of the imbalance appears to be calcium contamination of the sample.

5.2.2 Stable Isotopes

The stable isotope ratios are reported in the standard δ notation:

$$\delta^{2\text{H}}, \delta^{18\text{O}}, \delta^{34\text{S}(\text{SO}_4)} = \frac{R_{\text{Sample}}}{R_{\text{Standard}}} - 1 \times 1000$$

For deuterium, $\delta^{2\text{H}}$, $R = {}^2\text{H}/{}^1\text{H}$ and the standard is the mean composition of ocean water (SMOW) (Craig 1961). For $\delta^{18\text{O}}$, $R = {}^{18}\text{O}/{}^{16}\text{O}$ and the standard is also SMOW. For $\delta^{34\text{S}(\text{SO}_4)}$, $R = {}^{34}\text{S}/{}^{32}\text{S}$ and the standard is the Cañon Diablo meteorite. Values are reported in parts per thousand (0/00). A sample that is +10 0/00 contains 10 parts per thousand or 1% more than the standard.

5.2.3 Hydrogen and Oxygen

There are two stable isotopes of hydrogen: ${}^1\text{H}$ with a relative abundance of 99.984%; and ${}^2\text{H}$ (deuterium) with a relative abundance of 0.015%. Oxygen has three stable isotopes: ${}^{16}\text{O}$ with a relative abundance of 99.76%; ${}^{17}\text{O}$ with a

relative abundance of 0.037%; and ^{18}O with a relative abundance of 0.1%. The isotope ^{17}O is not presently used in environmental studies (Fritz and Fontes 1980).

Craig (1961) demonstrated a linear relationship between deuterium and oxygen-18. This relationship was established from analyses of meteoric waters collected from several hundred stations and around the world and is referred to as the global meteoric line. The equation for this line is $\delta^2\text{H} = 8 \delta^{18}\text{O} + 10$.

The linear relationship between deuterium and oxygen-18 arises from the fact that condensation from the atmosphere is essentially an equilibrium process. The fractionation of deuterium to hydrogen is proportional to the fractionation of oxygen-18 to oxygen-16. Secondary fractionation processes result in deviations from the meteoric water line.

One of the more frequent and recognizable secondary fractionation processes is evaporation. Generally, the slope of an evaporation line is within the range of 2 to 5, compared with 8 for the global meteoric line (Fontes 1980). As a result of this process, there is a net decrease in the heavier isotopes in precipitation as it moves from the ocean across a continental land mass. The deuterium and oxygen-18 content of precipitation is also affected by latitude, altitude, temperature and amount of precipitation.

The $\delta^2\text{H}$ and $\delta^{18}\text{O}$ values for the various ground-water samples are plotted in Figure 11. A curve is fitted to these data by linear regression. The global meteoric line and the local meteoric line are plotted for comparison. The slope of the local meteoric line determined from samples collected in the nearby Rattlesnake Hills area is 5.8 (Graham 1983). This shift from the global meteoric line probably results from evaporation in the arid climate and fractionation as the water vapor moves inland from the coast over the Cascade Range. As expected, the equation for the line fitted to the ground-water samples is similar to the local meteoric line equation.

5.2.4 Sulfur

Sulfur has four stable isotopes; the two most common of which are ^{32}S with a relative abundance of 94.95%, and ^{34}S with a relative abundance of 4.3%. The other two isotopes, ^{33}S and ^{35}S , constitute the remaining 0.8%.

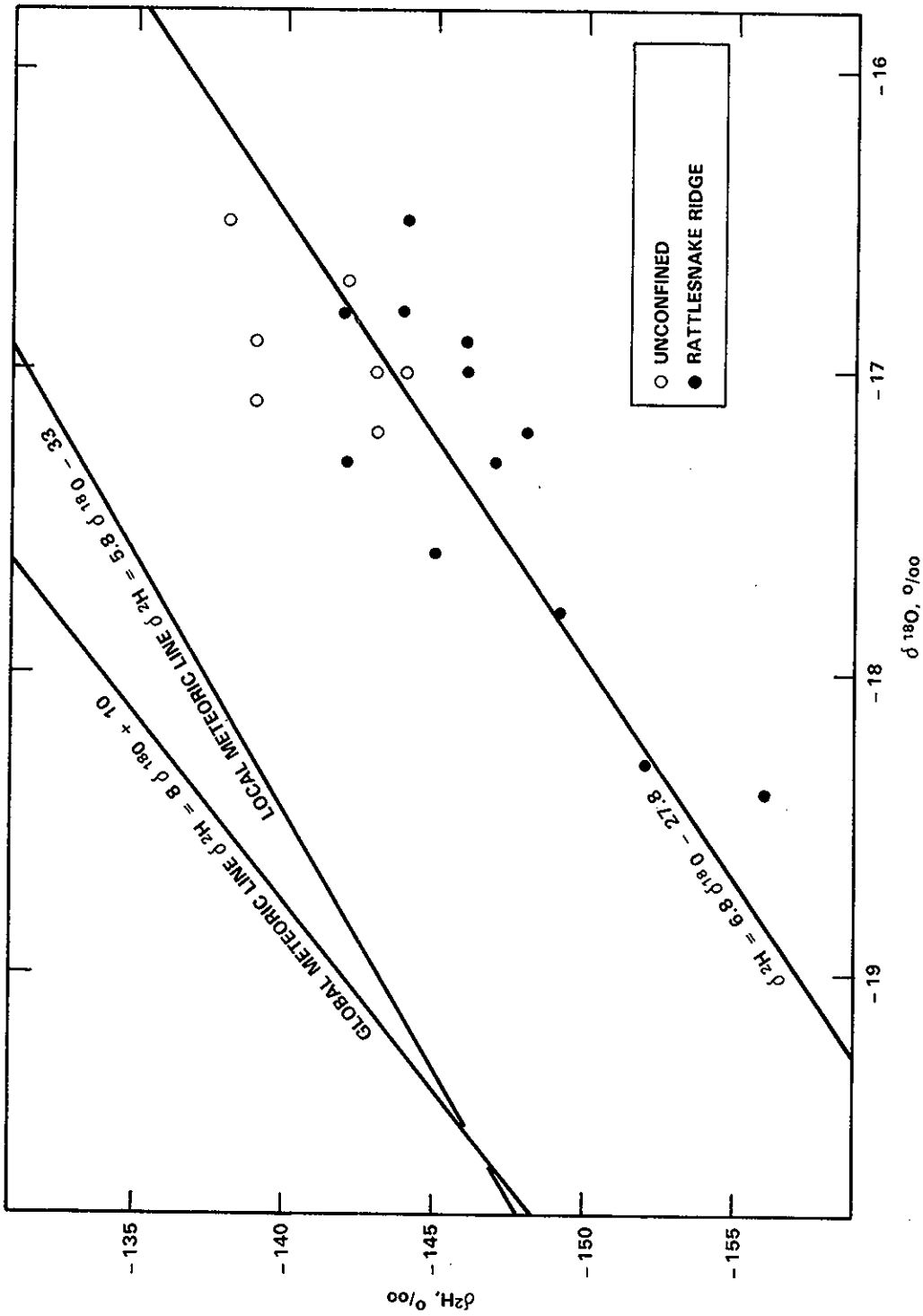


FIGURE 11. Plot of 2H and ^{18}O Values for Ground-Water Samples Collected in the Study Area Compared to Local and Global Meteoric Lines

The sulfate concentrations and the $\delta^{34}\text{S}$ values for the ground-water samples vary over a wide range. The sulfate ranges from 1 to 305 mg/L; $\delta^{34}\text{S}$ values range from -9.1 ‰ to +7.9 ‰. The higher values of sulfate are generally associated with the unconfined aquifer. The unconfined aquifer samples are also generally depleted in ^{34}S in comparison to the Rattlesnake Ridge samples.

Sulfate concentrations and $\delta^{34}\text{S}$ values from the ground-water samples are plotted in Figure 12. Sources of sulfate in ground water include evaporite-mineral dissolution, oxidation of sulfide minerals, and rainfall (Pearson and Rightmire 1980; Hem 1970). The presence of accessory sulfide minerals has been identified in the Columbia River Basalts (Ames 1980). In arid regions sulfate may be derived from windblown mineral-sulfate dust obtained from soils and playas (Pearson and Rightmire 1980). Sulfate in the ground water has many possible sources, which would account for the wide range of sulfate concentrations and sulfur-34 values.

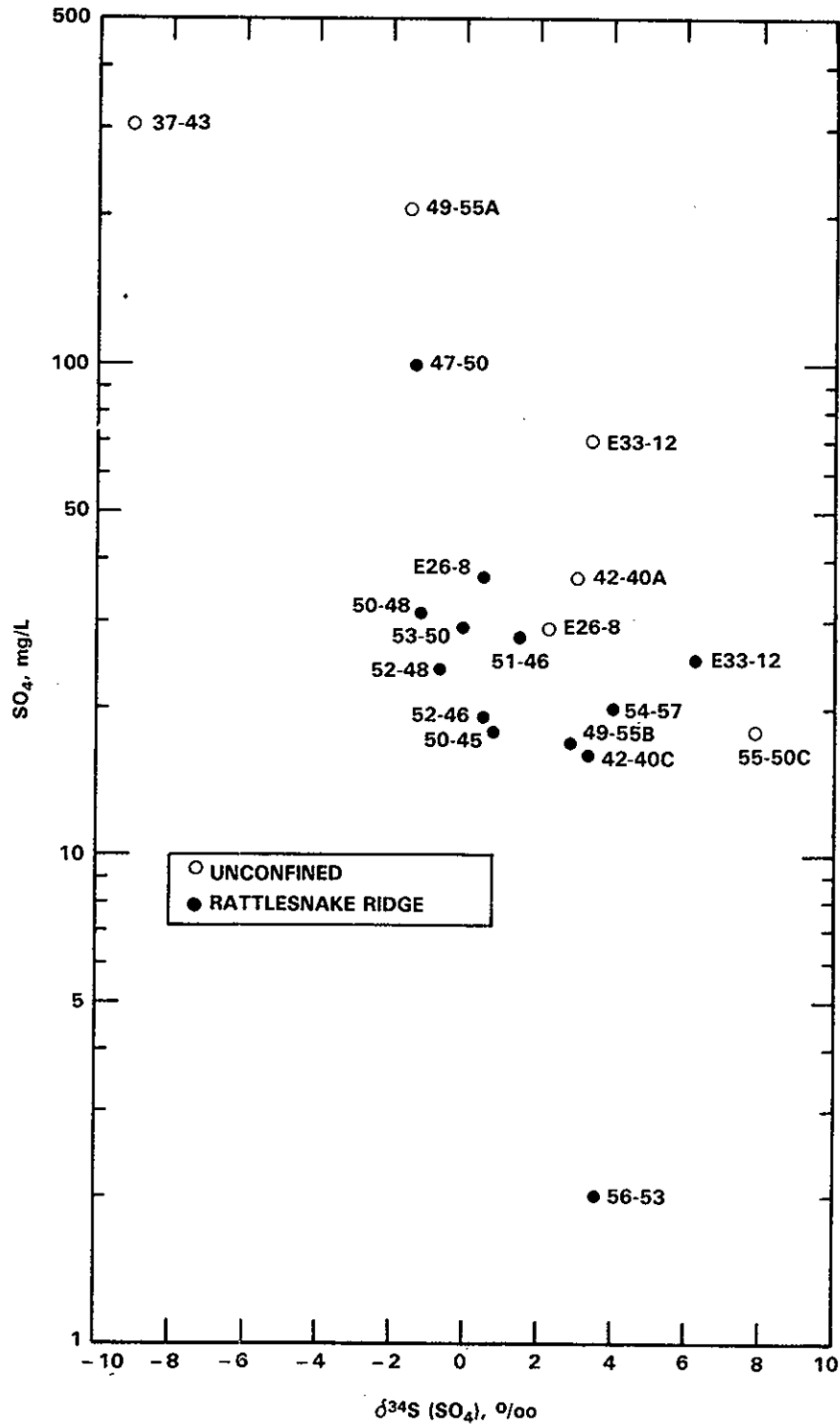


FIGURE 12. Plot of SO_4 Concentration and ^{34}S Values for Ground-Water Samples Collected in the Study Area

6.0 DATA INTERPRETATION: A CONCEPTUAL MODEL

The geologic framework of the study area includes the stratigraphy, structure, and geomorphology. An interpretation of the ground-water flow system in the unconfined and Rattlesnake Ridge aquifers in the study area was developed from head data collected in the aquifers from June 1982 to June 1983. The regional flow system of the Rattlesnake Ridge aquifer was also constructed. An interpretation of the intercommunication between the two aquifers was made by evaluating the locations of erosional areas in the confining bed and comparing hydraulic head values in the two aquifers to define the areas of downward gradients. The limited data collected on the Elephant Mountain interflow zone (Elephant Mountain aquifer) were also interpreted. The hydrogeochemistry of the ground waters was used to evaluate mixing of unconfined water in the Rattlesnake Ridge aquifer. The levels of radionuclide contamination in the Rattlesnake Ridge aquifer were also defined.

6.1 GEOLOGIC FRAMEWORK

A basic understanding of the geology of the study area is needed to define the framework for the ground-water flow system. The nature and distribution of aquifers and aquitards are primarily controlled by the lithology, stratigraphy, and structure of the geologic deposits and formations (Freeze and Cheery 1979). The stratigraphy (including lithologic descriptions) describes the geometric relationships between the principal geologic units and their physical make up. These relationships influence not only the distribution of aquifers and aquitards, but also homogeneity and isotropy of the ground-water system. Structural features such as fractures, folds, and faults primarily control the location of recharge, discharge, and no-flow boundaries.

6.1.1 Stratigraphy

The geologic units of principal interest are, in ascending order: the Pomona Member, a thick and dense basalt flow(s) that forms the base of the Rattlesnake Ridge aquifer; the Rattlesnake Ridge interbed, which forms the physical framework of the uppermost confined aquifer; the Elephant Mountain Member, which forms the confining bed over the Rattlesnake Ridge aquifer; and the

Ringold Formation and Hanford formation, which form the framework of the unconfined aquifer (Figure 4 and Appendix K).

The Pomona Member averages about 56 m thick in the study area, and thickens slightly to the south (Figure 13). On the western Gable Mountain anticline it is typified by four major intraflow structures: basal colonnade, entablature, upper colonnade, and flow top (Fecht 1978). The basal colonnade has large, blocky, well-developed columns, approximately 50 cm in diameter. The entablature consists of long, undulating, well-developed, slender columns (averaging only about 25 cm in diameter) and grades abruptly into the upper colonnade, where the columns average about 75 cm in diameter. The upper colonnade has many cross-joints and large scattered vesicles. In places, zones of glassy, vesicular basalt extend the full length of the upper colonnade. The flow top is highly vesicular and glassy and averages approximately 2 m thick throughout the study area (where not locally eroded away).

Hydrologically, the Pomona member behaves as an aquiclude in that it has extremely low permeability and does not transmit significant quantities of groundwater. Hydraulic conductivity of the Columbia River basalt flow interiors is extremely low, ranging from 10^{-6} to 10^{-8} m/day (BWIP staff 1982). The flow top of the Pomona I flow may, however, transmit enough water to be considered a potential aquifer. Flow tops of the Saddle Mountain Basalts typically have equivalent hydraulic conductivities of 10^2 to 10^{-2} m/day (BWIP staff 1982).

The Rattlesnake Ridge interbed is the most significant geologic unit in the present study. This unit forms the physical make up of the uppermost confined aquifer. Thus, its lithologies control the storativity and movement of ground water within the aquifer.

The Rattlesnake Ridge interbed was deposited on the weathered surface of the Pomona. Its thickness varies from a thin 1.5 m over Gable Mountain to over 25 m in the southwest portion of the study area (Figure 14). Its average thickness is 15.6 m. Locally, it has been divided into four facies on the basis of composition. These facies are, in ascending order: 1) a clayey basalt conglomerate formed by the weathering and reworking of the Pomona flow top, (2) an epiclastic fluvial-floodplain unit deposited by the ancestral Columbia River

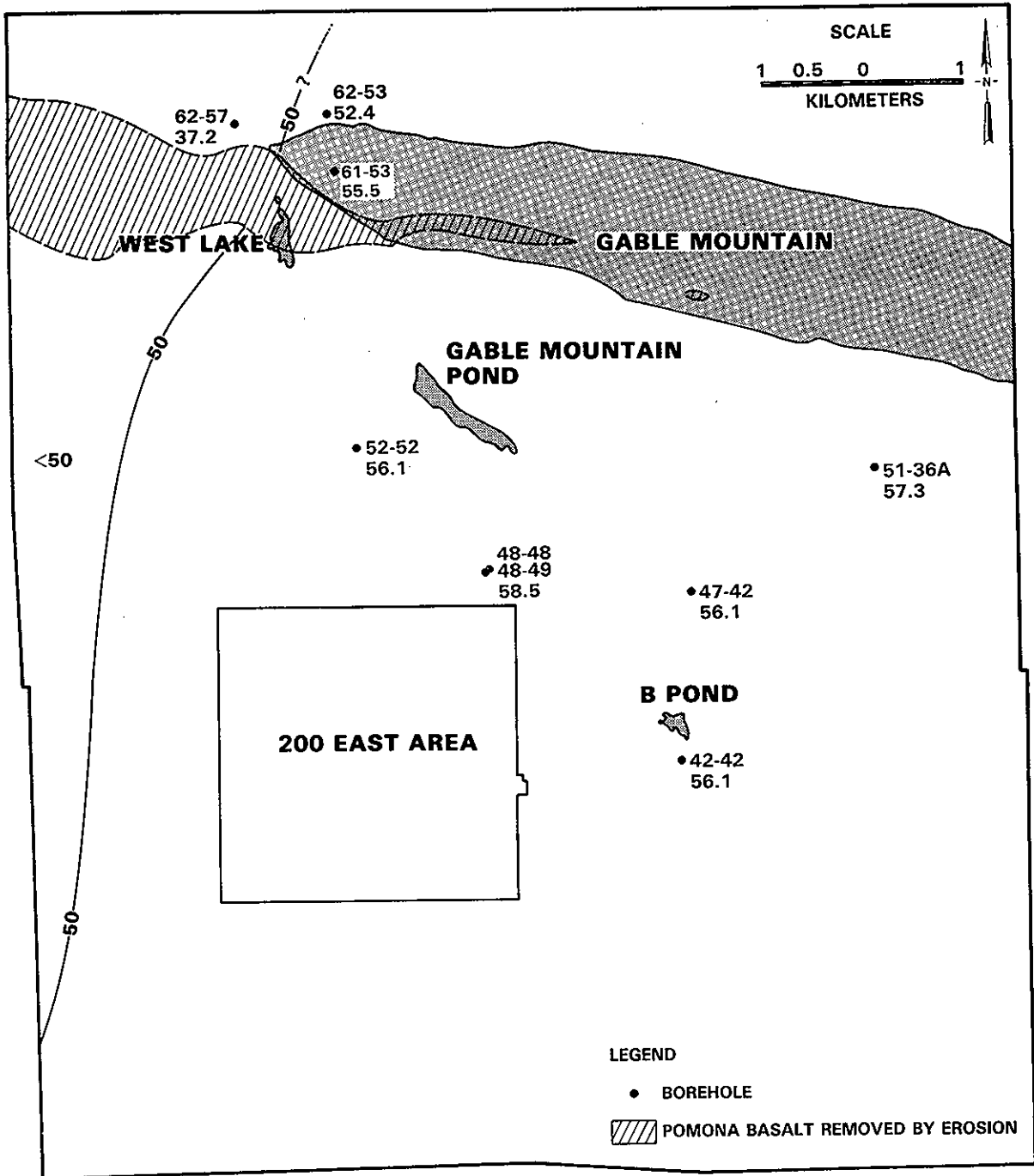


FIGURE 13. Isopach Map of the Pomona Member Within the Study Area (from Myers and Price 1981)

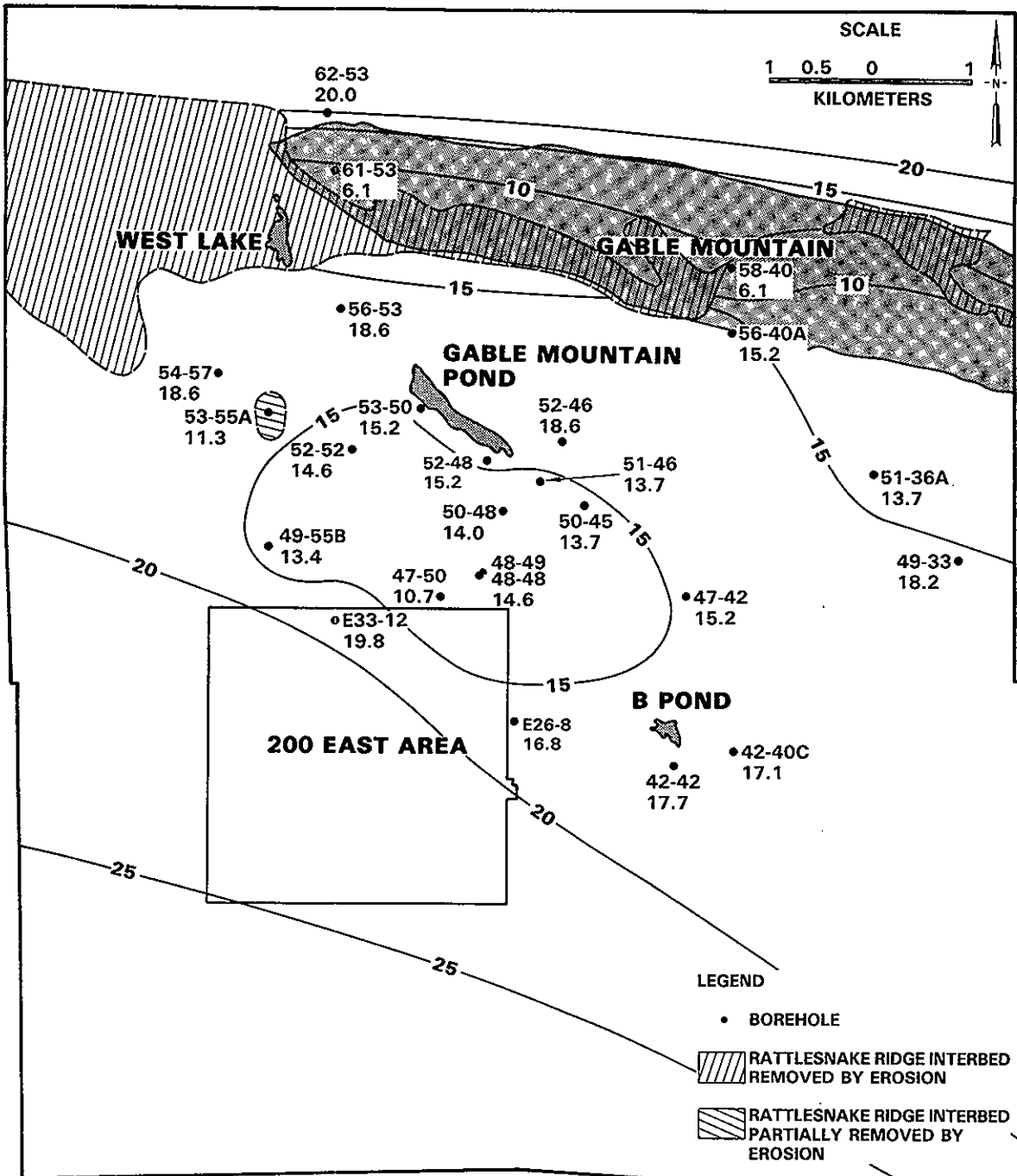


FIGURE 14. Isopach Map of the Rattlesnake Ridge Interbed

system, (3) a tuff made up of an air fall ash, and (4) a tuffite derived from fluvially reworking the tuff and epiclastic detritus. The tuff and tuffite units, when present, differ from the epiclastic and clayey basalt conglomerate units by exhibiting higher natural radioactivity (as indicated by the natural gamma logs in Appendix B) and by the high glass content found in borehole samples. The tuff and tuffite remain relatively constant in grain size but vary in thickness due to erosion and/or nondeposition. The epiclastic unit varies in thickness and grain size. Its grain size ranges from sandy gravel to sands and silts. These appear to interfinger and grade laterally into one another.

The Rattlesnake Ridge interbed forms the uppermost, regionally extensive, confined aquifer. The varying lithologies produce some degree of anisotropy and heterogeneity within the aquifer, which to some extent can be seen in the velocity profiles in Appendix J. Hydraulic conductivities range from 10^1 to 10^{-2} m/day (BWIP Staff 1982).

The Elephant Mountain Member (10.5 mybp) is the uppermost and youngest basalt member the study area. It is generally conformable to the surface of the Rattlesnake Ridge interbed, but in areas has been found to be invasive into the underlying sediments (Fecht 1978). The member consists of two flows or flow lobes. The lowermost flow (Elephant Mountain I) is continuous over most of the study area, ranging in thickness from 35 m to 11.5 m (where partially eroded away) and thins to about 6 m over Gable Mountain (Figure 15). Fecht (1978) describes three intraflow structures in the lower flow (Elephant Mountain I). These are, in ascending order: colonnade, entablature, and flow top. The colonnade makes up approximately one-third of the flow. Its base is nonvesicular with numerous cross-fractures and platy joints. Above this the colonnade grades from moderate- and well-developed columns into a platy cross-fractured colonnade and then into a hackly entablature. The entablature has numerous, irregular cross-fractures, vertical fractures, and small scattered vesicles near its top. The flow top has been largely eroded from Gable Mountain, but, where it is present, it is brecciated and/or palagonitic.

The upper flow (Elephant Mountain II) is present in the southeast and northern portions of the study area, identified only from boreholes (Figure 15).

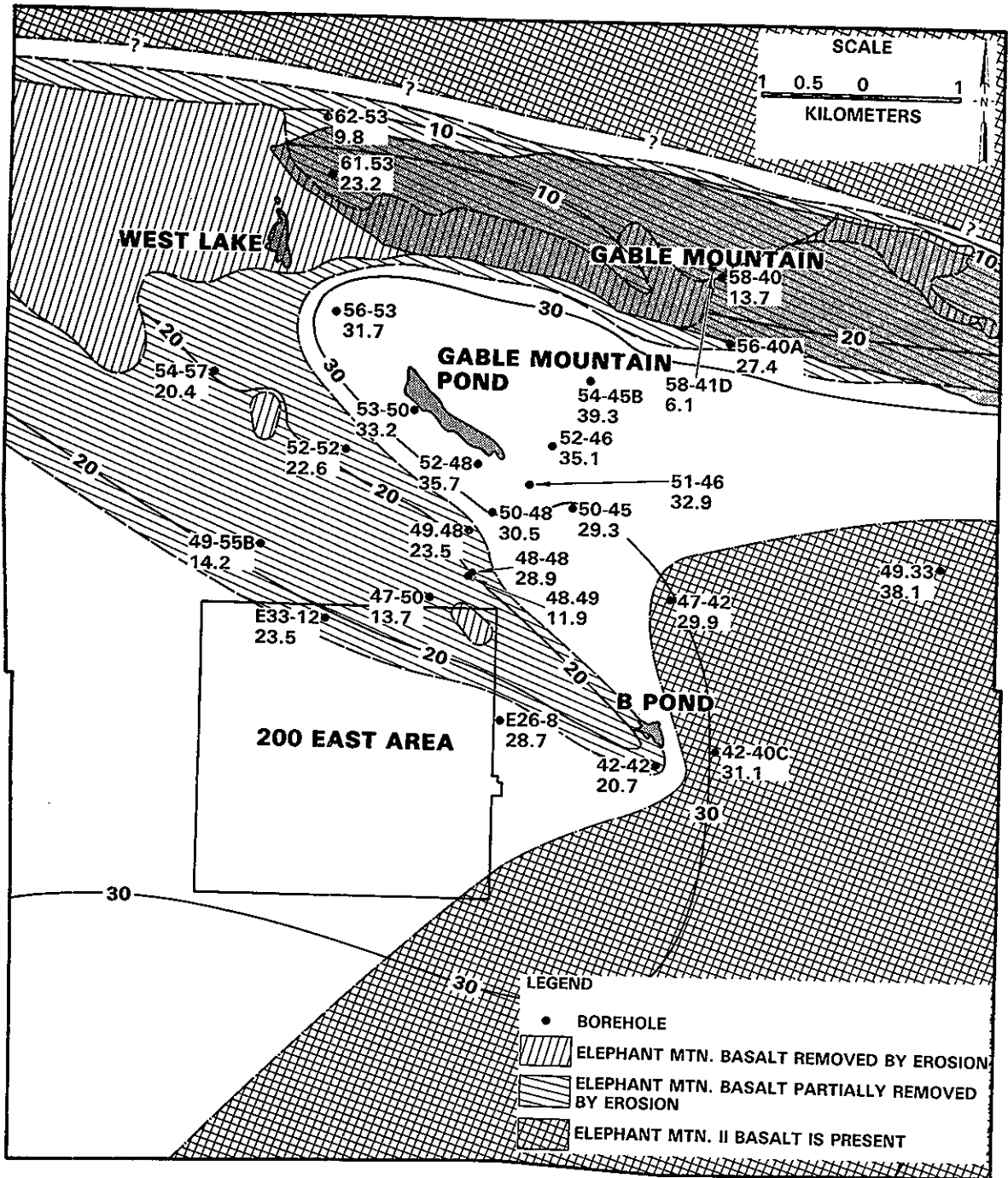


FIGURE 15. Isopach Map of the Elephant Mountain Member

This flow is roughly one-quarter the thickness of the Elephant Mountain I flow (averaging 7.7 m) and thickens to the southeast and north. An interflow zone separates the flows and was encountered in Wells 299-E16-1 and 699-42-40C. Well 299-E16-1 was completed in the interflow zone where approximately 3 m of silt were penetrated.

The Elephant Mountain Member forms the bedrock surface beneath the study area, except where it has been locally eroded exposing the older units. Much of this erosion occurred during the deposition of Ringold sediments, as the ancestral Columbia River flowed through the structural low west of Gable Mountain. Further erosion occurred following deposition of the Ringold, as Pleistocene catastrophic floods inundated the area. Figure 16 shows the geologic contacts and topography of the bedrock surface.

Hydrologically, the Elephant Mountain member has the character of an aquiclude, acting to confine the Rattlesnake Ridge aquifer. The Elephant Mountain interflow zone has interconnecting vesicles and rubbly zones, enabling it to produce a fair amount of groundwater. Hydraulic conductivity of this zone has been found to be in the range of 622 m/day (Graham, et al. 1981). This zone is considered an aquifer, confined by the overlying Elephant Mountain II flow. Both the Elephant Mountain I and II flows are dense, low permeability, basalt flows with very low hydraulic conductivities typical of the Columbia River Basalts. The Elephant Mountain II flow top has a hydraulic conductivity ranging between 10^2 to 10^{-2} m/day (BWIP Staff 1982).

The Ringold Formation is present throughout the study area except over Gable Mountain where the Ringold Formation was apparently not deposited, and in the area north of the 200-E Area where main stream currents of late Pleistocene flooding have completely removed it (Figure 17). The Ringold Formation generally thickens to the south into the Cold Creek syncline. Its thickness varies from zero in the Gable Mountain/Gable gap area to a maximum thickness of about 215 m in the southeast corner of the study area. The basal, lower, and middle units of the Ringold Formation are present within the study area, whereas the upper Ringold unit appears to be completely missing.

The basal Ringold, the oldest and lowermost of the Ringold units, directly overlies the Elephant Mountain Member. In the southern portion of the study

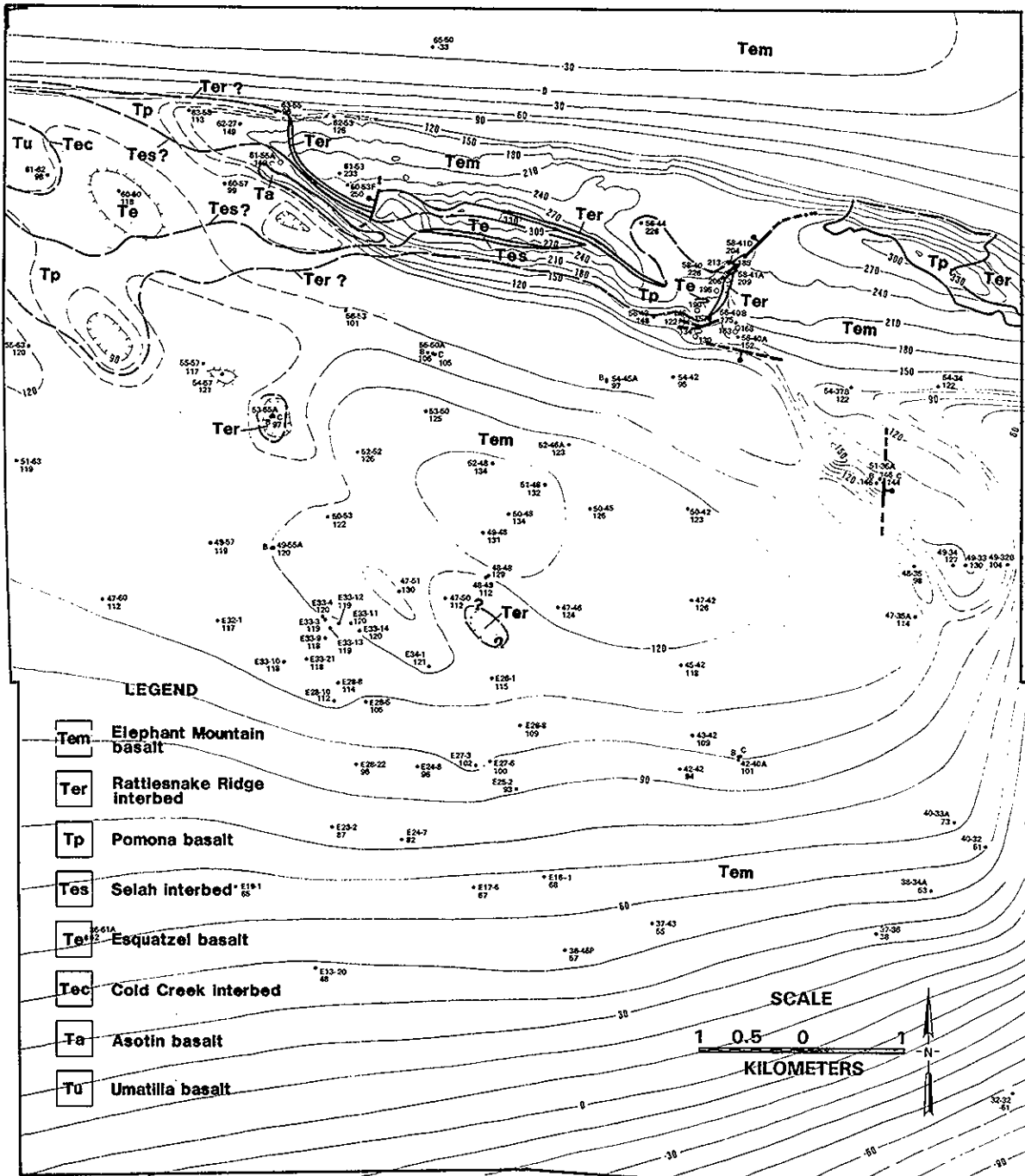


FIGURE 16. Geologic Map of the Bedrock Surface

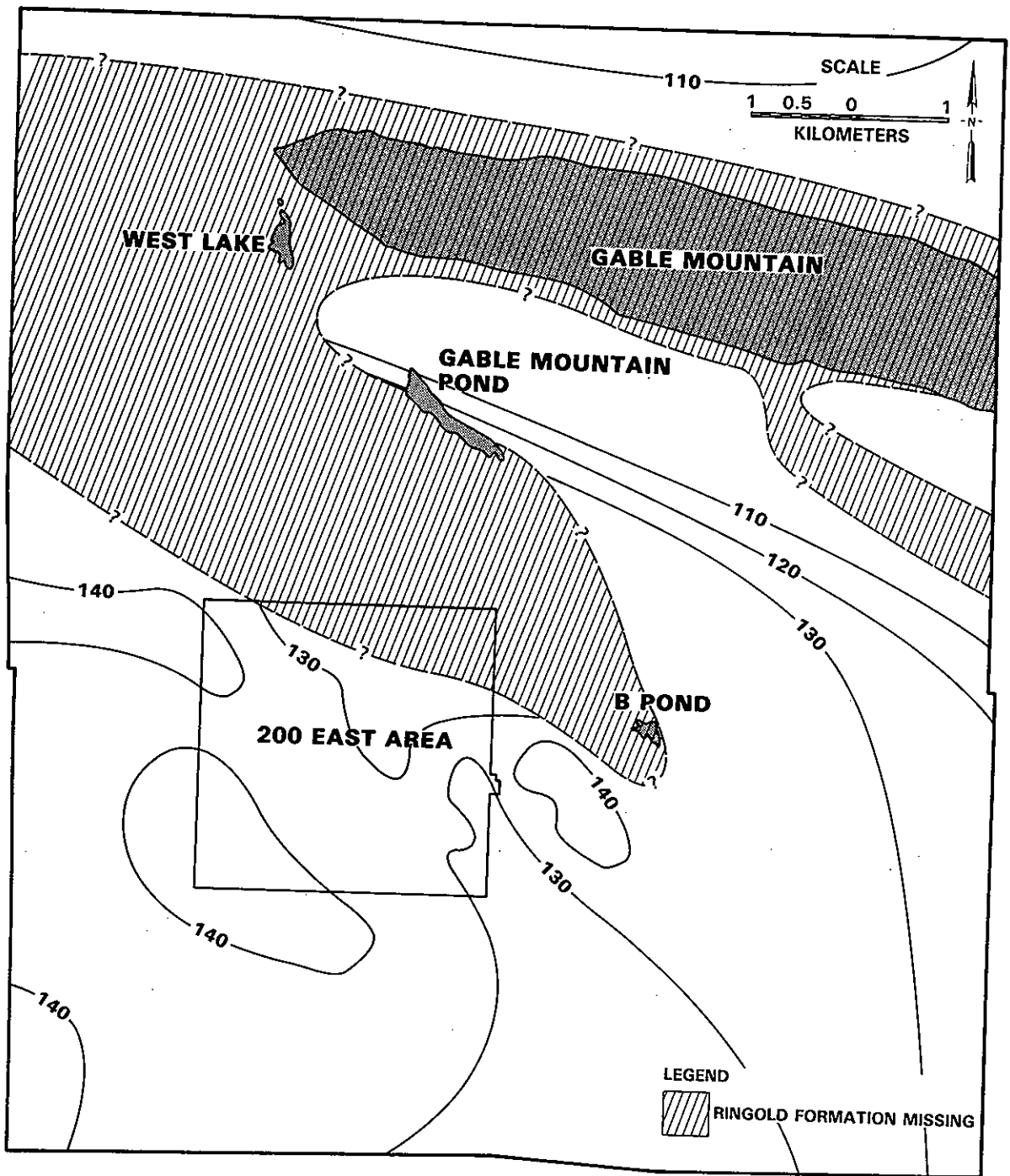


FIGURE 17. Map of the Surface of the Ringold Formation (Modified from Tallman et al. 1979; Brown 1959; Fecht 1979)

area, the basal Ringold is overlain by the lower Ringold unit and is well defined. In the central portion, the lower Ringold unit apparently pinches out, making definition of the basal Ringold difficult due to its similarities to the now overlying middle Ringold unit. The basal Ringold thickens southward from about 15 to 38 m in the Cold Creek Syncline.

The lower Ringold unit ranges from silty coarse to medium sand, to a sandy silt to clay (Tallman et al. 1979) and locally includes some gravel stringers. The lower Ringold sediments are generally compacted and have variable degrees of induration.

The middle Ringold unit occurs throughout the study area except over Gable Mountain and in the deeply eroded channels adjacent to Gable Mountain. The elevation of its surface ranges from about 120 to 150 m above mean sea level. Its thickness increases to 100 m in the southern part of the study area, thinning toward the north and east. Erosion by normal fluvial processes and/or Pleistocene proglacial flood waters has modified the surface of the middle Ringold throughout most of the study area (Figure 17). Reworked portions are often difficult to differentiate from the undisturbed portions. The middle Ringold unit consists of well-rounded pebble-to-cobble size gravel with a matrix of sand, silt, and some clay. Induration of the unit varies from virtually no cement to well cemented by calcium-carbonate and/or silica. Consolidation of the unit varies from matrix-supported conglomerate to open-work uncemented gravel (Tallman et al. 1979).

The upper Ringold unit is completely missing from the study area, except perhaps along the most northern boundary. It probably was never deposited on Gable Mountain and elsewhere was removed by erosion. Thus, the middle Ringold unit is the uppermost Ringold unit in the study area, and its surface is an erosional unconformity.

The Ringold Formation has a variety of hydrologic conditions including aquifer, aquitard, unconfined aquifer and unsaturated. The basal Ringold forms a confined aquifer in the southwest portion of the study area where it is capped by the lower Ringold unit. In this area, the lower Ringold acts as an aquitard to retard the vertical movement of groundwater. Here the middle Ringold contains the unconfined aquifer. In other portions of the study area

the lower Ringold is missing and the basal Ringold and middle Ringold jointly contain the unconfined aquifer. Those portions of the Ringold Formation extending above the water table are unsaturated. The variability of the sediments also produces various modifications to these generalized conditions. Hydraulic conductivities of the Ringold Formation range from 3 to 70 m/day for the middle Ringold units and 1 to 1.36 m/day for the lower Ringold unit (Graham 1981).

The surface and near-surface deposits of unconsolidated sand and gravel are glaciofluvial sediments of the Hanford formation. The thickness of the Hanford formation varies from 0 m on Gable Mountain to a maximum of about 90 m in the southern portion of the study area.

The lowermost textural facies of the Hanford formation is medium grained, ranging from coarse to fine sand to slightly gravelly, very coarse to medium sand beneath 200 East Area. To the north, this textural unit appears to thin and pinch out, while generally getting coarser. Gravel units also occur but mostly are channel fill within the sand units. Overlying the medium-grained textural facies is relatively coarse grained detritus that ranges from a gravelly sand in the topographically higher southern portion of the study area to boulders along the southern banks of the old flood channels immediately south of Gable Mountain.

Many varied bedding forms have been observed in the Hanford formation. Bedding forms provide indications of the depositional environment and of the stream's current direction. Unsaturated flow through these sediments in the vadose zone is partially controlled by these bedding forms. Horizontal bedding with fine laminations impedes downward migration of water and promotes lateral spreading, creating perched water zones beneath active disposal sites. Forset bedding enhances downward migration along the bedding planes. A good description of the various bedding forms observed in the Hanford formation can be found in Tallman et al. (1979).

Another common feature of the Hanford formation is the occurrence of clastic dikes (Black 1979). These sedimentary dikes are composed of numerous small dikes of clay-to-gravel sized clastic sediments separated by clay skins. These vertical dikes intersect each other at regular intervals, and where exposed at

the surface they form polygonal patterns much like giant mud cracks. These dikes are also generally associated with slump features and soft sediment deformation features. Clastic dikes, although predominately found in the Hanford formation, have also been observed in the Elephant Mountain Member and Rattlesnake Ridge interbed within the study area. The origin of clastic dikes is still under considerable controversy. Their significance to waste management, however, is apparent. These vertical features can potentially act as vertical conduits, promoting the vertical movement of contaminants and impeding horizontal movement.

The Hanford formation generally contains only the upper portion of the unconfined aquifer; however, around Gable Mountain Pond the unconfined aquifer is totally within the Hanford formation. The upper portion of the Hanford formation is generally unsaturated except for local perched water zones beneath the active waste disposal sites. Hydraulic conductivities of the Hanford formation are generally more than an order of magnitude higher than those of the middle Ringold unit, ranging from 600 to 3,000 m/day (Graham, et al. 1981).

6.1.2 Structure

The study area is located near the center of the Pasco Basin and covers portions of three first-order folds: the Umtanum Ridge-Gable Mountain structure, the Wahluke syncline, and the Cold Creek syncline.

The Umtanum Ridge--Gable Mountain structure is the dominant structural feature in the study area. Repeated folding of this east-west trending asymmetrical anticline has sharply raised the Rattlesnake Ridge interbed above its regional piezometric surface. Thus, the Rattlesnake Ridge interbed is dry on Gable Mountain and represents a no flow boundary.

North of the Umtanum Ridge--Gable Mountain structure and trending parallel to the structural ridge is the Wahluke syncline. This syncline appears to be a very broad, open depression that plunges gently westward in the study area. The Cold Creek syncline is situated south of the Umtanum Ridge--Gable Mountain structure and north of Yakima Ridge. In the study area, only the north limb of the syncline is present.

Six known faults have been mapped in the study area based on surface exposures and boreholes. These faults are generally associated with areas of intense deformation of the basalt on Gable Mountain (Figure 18).

The central Gable Mountain fault is an arcuate reverse fault that lies northwest of an eroded fault-line scarp in the saddle of Gable Mountain. Hence, the Elephant Mountain and Pomona members and the Rattlesnake Ridge interbed have been thrust to the northwest over the Elephant Mountain Member. The gouge zone ranges in thickness from 12.2 to 15.2 m near the center of Gable Mountain, to 5 cm near the northeast end before the fault dies out. The fault displaces glaciofluvial units of the Hanford formation that are as young as late Pleistocene age (13,000 to 19,000 ybp) (Puget Sound Power and Light Company 1982).

Two faults have been observed in trenches and boreholes in the southcentral Gable Mountain area; the south fault and north-dipping reverse fault (Puget Sound Power and Light Company 1982). The south fault is characterized by a 7- to 10-cm-thick clay gouge zone. The north-dipping reverse fault was encountered during drilling of boreholes on the south flank of Gable Mountain. The length of the fault is estimated to be less than 6.4 km based on its apparent relationship with the western Gable Mountain anticline. Within the core from the boreholes, the zone of brecciation and fault gouge ranges from 6.1 to 18.3 m in thickness.

The western Gable Mountain fault is located on the western Gable Mountain anticline. At the southern end of the fault, the fault zone is composed of brecciated bedrock and clay gouge 3 m wide and exhibiting about 4.6 m of offset. To the southeast the fault zone narrows to 0.5 m or less, dips nearly vertical, and the offset dies out.

Two faults were reported by Myers and Price et al. (1979), in the core from Borehole DB-10 (699-51-36A) drilled on the buried south flank of the Umtanum Ridge--Gable Mountain structure, based on zones of breccia and gouge. The faults offset bedrock units and have a reverse sense of displacement with a vertical throw of about 49 meters.

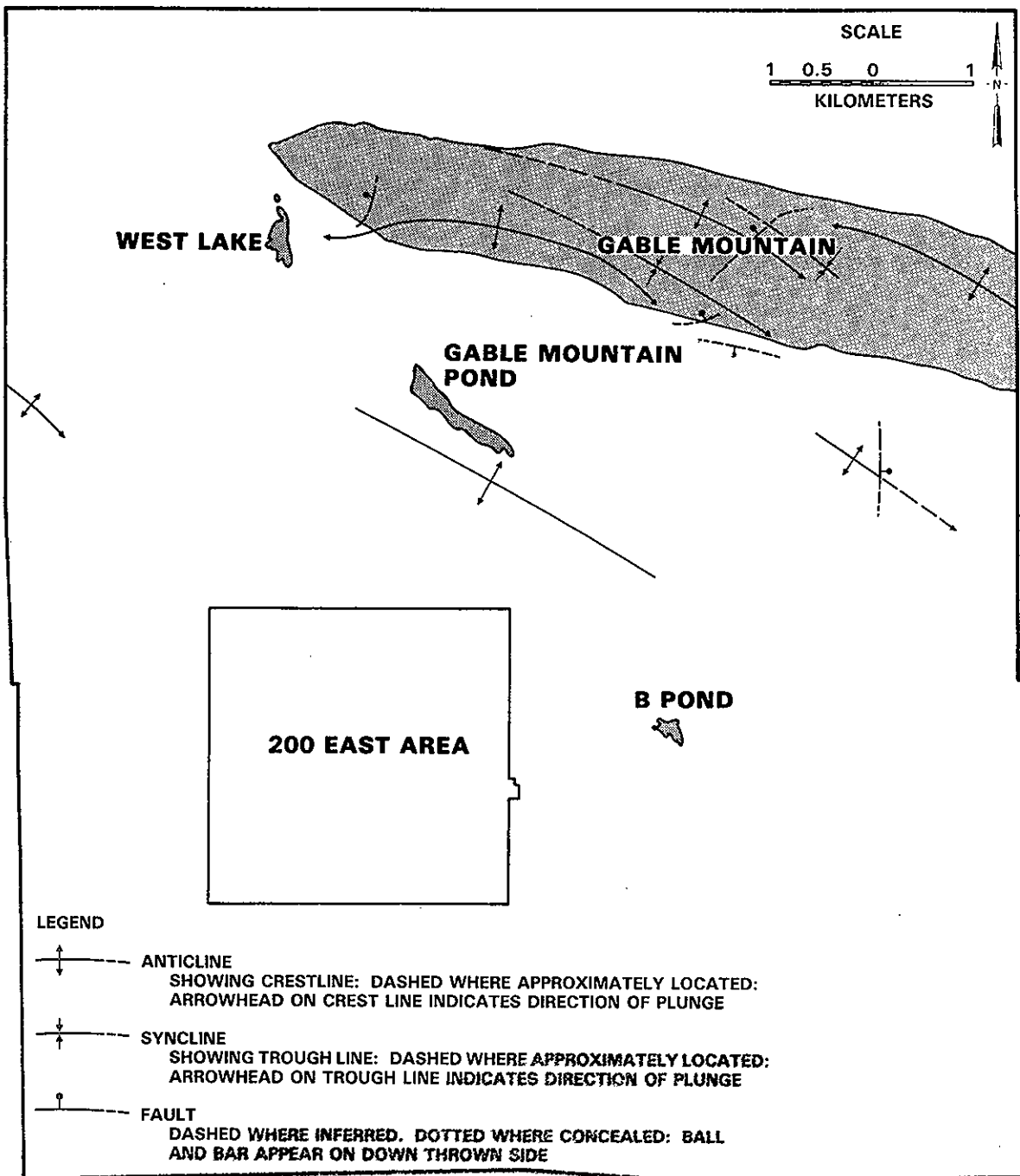


FIGURE 18. Location Map of Faults and Folds Within the Study Area

6.1.3 Geomorphology

Fluvial processes have been active in the vicinity of the study area since the diversion of the Columbia River into the central Pasco Basin after about 8.5 million years before present. Erosion of the structural low, known as Gable Gap, between Gable Butte and Gable Mountain and south into the study occurred in two phases. First, the Columbia River eroded a channel at Gable Gap as the Columbia River maintained its base level during uplift of the Umtanum Ridge--Gable Mountain structure. Secondly, multiple periods of Pleistocene preglacial catastrophic flooding of the Pasco Basin resulted in scouring of the land surface on and around Gable Butte and Gable Mountain and deeper erosion in the Gable Gap area. Figures 15, 16, 17 and Appendix K illustrate the extent of erosion of the major geologic units in the study area.

In the Gable Gap area, the basalt flows, including the Elephant Mountain basalt, and interbedded sediments have been extensively eroded. Two other erosional "windows" have been identified through the Elephant Mountain basalt (Figures 15 and 16). The northernmost "window" occurs at Well 699-53-55A where the Elephant Mountain basalt is conspicuously absent and the Rattlesnake Ridge interbed is abnormally thin. The southernmost "window" is only postulated to exist based on abnormally thin Elephant Mountain basalt in this area and hydrologic data collected during this study. This is consistent with the erosional channel identified in the basalt surface aligning with the northern "window" and the extensively eroded Gable Gap area. Erosion of the basalt in this area may have either completely removed or significantly thinned the confining bed. Erosional thinning of the basalt may have drastically increased the hydrologic effects of the vertical jointing by reducing the pathway lengths. This area may have been even further affected by the secondary permeability induced by the area's location on or near the central axis of the second-order anticlinal fold.

6.2 GROUND-WATER FLOW

This discussion covers the recharge, discharge, and movement of ground waters within the unconfined aquifer and the Rattlesnake Ridge aquifer. The section on aquifer intercommunication includes an analysis of barometric

efficiencies in relation to erosional areas of the confining bed and a comparison of hydraulic heads in both aquifers.

6.2.1 Unconfined Aquifer

The unconfined aquifer is contained within the Hanford and Ringold sediments. The depth to the water table ranges from a few meters in the northern portion of the study area to over 100 meters in the southern portion, where the maximum aquifer thickness (~230 meters) also occurs. The unconfined aquifer thins to zero thickness at basalt outcrops. Recharge to the unconfined aquifer occurs artificially from the liquid wastes discharged to the ground and naturally from precipitation and runoff on the higher elevations to the west of the Hanford Site. The primary sources of artificial recharge within the study area are Gable Mountain Pond and B Pond, which received a combined total of approximately 1×10^{10} liters of water in 1982. Measurements of the vertical head distribution near B Pond indicate a downward potential induced by the artificial recharge of approximately 4 m of water over the 26-m thickness of the aquifer (Table 9). A downward potential near Gable Mountain Pond is also anticipated.

A water table map of the study area was constructed from water-level measurements in wells open to the top few meters of the aquifer (Figure 19). Ranges of values have been contoured to account for water-level fluctuations over the year. Although the head values at the bottom of the aquifer would be more appropriate for this study, limited data prevented an analysis of the

TABLE 9. Vertical Distribution of Heads in the Unconfined Aquifer from Wells 699-42-40A, B, and C near B Pond

<u>Well Number</u>	<u>Well Completion, m below water table</u>	<u>Head Value, m above mean sea level</u>
699-42-40A	6.9 to 18.4	129.83 ^(a)
699-42-40B	3.8 to 9.9	130.77 ^(a)
699-42-40C	25.9 to 31.4	126.46 ^(b)

(a) Taken in June 1983.

(b) Taken in April 1982.

distribution of these values. The water table map is a conservative estimate of heads at the bottom of the aquifer as the actual head values at the bottom of the aquifer will be less than at the surface of the aquifer.

The influence of the artificial recharge from the liquid waste disposal ponds on the unconfined aquifer is evident in Figure 19. The movement of ground water under B Pond is radially outward and combines with flow under Gable Mountain Pond. Basalt outcrops and subcrops above the water table are barriers to ground-water flow. West Lake is a naturally occurring feature and is, therefore, an expression of the water table. The discharge from the area is principally to the north past Gable Mountain and to the southeast and east. Ground waters from the study area eventually discharge to the Columbia River.

A hydrograph of Well 699-45-42, which is located near the center of the study area, shows the response of the water table to changes in waste disposal practices (Figure 20). The water table dropped in 1952 when liquid-waste disposal to the 200-North area facilities (located northwest of 200-East Area) was terminated. The water-table elevation increased approximately 6 meters when Gable Mountain Pond began to be used for disposal in 1957. The highest elevation occurred in the late 1960's and early 1970's when the water table was almost one meter higher than present.

6.2.2 Rattlesnake Ridge Aquifer

A potentiometric surface map of the Rattlesnake Ridge aquifer was constructed from water-level measurements in the 13 wells penetrating the aquifer (Figure 21). Again, ranges of values were contoured to account for fluctuations over the one-year period of measurement.

6.2.2.1 Recharge

In order to evaluate ground-water flow into the study area, a regional potentiometric surface map of the Rattlesnake Ridge aquifer was prepared from data collected during this investigation and other published reports (Figure 22). Recharge to the Rattlesnake Ridge aquifer appears to occur along the higher elevations surrounding the basin to the west, north, and northeast.

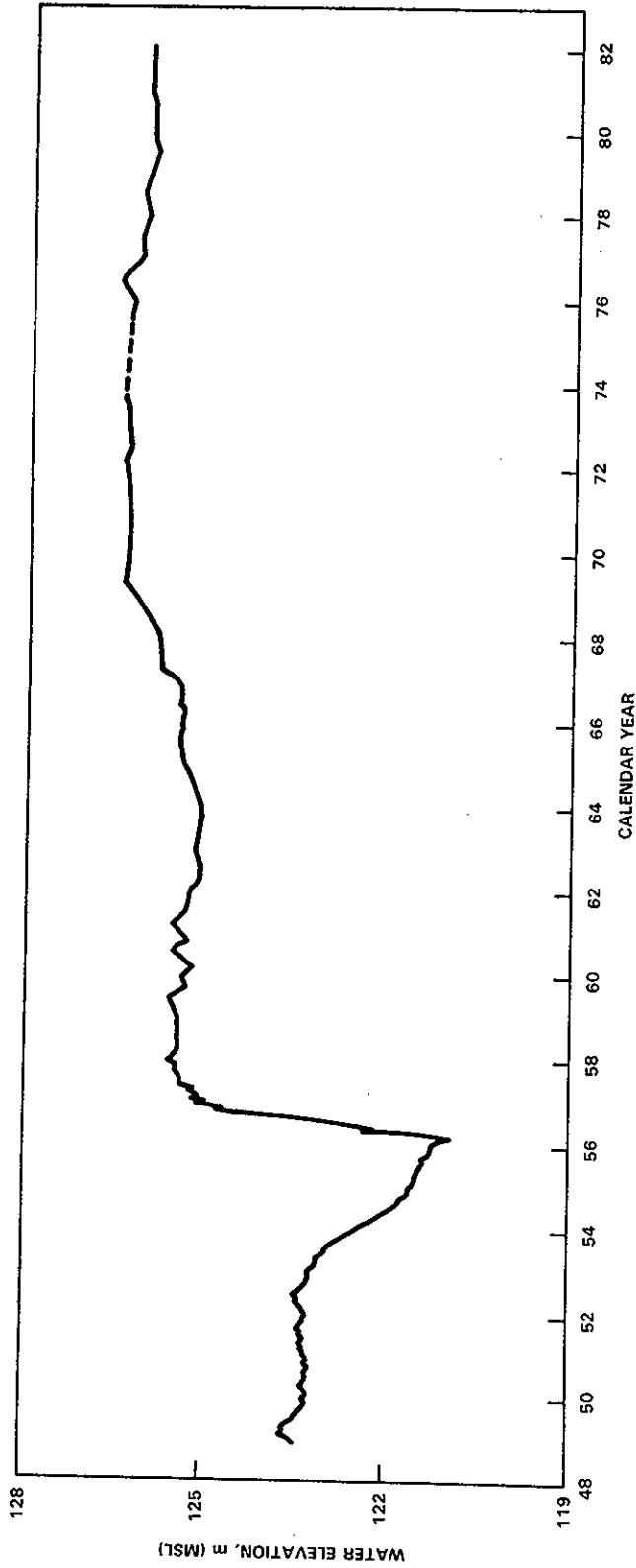


FIGURE 20. Hydrograph of Well 699-45-42

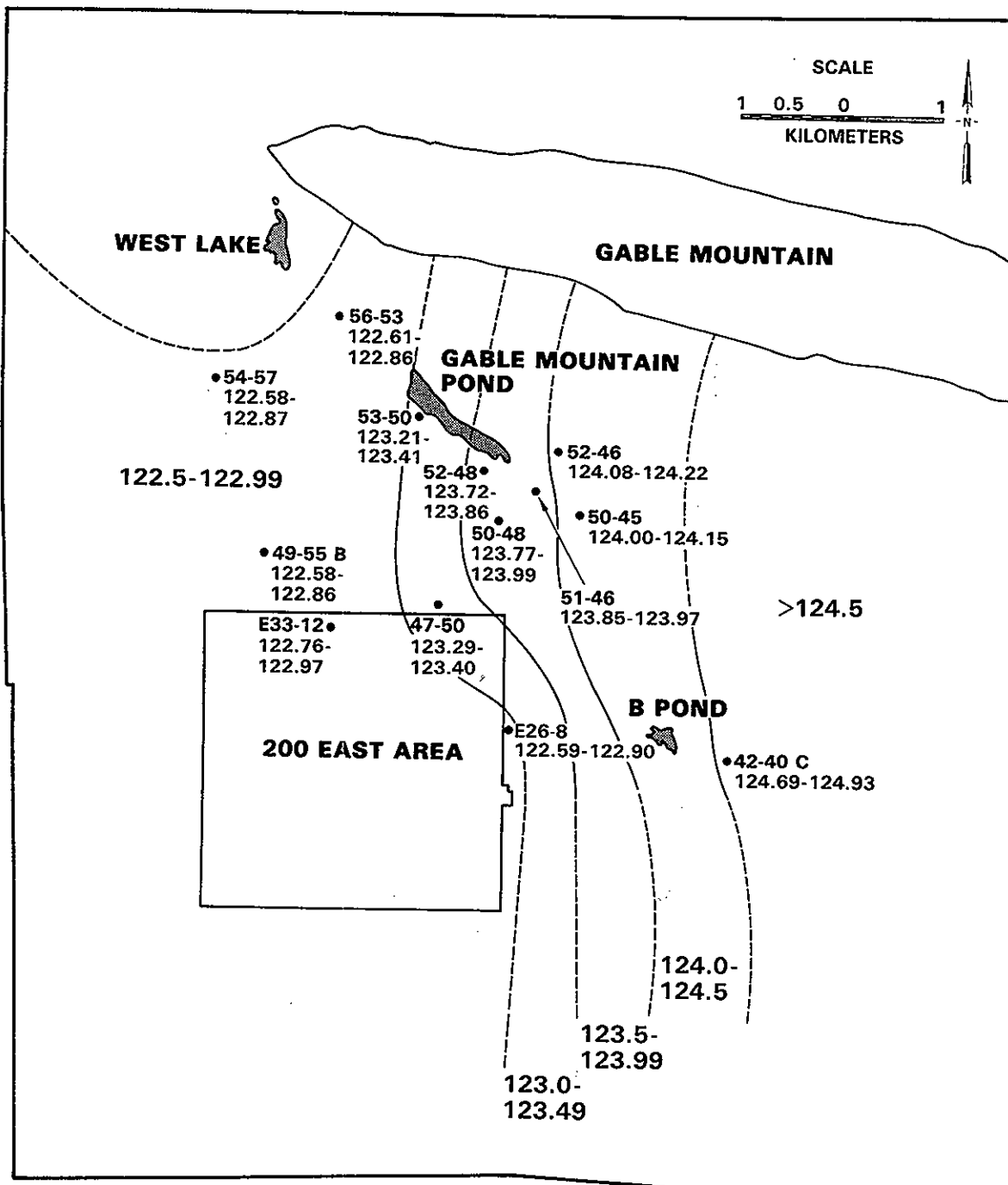


FIGURE 21. Potentiometric Surface Map in Meters Above Sea Level of the Rattlesnake Ridge Aquifer Within the Study Area

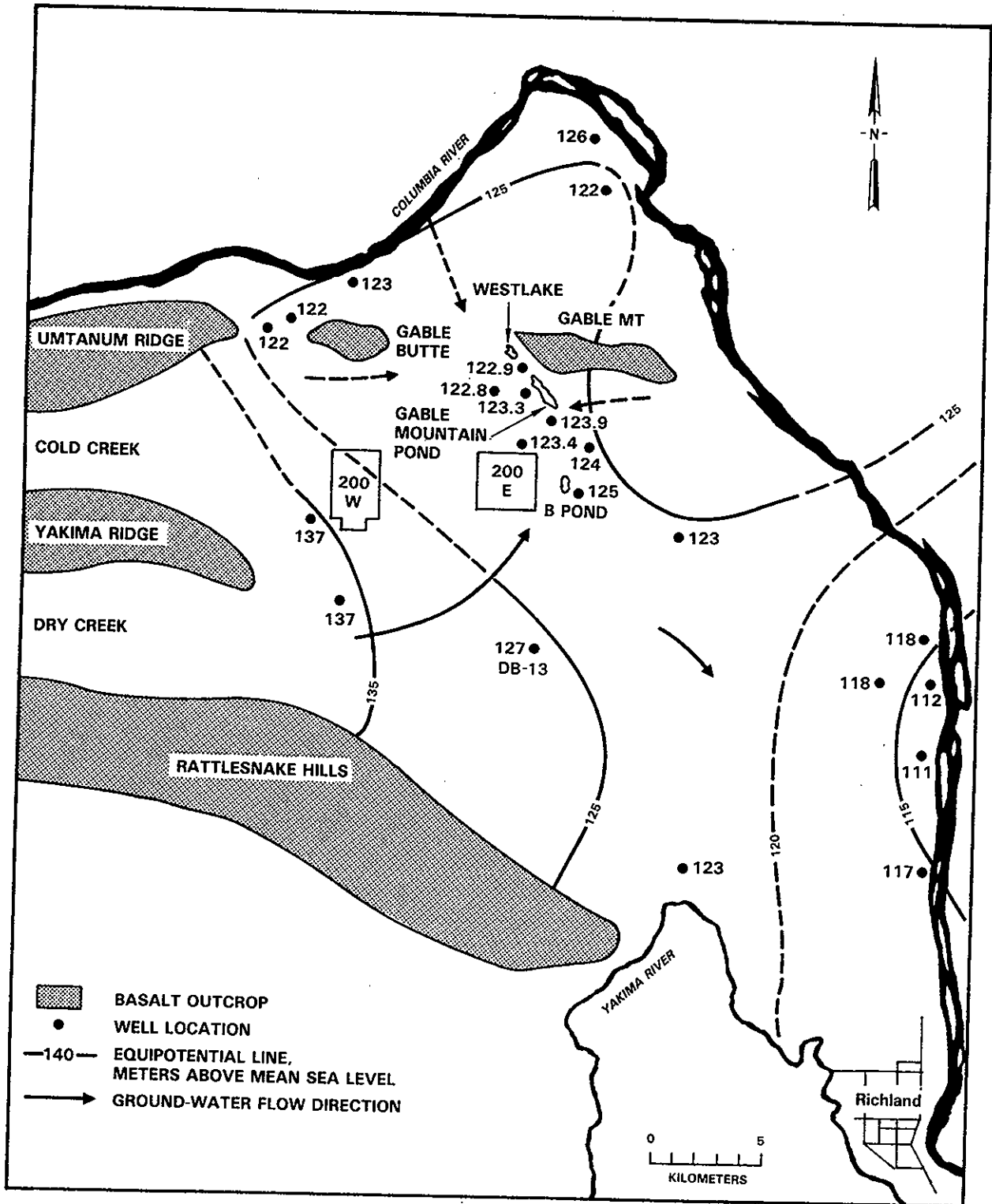


FIGURE 22. Potentiometric Surface Map of the Rattlesnake Ridge Aquifer Within the Hanford Site

6.2.2.2 Movement

Within the study area, ground-water flow is predominantly east to west-northwest. Although there is no indication in Figure 22 of flow entering the study area from the west, water-level measurements taken in May and June of 1982 showed easterly flow from Wells 699-54-57 to 699-56-53 (Appendix D). This may be an indication of ground water entering the study area from the west during that time.

The results of the single-borehole tracer tests (Appendix J) were interpreted to better quantify the movement of ground water within the Rattlesnake Ridge aquifer. The vertical distribution of ground-water velocities is a function of the local lithology of the aquifer. For example, in Well 699-42-40C, ground-water flow occurs predominantly in the top of the interbed or the flow bottom of the Elephant Mountain basalt (Appendix J). In Well 699-49-55B, however, a zone of high ground-water velocity is associated with the bottom of the interbed or the flow top of the Pomona basalt.

Two ground-water flow regimes were identified within the study area: a zone of low flow (maximum velocity <0.5 m/day) and a zone of high flow (maximum velocity >1.0 m/day) (Figure 23). The low ground-water flow regime is associated with low transmissivities and/or low hydraulic gradients. The high ground-water velocities in the vicinity of Wells 699-42-40C and 299-E26-8 are the result of the steeper hydraulic gradients (approximately 10^{-3} m/m) in this area.

The observed ground-water velocities in Wells 299-E33-12 and 699-49-55B cannot be explained in terms of flow inferred from the potentiometric surface map. These two wells are situated along a flow path from the low ground-water flow regime in an area of flat hydraulic gradients (approximately 4×10^{-4} m/m). These velocities indicate that ground water may be moving into this area from the south or southeast (Figure 23).

The observed high ground-water velocity in Well 699-56-53 is also an anomaly. This well is downgradient from, and surrounded by, the low ground-water flow regime in an area of flat hydraulic gradients (approximately 5×10^{-4} m/m). A possible source for this ground-water flow observed in Well

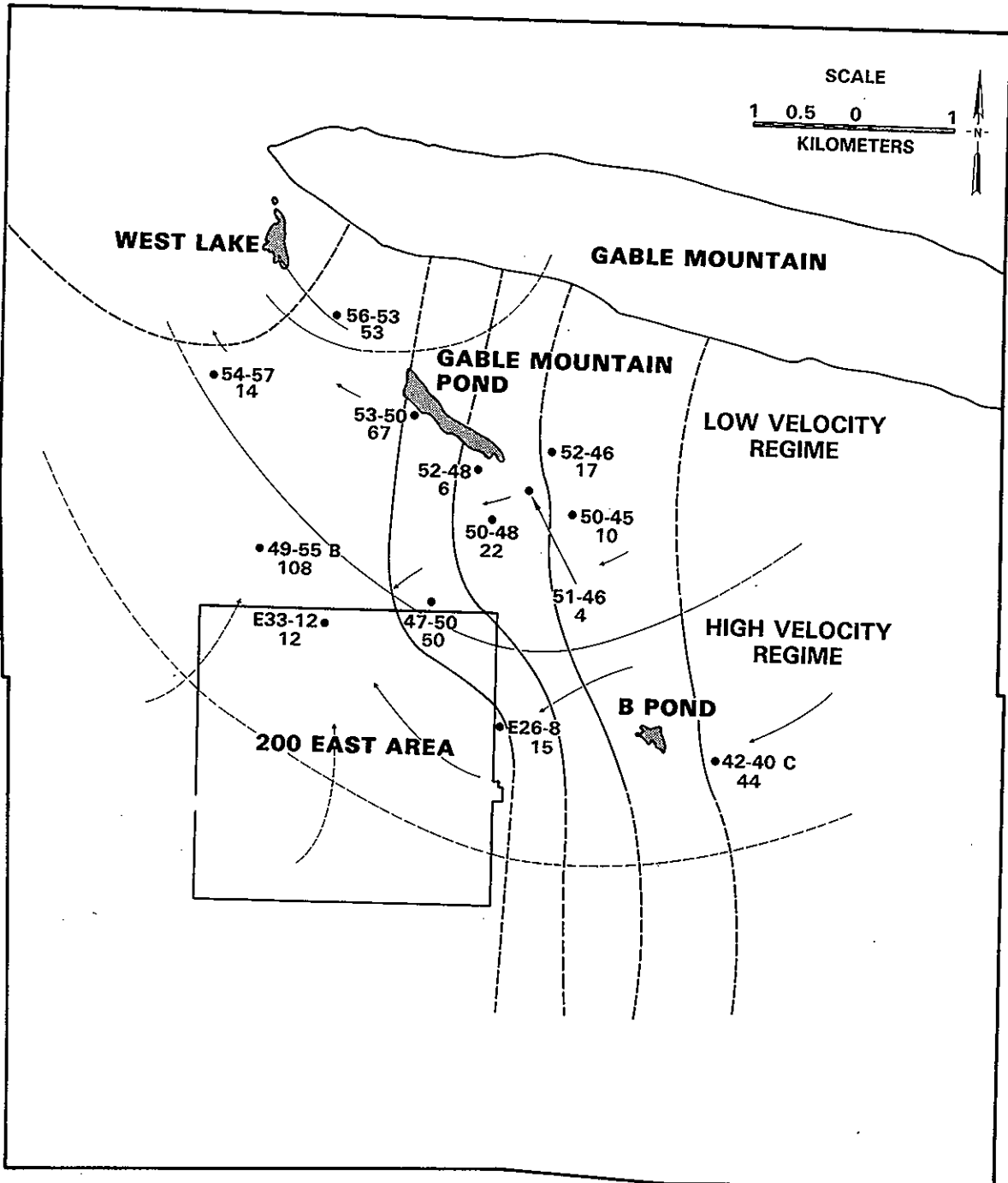


FIGURE 23. Ground-Water Flow Regimes and Relative Velocity Vectors in the Rattlesnake Ridge Aquifer Within the Study Area. (Transmissivities (m^2/day) given for comparison)

699-56-53 is leakage from underlying aquifers. Although there are insufficient head data to support this hypothesis, the area is structurally complex and the gradient is upward from the Rattlesnake Ridge aquifer to the unconfined aquifer. Ground water may be moving up from a deeper aquifer along joints or fractures associated with the Gable Mountain anticline.

6.2.2.3 Discharge

The Elephant Mountain basalt and Rattlesnake Ridge interbed have been eroded in the vicinity of West Lake (Fecht 1978). There is direct evidence that the Rattlesnake Ridge aquifer is discharging to the unconfined aquifer in this area. Well 699-59-55, located adjacent to West Lake (Figure 19), is completed 35 m below the water table. A water-level elevation measurement in this well (122.95 m above mean sea level) taken in June 1983, compared to the elevation of West Lake (122.63 m above mean sea level) indicates an upward potential of approximately 0.4 m. This upward movement of water within the aquifer is the result of the Rattlesnake Ridge aquifer (and possibly deeper confined aquifers) discharging to the unconfined aquifer. The confined waters discharged to the unconfined aquifer move within the unconfined aquifer and eventually discharge to the Columbia River.

6.2.3 Elephant Mountain Aquifer

The interflow zone between upper and lower units of the Elephant Mountain basalt is referred to as the Elephant Mountain aquifer. The Elephant Mountain aquifer was hydrologically tested in two wells in the study area, 299-E16-1 and 699-42-40C; and in one well south of the study area, DB-13 (Figure 22; Gephart et al. 1979). The flow system of the Elephant Mountain aquifer is thought to parallel that of the Rattlesnake Ridge aquifer, as the hydraulic head values of the two aquifers are approximately equal. A hydraulic head value, taken on 4/15/82 in Well 699-42-40C, for the Elephant Mountain aquifer of 124.69 meters above sea level falls within the range of values for the Rattlesnake Ridge aquifer in that well (Appendix E). Also, the hydraulic head values reported for the two aquifers in Well DB-13 are the same (Gephart et al. 1979). The Elephant Mountain aquifer is in contact with the unconfined aquifer in the vicinity of B-Pond, where the upper unit of the Elephant Mountain basalt is

absent. The Elephant Mountain aquifer probably discharges to the unconfined aquifer, although it may be influenced locally by the ground-water mound under B-Pond.

A fracture zone within the upper unit of the Elephant Mountain basalt is another confined aquifer between the unconfined and Rattlesnake Ridge aquifers. This aquifer was hydrologically tested in Well 299-E16-1. This fracture zone was not encountered in any of the other wells drilled for this investigation. Therefore the flow characteristics of this fracture zone aquifer cannot be determined.

6.3 AQUIFER INTERCOMMUNICATION

The areas of erosion of the Elephant Mountain basalt estimated from geologic evidence and the barometric efficiencies for the Rattlesnake Ridge aquifer wells are plotted for comparison in Figure 24. In unconfined aquifers, the changes in barometric pressure are evenly distributed over the entire water table. Thus, water levels in unconfined aquifer wells do not respond to changes in barometric pressure. Correspondingly, a confined aquifer underlying an unconfined aquifer in regions where the confining bed is absent will exhibit low barometric efficiencies. Wells located near known or suspected areas of erosion (Wells 699-47-50, 699-54-57, and 699-56-53) exhibit relatively low barometric efficiencies (13.3 to 25.4 percent). Wells 299-E26-8 and 699-51-46, with barometric efficiencies of 24.5 and 28.5 percent, respectively, are also low barometric efficiency wells. These relatively low barometric efficiencies may be an indication of erosion of the Elephant Mountain basalt in the vicinity of Wells 299-E26-8 and 699-51-46.

A comparison is made of the present water table with the potentiometric surface of the Rattlesnake Ridge aquifer to indicate areas of downward gradient (Figure 25). The areal extent of downward gradient between the aquifers was overestimated because, again, the head values at the bottom of the unconfined aquifer should be less than the water table within the study area. The hydrograph of the unconfined aquifer well (Figure 20) indicates that the water table in the late 1960s and early 1970s was somewhat higher than present day conditions. However, a lack of historical water-level data from the Rattlesnake

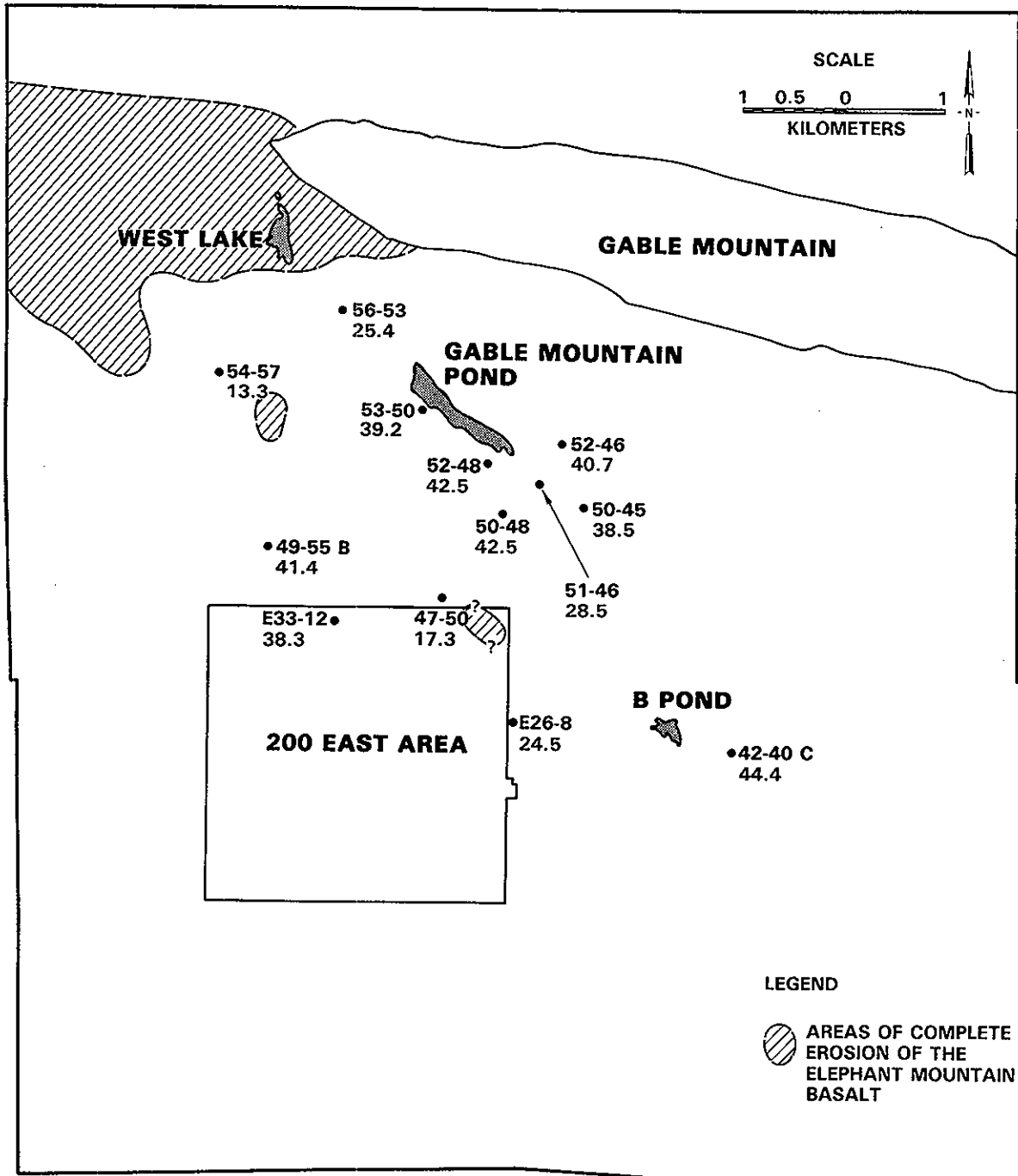


FIGURE 24. Comparison of Areas of Erosion of the Elephant Mountain Basalt and the Barometric Efficiencies of the Test Wells

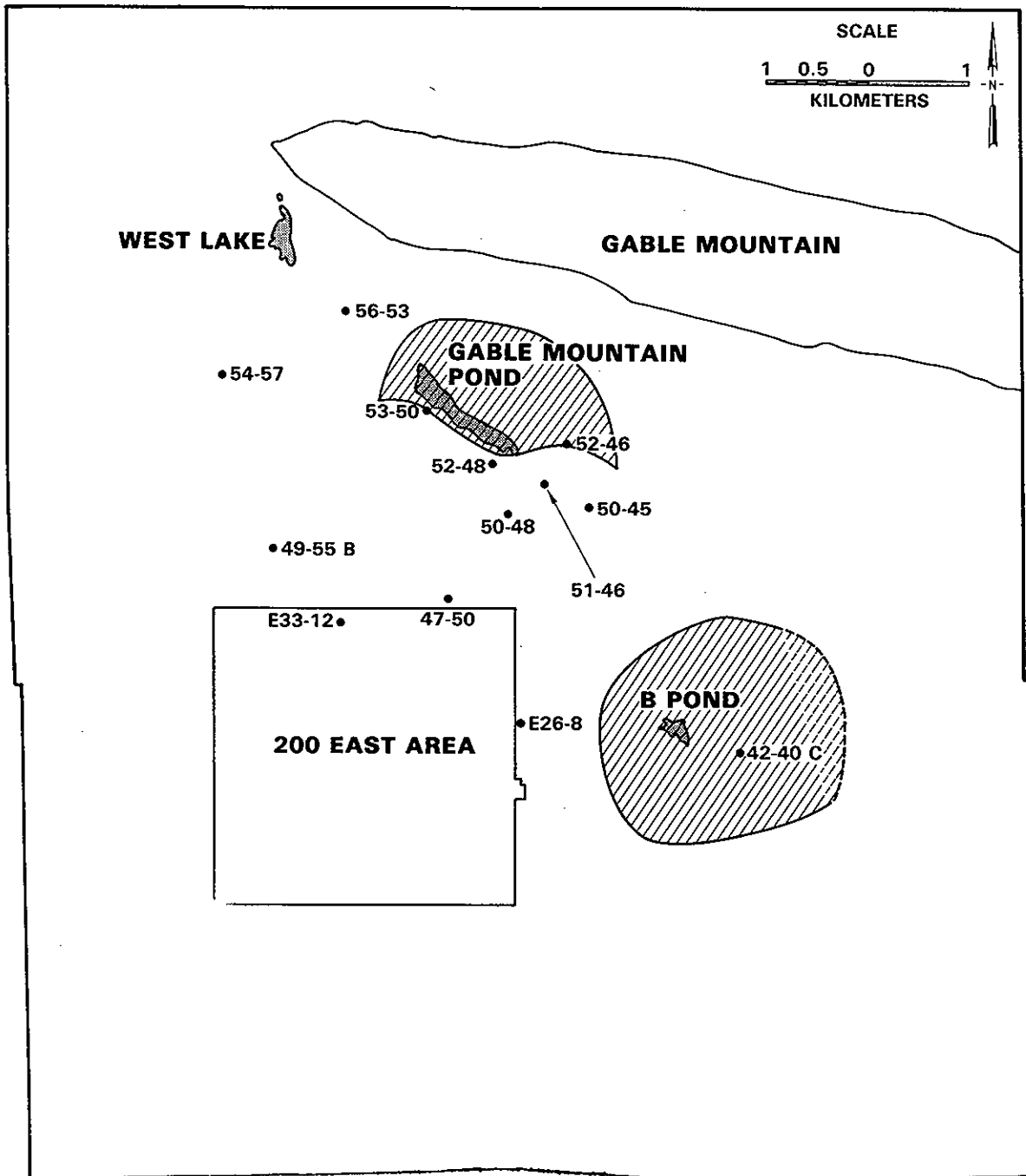


FIGURE 25. Areas of Present-Day Downward Gradient from the Unconfined Aquifer to the Rattlesnake Ridge Aquifer Within the Study Area

Ridge aquifer precludes a comparison between the aquifers during this time. If steady-state conditions within the Rattlesnake Ridge aquifer are assumed, the areas of downward gradient would have been more extensive and may have included the areas of erosion.

6.4 GROUND-WATER CHEMISTRY

Nine samples were collected from the unconfined aquifer. Samples from the bottom of the unconfined aquifer were collected in Wells 299-E26-8, 299-E33-12, 699-42-40C, and 699-49-55A. Well 699-60-57 is located in an area where the Elephant Mountain basalt has been removed by erosion. Well 699-42-40A is completed in the middle of the aquifer. The remaining unconfined aquifer samples were collected from near the surface of the aquifer. The hydrochemistry of the Rattlesnake Ridge aquifer was evaluated to infer ground-water flow and aquifer intercommunication.

6.4.1 Major Cations and Anions and Trace Metals

Stiff diagrams were constructed to indicate the EPM of the major cations and anions in the unconfined aquifer water samples (Figure 26). A stiff diagram for Columbia River water is given for comparison. The prevalent cation is calcium; however, in samples from Wells 299-E33-12, 699-42-40A and C, and 699-60-57, the combination of sodium and potassium exceeded the calcium EPM. Sodium hydroxide is used extensively in the chemical processes at Hanford and is present in the liquid effluents discharged to the ground; therefore, the sodium concentrations observed in Wells 299-E33-12 and 699-42-40A and B may result from these effluents. The prevalent anion in the samples from the unconfined aquifer was bicarbonate, with the exception of sulfate in samples from Wells 699-49-55A and 699-37-43 (Figure 26). There was also significant (>1.0 meq/L) sulfate in the sample from Well 299-E33-12. This sulfate may originate from sulfuric acid in the waste stream or the dissolution of gypsum in the sediments. The chemistry of the sample from Well 699-60-57 was another indication that the deeper aquifers are discharging to the unconfined aquifer in the West Lake area. The principal aquifer in the Saddle Mountains basalt is the Mabton interbed. The prevalent chemical character of samples from the

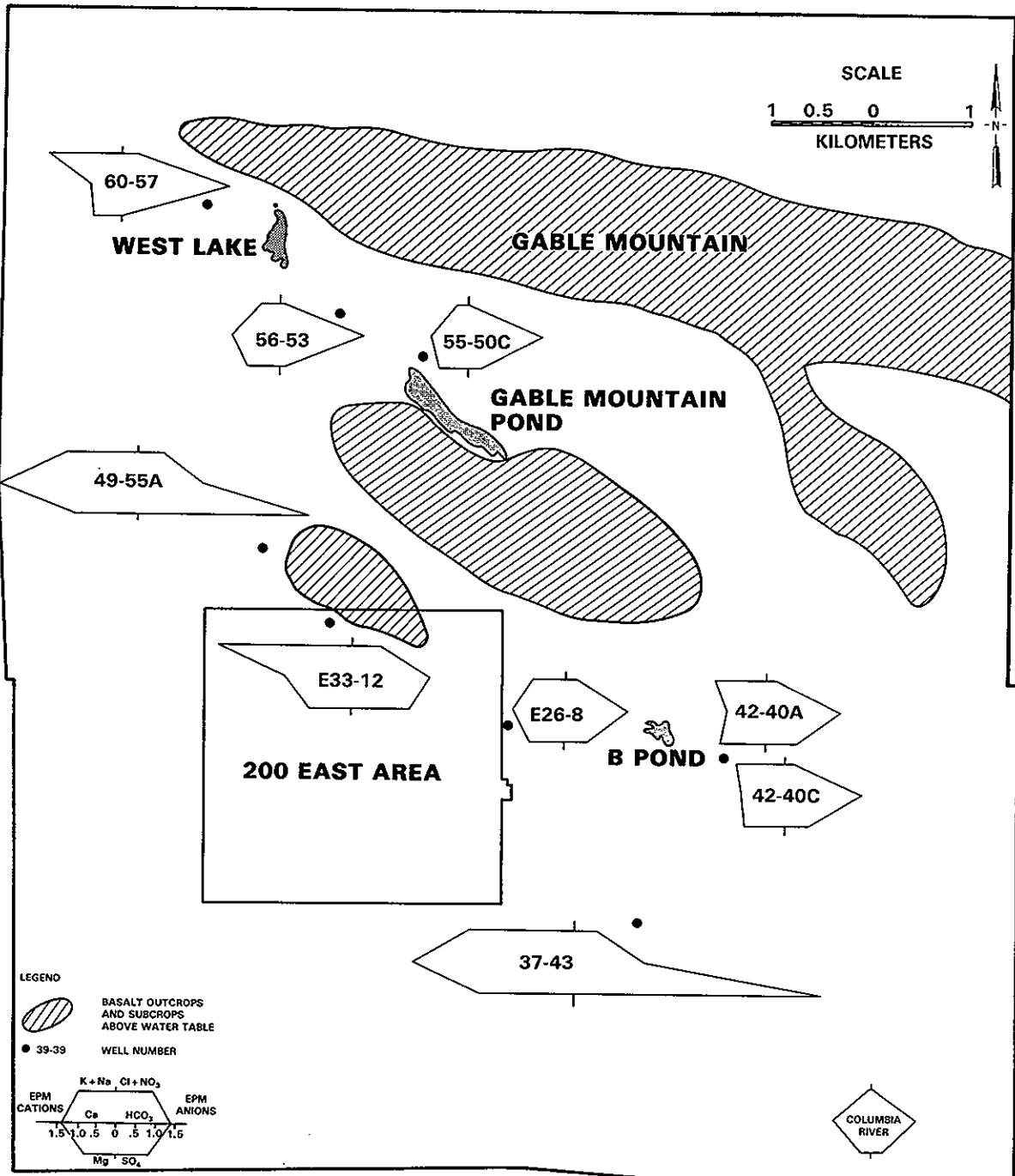


FIGURE 26. Stiff Diagrams for the Unconfined Aquifer Samples Within the Study Area

Mabton interbed is sodium bicarbonate (Gephart et al. 1979), the same as the sample from Well 699-60-57.

Stiff diagrams for the Rattlesnake Ridge samples also were constructed (Figure 27). Ground-water moving into the study area from the east is predominantly a sodium bicarbonate water (Well 699-42-40C). However, in the vicinity of Gable Mountain Pond, the prevalent chemical character of the ground water shifts from a sodium bicarbonate (in Well 699-52-48) to a calcium bicarbonate water (e.g., Well 699-52-46). This may indicate a mixing of calcium bicarbonate waters from the unconfined aquifer with the sodium bicarbonate waters in the Rattlesnake Ridge aquifer. The ground water in Well 299-E26-8 showed a similar pattern when compared with Well 699-42-40C.

The chemistry in Well 699-47-50 is an anomaly. The well is located adjacent to a suspected area of erosion in the Elephant Mountain basalt. The chemistry of the samples from this well indicated that unconfined ground water has migrated into the Rattlesnake Ridge aquifer in this area. The additional hydrochemistry data corroborated the observations made on ground-water flow in the Rattlesnake Ridge aquifer--Well 299-E33-12 indicates a mixing of waters from the east (Well 299-E26-8) and south-southwest (Well 699-49-55B). Water in Well 699-56-53 indicated a mixing of low-sodium water from the west (Well 699-54-57) with a higher sodium water, possibly from deeper aquifers.

Of the trace metals, barium and zinc were detectable consistently in the ground-water samples (Appendix I). Barium is more abundant in igneous rocks than in sedimentary rocks (Horn and Adams 1966). This may account for its presence in the ground-water samples. The likely control over the concentration of barium is the solubility of barite (BaSO_4) (Hem 1970). At sulfate molar activity near 10^{-4} (~10 mg/L) or 10^{-3} (~100 mg/L) the corresponding equilibrium molar activities of barium would be 10^{-6} (~140 $\mu\text{g/L}$) or 10^{-7} (~14 $\mu\text{g/L}$), respectively. Barium ranged from 14.7 $\mu\text{g/L}$ to 58.7 $\mu\text{g/L}$ in the unconfined aquifer. The barium concentrations were generally higher in the Rattlesnake Ridge aquifer than in the unconfined aquifer. This is attributed to the lower concentrations of sulfate in the Rattlesnake Ridge aquifer. However, in samples from wells located south of Gable Mountain Pond to 200 East Area, the concentrations were less than 90 $\mu\text{g/L}$ (Figure 28). This may indicate

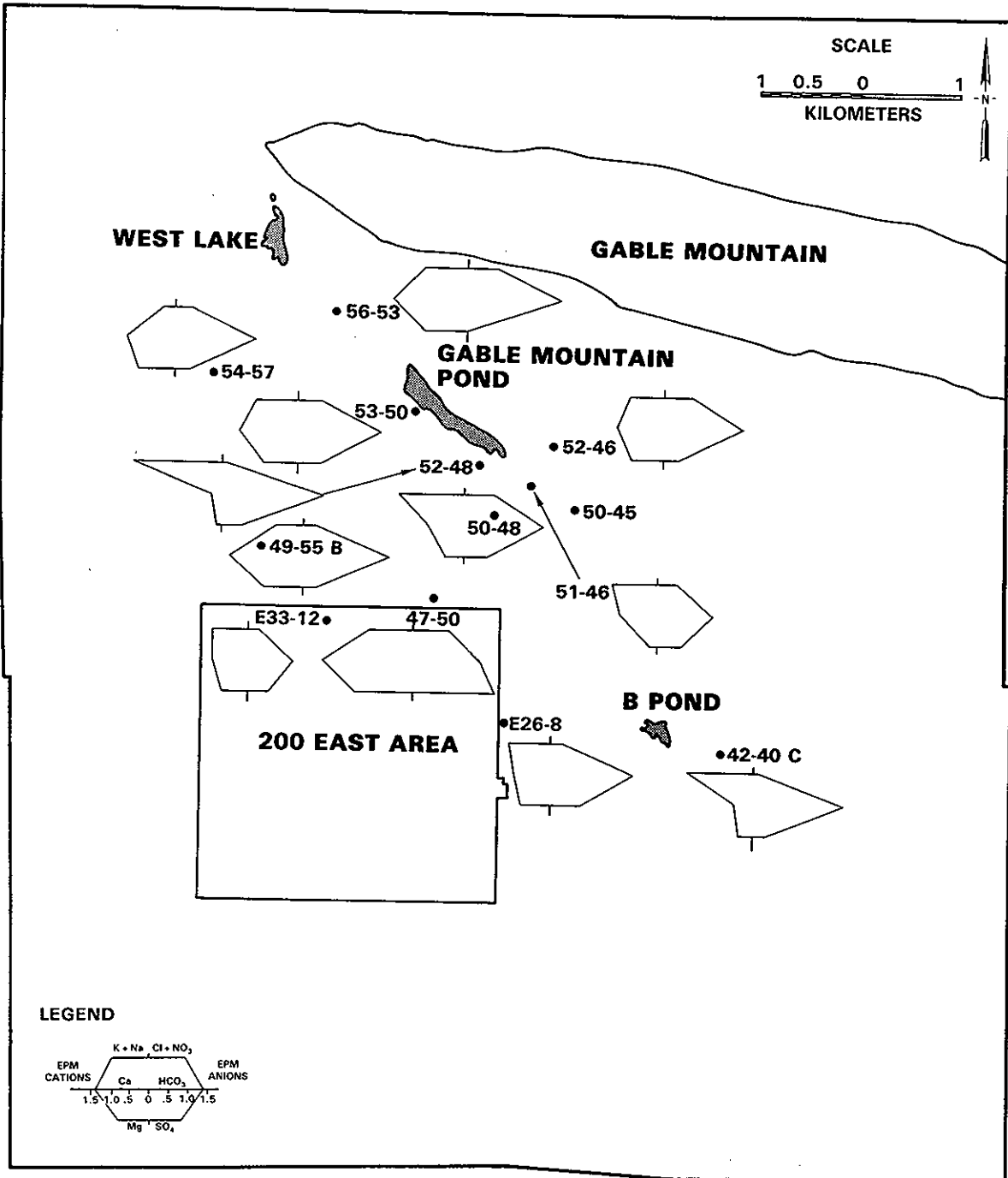


FIGURE 27. Stiff Diagrams for the Rattlesnake Ridge Aquifer Samples Within the Study Area

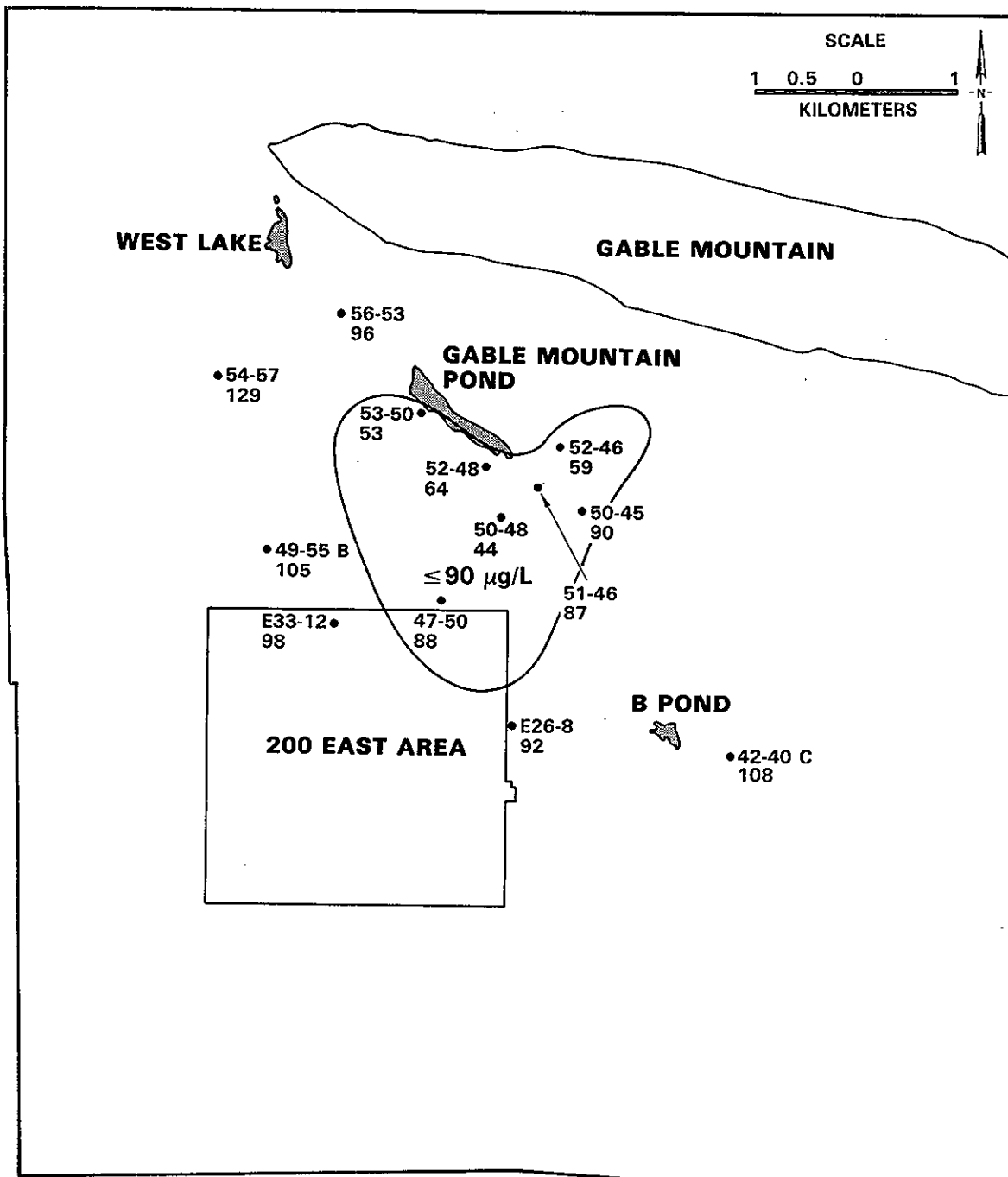


FIGURE 28. Distribution and Concentrations of Barium, $\mu\text{g/L}$, in the Rattlesnake Ridge Aquifer Within the Study Area

the migration of water from the unconfined aquifer into the Rattlesnake Ridge aquifer. Zinc concentrations in the unconfined aquifer range from 84 g/L to 180 g/L. The concentrations of zinc in the Rattlesnake Ridge aquifer are similar to those observed in the unconfined aquifer. These concentrations of zinc may represent background levels present in the area, although some zinc may result from the chemical processes.

6.4.2 Stable Isotopes

The deuterium-oxygen-18 values and the sulfate concentrations-sulfur-34 values for the unconfined aquifer and Rattlesnake Ridge aquifer samples are compared to determine areas where aquifer intercommunication has occurred.

6.4.2.1 Deuterium and Oxygen-18

There is very little scatter in the deuterium and oxygen-18 values of the samples from the unconfined aquifer (Appendix G). The range of deuterium values is -139 to -144, with a mean value of -141. The range of oxygen-18 values is -16.5 to -17.2, with a mean value of -16.9. These values are similar to those reported for B Pond and Gable Mountain Pond of -124 to -130 for deuterium and -16.1 to 17.2 for oxygen-18 (Strait and Moore 1982).

This small range of deuterium and oxygen-18 values indicates that extensive mixing has taken place in the unconfined aquifer. Approximately 4×10^{11} liters of liquid wastes have been discharged to the ground in the study area through 1982. Artificial recharge to the unconfined aquifer as a result of these discharges is at least an order of magnitude greater than the natural recharge to the area (Graham et al. 1981). This dominance of artificial recharge probably is responsible for the thorough mixing of waters within the unconfined aquifer.

The deuterium and oxygen-18 values for the Rattlesnake Ridge and unconfined aquifers are plotted (Figure 29) in order to infer flow within the Rattlesnake Ridge and aquifer intercommunication. Inflow to the study area from the east is represented by samples from Well 699-42-40C, which are depleted in deuterium and oxygen-18 with respect to the other samples. There is evidence of ground-water recharge to the study area from the west in Wells 699-54-57 and 699-49-55B. Samples from these wells are somewhat more enriched

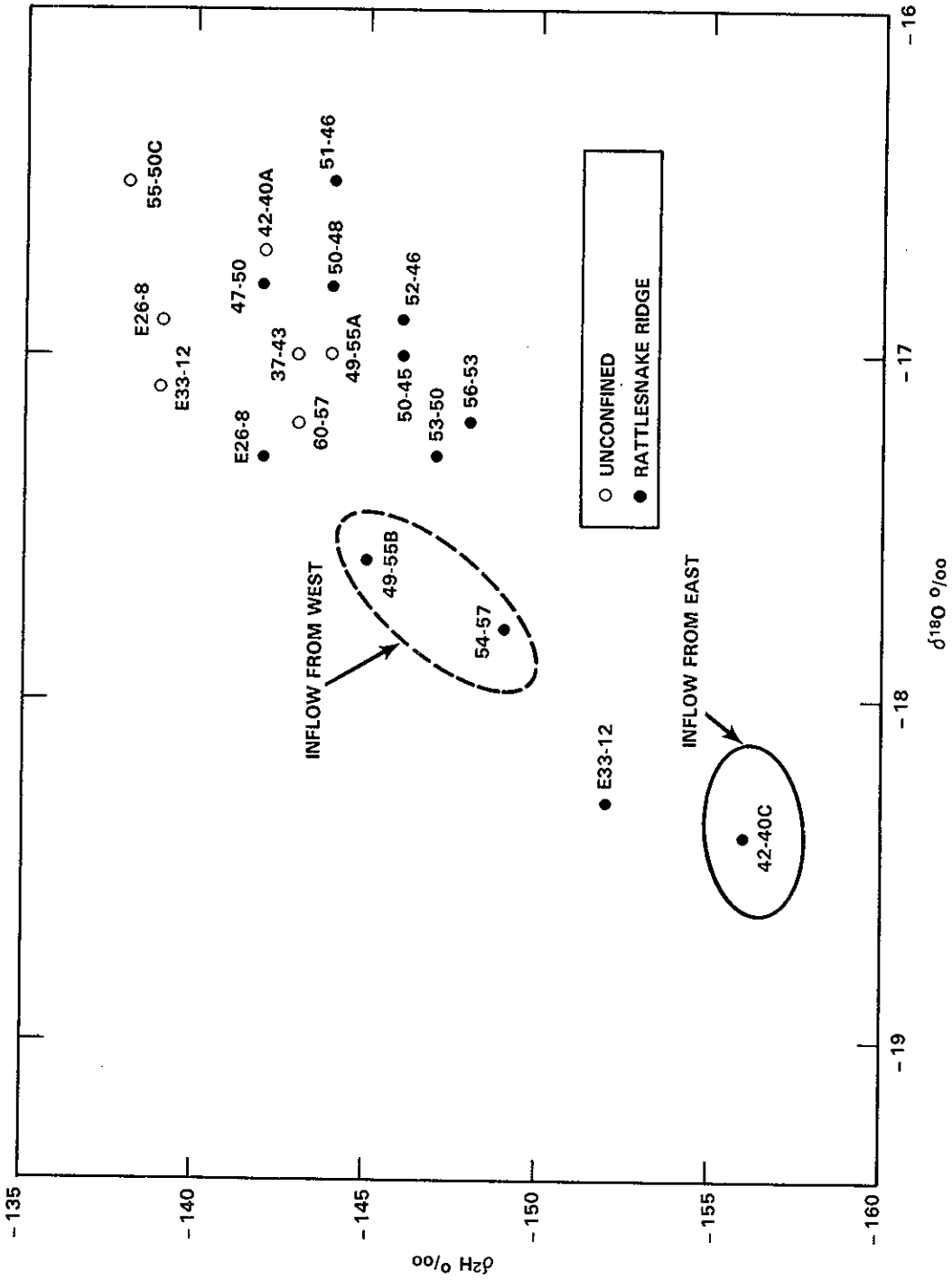


FIGURE 29. Inflow of Ground Water to the Study Area Within the Rattlesnake Ridge Aquifer and Aquifer Intercommunication Inferred from the δ^2H and $\delta^{18}O$ Values

in deuterium and oxygen than the recharge from the east. The deuterium and oxygen-18 values in Well 299-E33-12 plot between the east and west values indicating a mixing of these waters.

The aquifer intercommunication, inferred from the cation and anion data, to the south and east of Gable Mountain Pond and in the vicinity of Well 699-47-50 is also evident from the deuterium and oxygen-18 relationships. This zone where aquifer intercommunication has occurred can be defined by the deuterium values exceeding -145 0/00 (Figure 30). The plots of deuterium and oxygen-18 values for Wells 699-50-45, 699-52-46, 699-52-48, 699-53-50, and 69-56-53 lie between the range of values for the unconfined aquifer and the values for the Rattlesnake Ridge waters from the east. This may be an indication of a lesser amount of aquifer intercommunication in this area. However, the waters in the vicinity of Well 699-56-53 also may be influenced by flow from the west and upward leakage from deeper aquifers.

6.4.2.2 Sulfur-34

As stated earlier, there is a wide range of sulfur-34 values, -9.1 to 7.4, in the samples from the unconfined aquifer, which probably indicates that there are several sources of sulfate in the ground water. However, sulfate in water near the bottom of the aquifer may result predominantly from one source (i.e., oxidation of pyrite in the basalt). Samples collected from near the bottom of the unconfined aquifer and the corresponding sulfur-34 values are: Well 299-E26-8, 2.2; Well 299-E33-12, 3.4; Well 699-42-40A, 3.0; and Well 699-49-55A, -1.5. These samples do exhibit a much smaller range of sulfur-34 values and are more representative of the waters that would migrate to the Rattlesnake Ridge aquifer.

The sulfate concentrations and the sulfate-34 values for these unconfined aquifer samples and the Rattlesnake Ridge aquifer samples are plotted in Figure 31. The same general patterns hold as those observed in the deuterium and oxygen-18 values. The Rattlesnake Ridge waters flowing into the study area from the east and west contain similar concentrations of sulfate and sulfur-34. The samples from Well 299-E33-12 contain higher concentrations of sulfate than the inflowing waters. This is attributed to the high salt waste that migrated into the Rattlesnake Ridge aquifer during the time the well was open to the

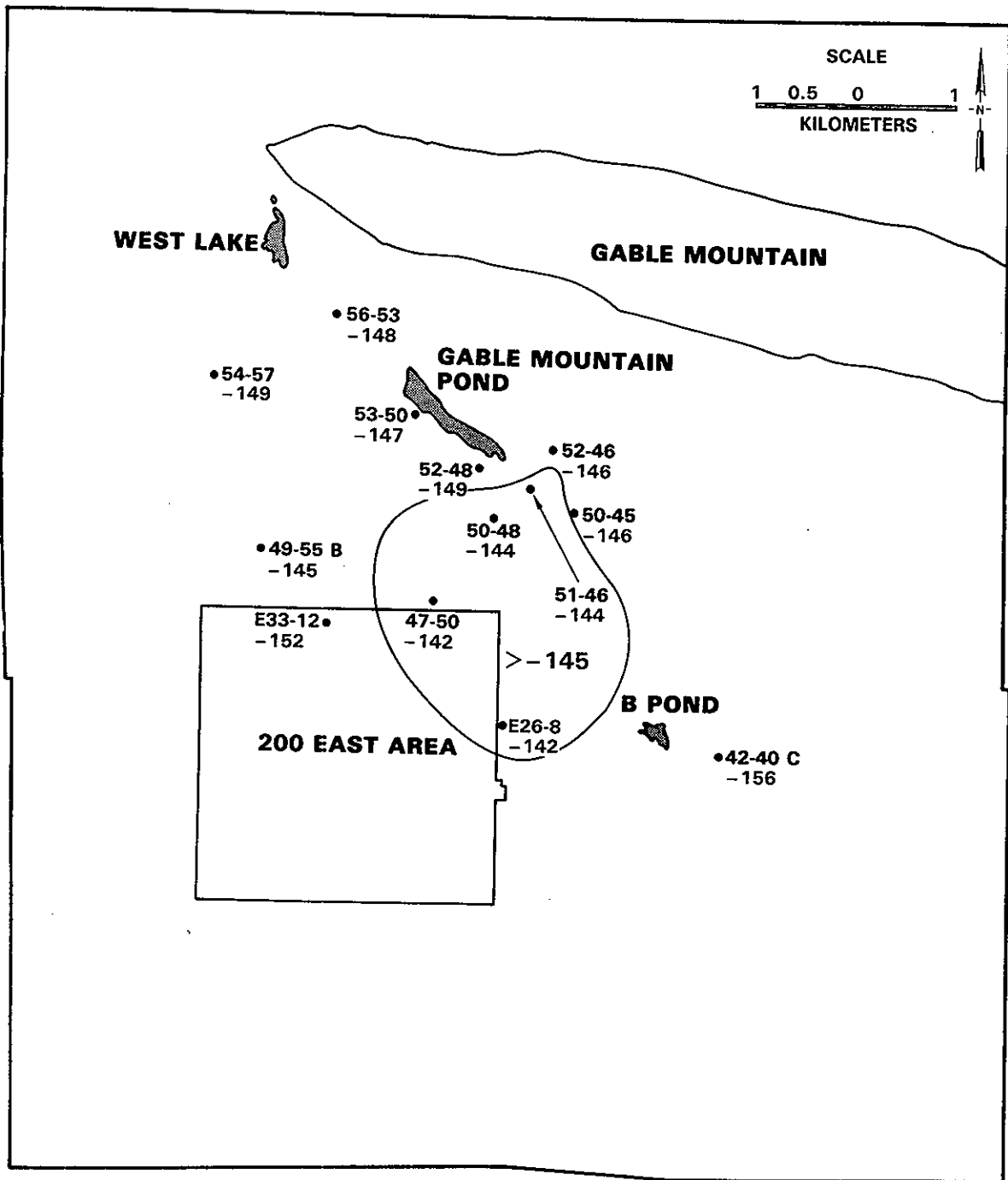


FIGURE 30. Area of Deuterium Values Less Than -145, Indicating Aquifer Intercommunication Within the Study Area

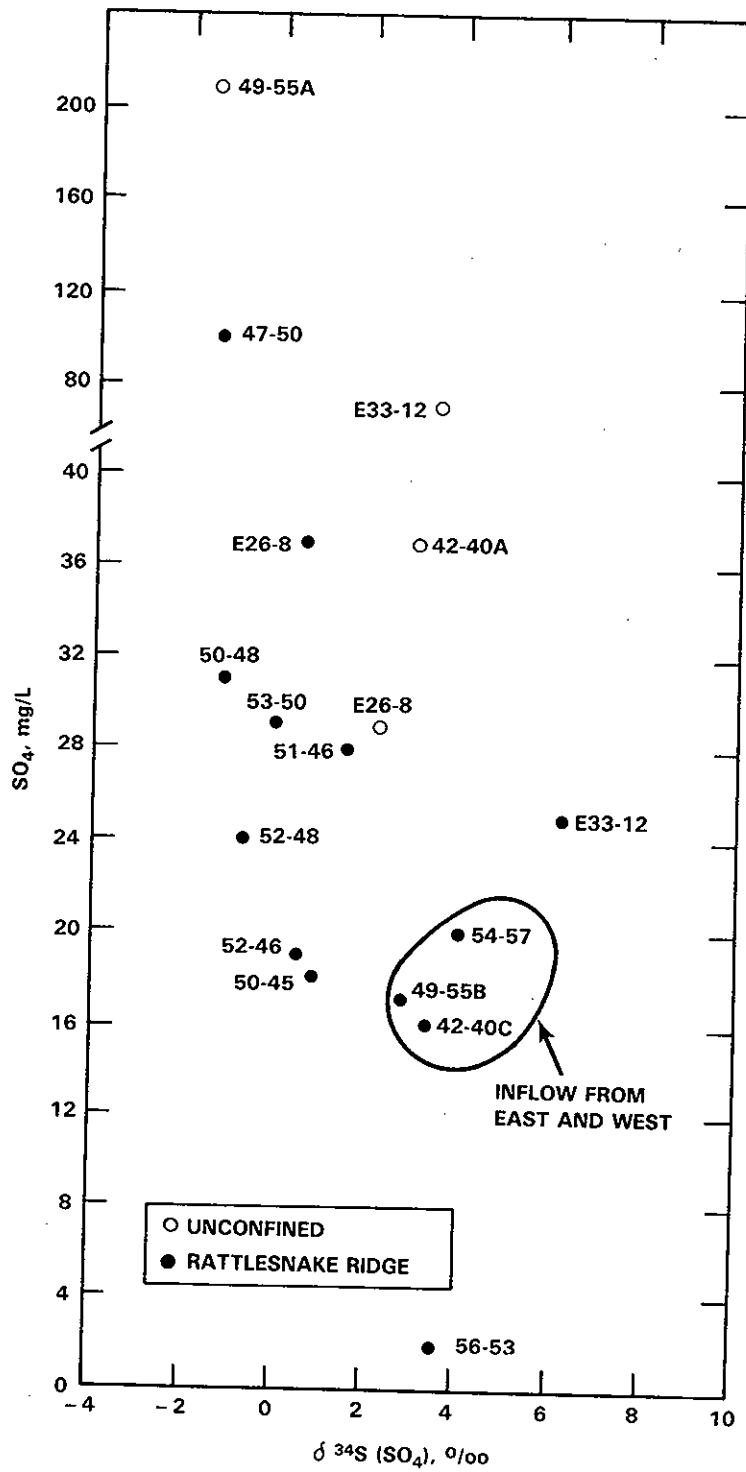


FIGURE 31. Inflow of Ground Water to the Study Area Within the Rattlesnake Ridge Aquifer and Aquifer Intercommunication Inferred from the Sulfate Concentrations and $\delta^{34}\text{S}$ Values

unconfined aquifer. The sulfate/sulfur-34 relationship in Rattlesnake Ridge aquifer samples from wells to the south and east of Gable Mountain Pond is similar to that in the lower unconfined aquifer samples. This indicates essentially the same area of aquifer intercommunication as inferred from the other hydrogeochemical data. The concentrations of sulfate and sulfur-34 in the remaining wells may be controlled by local effects.

6.4.3 Radioactive Isotopes

The various radionuclides present in the waste streams are monitored extensively in the unconfined aquifer at the Hanford Site (Wilbur et al. 1983; Eddy, et al. 1983). The most prevalent radionuclide in the unconfined aquifer is tritium, due to its concentrations in the waste streams and its nonsorbing character. The current distribution of tritium in the unconfined aquifer is controlled by the locations of past and present source terms and convection-dispersion in the aquifer. This distribution is defined from the analyses of samples collected near the surface of the aquifer, where the highest levels of contamination are expected (Figure 32). The concentrations of tritium in samples collected at depth within the aquifer again indicate that the aquifer is well mixed within the study area (Appendix I).

The concentrations of tritium in the confined aquifer test wells are given in Figure 33. Based upon hydrogeochemical evidence, the area of the most extensive aquifer intercommunication is to the south and east of Gable Mountain Pond (refer to Figure 30). The concentrations of tritium in the Rattlesnake Ridge wells located in this area range from 1.8 to 310 pCi/L. The control on these concentrations is the historical concentrations and distributions of tritium in the unconfined aquifer. Gable Mountain Pond receives cooling waters that contain very low levels of contamination. There are no subsurface disposal facilities in the area that would contribute higher levels of contamination. Consequently, contamination of the unconfined aquifer surrounding Gable Mountain Pond has been minimal. Also the basalt outcrop above the water table adjacent to the pond acts as a barrier to ground-water flow and contamination transport to the south.

Historically, the highest levels of contamination in the unconfined aquifer have occurred around 200-East Area disposal facilities. This would account

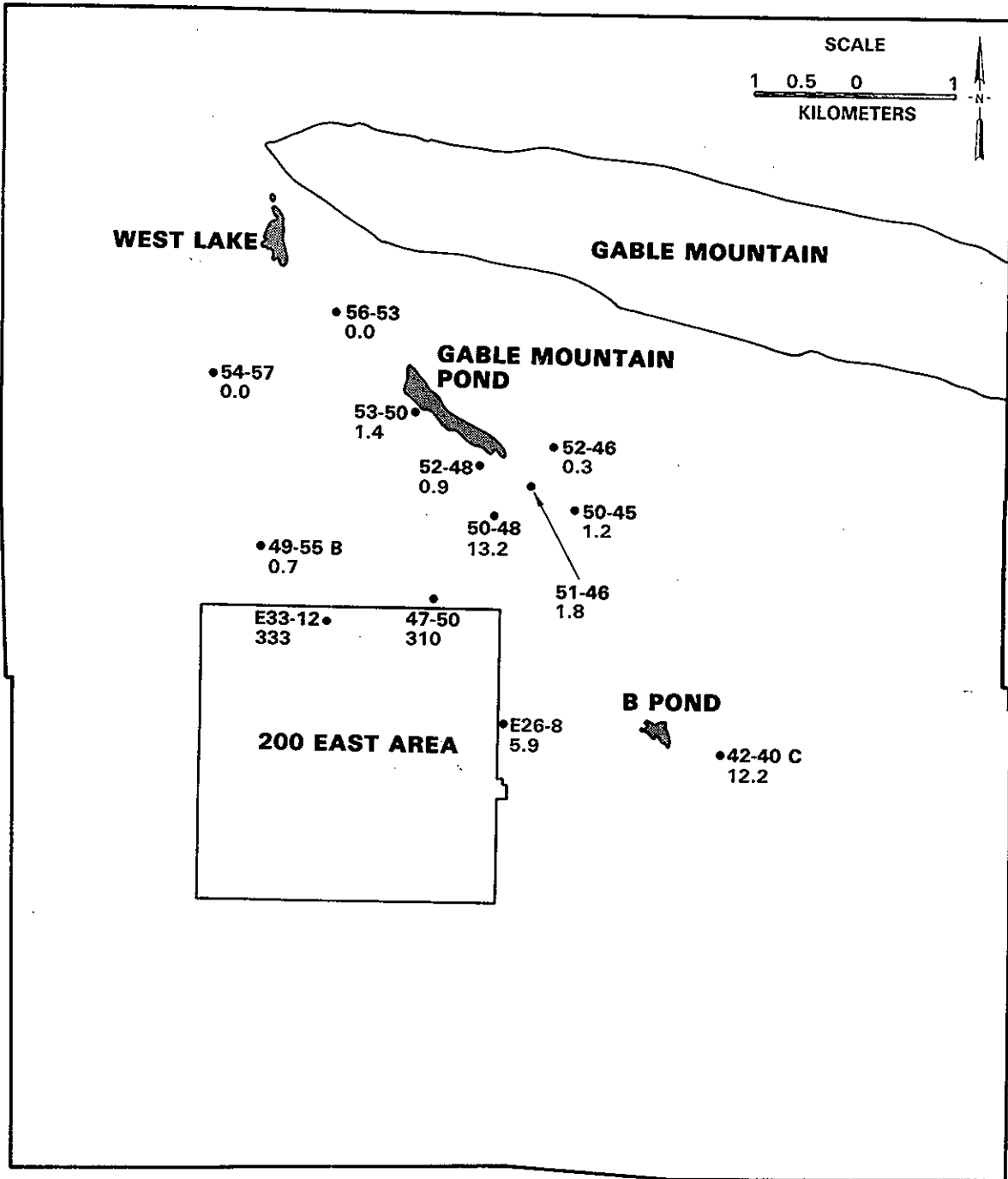


FIGURE 33. Distribution and Concentrations of Tritium, pCi/L, in the Rattlesnake Ridge Aquifer

for the higher levels of tritium observed in Well 699-47-50. The lower levels of tritium in Well 299-E26-8 (also located near 200-East Area) may be due to a greater distance from the source term. Further evidence of this is the increase in tritium concentrations during the pump test (Appendix I). Migration of contamination to the well from a distant source or contamination plume may have been induced from pumping. The highest tritium concentrations are in Well 299-E33-12 with 333 pCi/L. This contamination is attributed to the high-salt, dense waste that migrated by density flow into the well when it was open to the unconfined aquifer. There is no indication, from the hydrogeochemical data, that unconfined aquifer waters are present in the Rattlesnake Ridge aquifer in the vicinity of Well 299-E33-12. The migration of this dense waste apparently was not accompanied by a significant inflow of unconfined aquifer waters. The contamination in Well 699-42-40C may have been induced during the construction of the well. The Elephant Mountain interflow zone encountered in drilling the well contained 1,200 pCi/L of tritium. The Rattlesnake Ridge aquifer was open to this interflow zone before the interflow zone was cemented. The contamination in the Rattlesnake Ridge aquifer decreased from 39 to 12.2 pCi/L during the pump test, which is another indication that the contamination is very local. The other Rattlesnake Ridge wells contained tritium less than or equal to 1.4 pCi/L.

In addition to tritium, gamma scan and iodine-129 (half-life, 1.59×10^7 yr) data are available for the ground-water samples (Appendix I). The highest concentrations of iodine-129 in the unconfined aquifer samples are from Wells 699-37-43 (1.1 pCi/L) and 699-42-40A (2.5 pCi/L). The samples from these wells also contain the highest concentrations of tritium. These wells are located along a major flow path for contamination migration in the unconfined aquifer. This flow path carries contamination out of the study area to the south-east. The contamination is primarily the result of past disposal to facilities that are no longer active (Wilbur et al. 1983).

Iodine-129 concentrations in the Rattlesnake Ridge test wells are shown in Figure 34. The general patterns of iodine-129 contamination are the same as the tritium contamination. Again, the iodine-129 contamination observed in 699-42-40C is thought to have been induced during the construction of the

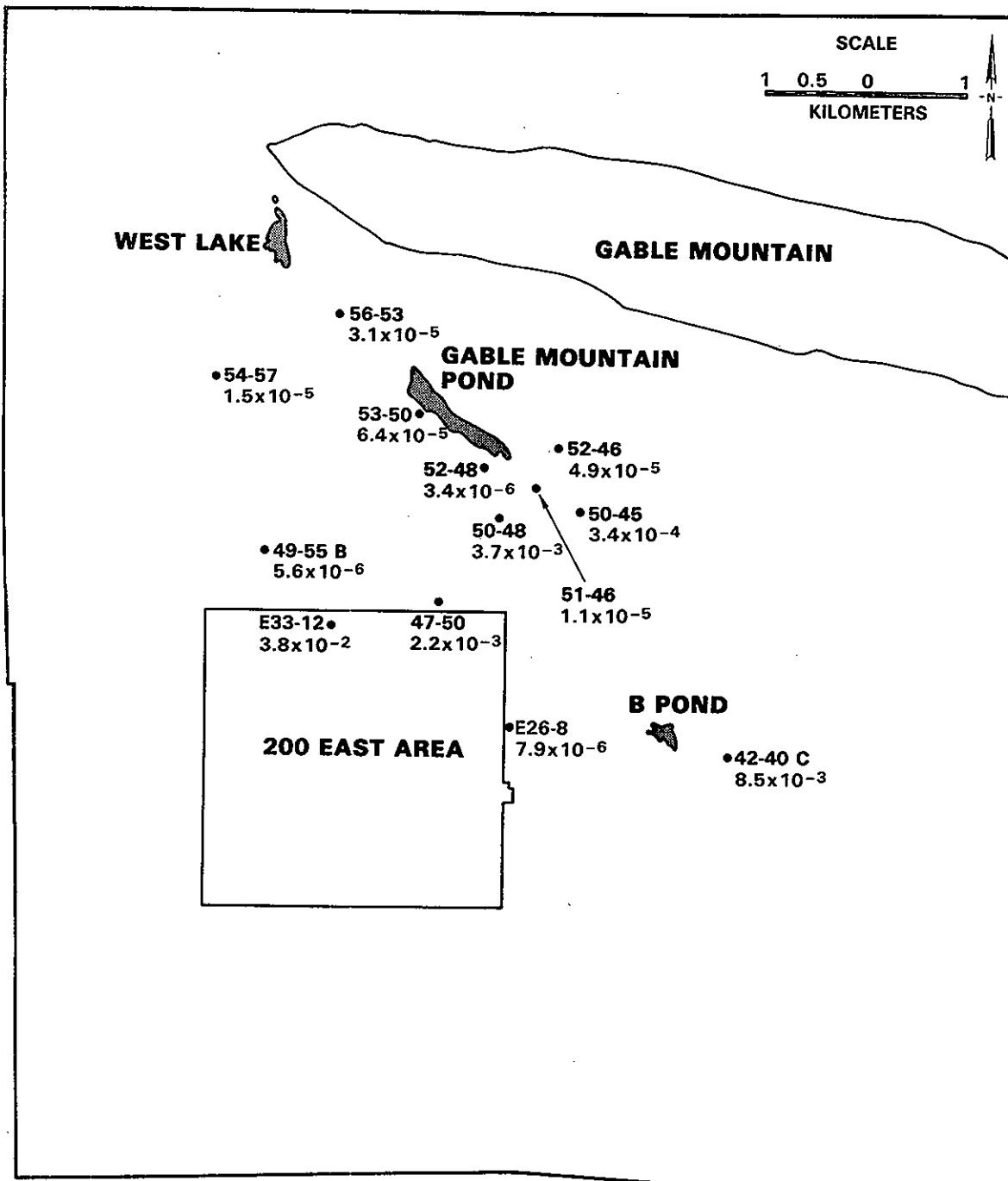


FIGURE 34. Distribution and Concentrations of Iodine-129, pCi/L, in the Rattlesnake Ridge Aquifer

well. The highest concentrations are in the vicinity north of 200-East Area. This contamination occurred from aquifer intercommunication in the vicinity of Wells 699-47-50 and 699-50-48, and migration by density flow down Well 299-E33-12 when the borehole was open to both aquifers.

7.0 DISCUSSION

Four plausible mechanisms can provide physical connections between the unconfined and Rattlesnake Ridge aquifers. These mechanisms are 1) the lithologic framework of the Elephant Mountain basalt, 2) stratigraphic unconformities, 3) structural deformation and/or rupture, and 4) human intrusion.

The framework of the Elephant Mountain basalt consists of numerous vertical and horizontal cooling joints, typical of all basalt flows. This jointing, if not sealed with secondary mineralization or forced together by tectonic or lithostatic pressures, can effectively form a network of interconnecting pathways between the aquifers. However, even in the presence of minor extensional deformation, this jointing is considered to be a negligible pathway for contaminants (when compared to other more direct pathways) unless the Elephant Mountain basalt is extremely thin.

Erosional unconformities are considered the principal mechanism for direct physical interconnection between the aquifers. These unconformities place the Rattlesnake Ridge lithologies in direct contact with the younger sands and gravels of the Hanford formation containing the unconfined aquifer. The large areas of erosion in the Gable Gap area and the northwestern most "window" at Borehole 699-53-55C are prime examples of this. The southernmost "window" is postulated to exist based on abnormally thin Elephant Mountain basalt in this area and low barometric efficiencies in Wells 699-47-50 and 299-E26-8.

Anticlinal deformation of the Elephant Mountain basalt, particularly in the hinge zone, may act to enhance the aperture of cooling joints, thus inducing secondary permeabilities through the confining bed. Another type of structural deformation, faulting, can provide a much more direct connection between the aquifers in two ways 1) by providing a vertical fracture (pathway) through the confining bed, and 2) by vertically offsetting the stratigraphy, thereby placing the Rattlesnake Ridge aquifer in direct contact with the unconfined aquifer's lithologies. However, interpretation of the available data does not indicate faulting to be a mechanism for the aquifers' interconnection within the study area.

Another mechanism for creating physical connections between the aquifers is human intrusion. Improperly constructed boreholes through the confining bed can provide a direct pipeline between the aquifers, as in the case of Well 299-E33-12.

Barometric efficiency data collected for this investigation are used to infer two areas of interconnection near Wells 299-E26-8 and 699-51-46. The low barometric efficiency of Well 699-47-50 supports the presence of the southernmost "window" that was postulated from the geologic data. This area of erosion actually may extend to the vicinity of Well 299-E26-8, thus accounting for the low barometric efficiency of that well. The presence of these areas is supported by the hydrogeochemical data.

The barometric efficiencies also have implications for the determination of ground-water flow. During periods of high barometric pressure, the water level in a high barometric-efficiency well will be lowered more than in an adjacent well with a lower barometric efficiency. If the gradient between the wells is slight, the direction of ground-water flow may appear to be from the low barometric efficiency well to the high barometric efficiency well. During periods of low barometric pressure, the water level in the high efficiency well will raise more than the well with lower barometric efficiency; thus, the flow will appear to be from the high efficiency well to the lower efficiency well. This is apparently the case with Wells 299-E33-12 and 699-47-50 with barometric efficiencies of 38.3 and 17.3 percent, respectively. Water levels taken over a long period of time are used to define the true ground-water flow directions.

The flow of ground water within the Rattlesnake Ridge aquifer is toward the center of the Hanford Site, from recharge areas located to the west, north and east. Within the study area, the flow is to the west and north toward West Lake, where the Rattlesnake Ridge and possibly deeper aquifers discharge to the unconfined aquifer.

Two areas of downward gradient between the unconfined aquifer and the Rattlesnake Ridge aquifer are identified under B-Pond and Gable Mountain Pond for present-day conditions. These areas may be somewhat over estimated because the elevation of the water table is used to define the potential in the unconfined aquifer. The head values in the bottom of the unconfined aquifer are

thought to be less than or equal to the water table throughout the study area, due to the large artificial recharge and the absence of discharge areas. Downward gradients presently do not occur in the areas where erosion of the confining bed is observed or suspected.

The various hydrogeochemical data indicate similar patterns of mixing of unconfined waters in the Rattlesnake Ridge aquifer. The deuterium-oxygen-18 data appear to be the most quantitative indicators of aquifer intercommunication. The area where aquifer intercommunication has occurred lies south and east of Gable Mountain Pond and extends to 200 East Area. The aquifer intercommunication occurred when the water table was at a higher elevation than the potentiometric surface of the Rattlesnake Ridge aquifer in this area, possibly in the late 1960s and early 1970s when the water table was at a higher elevation.

Contamination has migrated from the unconfined aquifer to the Rattlesnake Ridge aquifer in the area of aquifer intercommunication. Samples with the highest levels of contamination were collected from Well 299-E33-12, where contamination migrated by density flow down the borehole when it was open to both aquifers. The contamination in the Rattlesnake Ridge aquifer will eventually discharge back to the unconfined aquifer in the vicinity of West Lake; the unconfined aquifer discharges to the Columbia River. The levels of iodine-129 and tritium in the Rattlesnake Ridge aquifer are well below the EPA drinking water limits (based upon an annual 4 millirem whole body dose) of 0.5 and 20,000 pCi/L, respectively.

8.0 CONCLUSIONS

The following conclusions were drawn from interpretations of the hydro-geologic data collected during the investigation of aquifer intercommunication in the B Pond-Gable Mountain Pond Area.

- Erosional "windows" through the confining bed (Elephant Mountain basalt) provide direct physical interconnections between the unconfined and the Rattlesnake Ridge aquifers. Two areas of complete erosion of the Elephant Mountain basalt were identified in the study area. Two other areas of erosion were inferred from the barometric efficiencies of the wells.
- Within the Rattlesnake Ridge aquifer, ground water flows into the study area from recharge areas to the east, north, and west. The ground water flows to the west and north through the study area toward West Lake where the aquifer discharges to the unconfined aquifer via an area of extensive erosion. Two zones of downward gradient between the unconfined aquifer and the Rattlesnake Ridge aquifer were identified beneath B Pond and Gable Mountain Pond. Downward gradients presently do not occur in the areas where erosion of the confining bed is observed or suspected.
- A zone of mixing of unconfined aquifer water in the Rattlesnake Ridge aquifer that resulted from aquifer intercommunication was identified to the south and east of Gable Mountain Pond and extending to 200 East Area. The aquifer intercommunication occurred when there were downward gradients between the aquifers in this area, possibly in the late 1960s and early 1970s when the water table was at a higher elevation.
- Contamination in the Rattlesnake Ridge aquifer resulted from the aquifer intercommunication and by the migration of wastes by density flow down Well 299-E33-12 when the well was open, prior to this investigation, from the unconfined aquifer to the Rattlesnake Ridge aquifer.

- The distributions and concentrations of contamination (tritium and iodine-129) were determined for the unconfined and confined aquifers. The levels of iodine-129 and tritium in the Rattlesnake Ridge aquifer are well below the drinking water standards of 0.5 and 20,000 pCi/L, respectively.

9.0 REFERENCES

- Ames, L. L. 1980. Hanford Basalt Flow Mineralogy. PNL-2847, Pacific Northwest Laboratory, Richland, Washington.
- Baker, V. R. 1973. Paleohydrology and Sedimentology of the Lake Missoula Flooding in Eastern Washington. Geological Society of America Special Paper 144.
- Basalt Waste Isolation Project (BWIP) Staff. 1982. Site Characterization Report for the Basalt Waste Isolation Project. DOE/RL 82-3, 3 volumes, U.S. Department of Energy, Richland, Washington.
- Bierschenk, W. H. 1957. Hydraulic Characteristics of Hanford Aquifers. HW-48916, General Electric Company, Richland, Washington.
- Bierschenk, W. H. 1959a. Aquifer Characteristics and Ground-Water Movement at Hanford. HW-60601, General Electric Company, Richland, Washington.
- Bierschenk, W. H. 1959b. Observational and Field Aspects of Ground-Water Flow at Hanford. HW-SA-41, General Electric Company, Richland, Washington.
- Black, R. F. 1979. Clastic Dikes of the Pasco Basin, Southeastern Washington. RHO-BWI-C-64, Rockwell Hanford Operations, Richland, Washington.
- Bredhoeft, J. D., H. H. Cooper, Jr., and I. S. Papadopoulos. 1966. "Inertial and Storage Effects in Well Aquifer Systems: An Analog Investigation." Water Resources Res. 2(4):697-707.
- Bretz, J. H. 1923. "The Channeled Scablands of the Columbia Plateau." Journal of Geology 31:617-649.
- Bretz, J. H. 1959. Washington's Channeled Scabland, Washington Division of Mines and Geology Bulletin 45.
- Brock, M. R., and M. J. Grolier. 1973. Chemical Analyses of 305 Basalt Samples from the Columbia River Plateau, Washington, Oregon, and Idaho. Open File Report, U.S. Geological Survey, U.S. Government Printing Office, Washington D.C.
- Brown, D. J. 1959. Subsurface Geology of the Hanford Separations Areas. HW-61780. General Electric Company, Richland, Washington.
- Brown, D. J. 1960. An Eolian Deposit Beneath 200 West Area. HW-67549, General Electric Company, Richland, Washington.
- Brown, R. E., and D. J. Brown. 1961. The Ringold Formation and Its Relationship to Other Formations. HW-SA-2319, General Electric Company, Richland, Washington.

- Brown, R. E. 1975. "Groundwater and the Basalts in the Pasco Basin," in Proceedings of the Thirteenth Engineering Geology and Soils Engineering Symposium, Moscow, Idaho.
- Brown, R. E., and H. G. Ruppert. 1950. The Underground Disposal of Liquid Wastes at the Hanford Works, Washington. HW-17088, General Electric Company, Richland, Washington.
- Cooper, H. H., Jr., and C. E. Jacob. 1946. "A Generalized Graphical Method for Evaluating Formation Constants and Summarizing Well Field History," Trans. American Geophysical Union 27(IV):526-534.
- Cooper, H. H., Jr., J. D. Bredehoeft, and I. S. Papadopoulos. 1967. "Response of a Finite Diameter Well to an Instantaneous Charge of Water." Water Resources Res. 3(1):263-269.
- Craig, H.. 1961. "Standard for Reporting Concentrations of Deuterium and Oxygen-18 in Natural Waters." Science 133:1833-1834.
- Diediker, L. D., and R. K. Ledgerwood. 1980. Drilling History of Core Hole DB-15. RHO-BWI-LD-29, Rockwell Hanford Operations, Richland, Washington.
- DeWiest, R. J. M. 1965. Geohydrology, John Wiley, New York.
- Drost, W., et al. 1968. "Point Dilution Methods of Investigation Ground-Water Flow by Means of Radioisotopes." Water Resources Res. 4:125-146.
- Eddy, P. A., L. S. Prater, and J. T. Rieger. 1983. Ground-Water Surveillance at the Hanford Site for CY 1982. PNL-4659, Pacific Northwest Laboratory, Richland, Washington.
- Eliason, J. R. 1967. Earth Sciences Waste Disposal Investigation, July-December, 1966. BNWL-432, Pacific Northwest Laboratory, Richland, Washington.
- Fecht, K. R. 1978a. Geology Along Topographic Profile for Near-Surface Test Facility. RHO-BWI-LD-16, Rockwell Hanford Operations, Richland, Washington.
- Fecht, K. R. 1978b. Geology of the Gable Mountain--Gable Butte Area. RHO-BWI-LD-5, Rockwell Hanford Operations, Richland, Washington.
- Ferris, J. G., and D. B. Knowles. 1954. The Slug Test for Estimating Transmissivity. U.S. Geological Survey Ground-Water Note 26, U.S. Government Printing Office, Washington, D.C.
- Ferris, J. G., et al. 1962. Theory of Aquifer Tests. U.S. Geological Survey Water-Supply Paper 1536-E, U.S. Government Printing Office, Washington, D.C.
- Flint, R. F. 1938. "Origin of the Cheney-Palouse Scabland Tract." Geological Society of America Bulletin 49:461-524.

- Fontes, J. Ch. 1980. "Interpretation of Stable Isotopes of Sulfur and Oxygen." In Handbook of Environmental Isotope Geochemistry, Volume 1, The Terrestrial Environment, eds. P. Fritz and J. Ch. Fontes. A. Elsevier, New York.
- Freeze, R. A., and J. A. Cherry. 1979. Groundwater. Prentice-Hall, Inc., Englewood Cliffs, New Jersey.
- Fritz, P. and J. C. Fontes, eds., 1980. Handbook of Environmental Isotope Geochemistry, Vol. 1 - The Terrestrial Environment, A, Elsevier, New York, New York.
- Gephart, R. E., et al. 1979. Hydraulic Studies Within the Columbia Plateau, Washington: An Integration of Current Knowledge. RHO-BWI-ST-5, Rockwell Hanford Operations, Richland, Washington.
- Gephart, R. E., et al. 1976. Geohydrologic Study of the West Lake Basin. ARH-CD-775, Atlantic Richfield Hanford Company, Richland, Washington.
- Gilcreas, F. W., M. J. Taras and R. S. Ingols, eds. 1980. Standard Methods for the Examination of Water and Wastewater. Fifteenth Edition. American Public Health Association, New York.
- Graham, D. L. 1983. Stable Isotopic Composition of Precipitation from the Rattlesnake Hills Area of South-Central Washington. RHO-BW-ST-44P, Rockwell Hanford Operations, Richland, Washington.
- Graham, M. J., et al. 1981. Hydrology of the Separations Area. RHO-ST-42, Rockwell Hanford Operations, Richland, Washington.
- Hem, J. D. 1970. Study and Interpretation of the Chemical Characteristics of Natural Water. Second Edition. Geological Survey Water-Supply Paper 1473, U.S. Government Printing Office, Washington, D.C.
- Hooper, P. R., et al. 1976. Major Element Analyses of Columbia River Basalt Part I. Washington State University, Pullman, Washington.
- Horn, M. K., and J. A. S. Adams. 1966. "Computer-Derived Geochemical Balances and Elemental Abundances." Geschim. et Cosmochim-Acta 30:279-297.
- Horwitz, W. 1970. Official Methods of Analysis of the Association of Official Analytical Chemists, 11th Edition, Association of Official Analytical Chemists, p. 13.
- Jacob, C. E. 1940. "On the Flow of Water on an Elastic Artesian Aquifer." Trans. Amer. Geophysical Union 21:574-586.
- Jacob, C. E. 1963. Recovery Method for Determining the Coefficient of Transmissibility. U.S. Geological Survey Water-Supply Paper 15361, U.S. Government Printing Office, Washington, D.C.

- Jorgensen, D. G. 1980. Relationships Between Basic Soils - Engineering Equations and Basic Ground-Water Flow Equations. U.S. Geological Survey Water-Supply Paper 2064, U.S. Government Printing Office, Washington, D.C.
- Keys, W. Scott, and L. M. MacCray. 1971. Application of Borehole Geophysics to Water-Resources Investigations. Book 2 of Techniques of Water-Resources Investigations, U.S. Geological Survey, U.S. Government Printing Office, Washington, D.C.
- LaSala, A. M., Jr., and G. C. Doty. 1975. Geology and Hydrology of Radioactive Solid-Waste Burial Grounds at the Hanford Reservation, Washington. U.S. Geological Survey Open File Report 75-625, U.S. Government Printing Office, Washington, D.C.
- Ledgerwood, R. K., and R. A. Deju. 1976. Hydrology of the Uppermost Confined Aquifers Underlying the Hanford Reservation. ARH-SA-253, Atlantic Richfield Hanford Company, Richland, Washington.
- Ledgerwood, R. K., C. W. Myers and R. W. Cross. 1978. Pasco Basin Stratiographic Nomenclature. RHO-BWI-LD-1, Rockwell Hanford Operations, Richland, Washington.
- Lohman, S. W. 1972. Definitions of Selected Ground-Water Terms--Revisions and Conceptual Refinements. U.S. Geological Survey Water-Supply Paper 1988, U.S. Government Printing Office, Washington, D.C.
- Moore, B. A. 1982. Geophysical Investigations of the Gable Mountain Pond--West Lake Area, Hanford, South-Central Washington. RHO-SA-239, Rockwell Hanford Operations, Richland, Washington.
- Myers, C. W., and S. M. Price, eds. 1981. Subsurface Geology of the Cold Creek Syncline. RHO-BWI-ST-14, Rockwell Hanford Operations, Richland, Washington.
- Myers, C. W., and S. M. Price, et al. 1979. Geological Studies of the Columbia Plateau - A Status Report. RHO-BWI-ST-4, Rockwell Hanford Operations, Richland, Washington.
- Narasimhan, T. N., and B. Y. Kanehiro. 1980. "A Note on the Meaning of Storage Coefficient." Water Resources Res. 16(2):423-429.
- Neter, J., and W. Wasserman. 1974. Applied Linear Statistical Models. Richard D. Irwin, Inc., Homewood, Illinois.
- Newcomb, R. C., and J. R. Strand. 1953. Geology and Ground-Water Characteristics of the Hanford Reservation of the Atomic Energy Commission, Washington. U.S. Geological Survey WP-8, U.S. Government Printing Office, Washington, D.C.

- Newcomb, R. C., J. R. Strand and F. J. Frank, 1972. Geology and Ground-Water Characteristics of the Hanford Reservation of the U.S. Atomic Energy Commission, Washington. U.S. Geological Survey Professional Paper 717, U.S. Government Printing Office, Washington, D.C.
- Parker, G. G., and A. M. Piper. 1949. Geologic and Hydrologic Features of the Richland Area, Washington, Relevant to the Disposal of Wastes at the Hanford Directed Operations of the Atomic Energy Commission. U.S. Geological Survey WP-7, U.S. Government Printing Office, Washington, D.C.
- Patton, P. C., and V. R. Baker. 1978. "New Evidence for Pre-Wisconsin Flooding in the Channeled Scabland of Eastern Washington." Geology 6:567-571.
- Pearson, F. J., Jr. and C. T. Rightmire. 1980. "Sulphur and Oxygen Isotopes in Aqueous Sulphur Compound," in Handbook of Environmental Isotope Geochemistry, Vol. 1 - The Terrestrial Environment, A. Fritz, P. and J. C. Fontes, eds., Elsevier, New York, New York, pp. 227-258.
- Puget Sound Power and Light Company. 1982. Preliminary Safety Analysis Report for Skagit/Hanford Nuclear Project, Amendment 29. Bellevue, Washington.
- Richard, B. H. 1976. Residual Gravity Analysis of Selected Cross Sections of the Hanford Reservation. CA-200-BHR-1, Atlantic Richfield Hanford Company, Richland, Washington.
- Robinson, T. W. 1939. "Earth-Tides Shown by Fluctuations of Water-Levels in Wells in New Mexico and Iowa." Trans. Amer. Geophysical Union 20:656-666.
- Smith, R. M. 1980. 216-B-5 Reverse Well Characterization Study, RHO-ST-37, Rockwell Hanford Operations, Richland, Washington.
- Stone, W. A., D. E. Jenne and M. J. Thorp. 1972. Climatology of the Hanford Area. BNWL-1065, Pacific Northwest Laboratory, Richland, Washington.
- Strait, S. R., and B. A. Moore. 1982. Geohydrology of the Rattlesnake Ridge Interbed in the Gable Mountain Pond Area. RHO-ST-38, Rockwell Hanford Operations, Richland, Washington.
- Tallman, A. M., et al. 1979. Geology of the Separations Areas, Hanford Site, South-Central Washington. RHO-ST-23, Rockwell Hanford Operations, Richland, Washington.
- Theis, C. V. 1935. "The Relation Between the Lowering of the Piezometric Surface and the Rate and Duration of Discharge of a Well Using Ground-Water Storage." Trans. Amer. Geophysical Union 16:519-524.
- Wentworth, C. K. 1922. "A Grade Scale and Class Terms for Clastic Sediments", Journal of Geology, 30, p. 377-392.

Wenzel, L. K. 1942. Methods for Determining Permeability of Water-Bearing Materials. V. 5, U.S. Geological Survey Water-Supply, Paper 887, U.S. Government Printing Office, Washington, D.C.

Wilbur, J.S., M. J. Graham, and A. H. Lu. 1983. Results of the Separations Area Monitoring Network for 1982. RHO-RE-SR-83-24, Rockwell Hanford Operations, Richland, Washington.

APPENDIX A.

WELL CONSTRUCTION DIAGRAMS

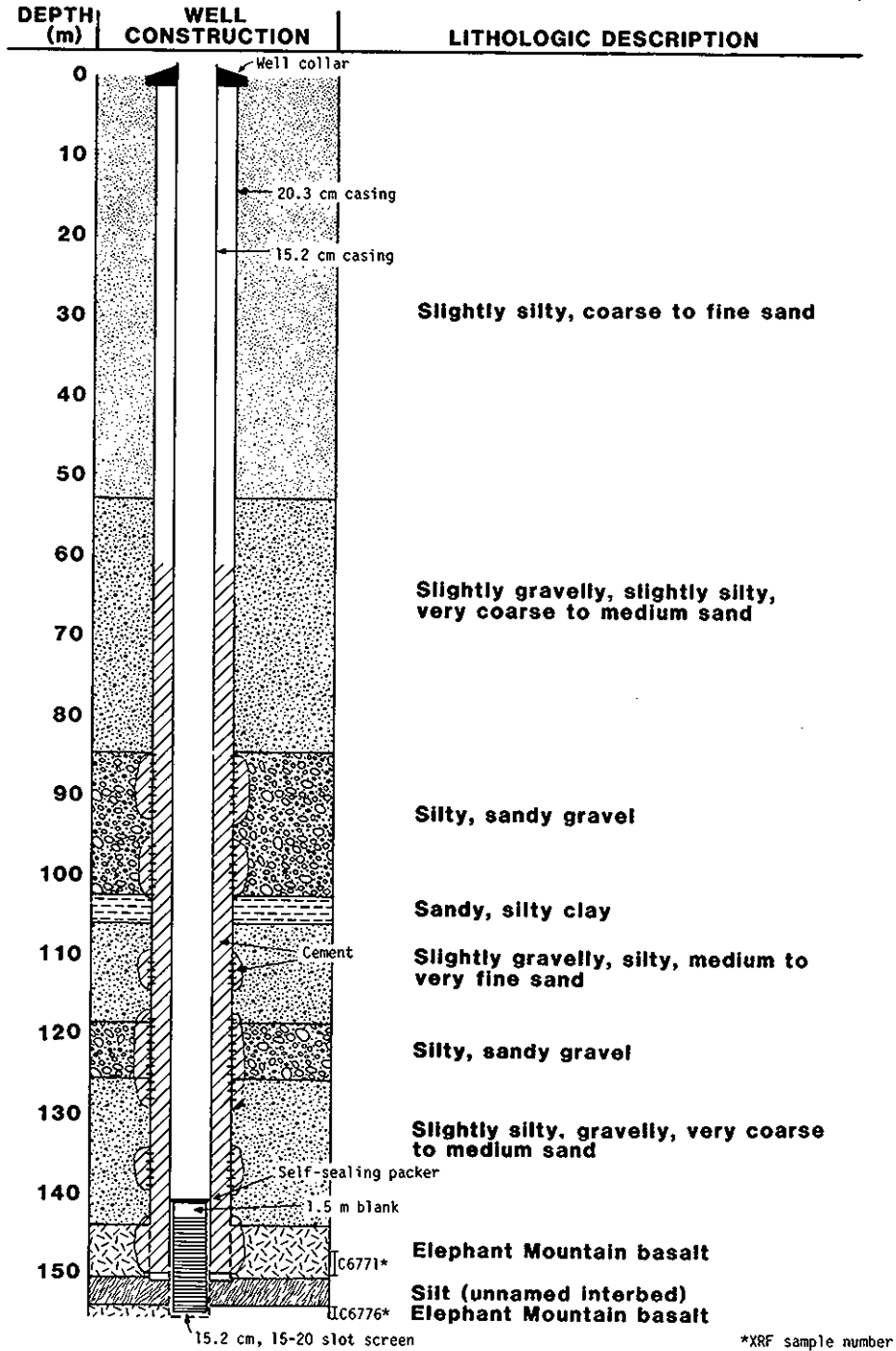


FIGURE A.1. Construction Diagram of Well 299-E16-1

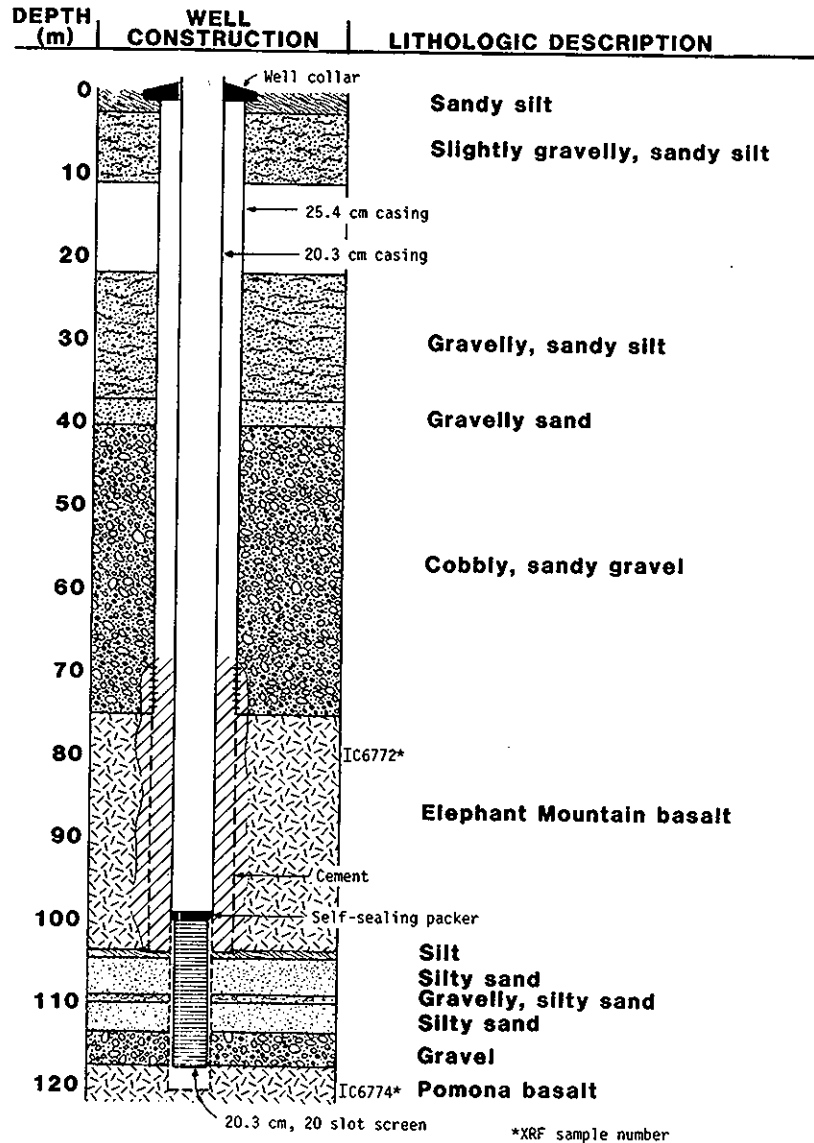


FIGURE A.2. Construction Diagram of Well 299-E26-8

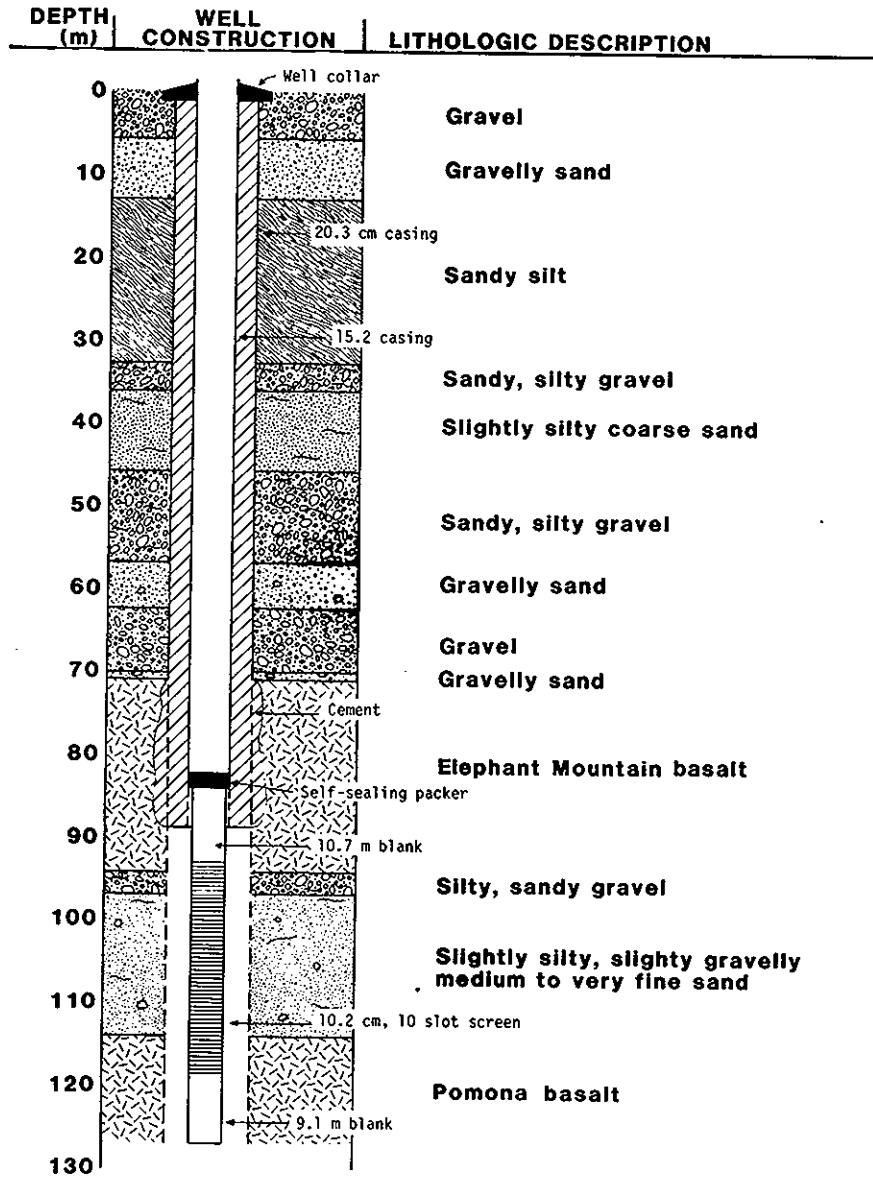


FIGURE A.3. Construction Diagram of Well 299-E33-12

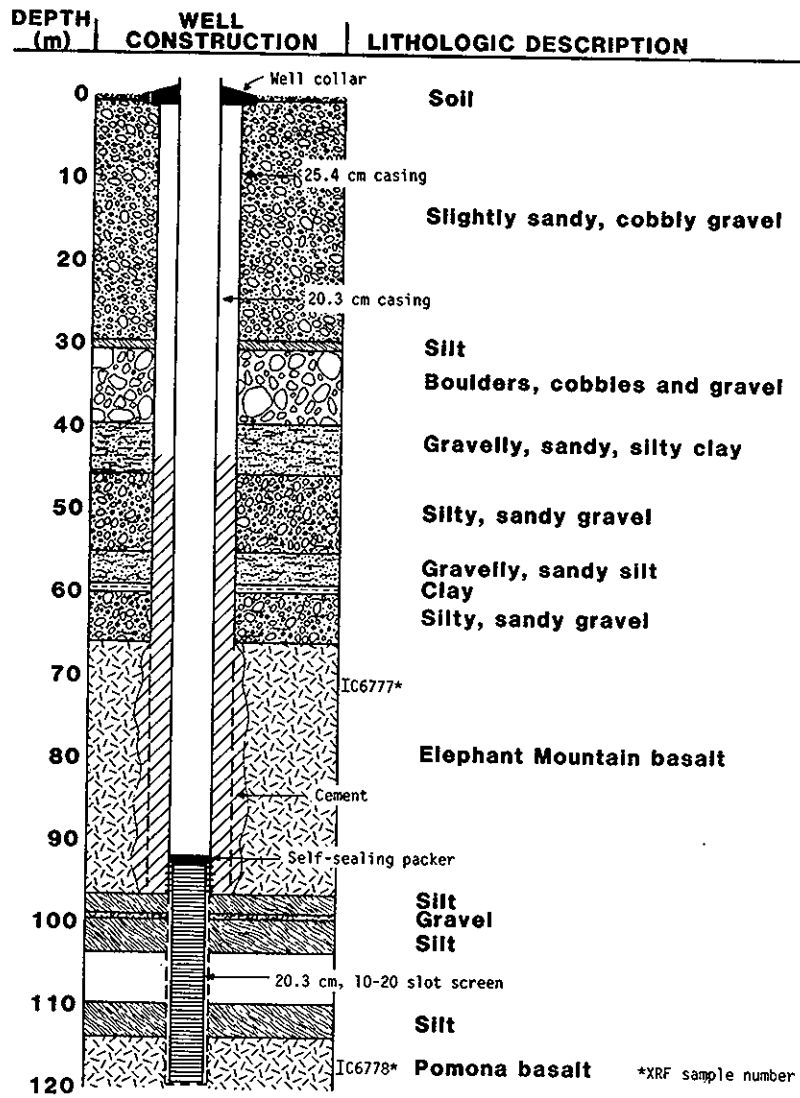


FIGURE A.4. Construction Diagram of Well 699-42-40C

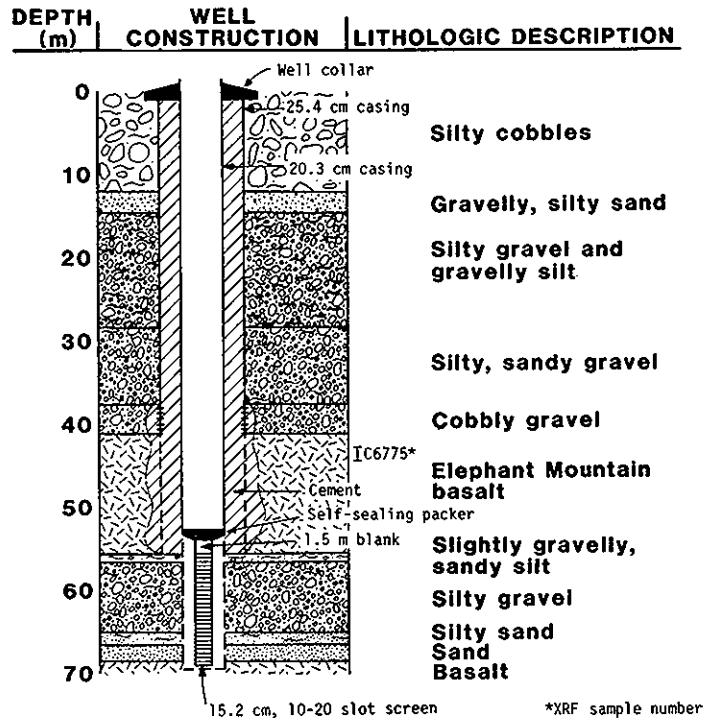


FIGURE A.5. Construction Diagram of Well 699-49-55B

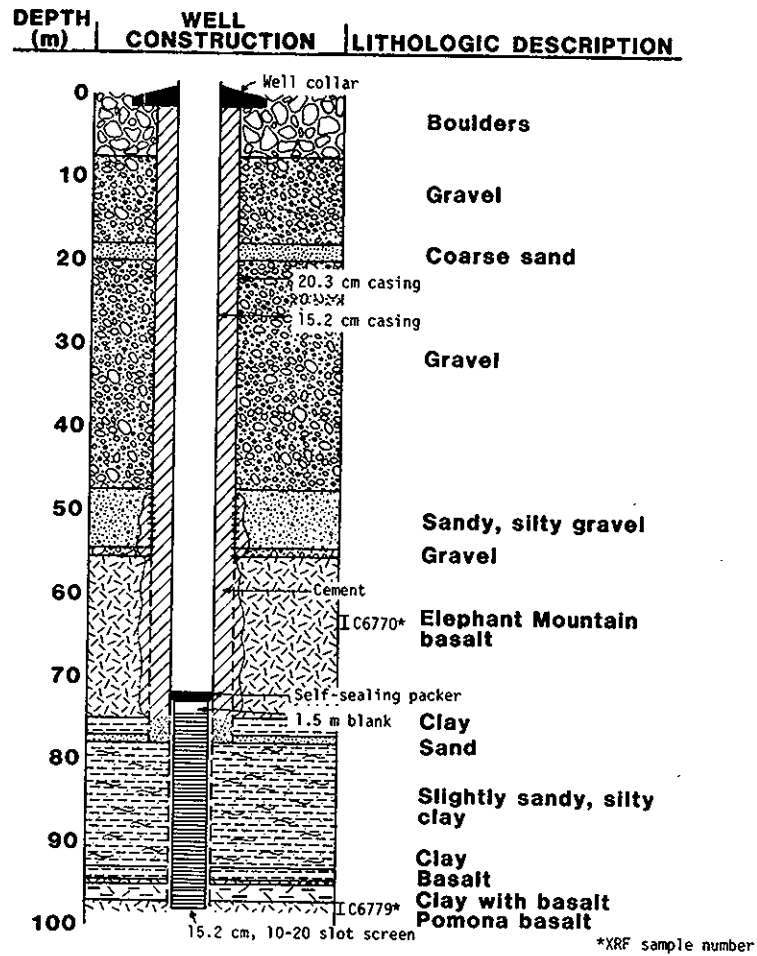


FIGURE A.6. Construction Diagram of Well 699-54-57

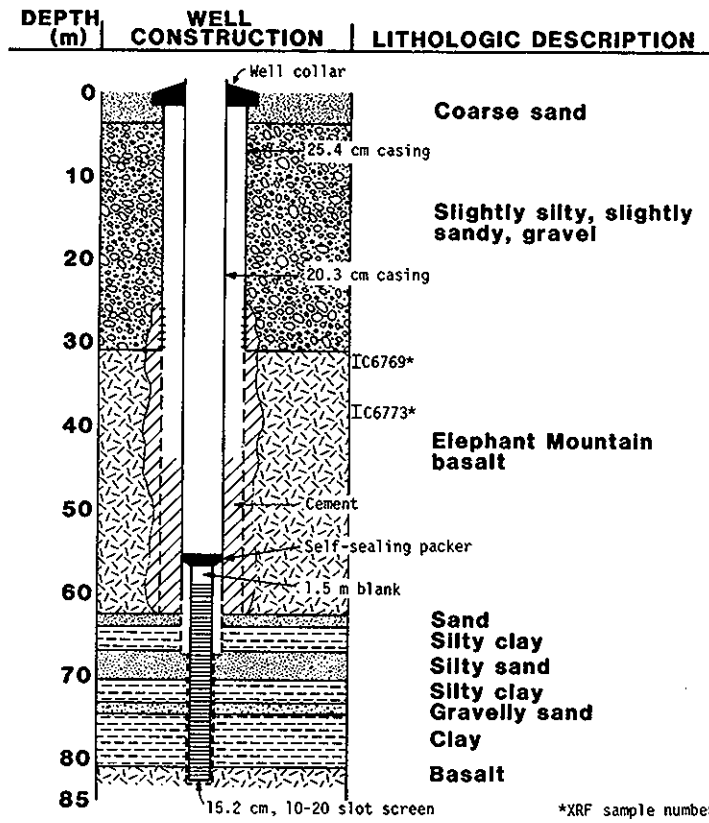
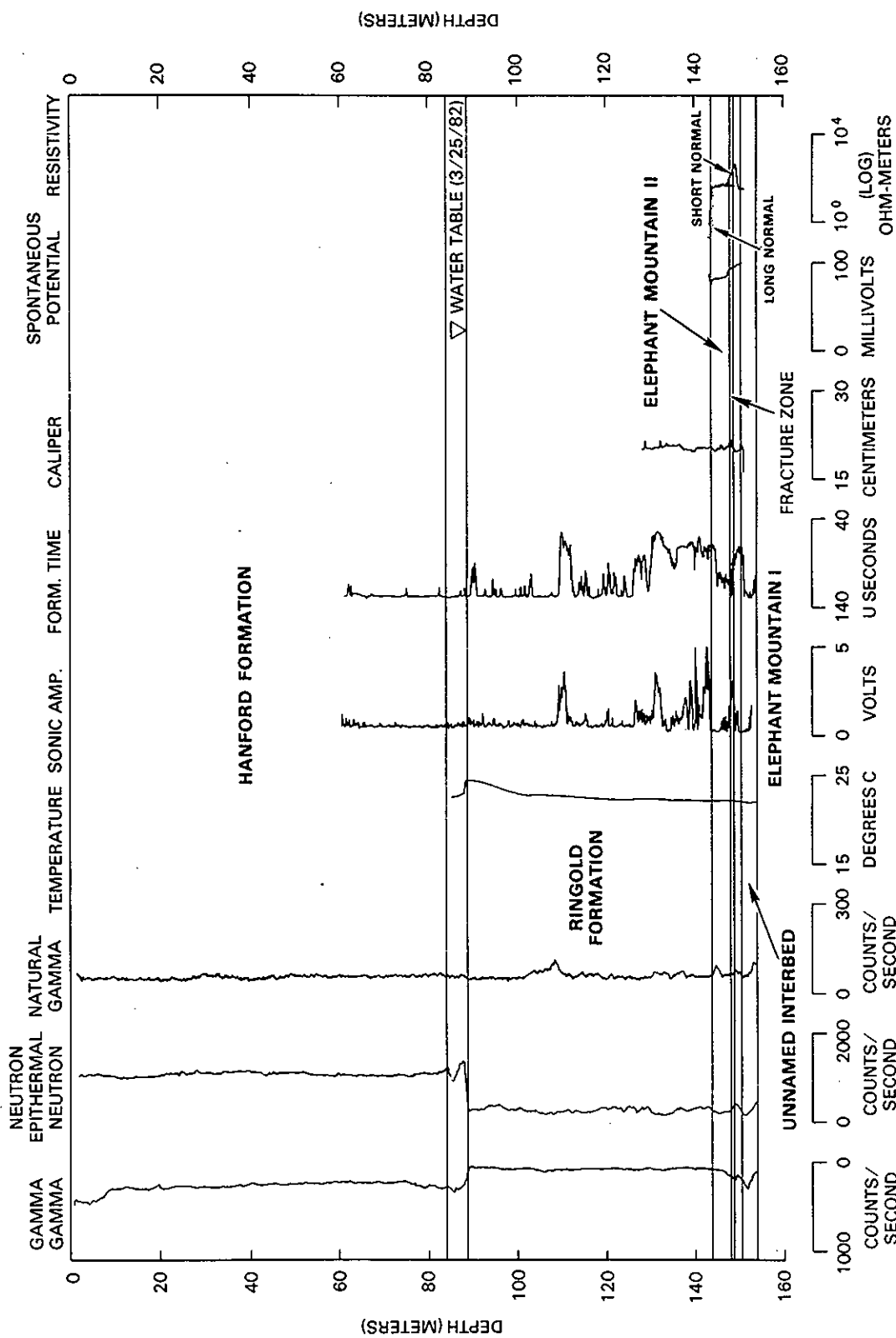


FIGURE A.7. Construction Diagram of Well 699-56-53

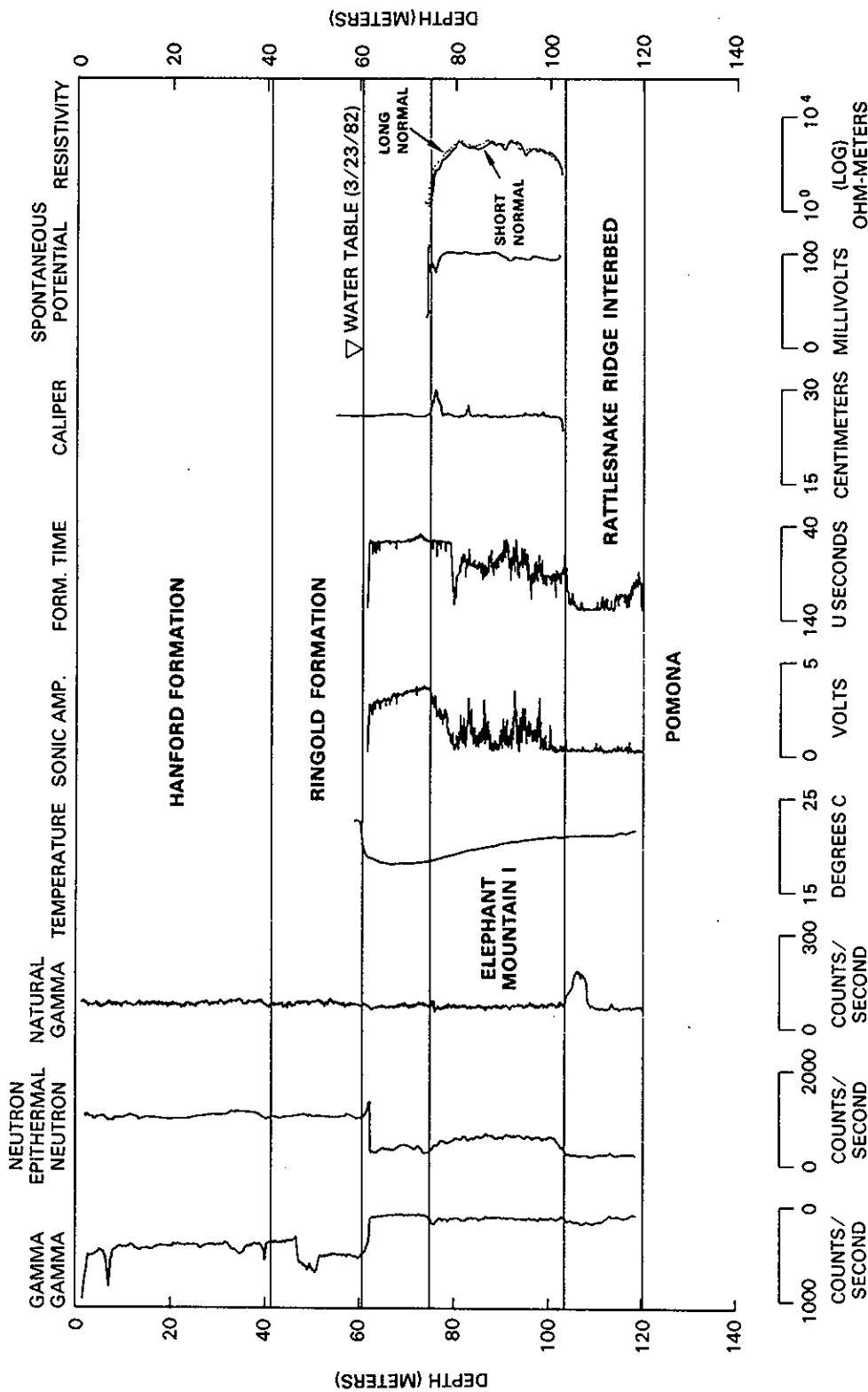
APPENDIX B

BOREHOLE GEOPHYSICAL LOGS
AND STRATIGRAPHIC COLUMNS



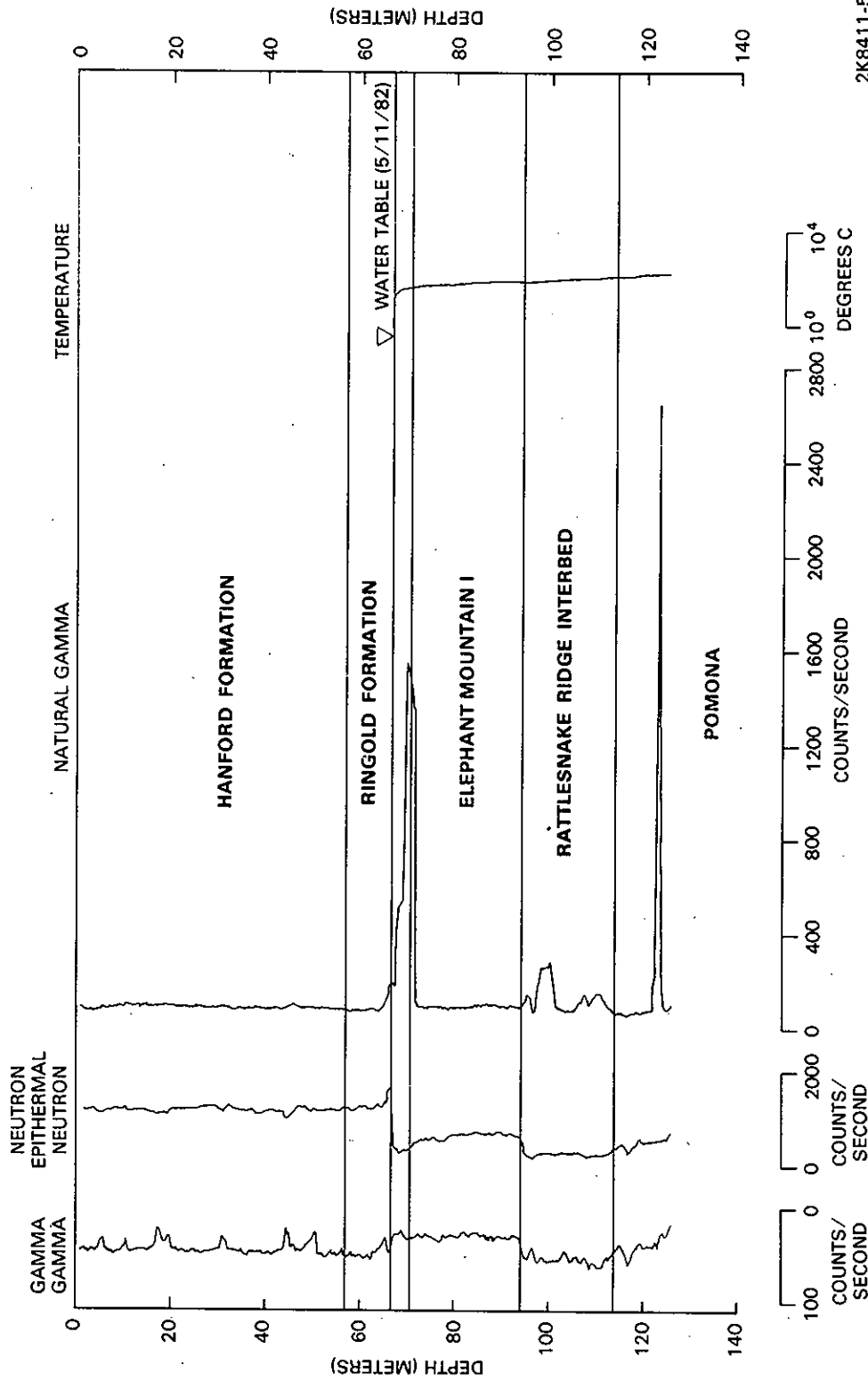
2K8411-5.1

FIGURE B.1. Geophysical Logs of Borehole 299-E16-1



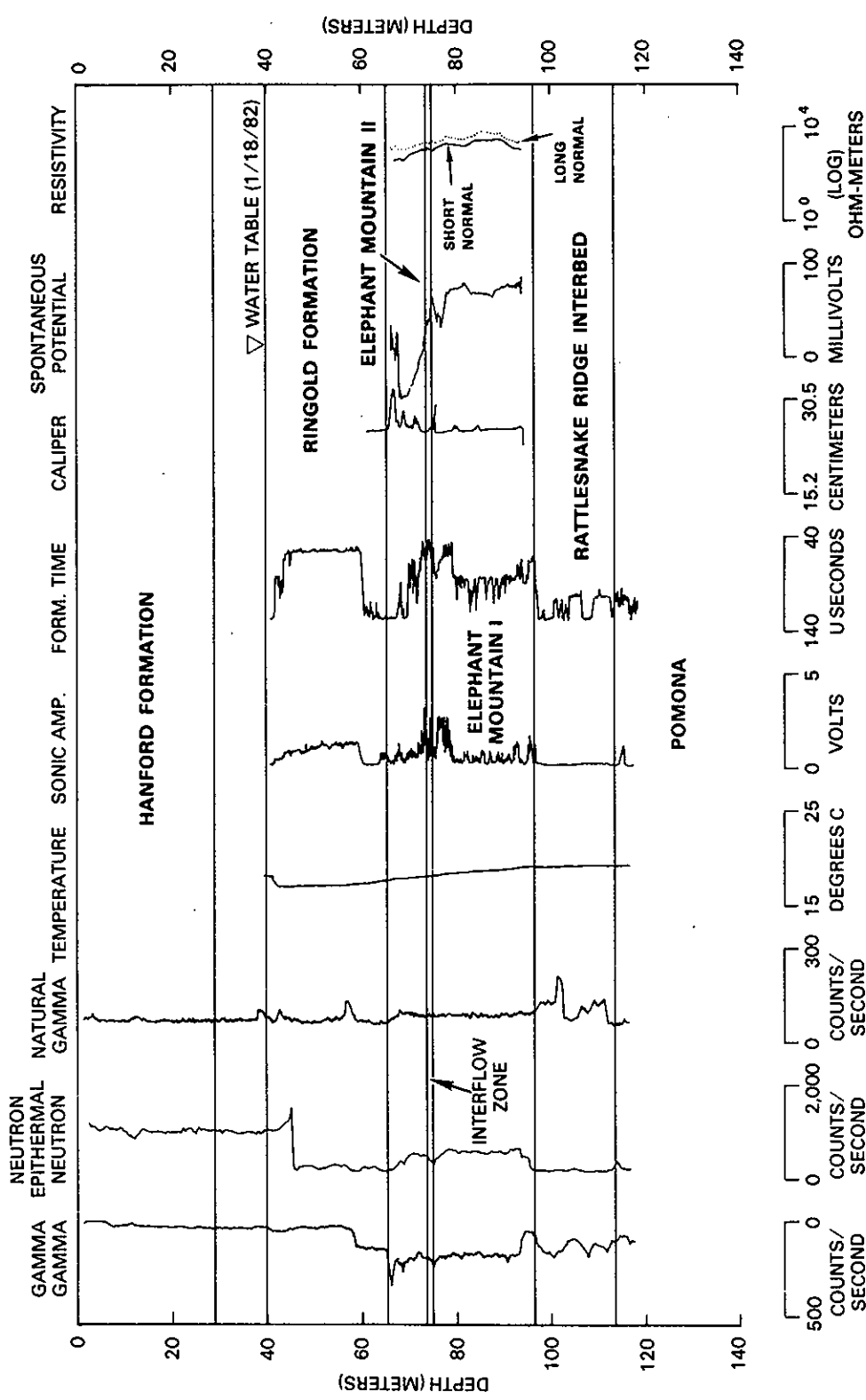
2K8411-5.2

FIGURE B.2 Geophysical Logs of Borehole 299-E26-8



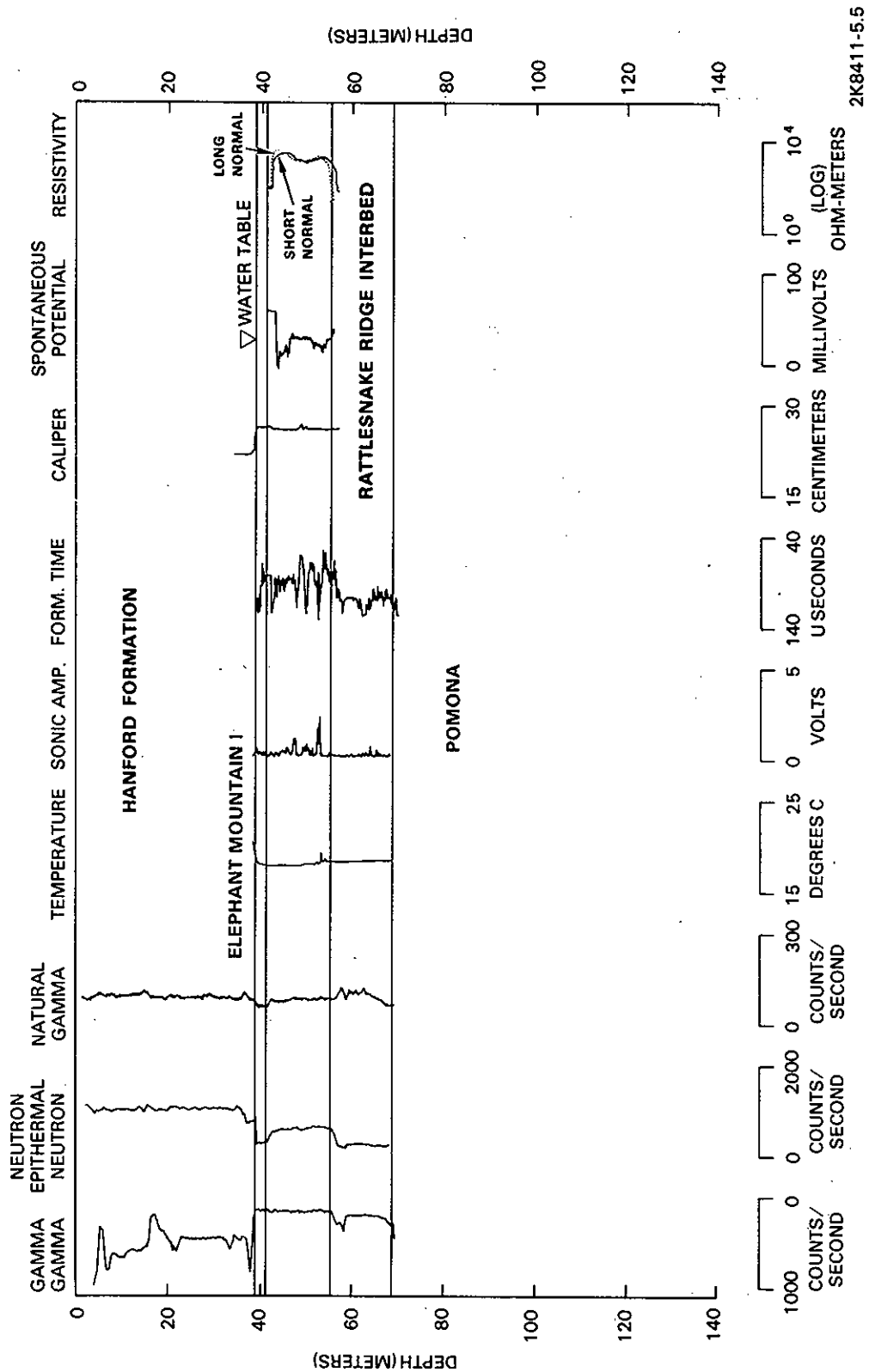
2K8411-5.3

FIGURE B.3. Geophysical Logs of Borehole 299-E33-12



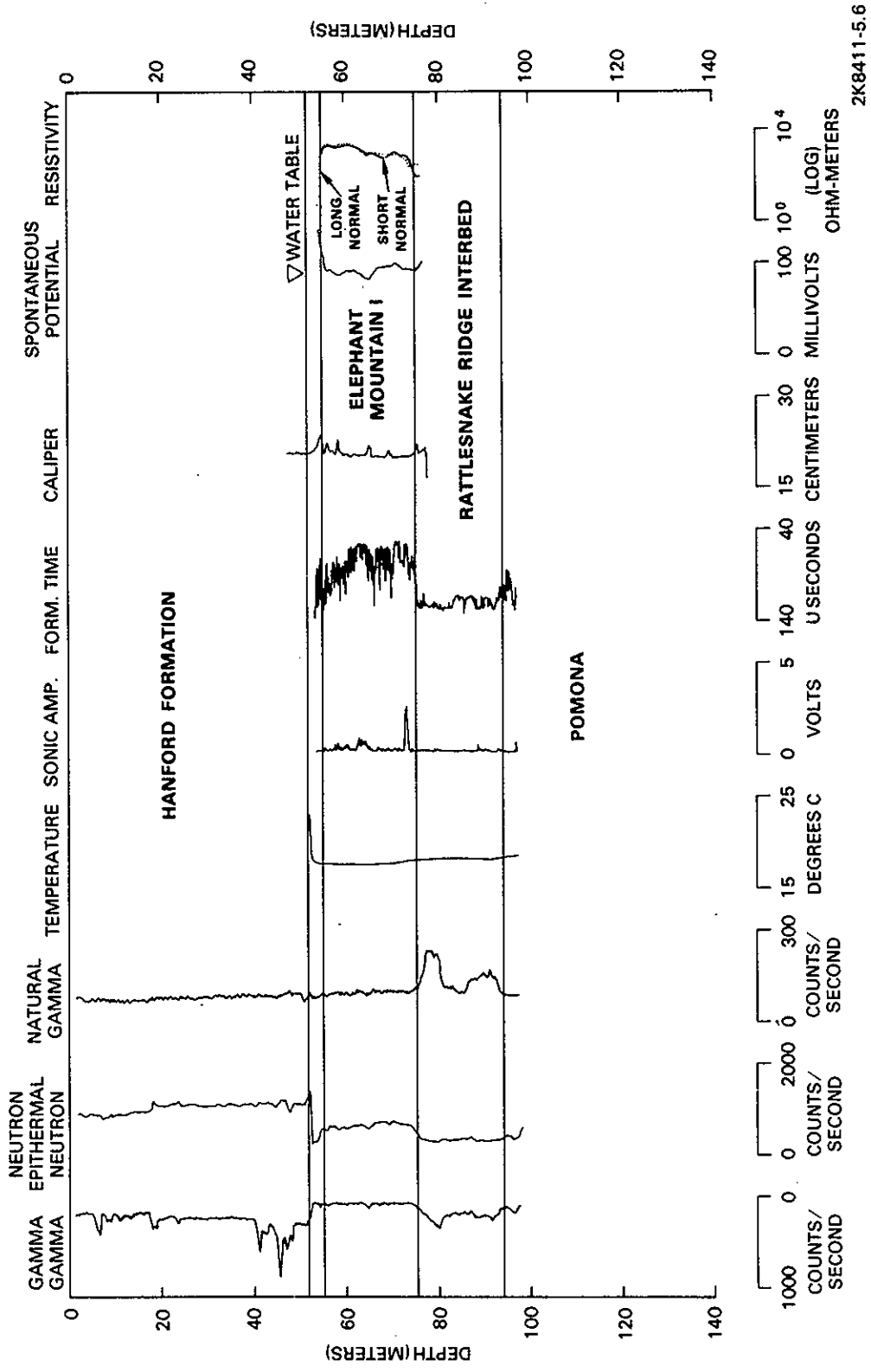
2K8411-5.4

FIGURE B.4. Geophysical Logs of Borehole 699-42-40 C



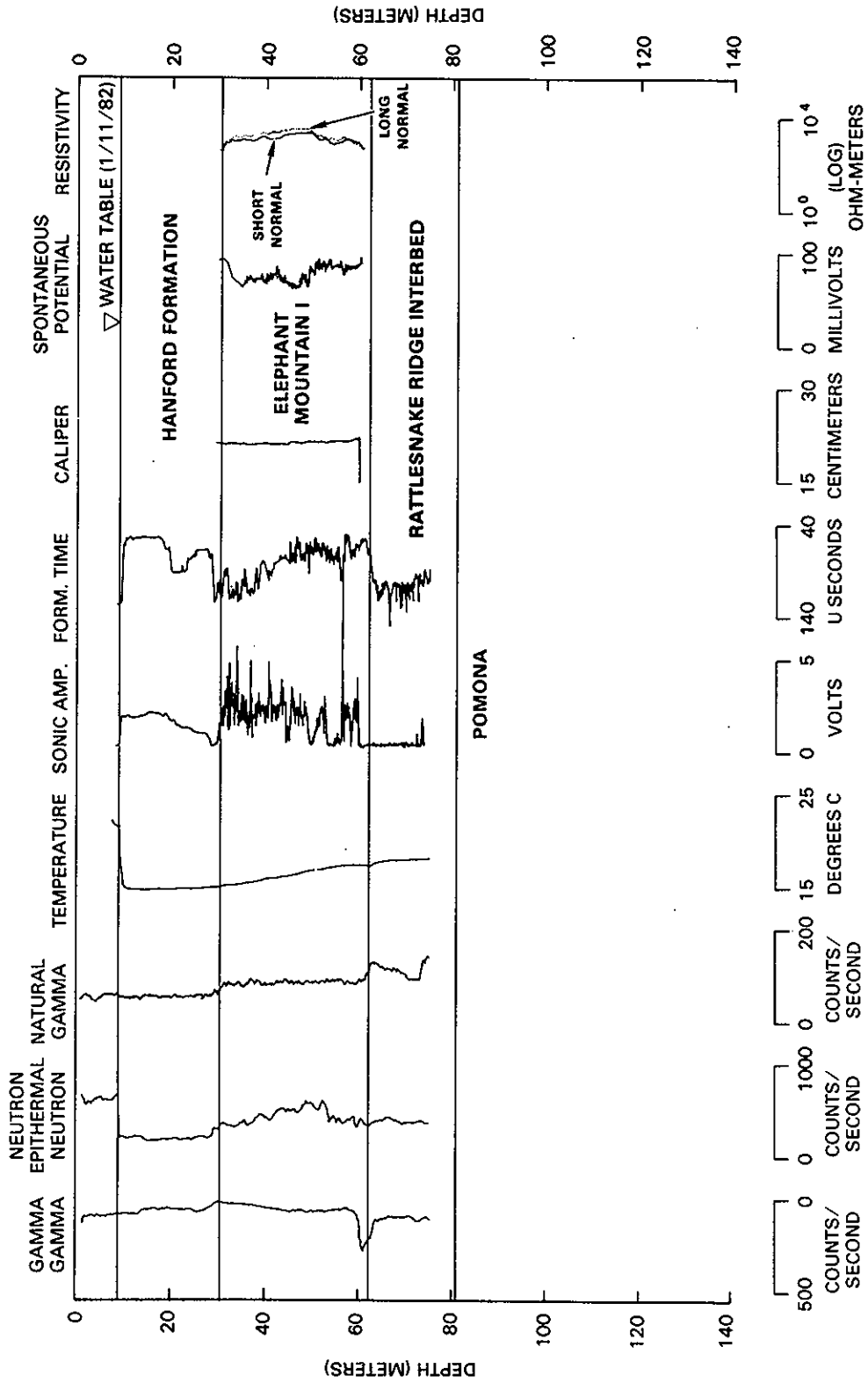
2K8411-5.5

FIGURE B.5. Geophysical Logs of Borehole 699-49-55 B



2K8411-5.6

FIGURE B.6. Geophysical Logs of Borehole 699-54-57

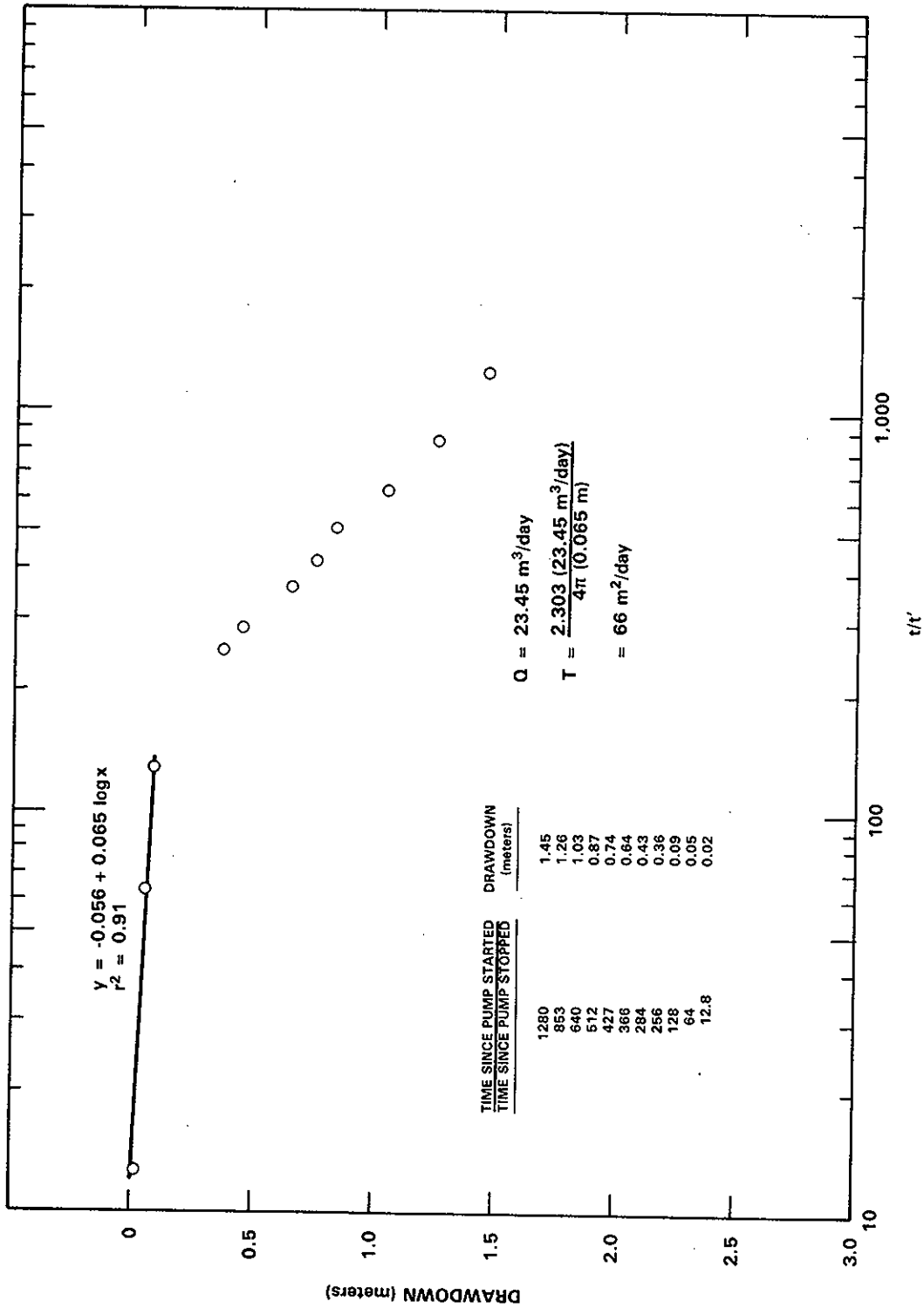


2K8411-5.7

FIGURE B.7. Geophysical Logs of Borehole 699-56-53

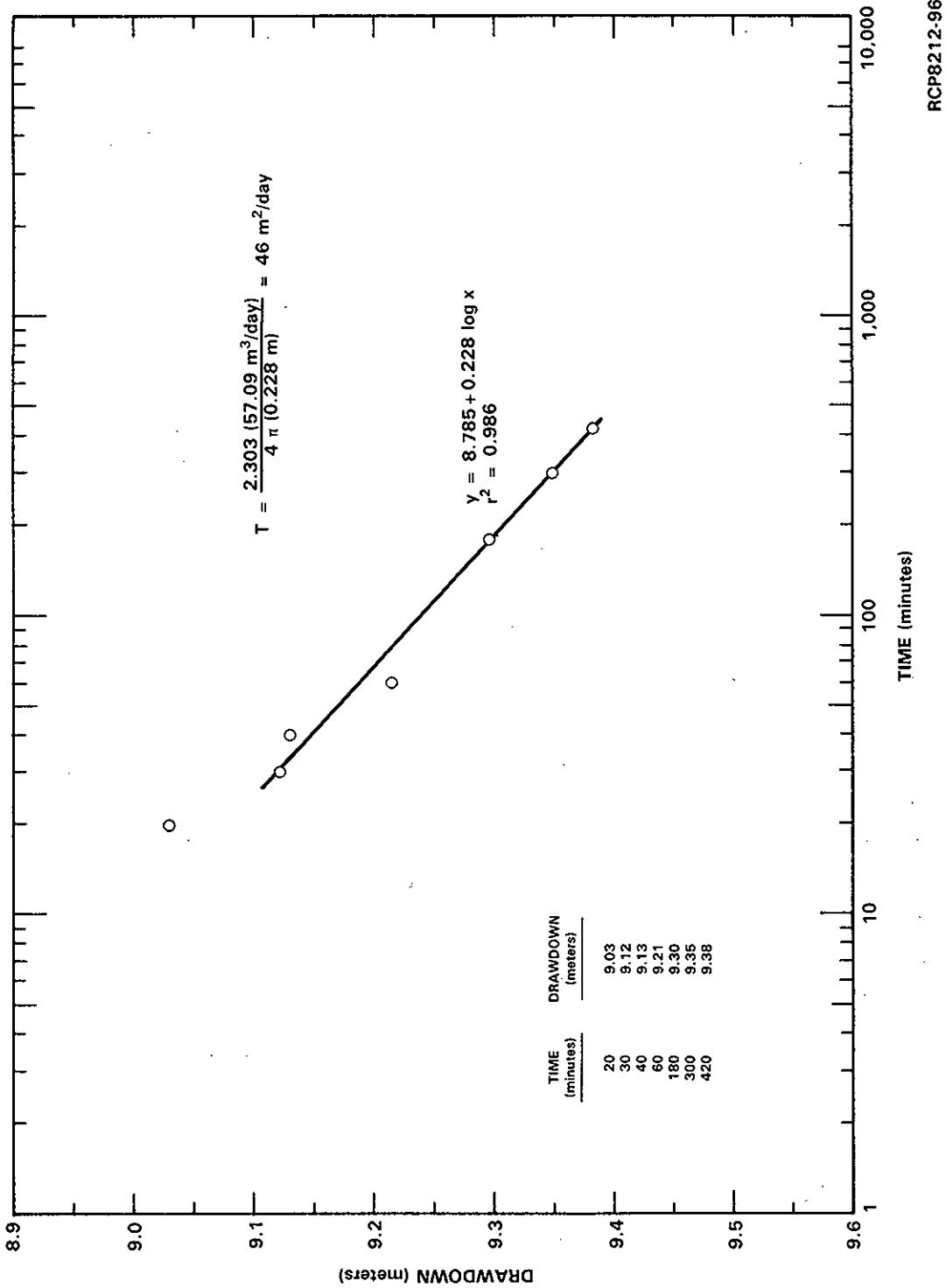
APPENDIX C

CONSTANT DISCHARGE AND RECOVERY
TEST DATA AND ANALYSES



RCP8302-30

FIGURE C.1. Recovery Test: 299-E16-1, 5/15/82, Elephant Mountain Fracture Zone



RCP8212-96

FIGURE C.2. Constant Discharge: 299-E16-1, 7/12/82, Elephant Mountain Interflow Zone

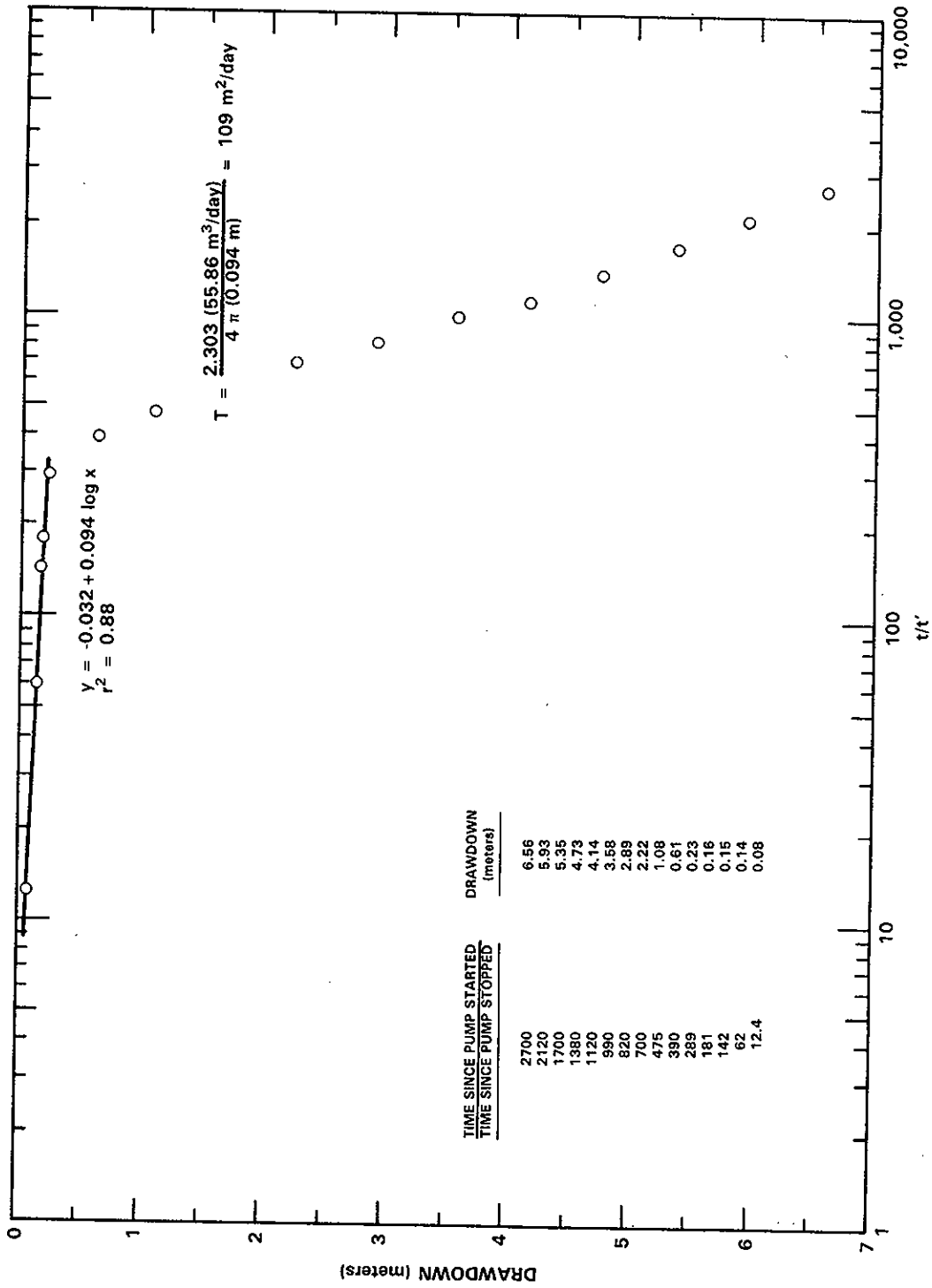
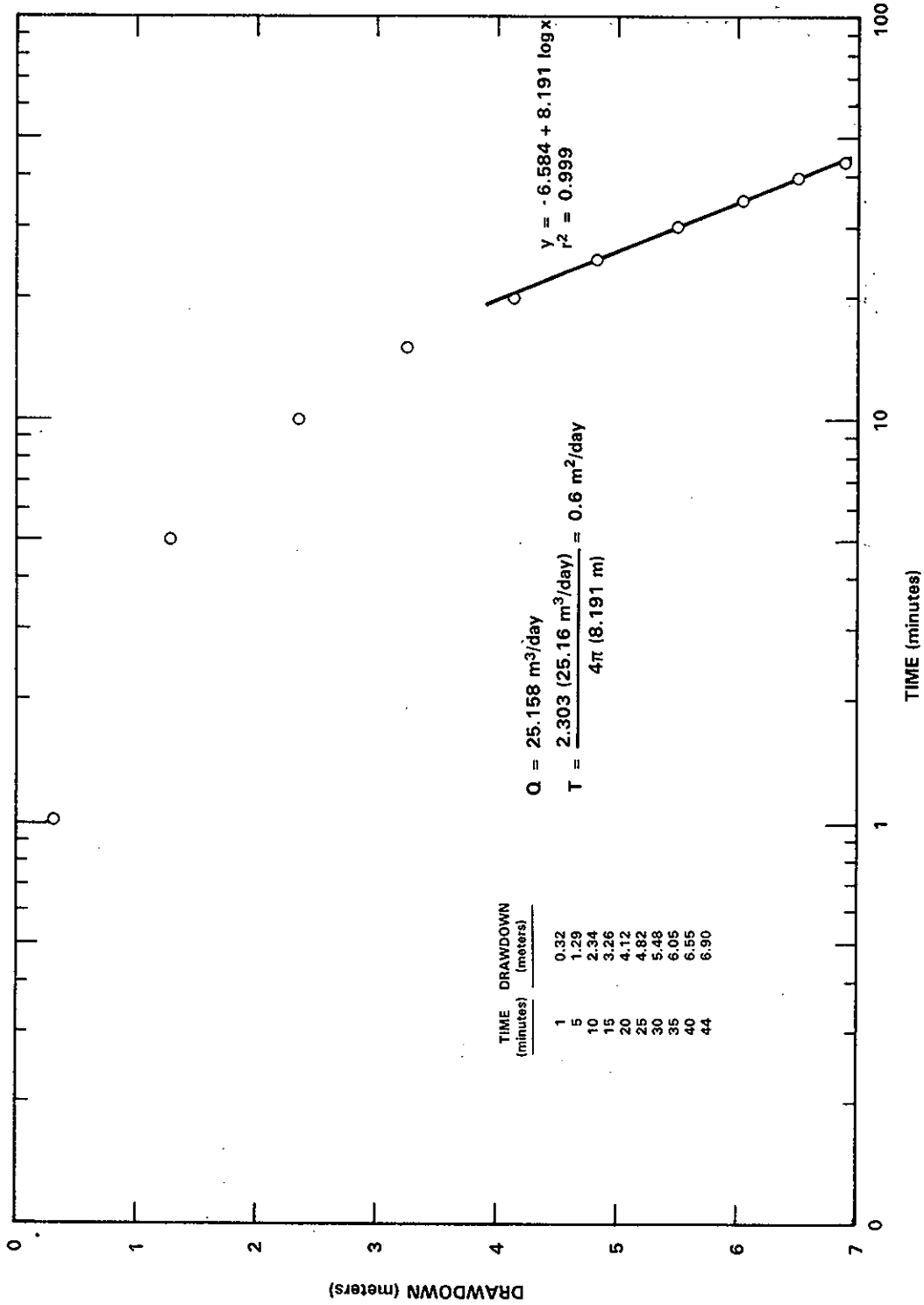
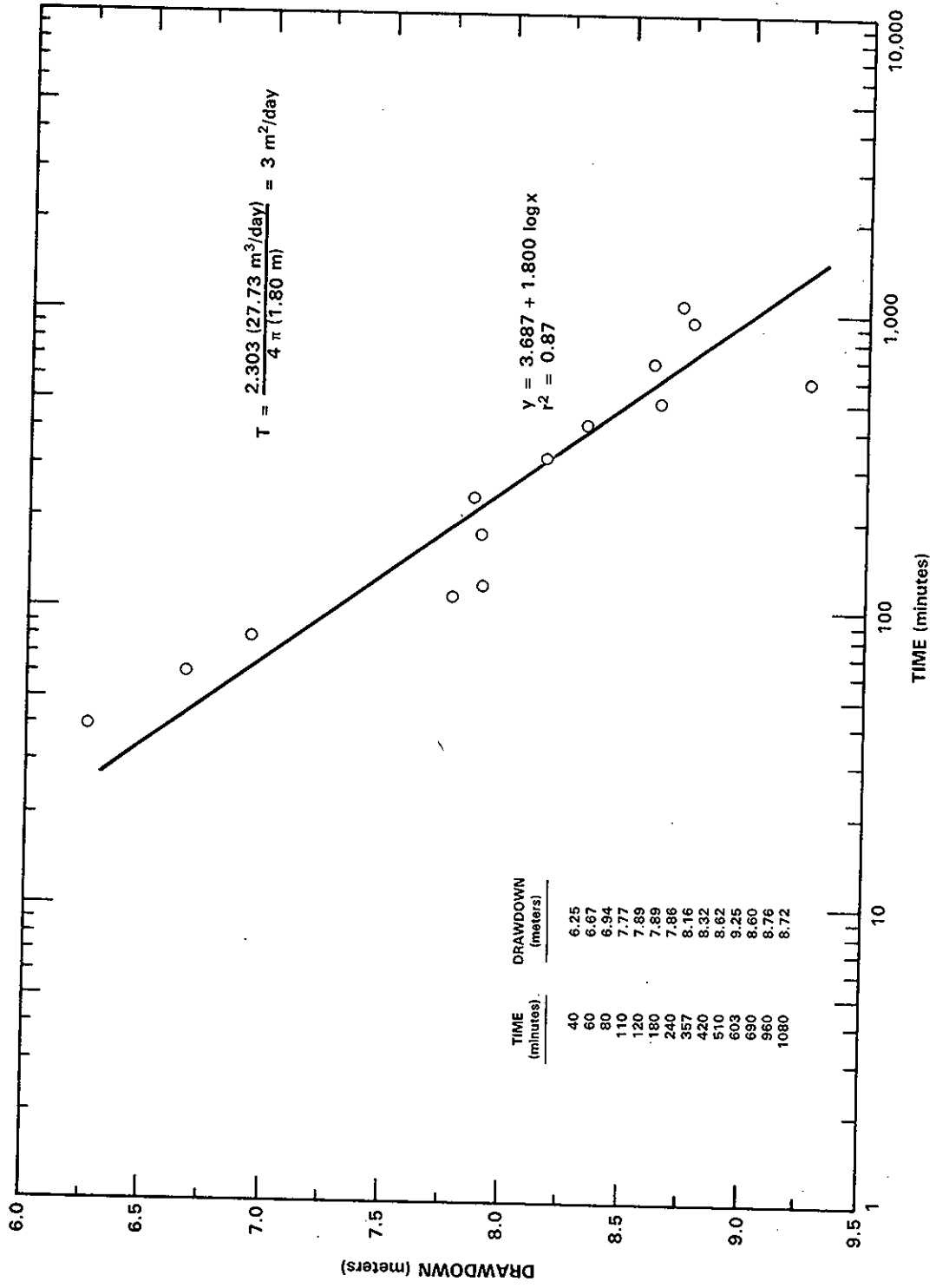


FIGURE C.3. Recovery Test: 299-E16-1, 7/13/82, Elephant Mountain Interflow Zone RCP8212-97



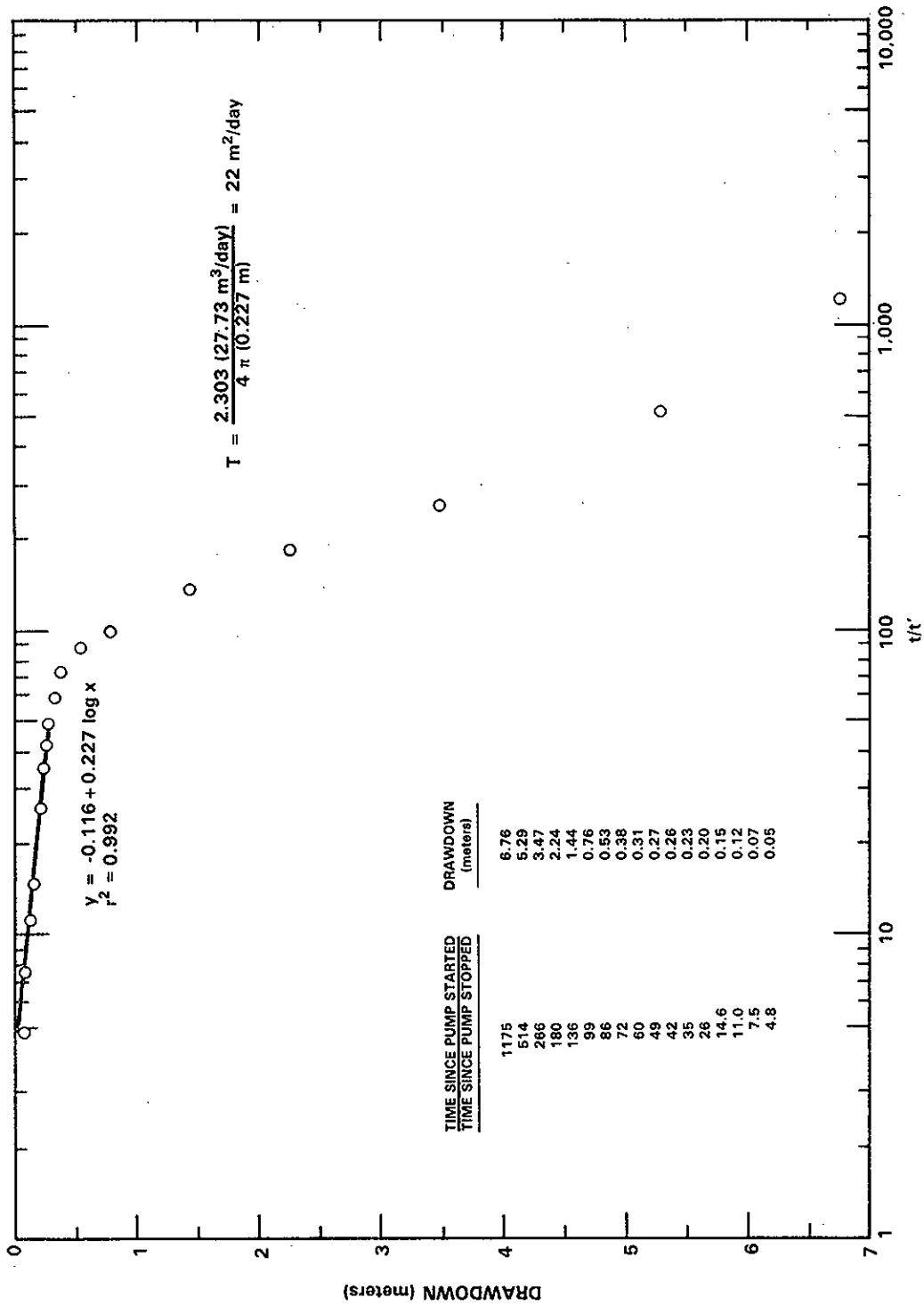
RCP8302-33

FIGURE C.4. Constant Discharge: 299-E26-8, 3/23/82, Lower Unconfined



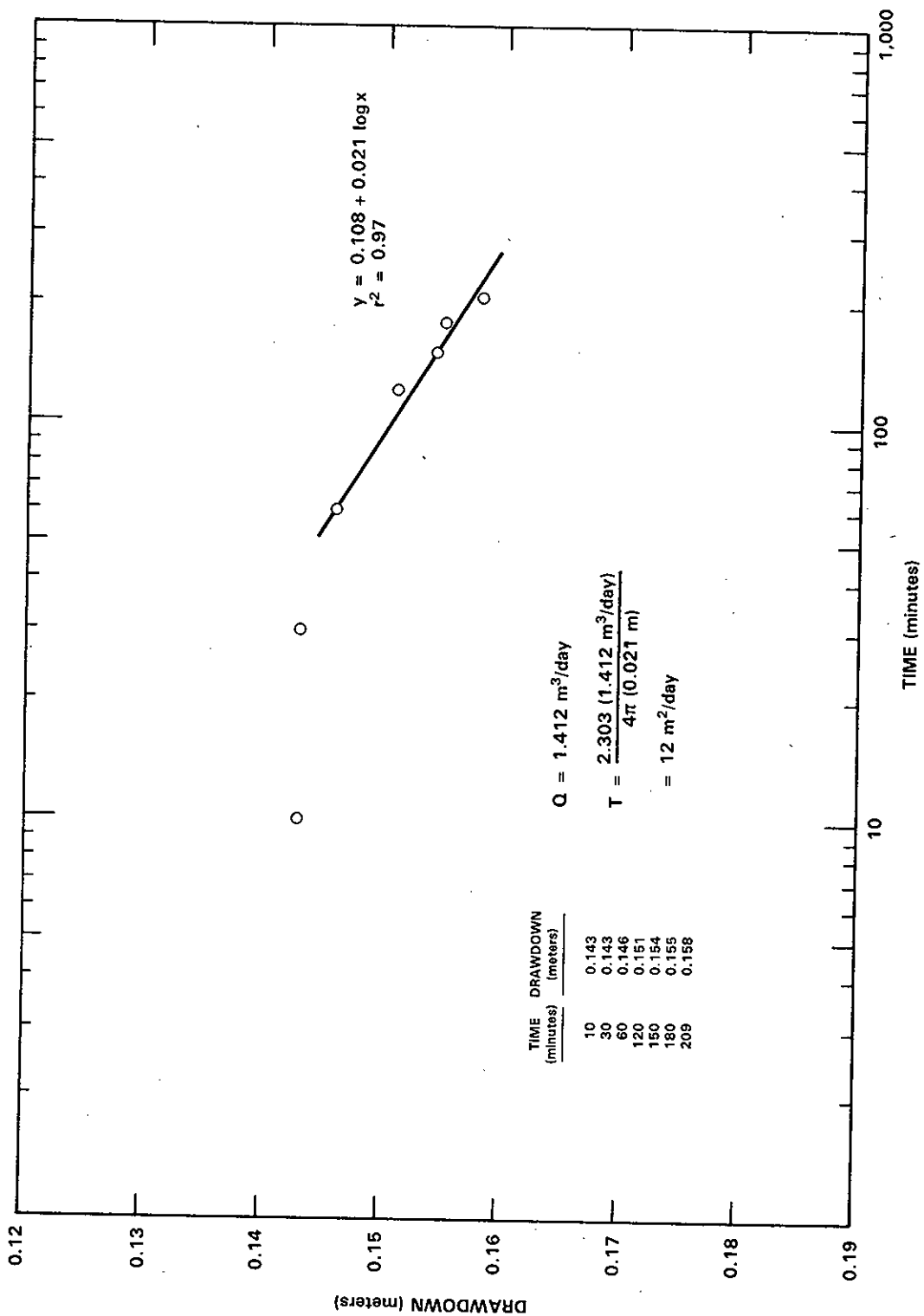
RCP8212-99

FIGURE C.5. Constant Discharge: 299-E26-8, 5/17-19/82, Rattlesnake Ridge



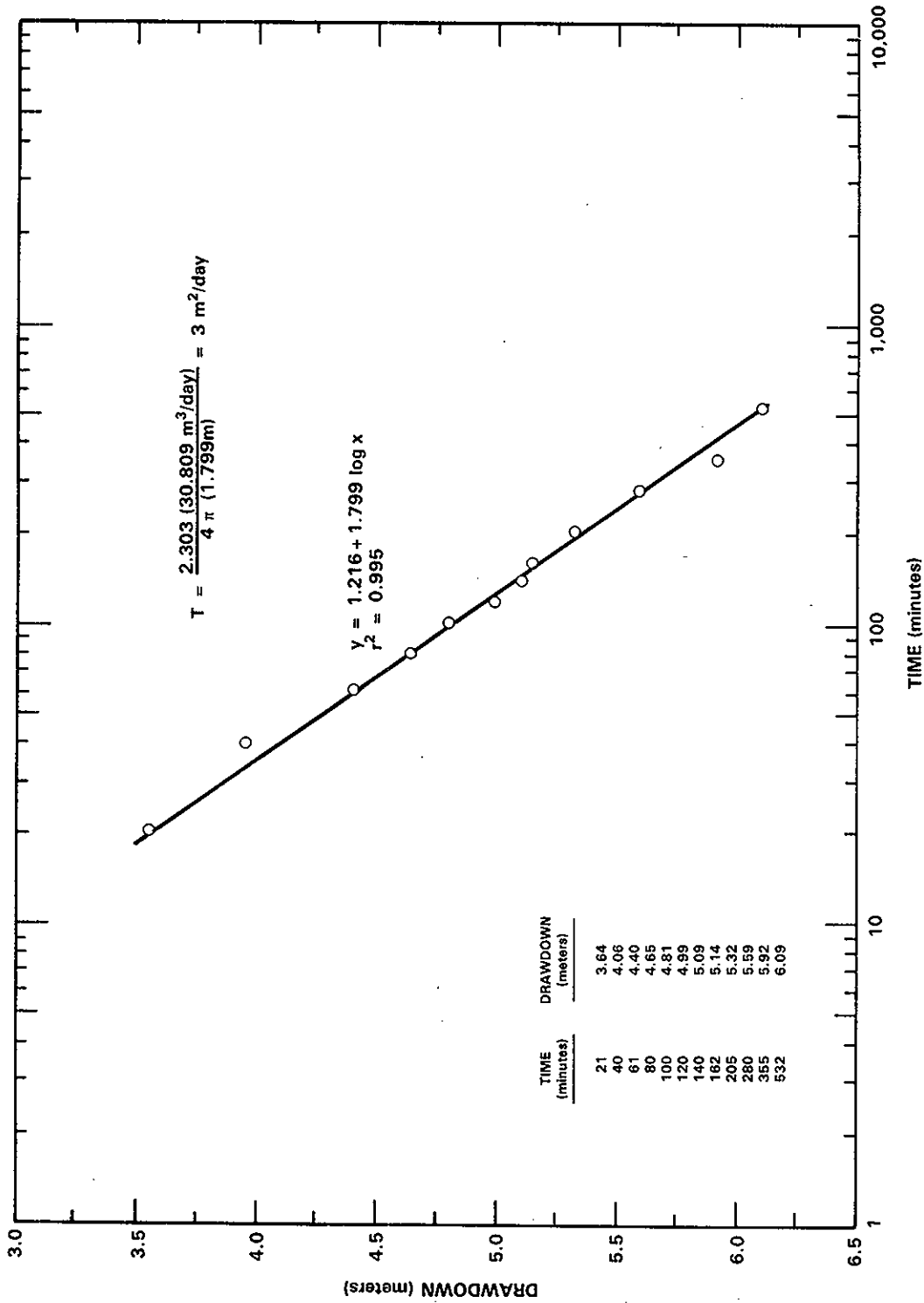
RCP8212-98

FIGURE C.6. Recovery Test: 299-E26-8, 5/19,20/82, Rattlesnake Ridge



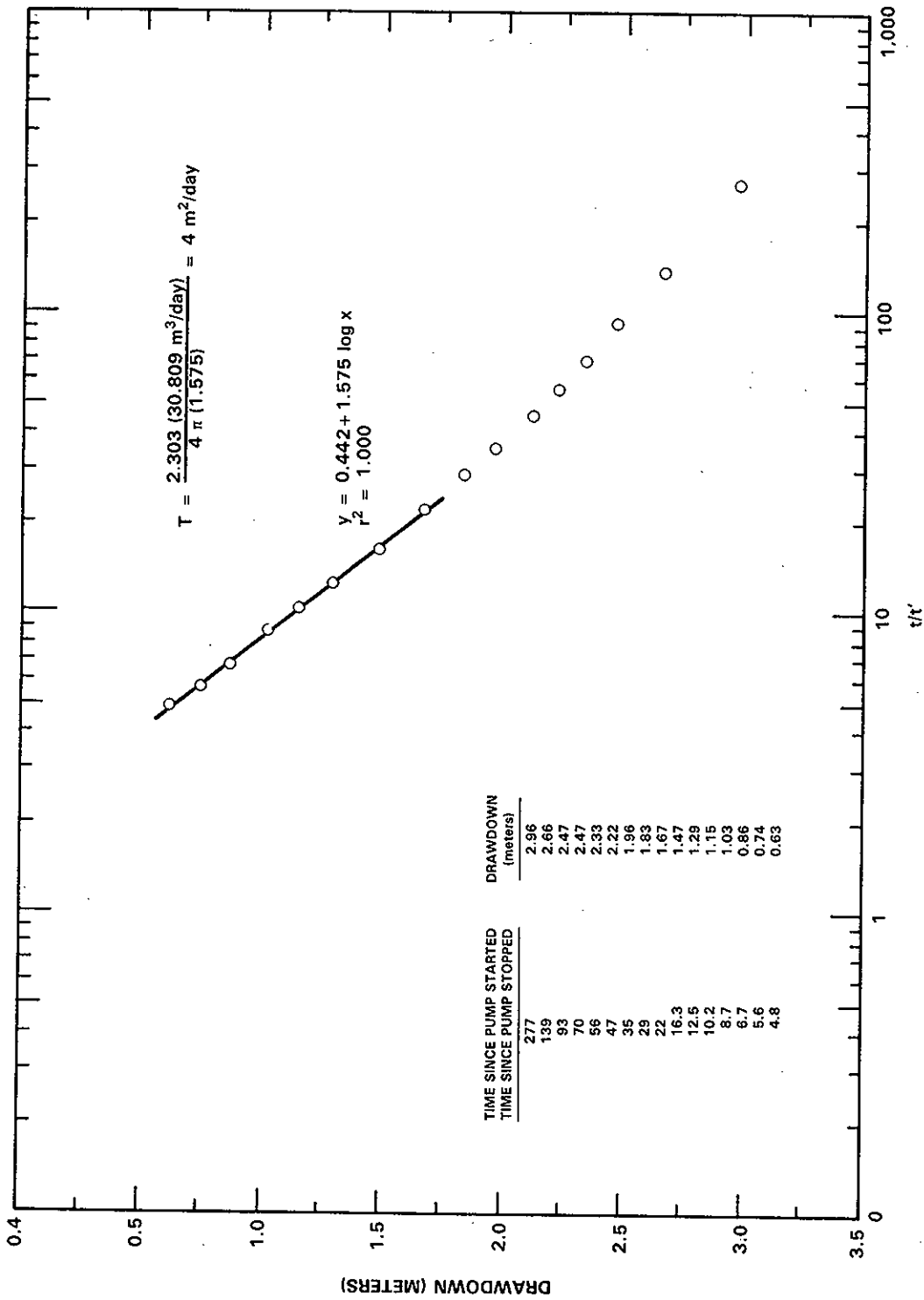
RCP8302-32

FIGURE C.7. Constant Discharge: 299-E33-12, 5/11/82, Lower Unconfined



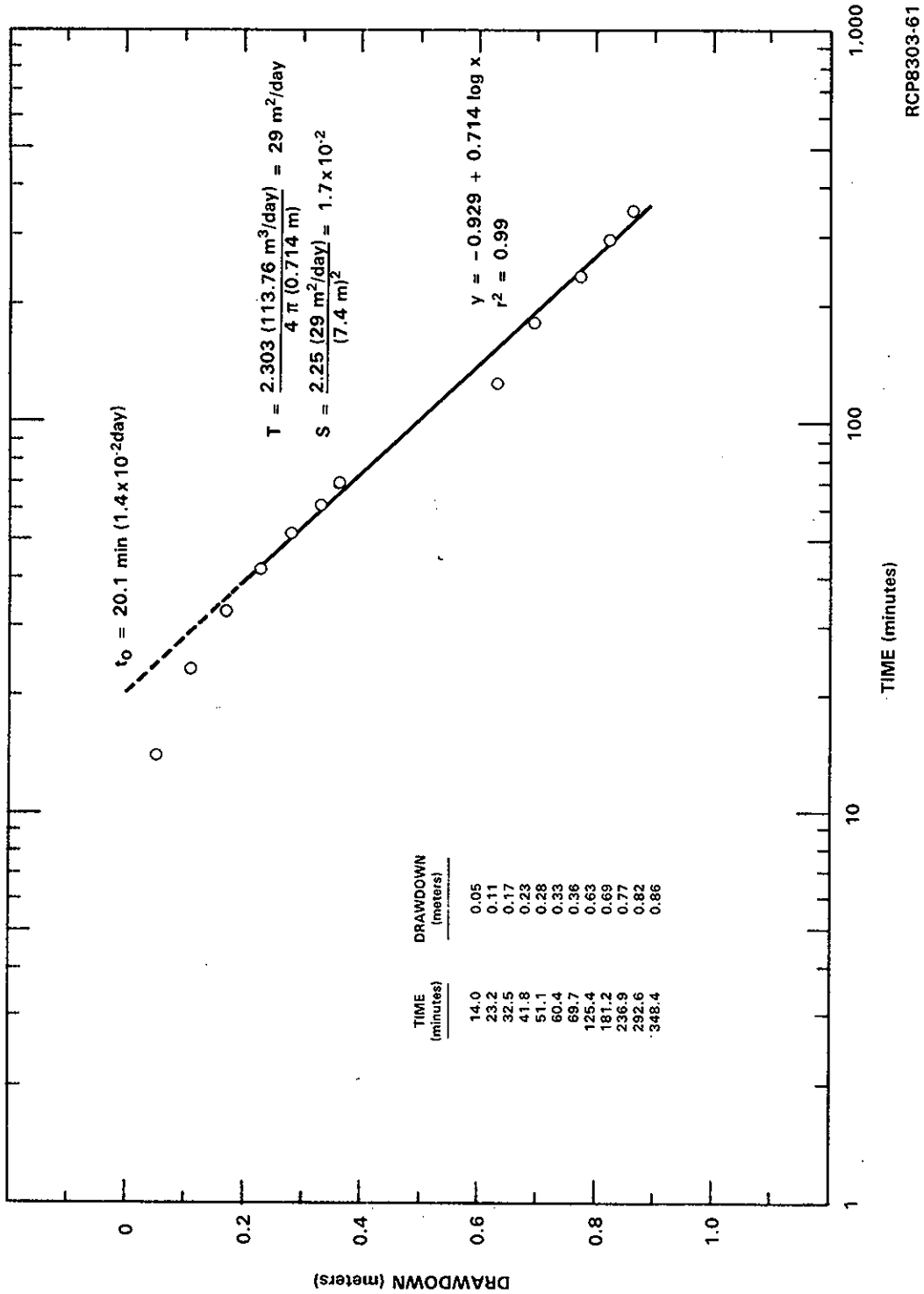
RCP8212-104

FIGURE C.8. Constant Discharge: 299-E33-12, 5/20-22/82, Rattlesnake Ridge



RCP8212-105

FIGURE C.9. Recovery Test: 299-E33-12, 5/22,23/82, Rattlesnake Ridge



RCP8303-61

FIGURE C.10. Constant Discharge: 699-42-40A, 1/18/82, Unconfined Aquifer

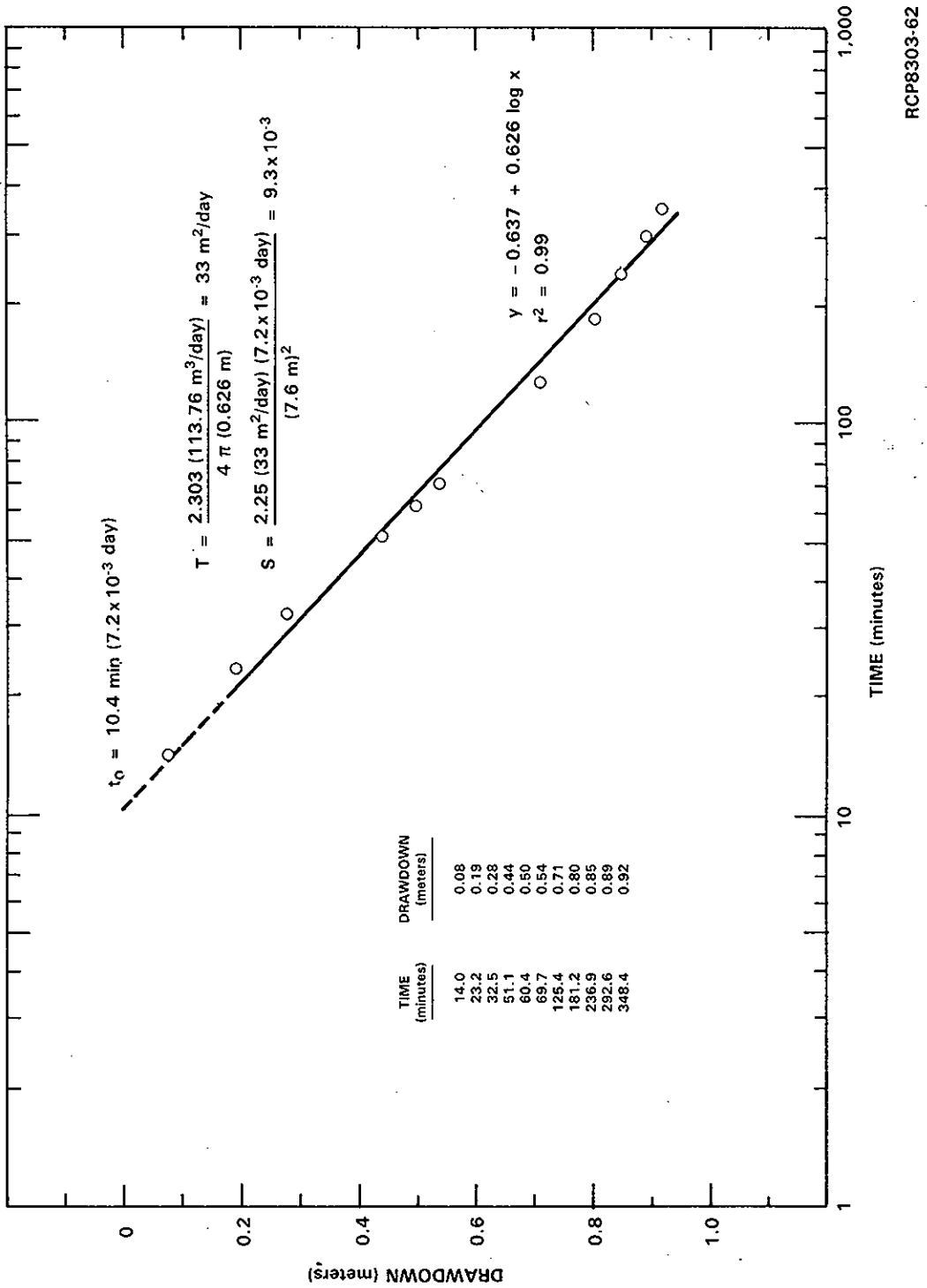


FIGURE C.11. Constant Discharge: 699-42-40B, 1/18/82, Unconfined Aquifer

RCP8303-62

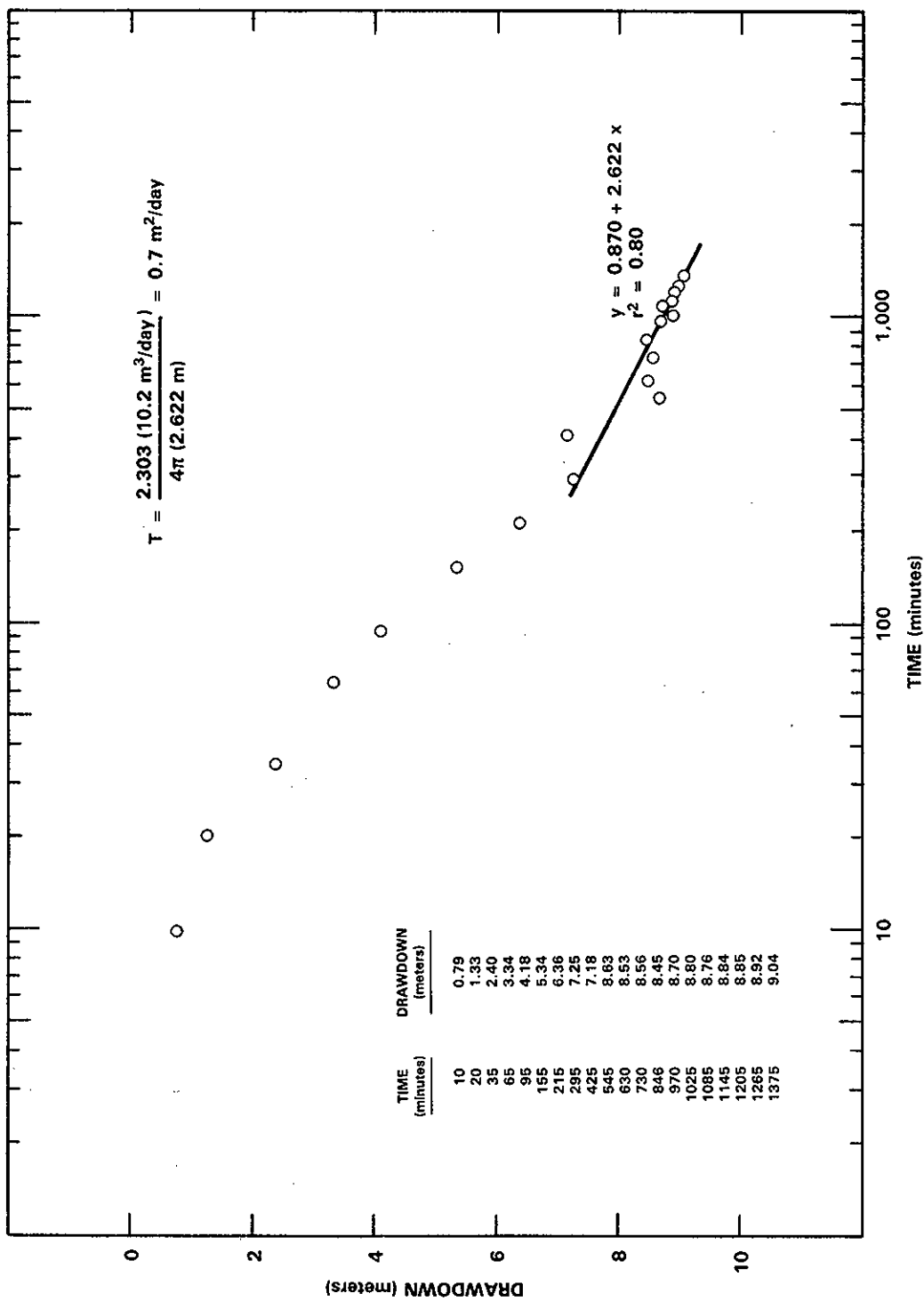
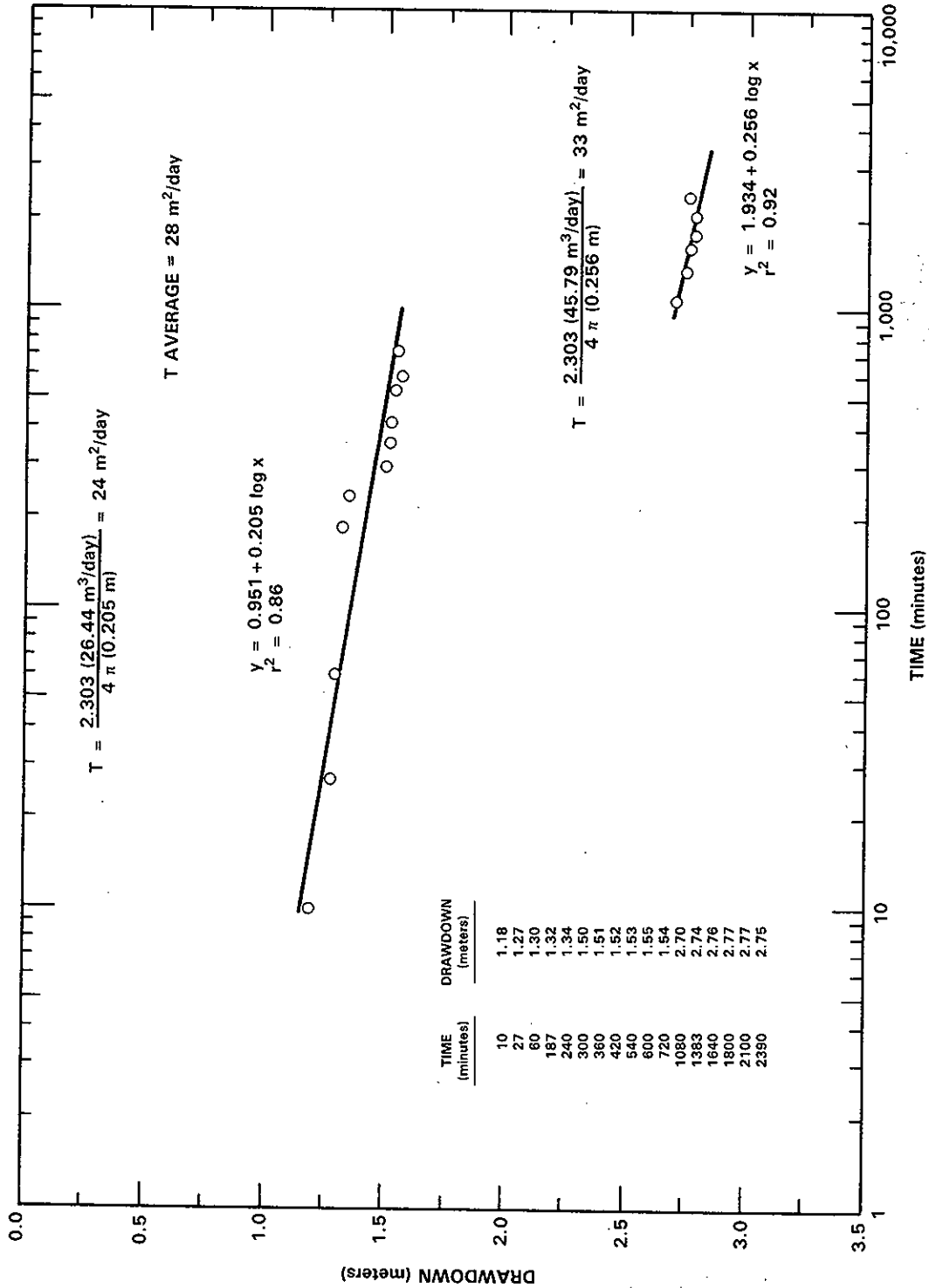


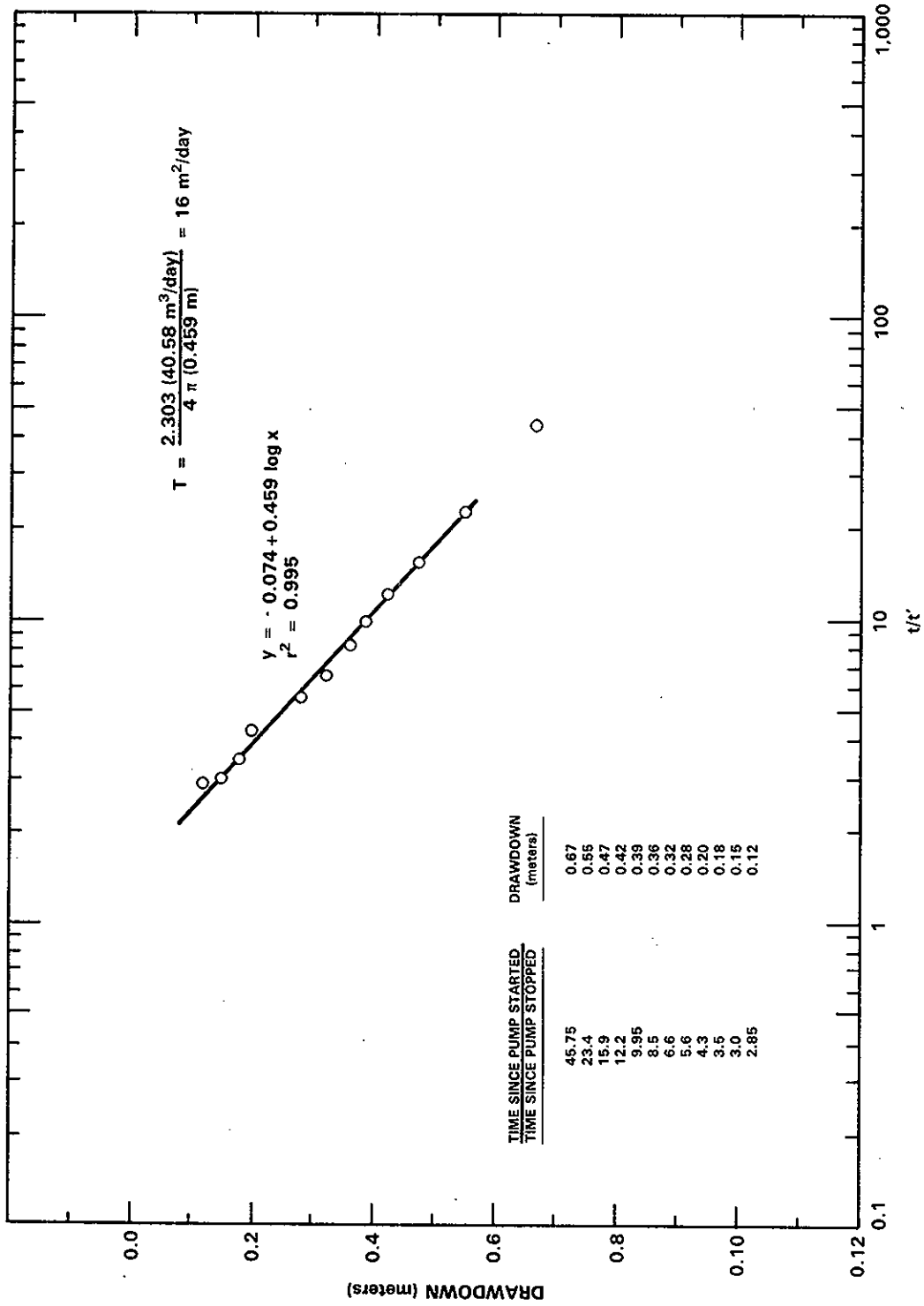
FIGURE C.12. Constant Discharge: 699-42-40C, 4/15/82 Elephant Mountain Interflow Zone

RCP8302-29



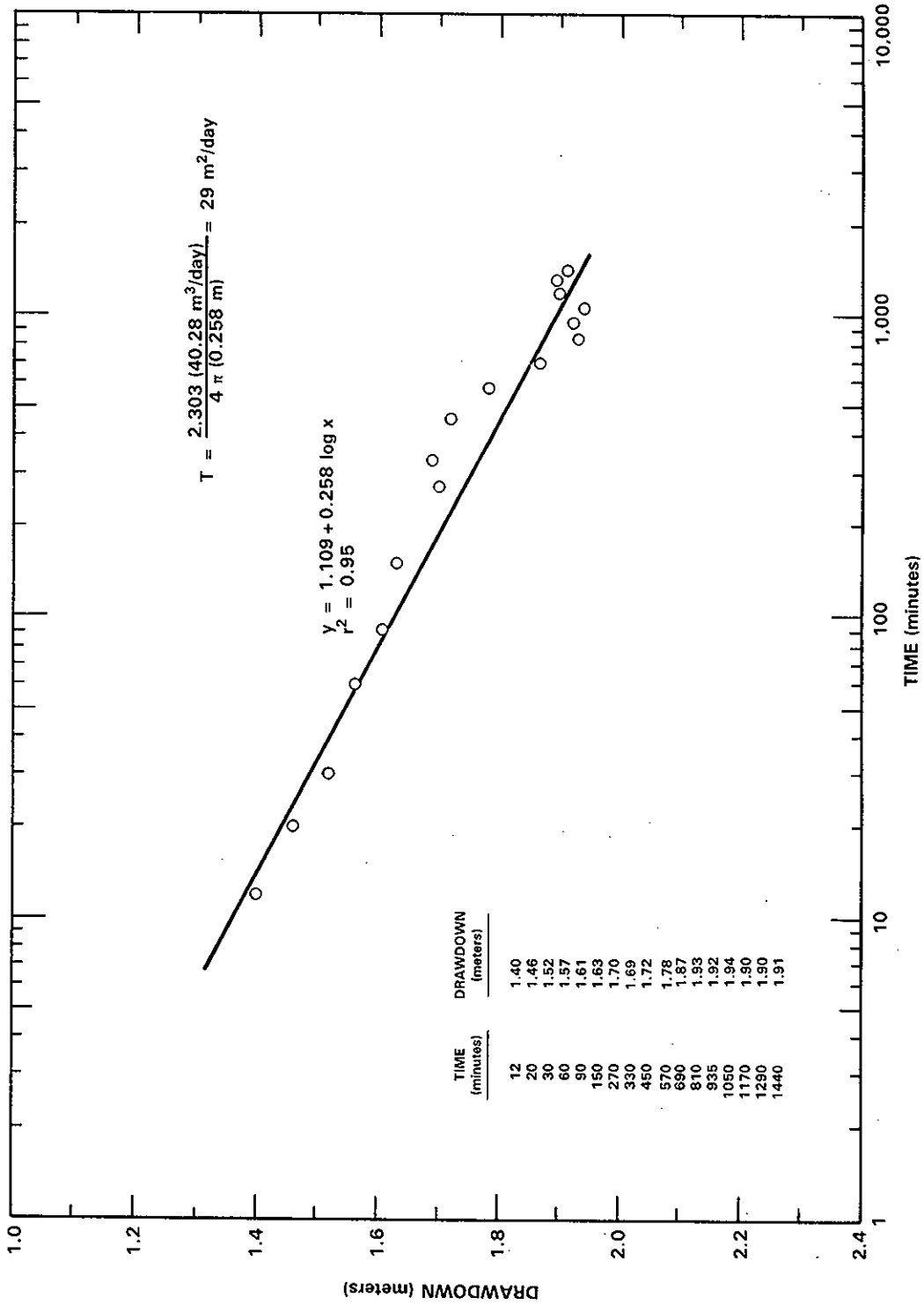
RCP8212-93

FIGURE C.13. Constant Discharge: 699-42-40C, 5/19-21/82, Rattlesnake Ridge



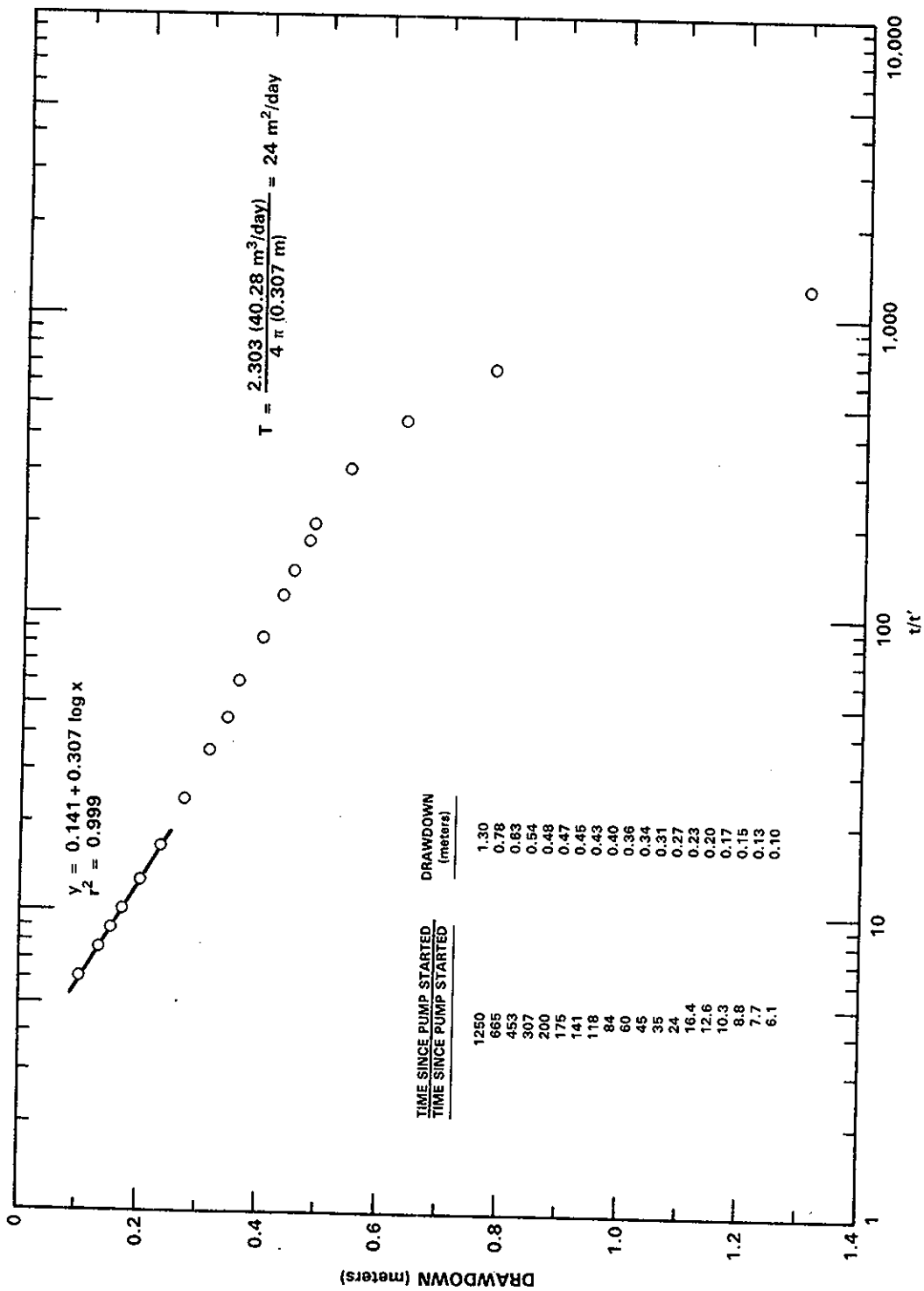
RCP8212-92

FIGURE C.14. Recovery Test: 699-42-40C, 5/21,22/82, Rattlesnake Ridge



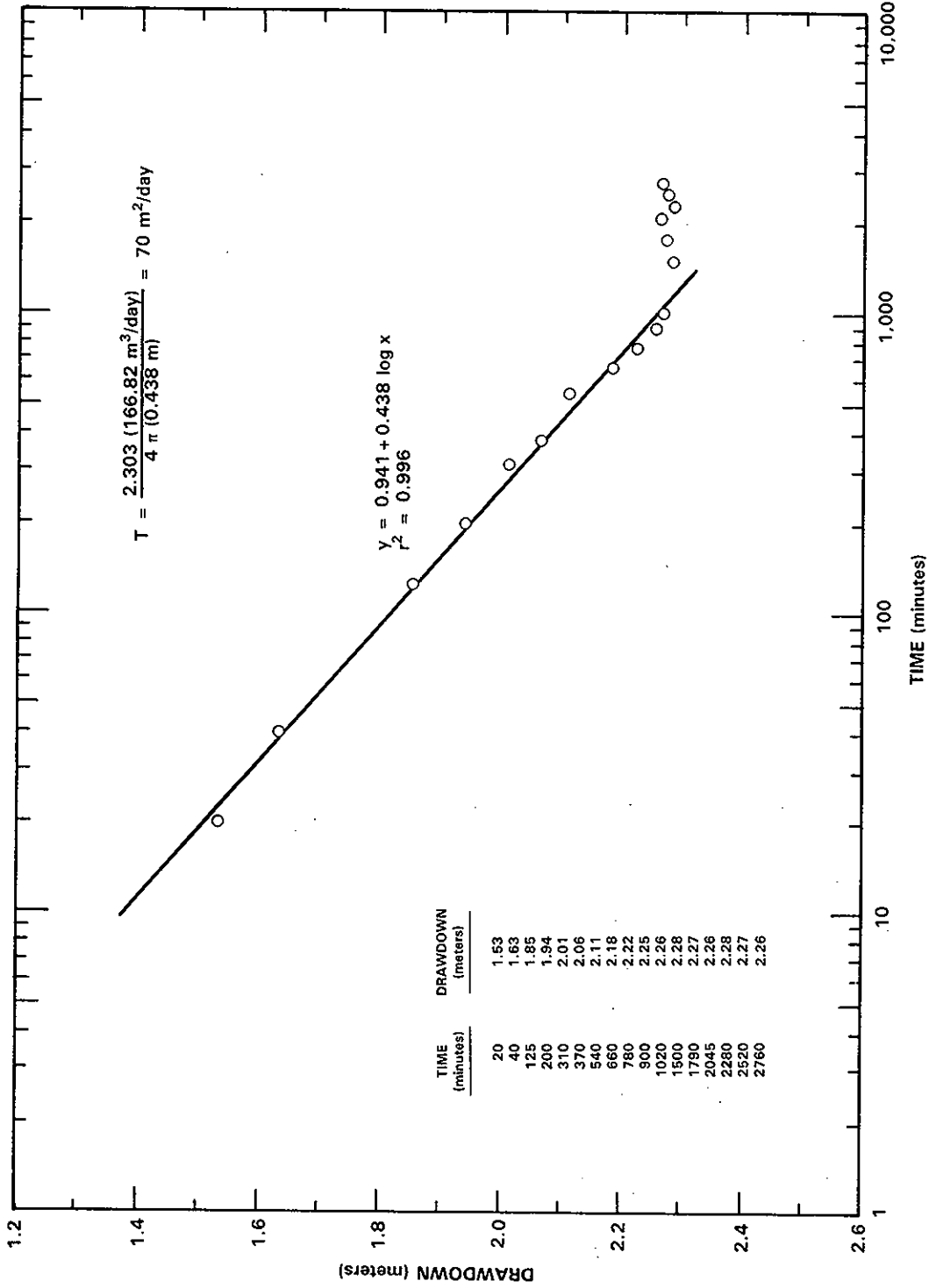
RCP8212-94

FIGURE C.15. Constant Discharge: 699-42-40C, 11/18,19/82, Rattlesnake Ridge



RCP8212-95

FIGURE C.16. Recovery Test: 699-42-40C, 11/19/82, Rattlesnake Ridge



RCP8212-100

FIGURE C.17. Constant Discharge: 699-40-55B, 5/26-28/82, Rattlesnake Ridge

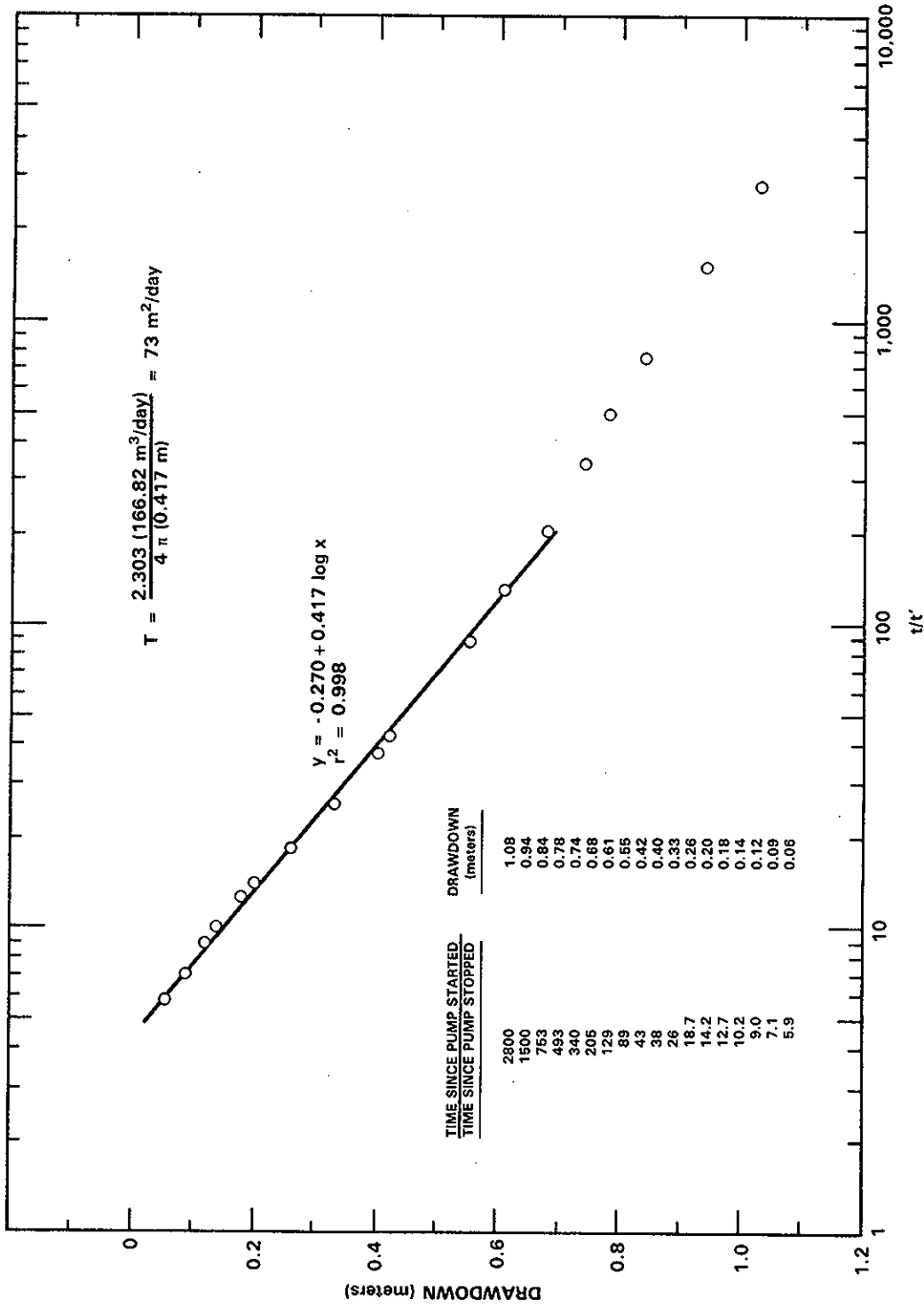
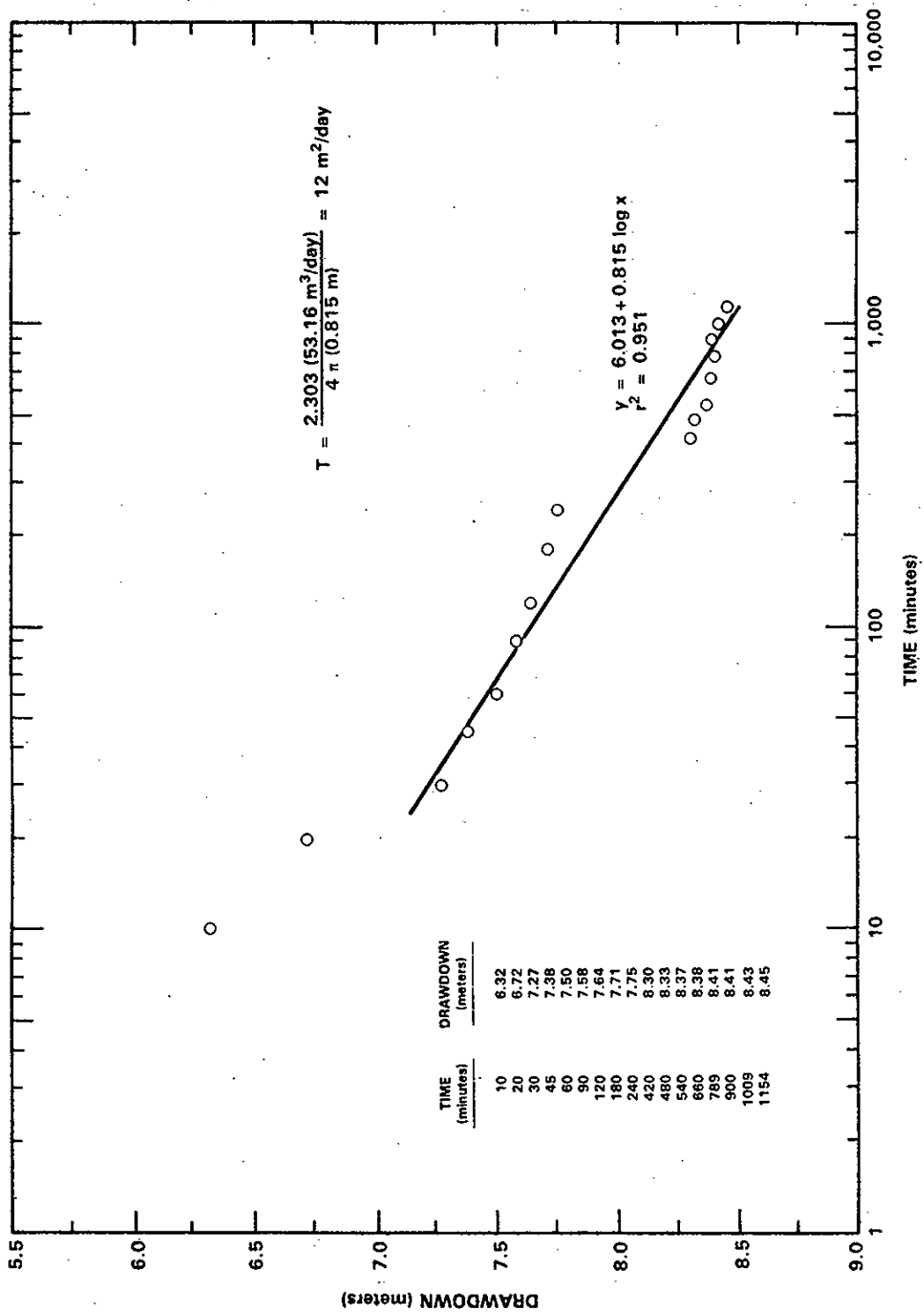
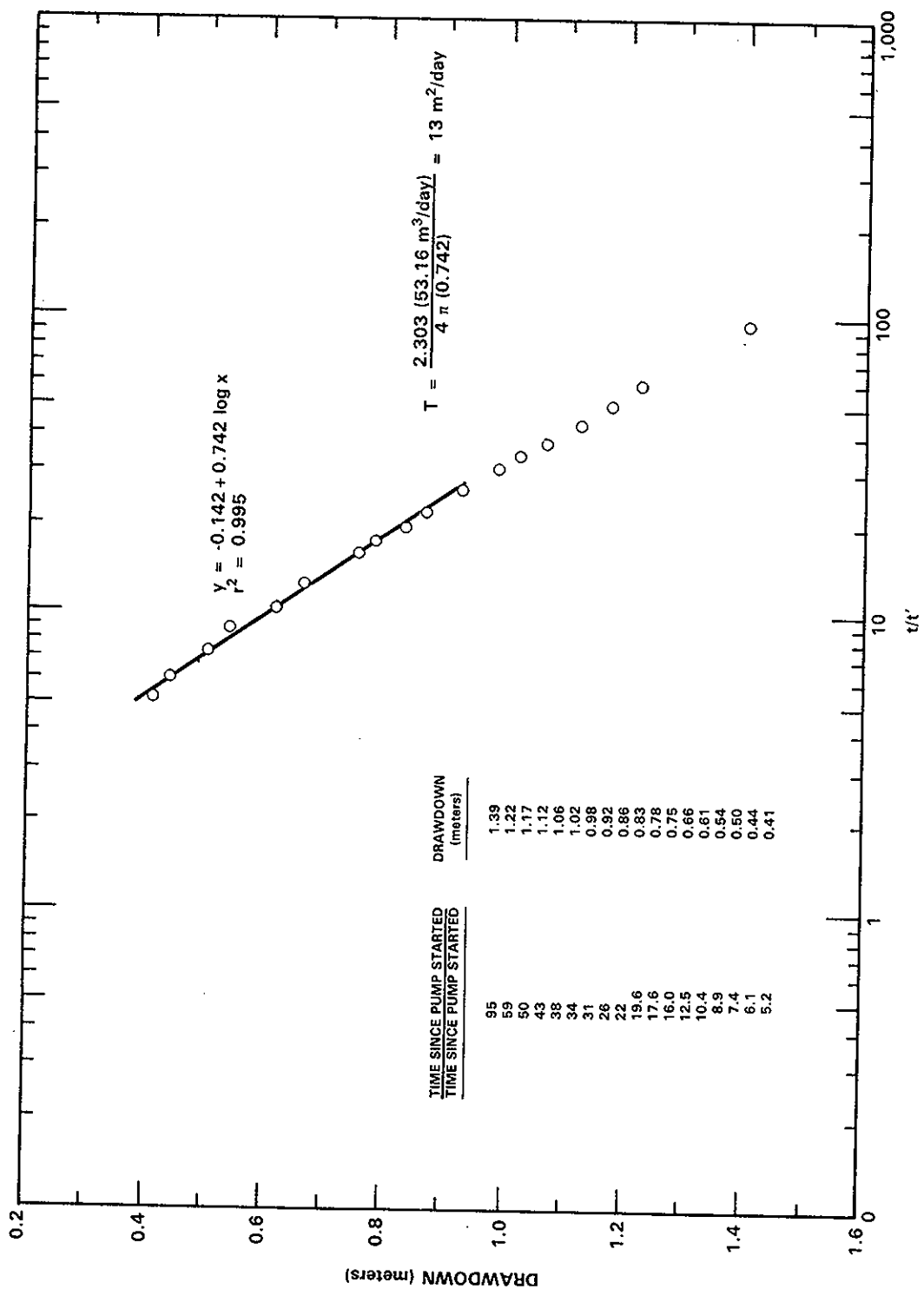


FIGURE C.18. Recovery Test: 699-49-55B, 5/28,29/82, Rattlesnake Ridge RCP8212-101



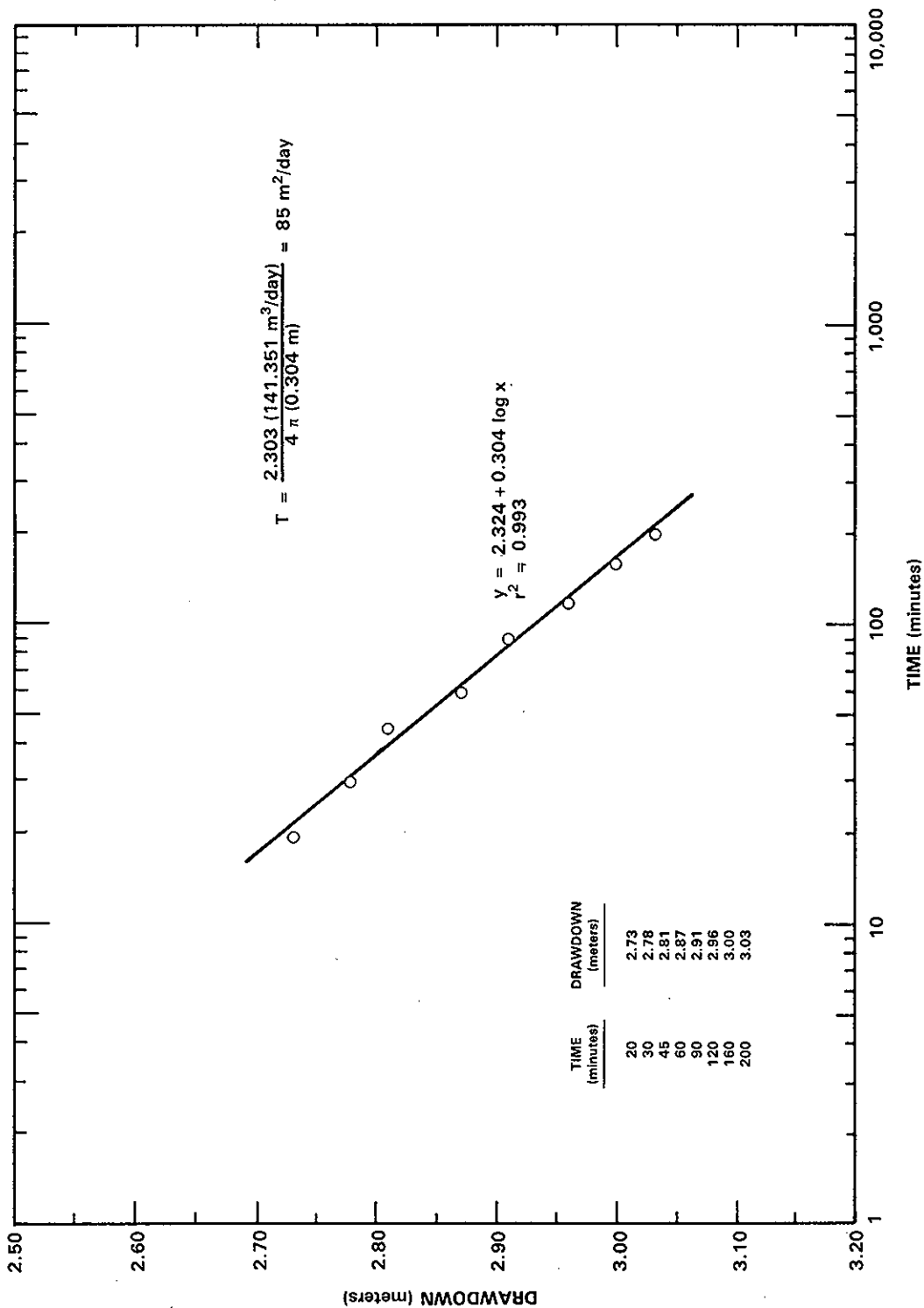
RCP8212-107

FIGURE C.19. Constant Discharge: 699-54-57, 5/17,18/82, Rattlesnake Ridge



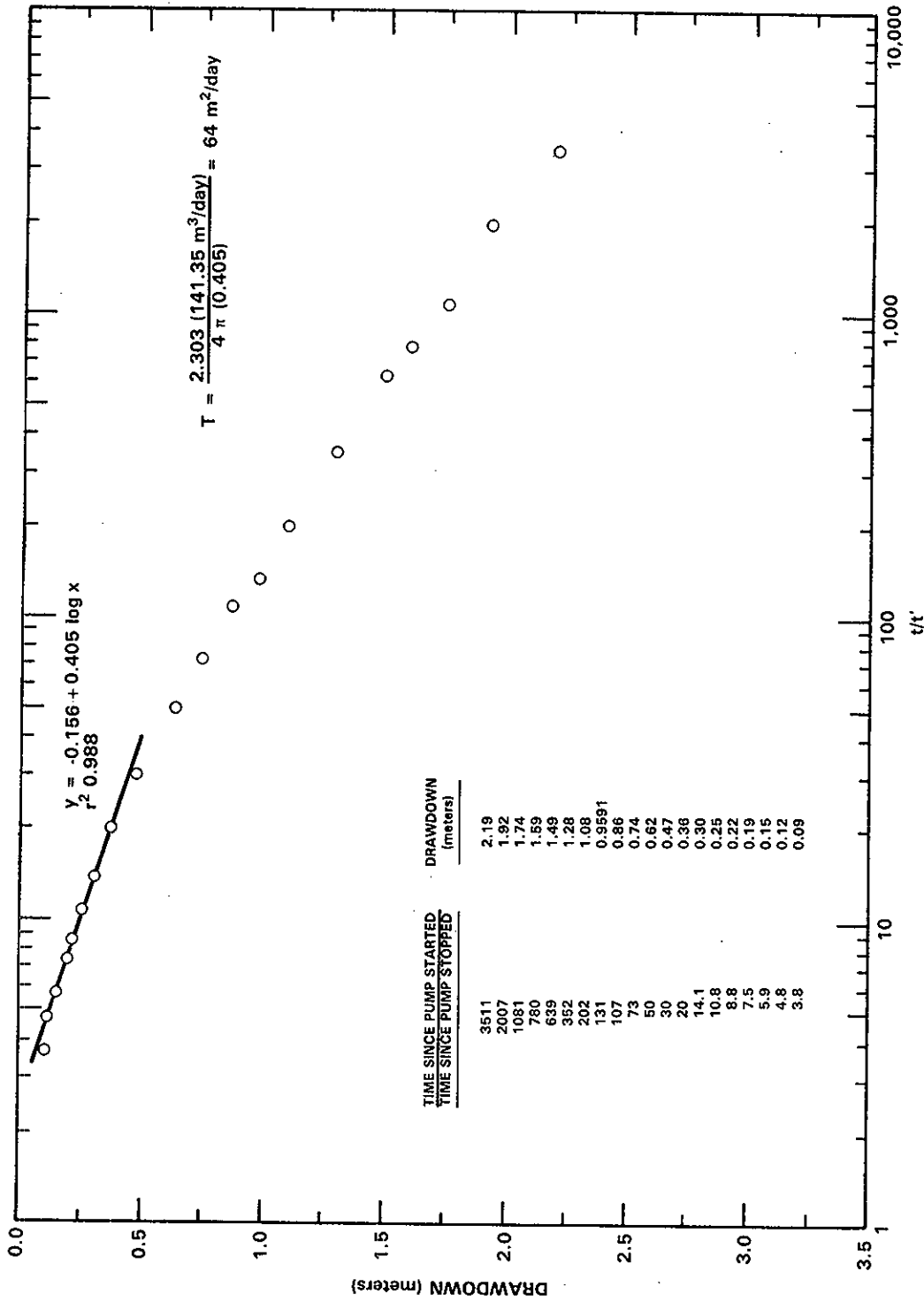
RCP8212-106

FIGURE C.20. Recovery Test: 699-54-57, 5/18/82, Rattlesnake Ridge



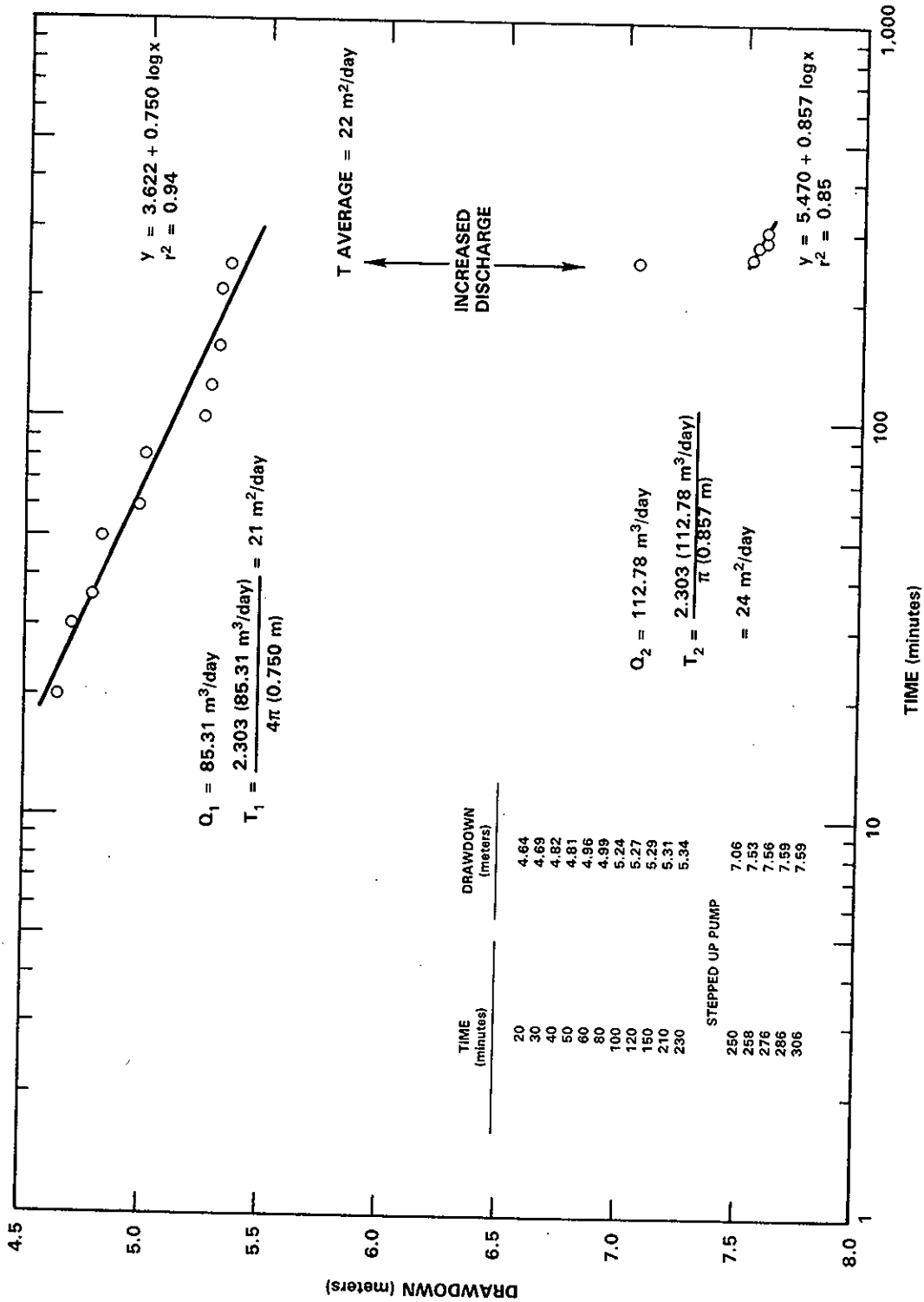
RCP8212-103

FIGURE C.21. Constant Discharge: 699-56-53, 6/2,3/82, Rattlesnake Ridge



RCP8212-102

FIGURE C.22. Recovery Test: 699-56-53, 6/3,4/82, Rattlesnake Ridge

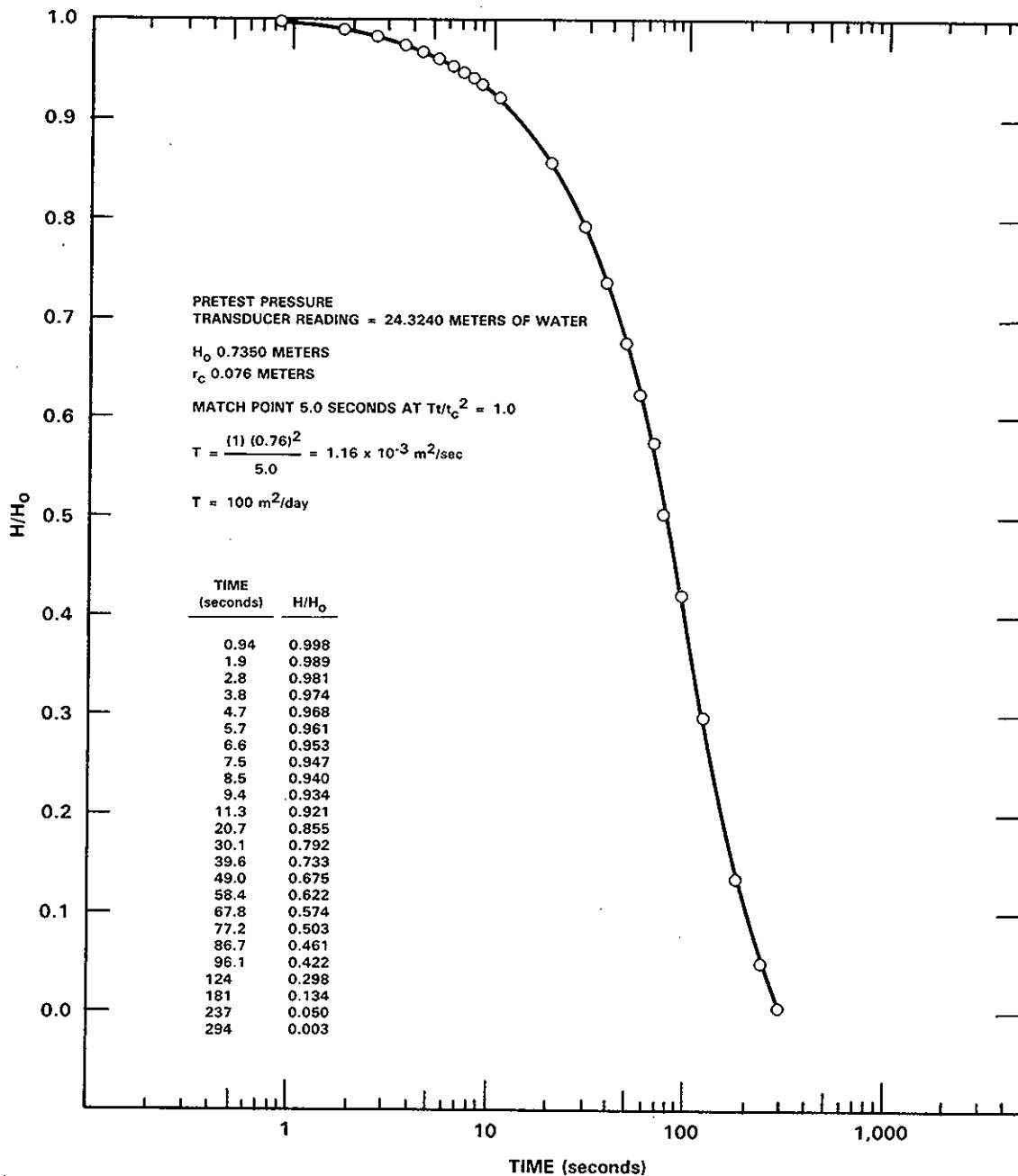


RCP8302-31

FIGURE C.23. Constant Discharge: 699-56-53, 11/11/82, Lower Unconfined

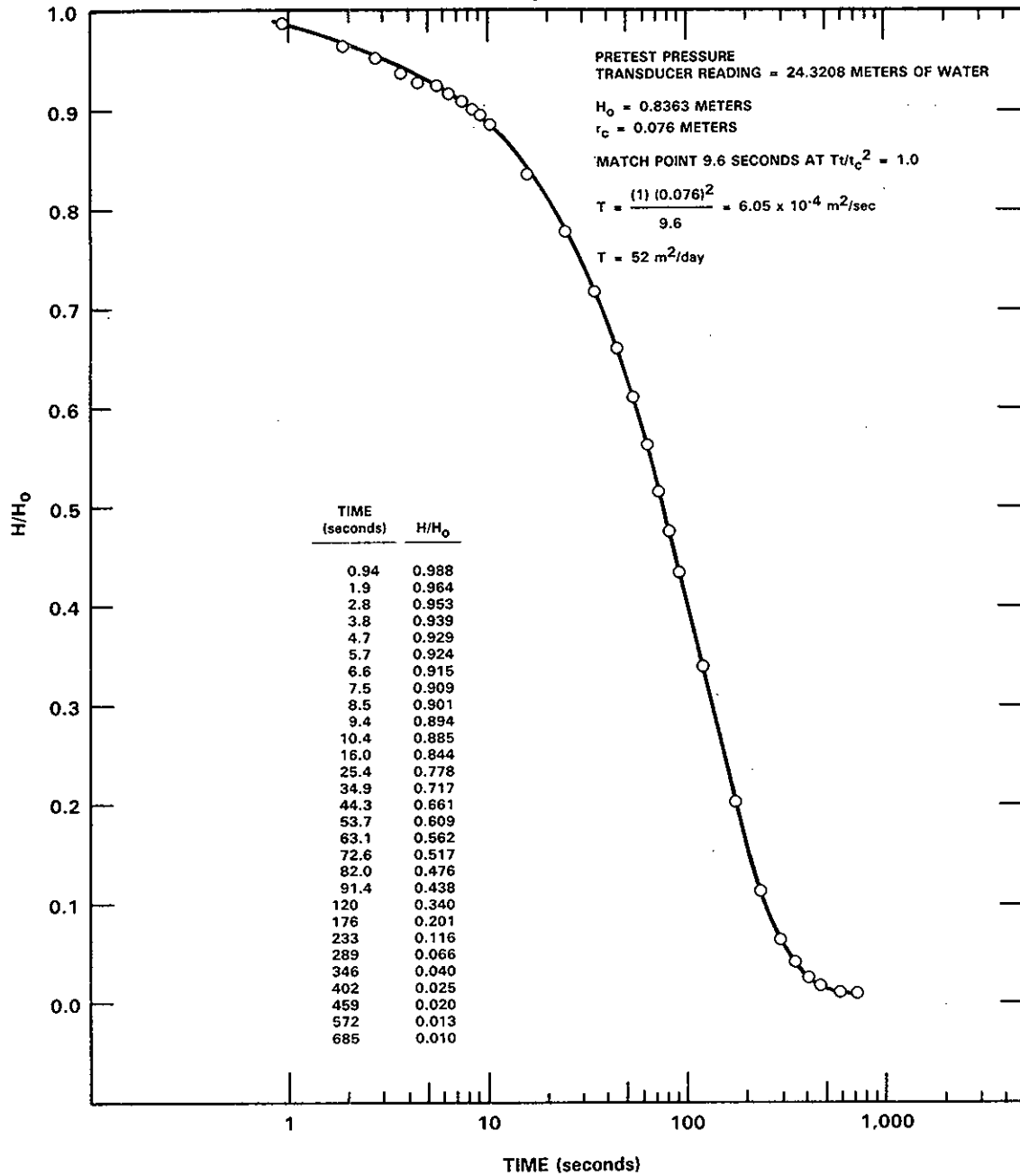
APPENDIX D

SLUG INJECTION AND WITHDRAWAL
TEST DATA AND ANALYSES



RCP8302-4

FIGURE D.1. Slug Injection Test: 299-E16-1, 11/30/82,
Elephant Mountain Interflow



RCP8302-3

FIGURE D.2. Slug Withdrawal Test: 299-E16-1, 11/30/82, Elephant Mountain Interflow

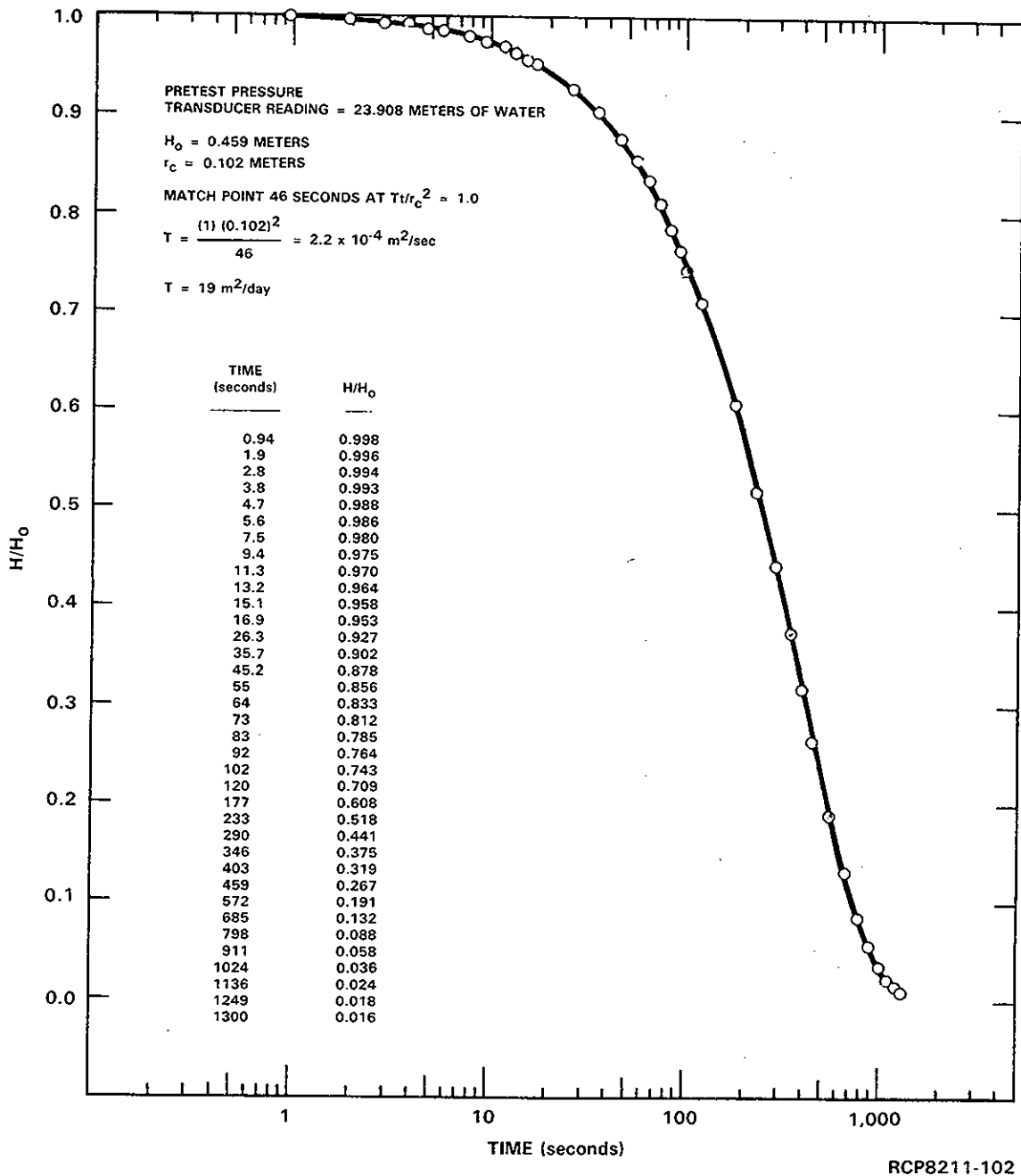
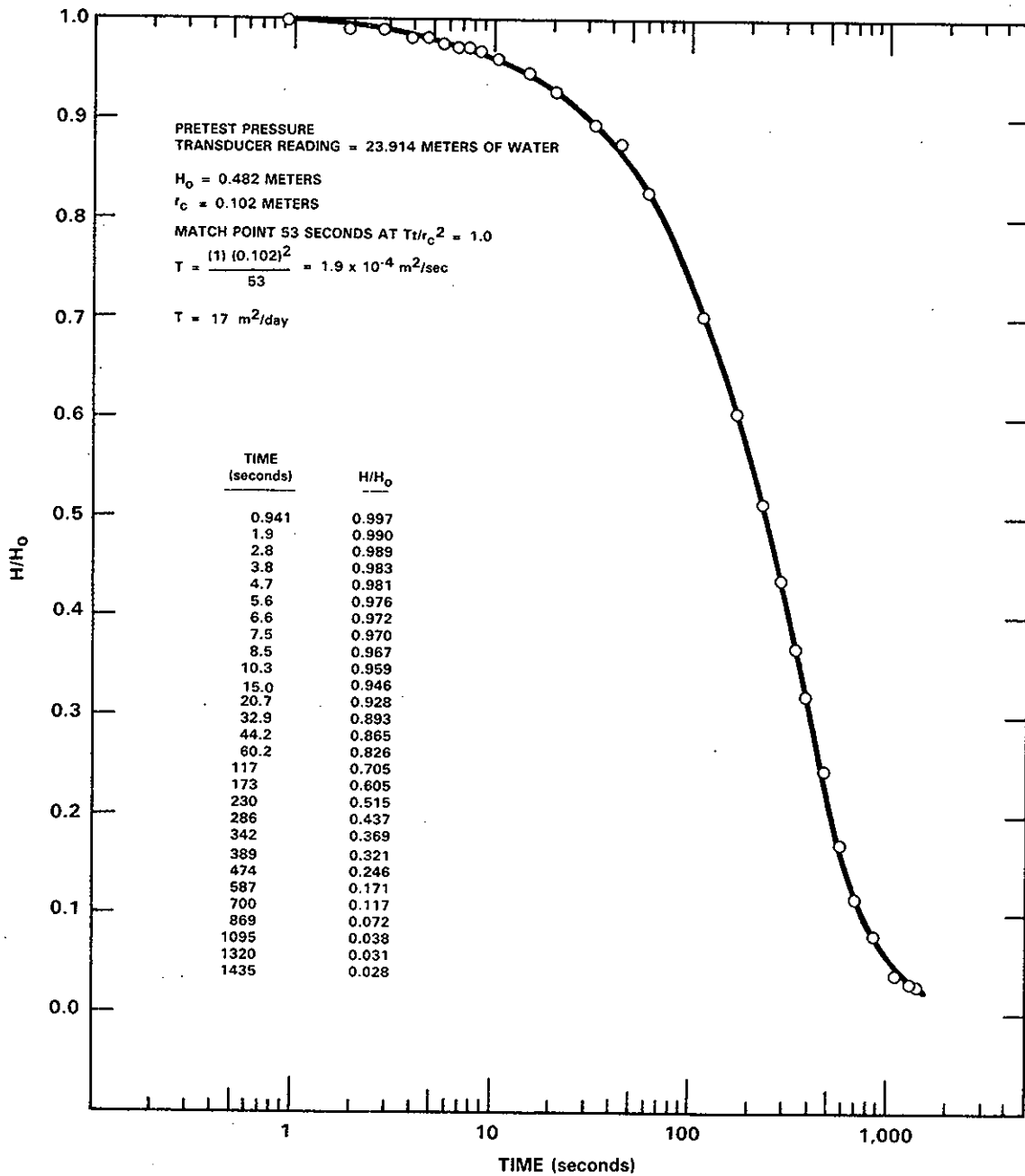


FIGURE D.3. Slug Injection Test: 299-E26-8, 11/9/82, Rattlesnake Ridge



RCP8211-103

FIGURE D.4. Slug Withdrawal Test: 299-E26-8, 11/9/82, Rattlesnake Ridge

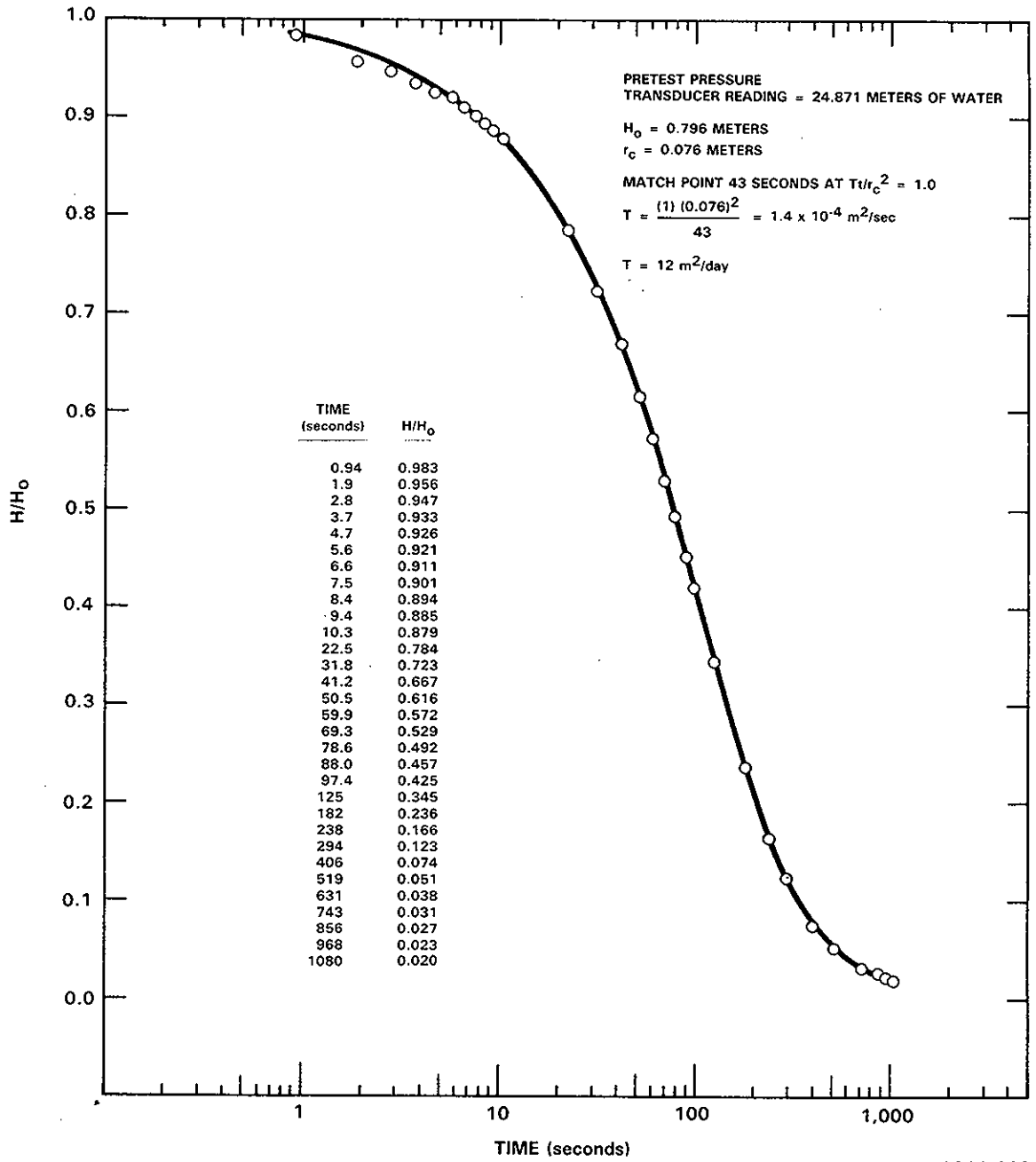
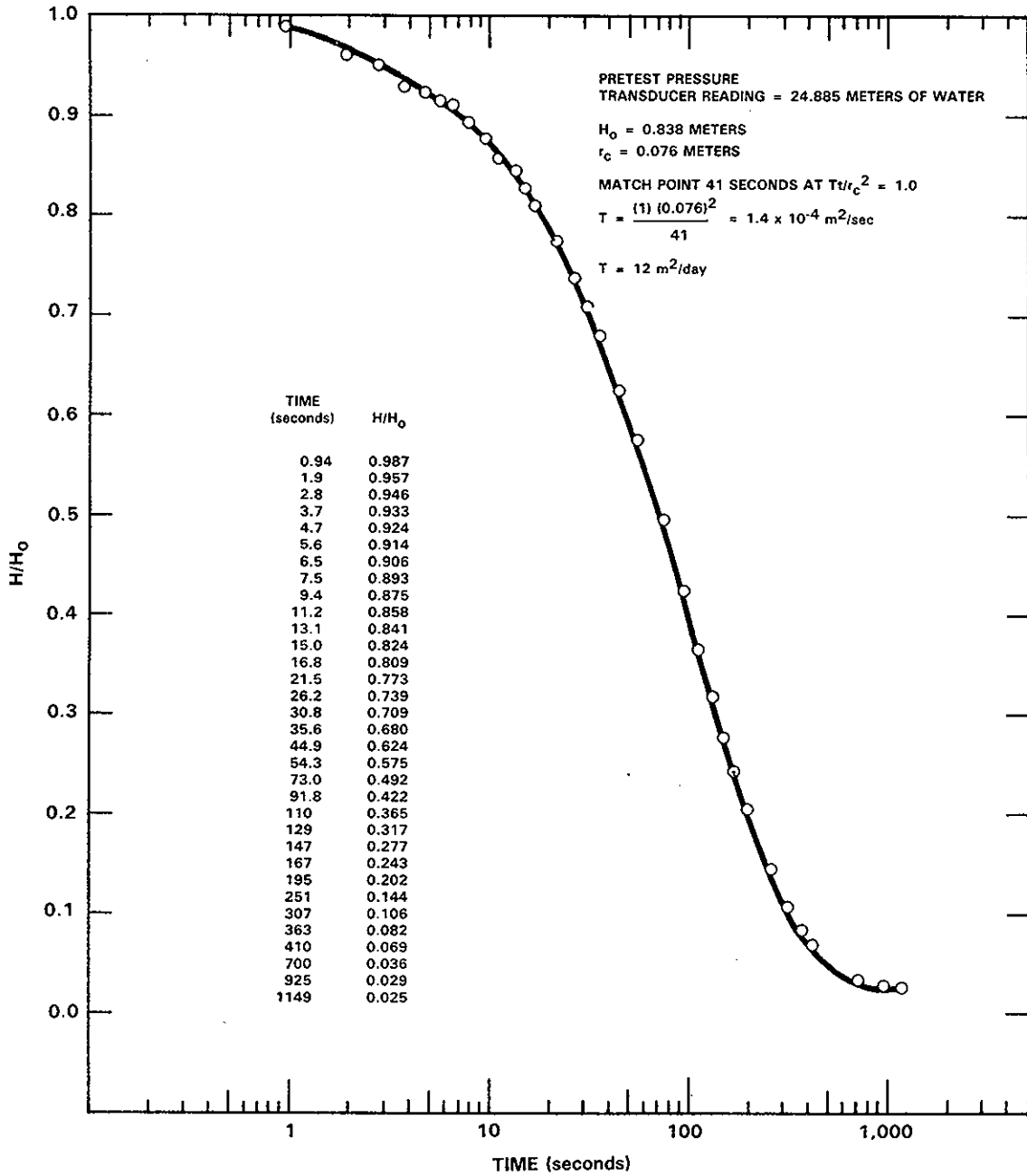


FIGURE D.5. Slug Injection: 299-E33-12, 11/11/82, Rattlesnake Ridge



RCP8211-110

FIGURE D.6. Slug Withdrawal Test: 299-E33-12, 11/11/82, Rattlesnake Ridge

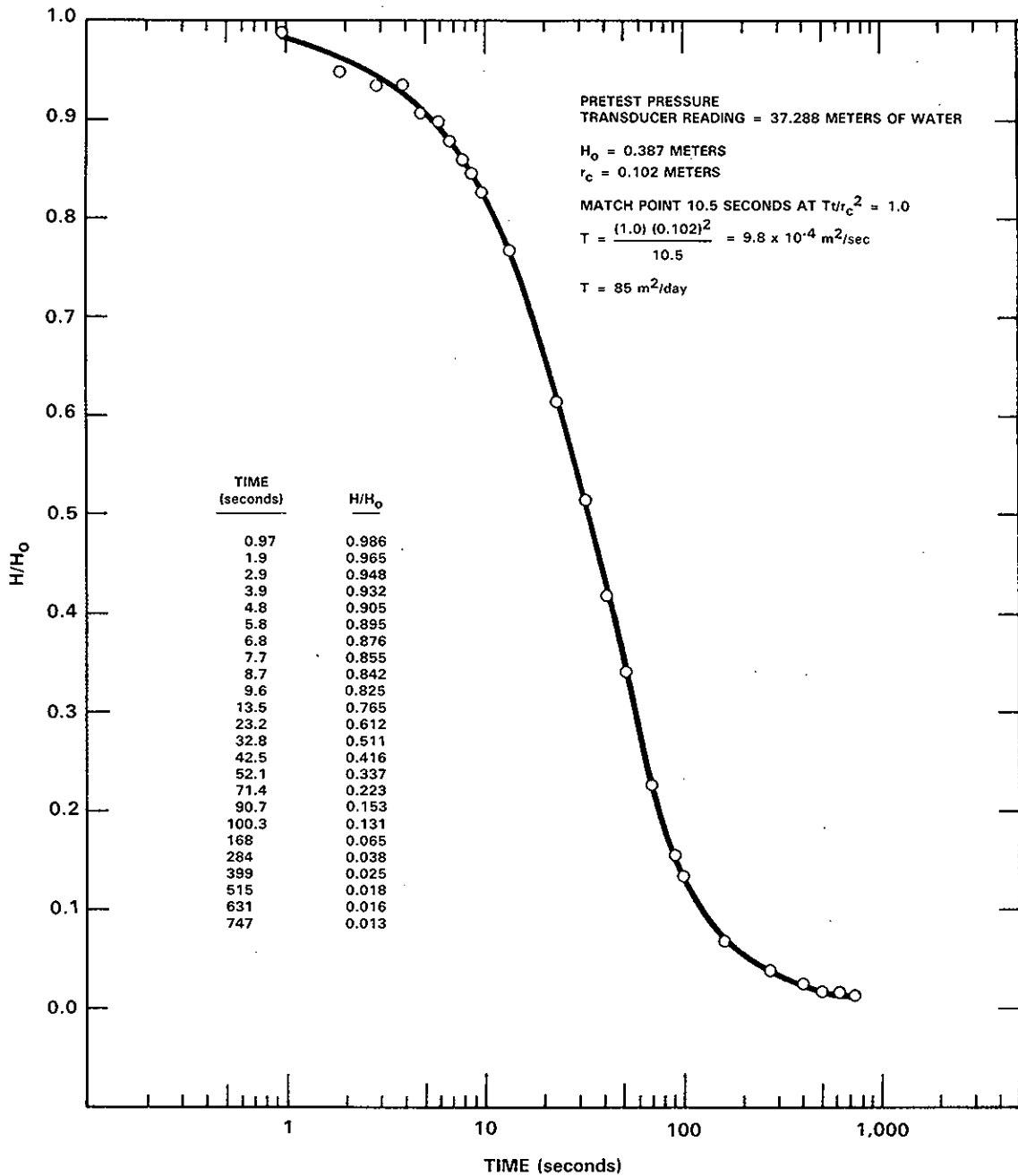
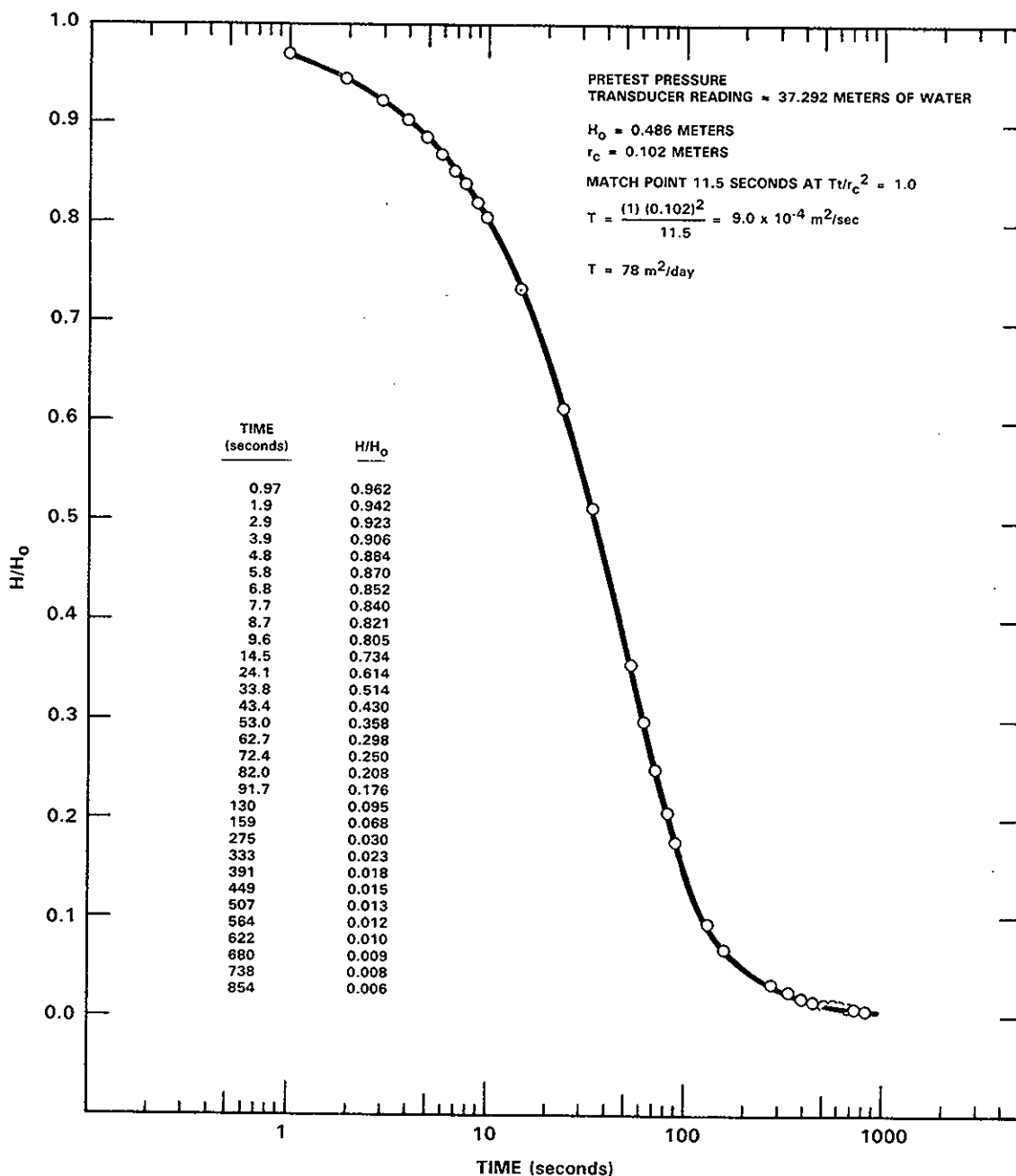


FIGURE D.7. Slug Injection Test: 699-42-40C, 10/30/82, Rattlesnake Ridge



RCP8211-104

FIGURE D.8. Slug Withdrawal Test: 699-42-40C, 10/30/82, Rattlesnake Ridge

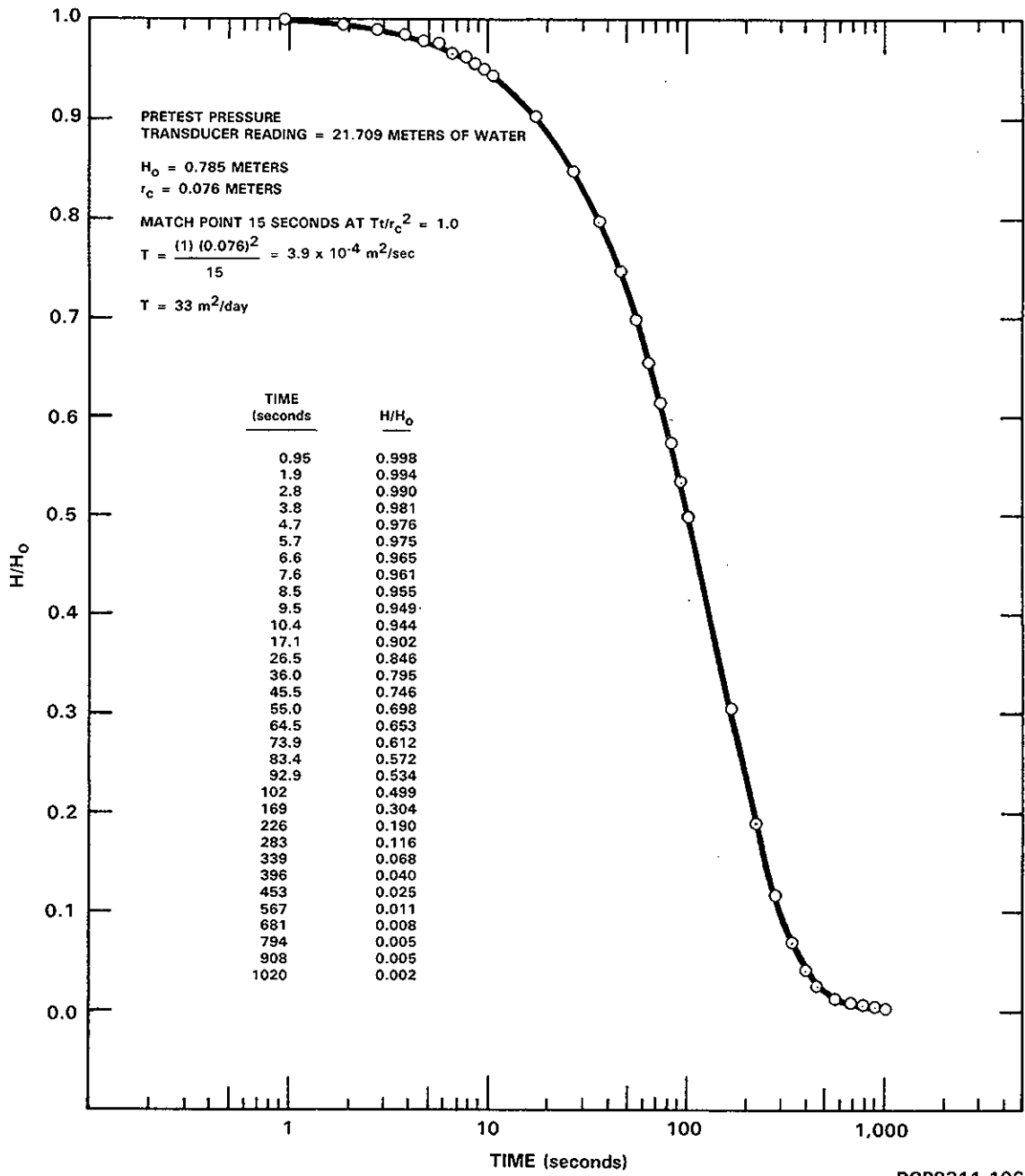
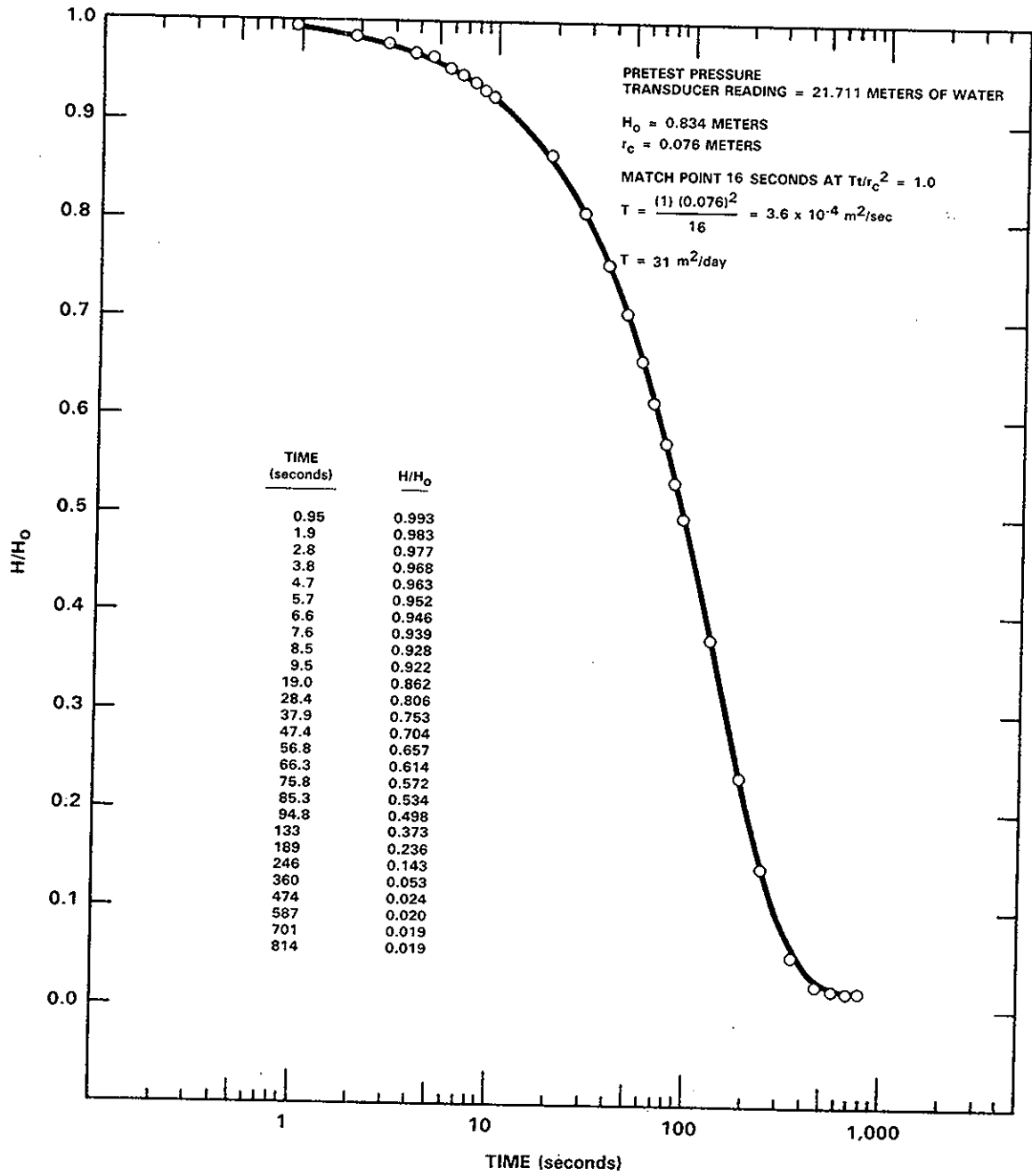
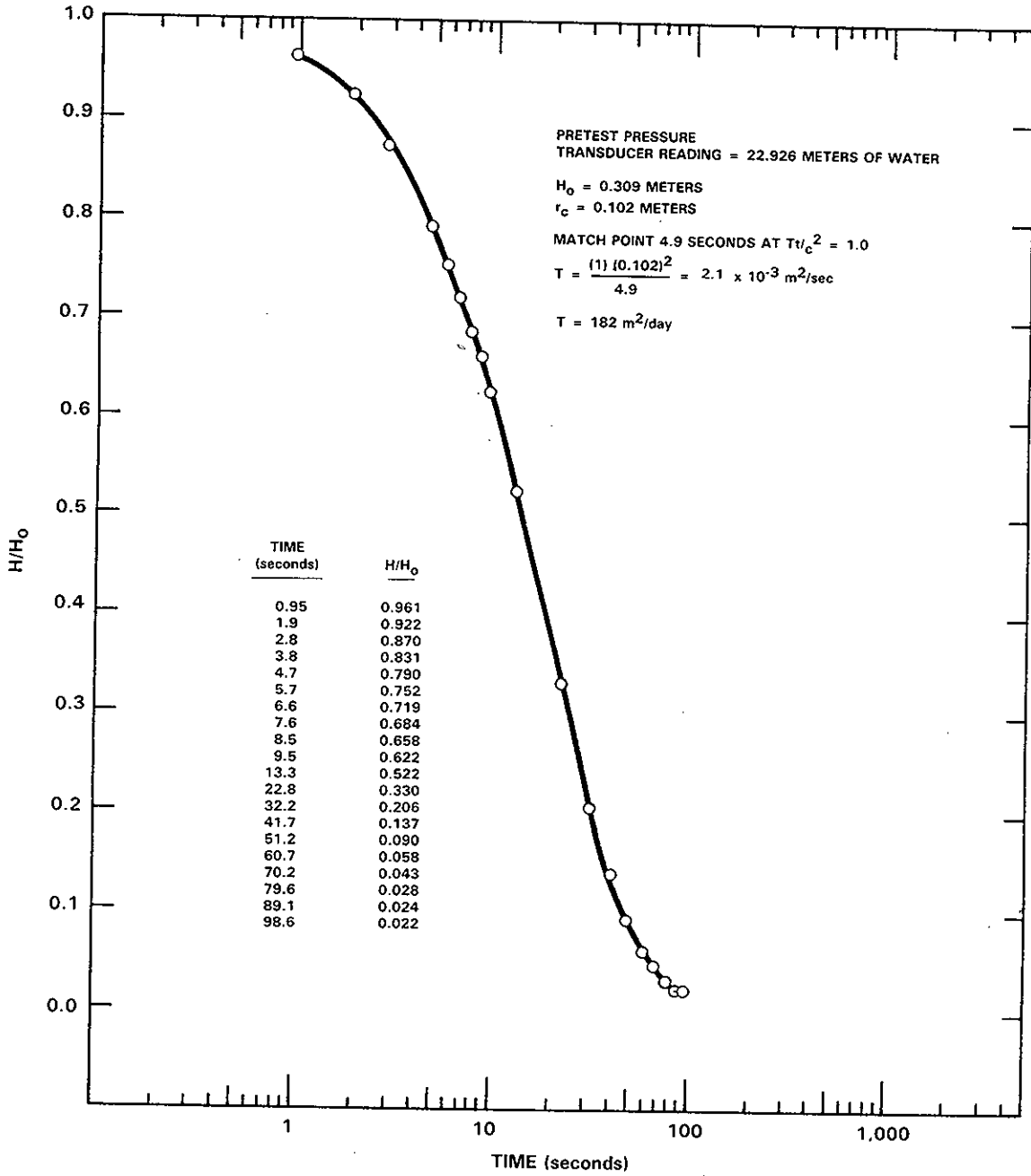


FIGURE D.9. Slug Injection Test: 699-47-50, 11/12/82, Rattlesnake Ridge



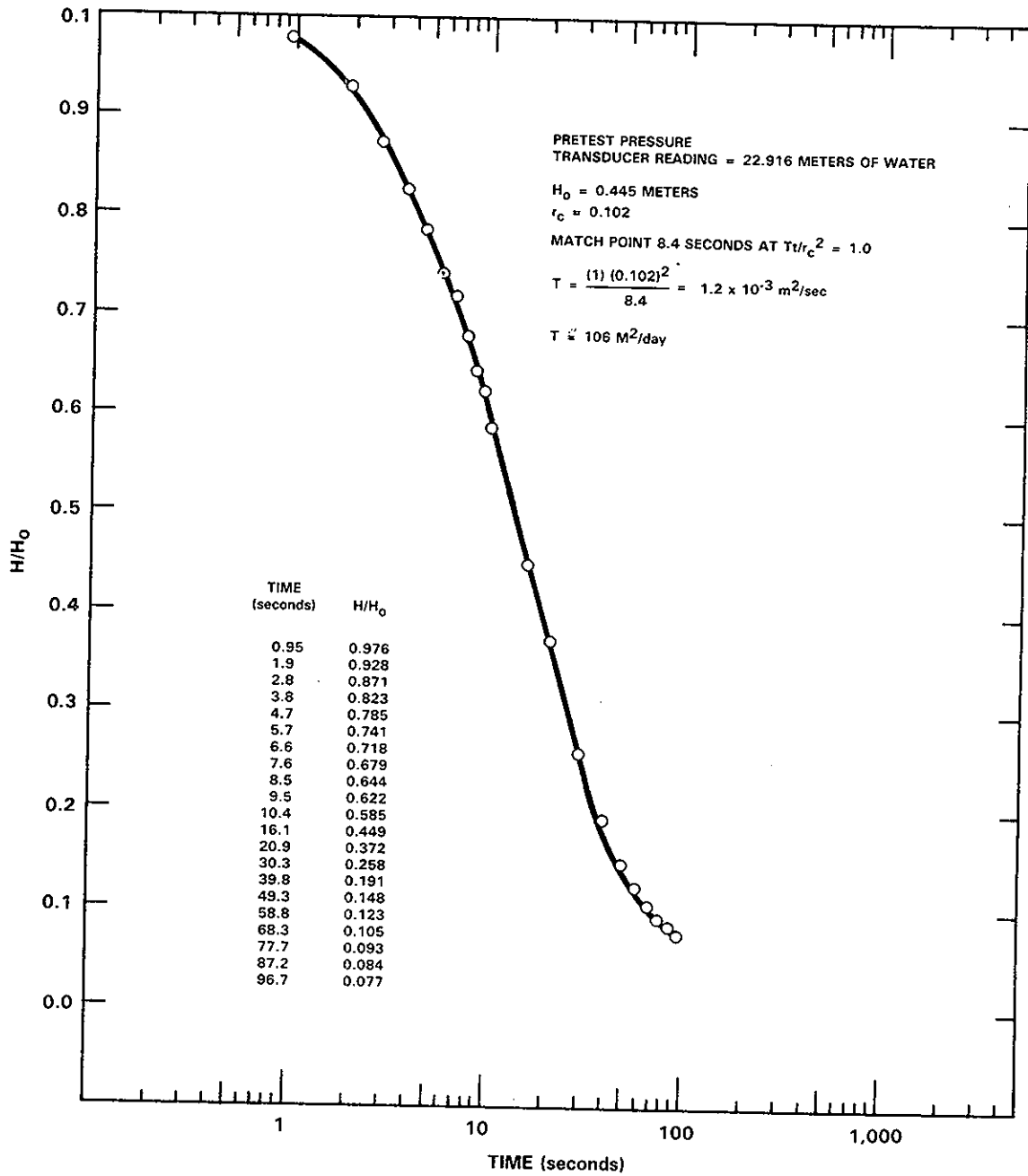
RCP8211-107

FIGURE D.10. Slug Withdrawal Test: 699-47-50, 11/12/82, Rattlesnake Ridge



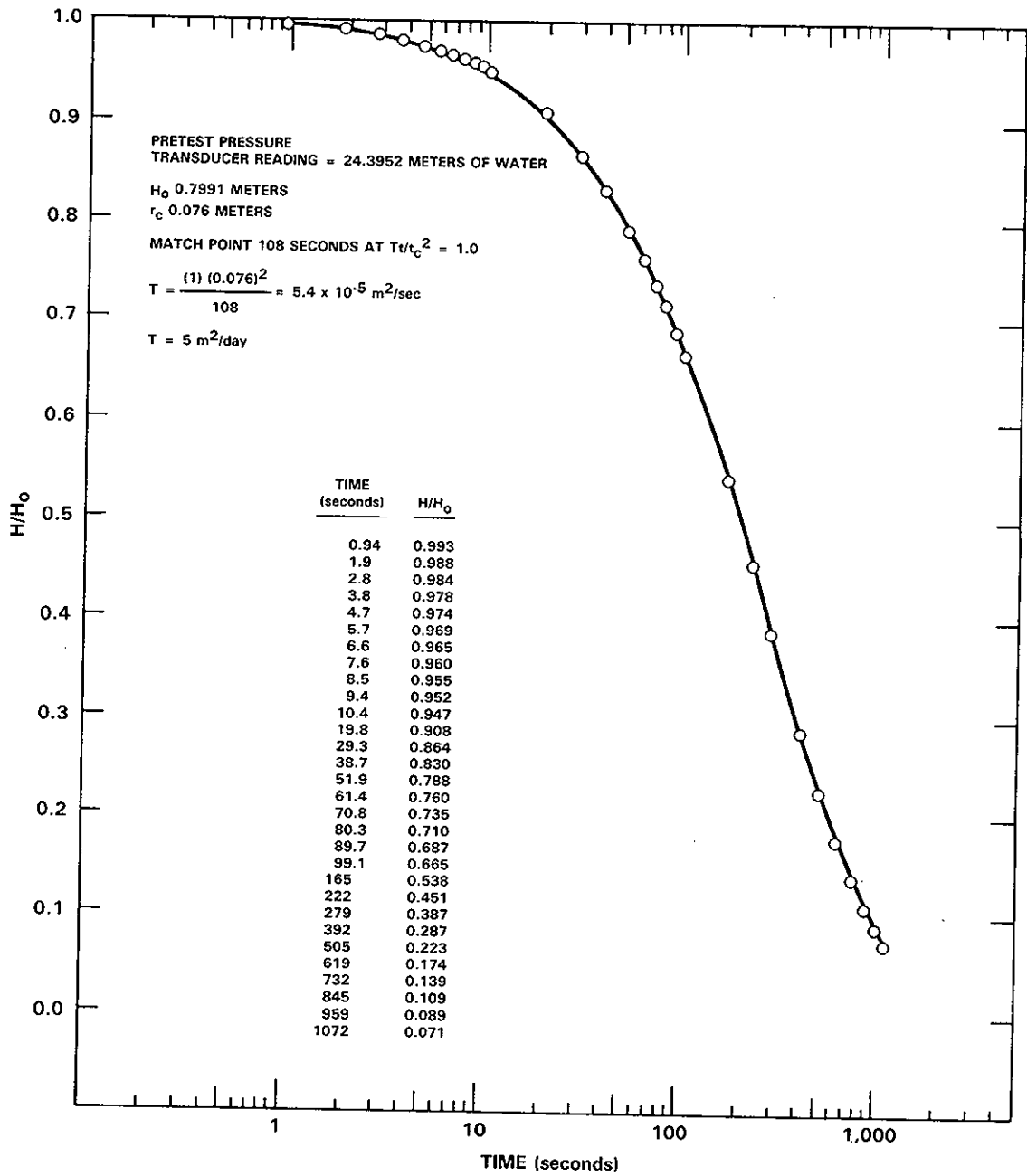
RCP8211-108

FIGURE D.11. Slug Injection Test: 699-49-55B, 11/12/82, Rattlesnake Ridge



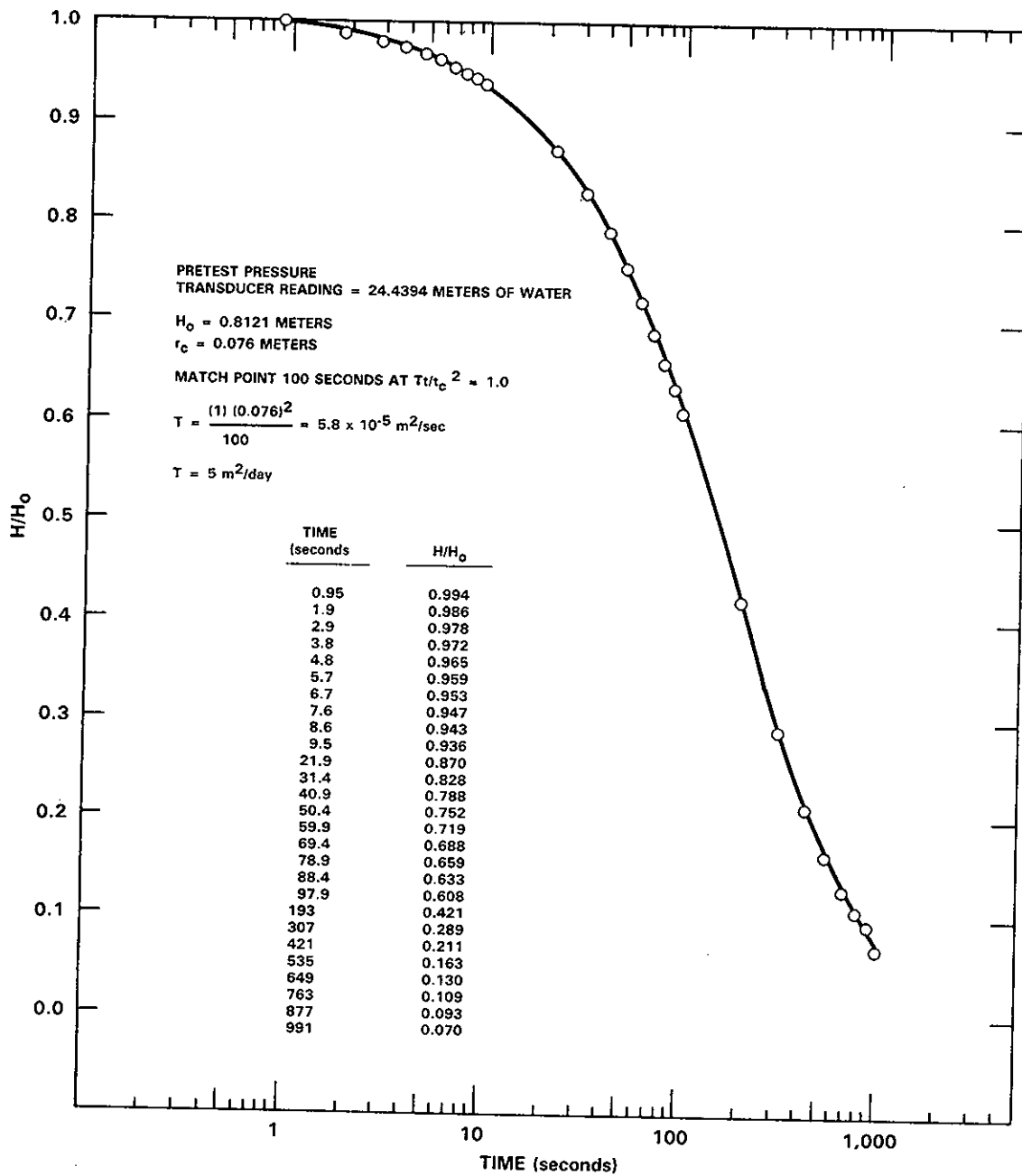
RCP8211-109

FIGURE D.12. Slug Withdrawal Test: 699-49-55B, 11/12/82, Rattlesnake Ridge



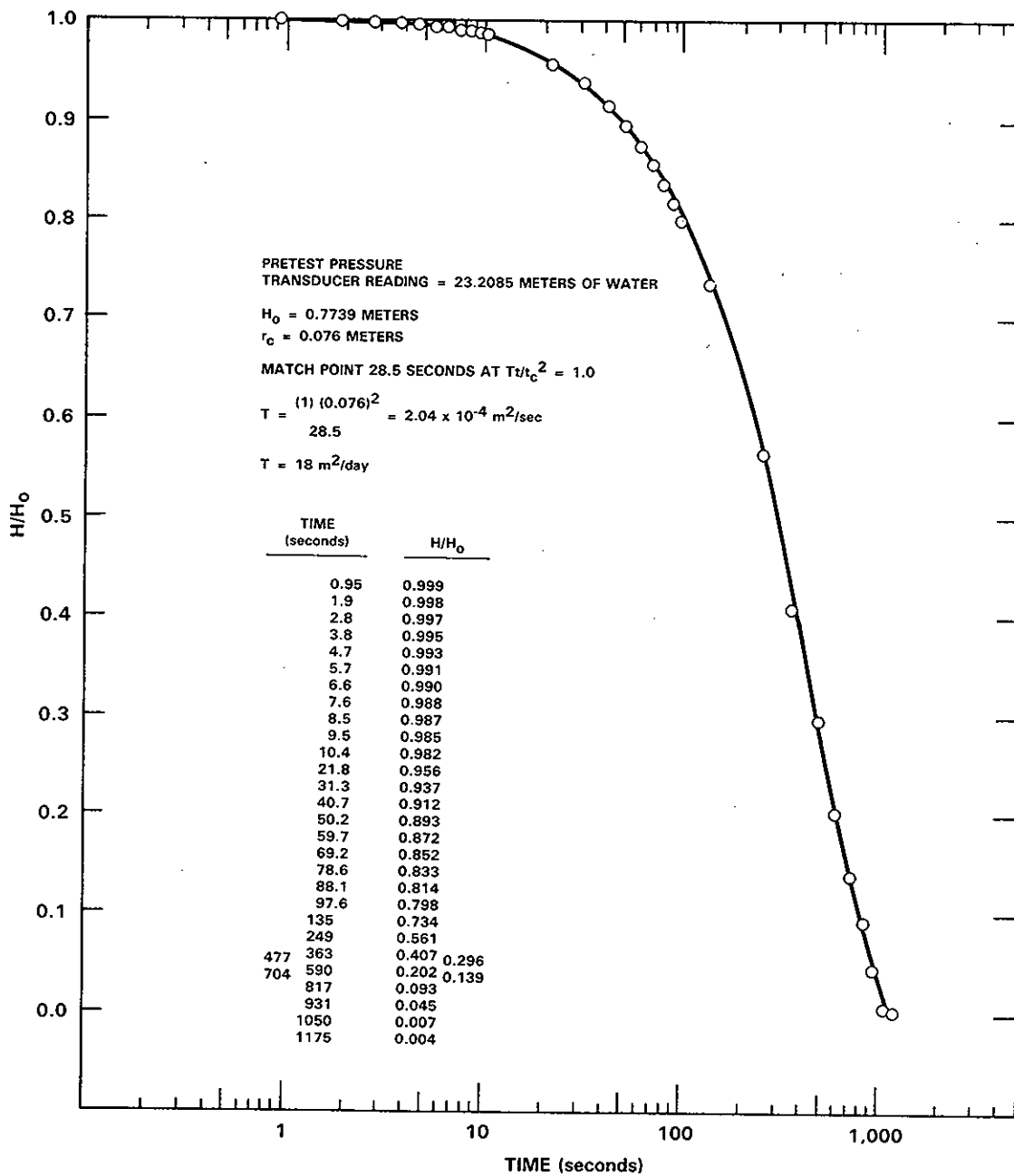
RCP8302-7

FIGURE D.13. Slug Injection Test: 699-50-45, 11/16/82, Rattlesnake Ridge



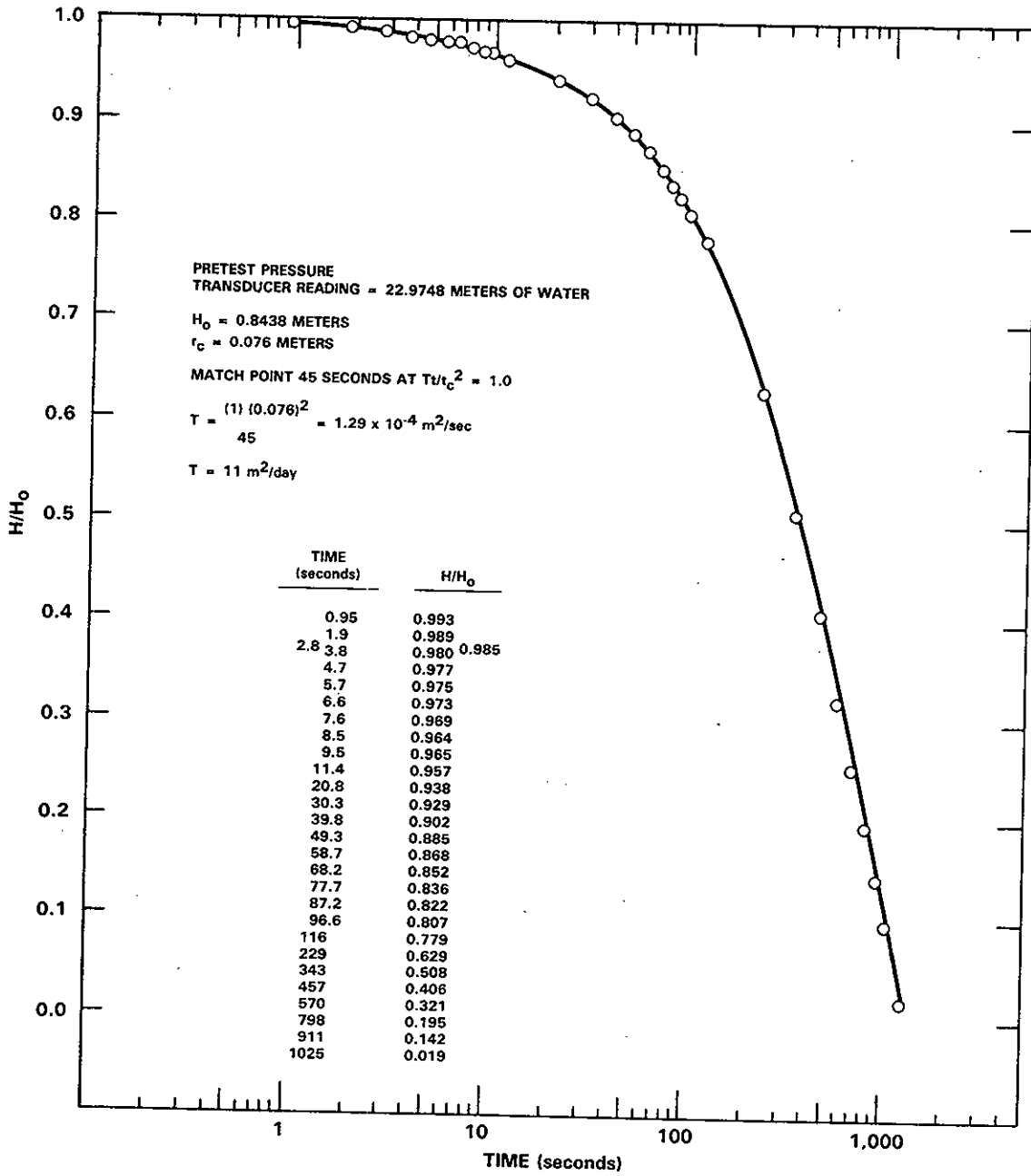
RCP8302-12

FIGURE D.14. Slug Withdrawal Test: 699-50-45, 11/16/82, Rattlesnake Ridge



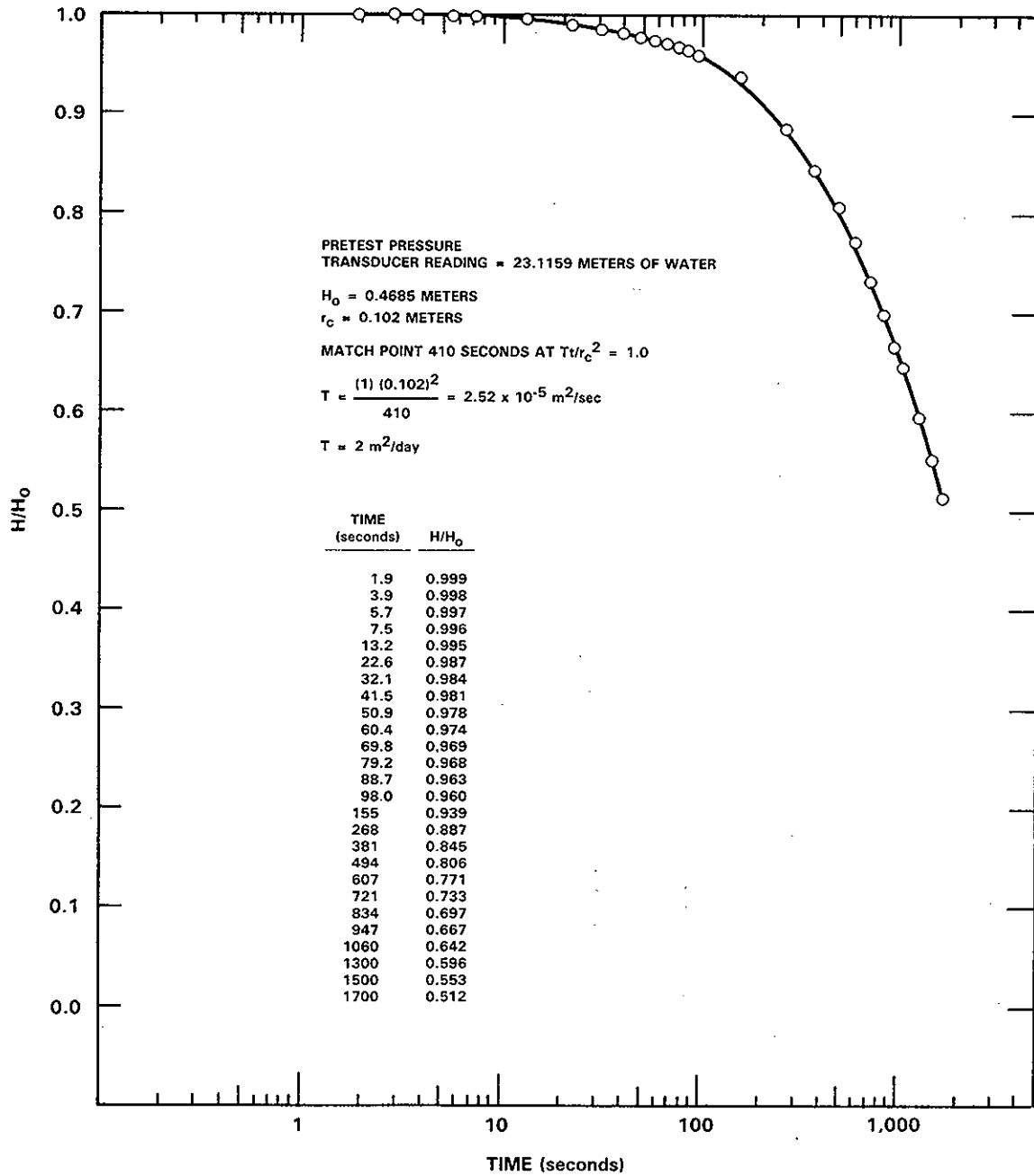
RCP8302-11

FIGURE D.15. Slug Injection Test: 699-50-48, 11/16/82, Rattlesnake Ridge



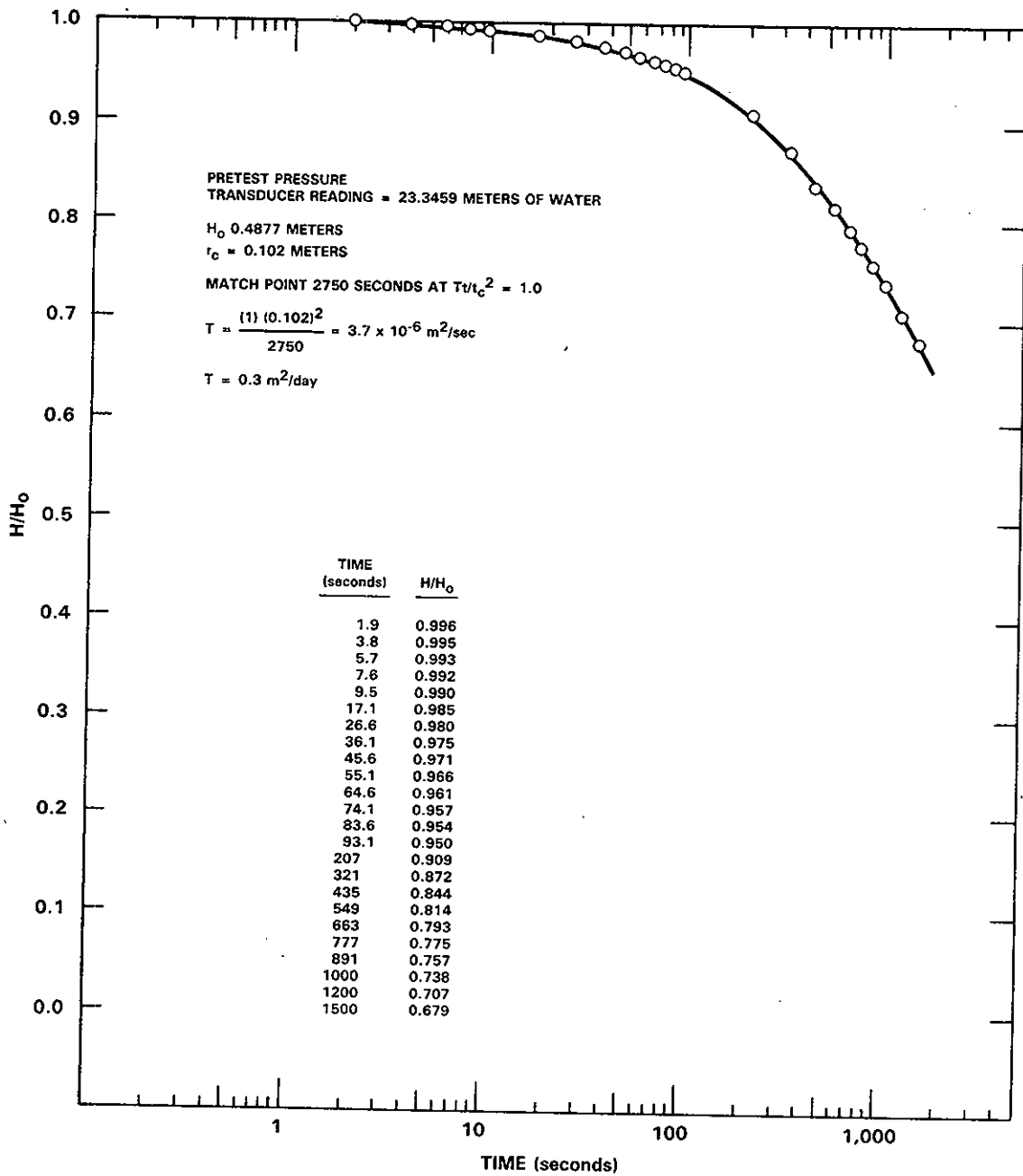
RCP8302-13

FIGURE D.16. Slug Withdrawal Test: 699-50-48, 11/16/82, Rattlesnake Ridge



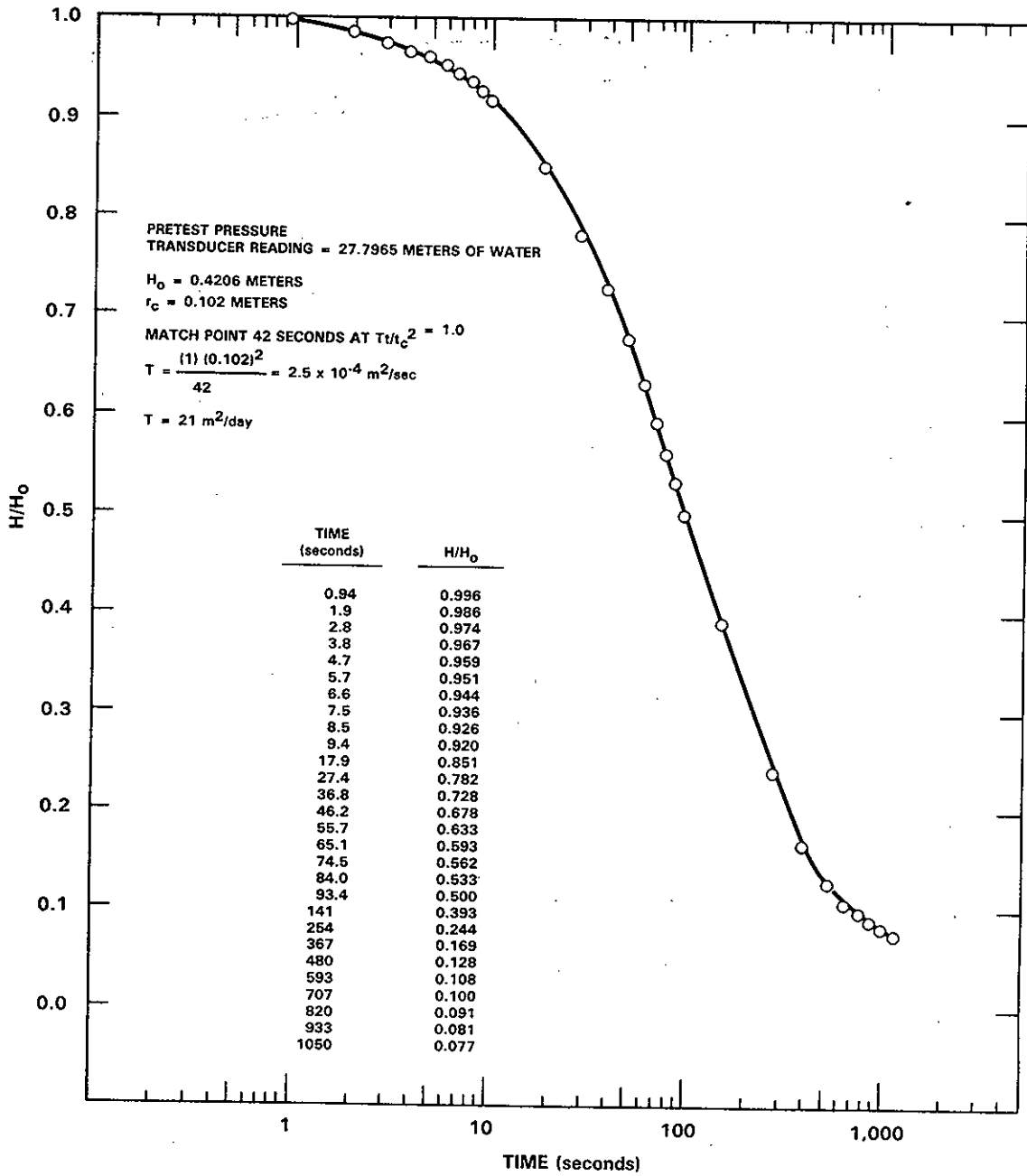
RCP8302-2

FIGURE D.17. Slug Injection Test: 699-41-46, 11/16/82, Rattlesnake Ridge



RCP8302-9

FIGURE D.18. Slug Withdrawal Test: 699-51-46, 11/16/82, Rattlesnake Ridge



RCP8302-15

FIGURE D.19. Slug Injection Test: 699-52-46, 11/16/82, Rattlesnake Ridge

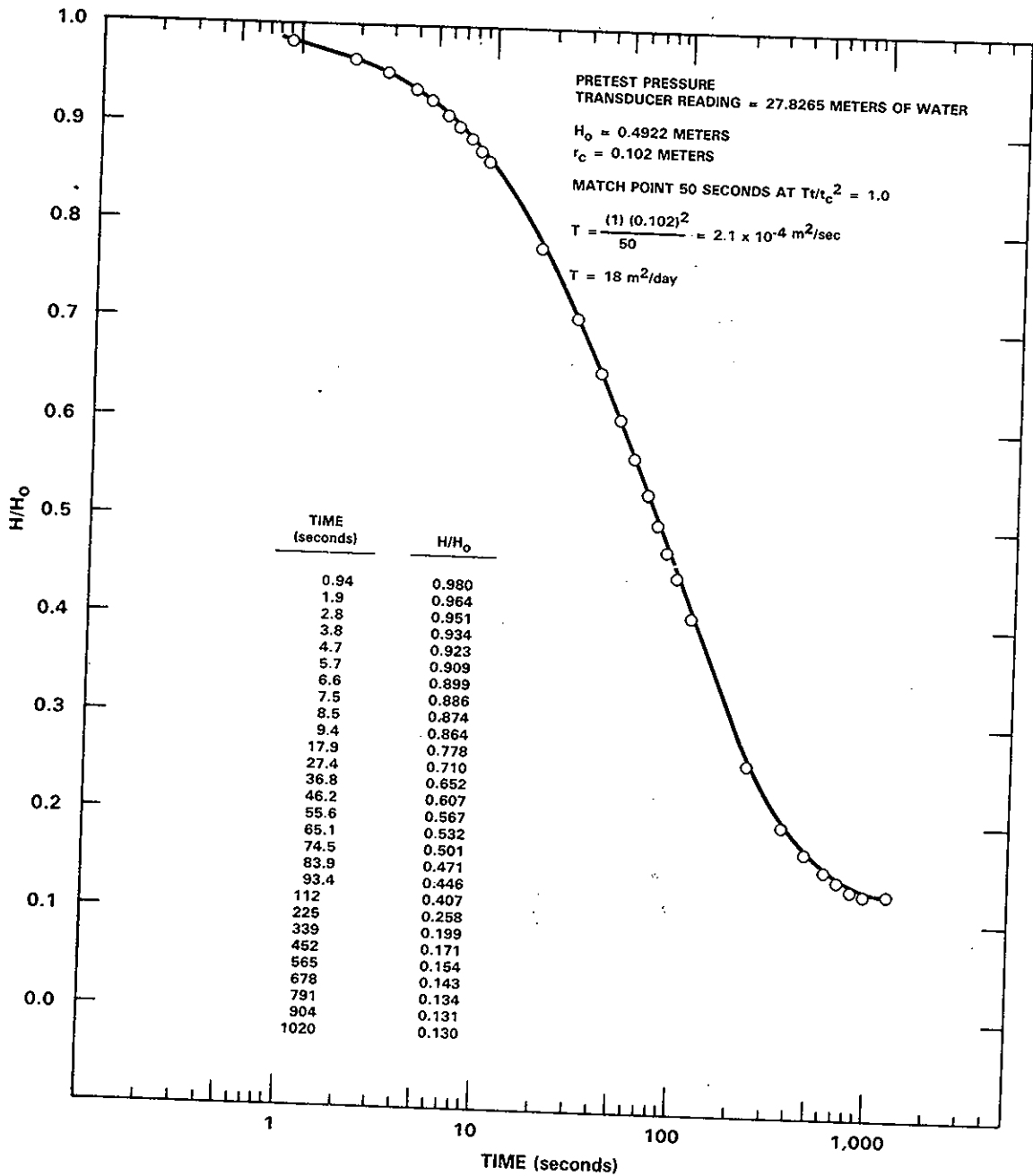
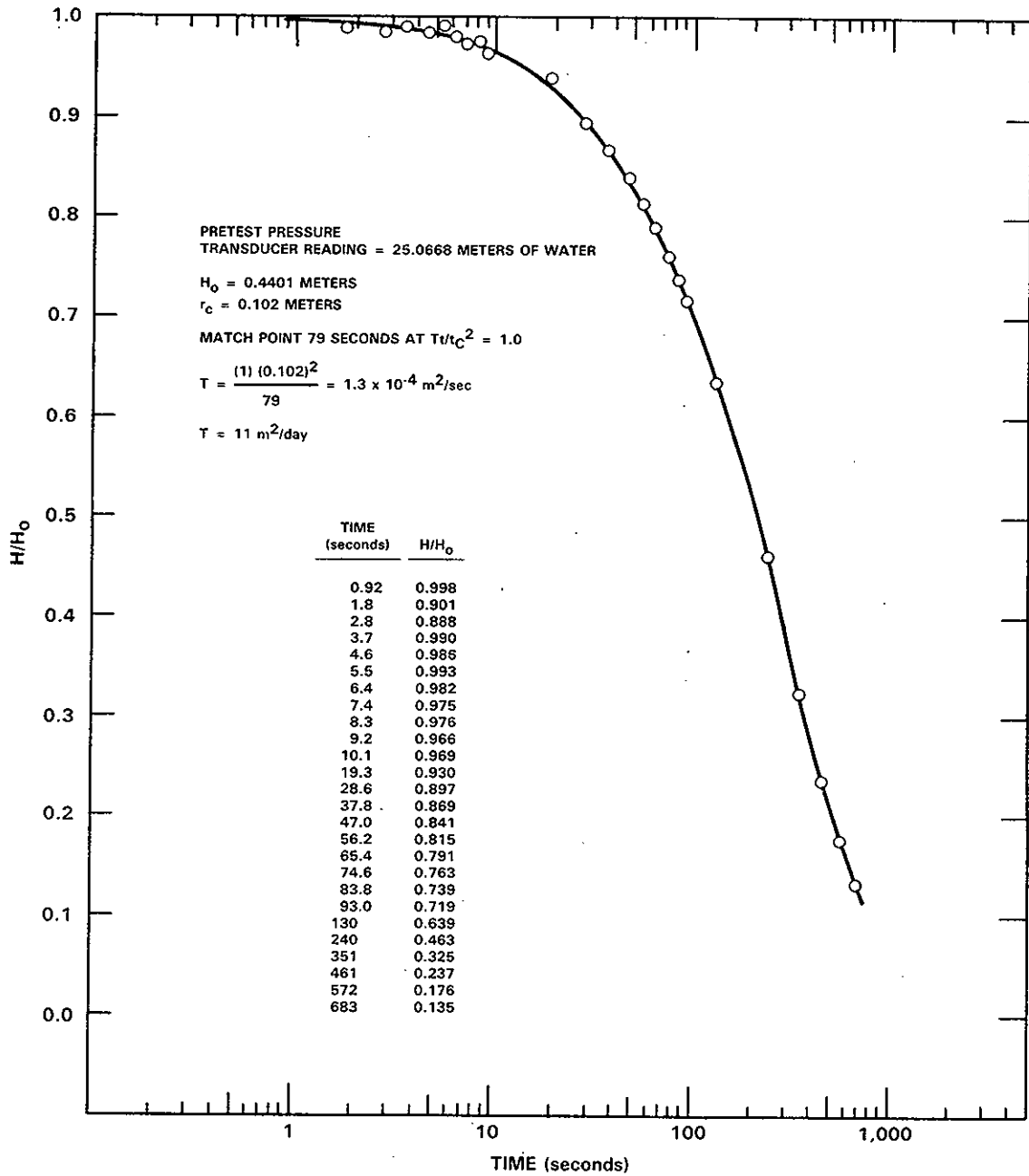


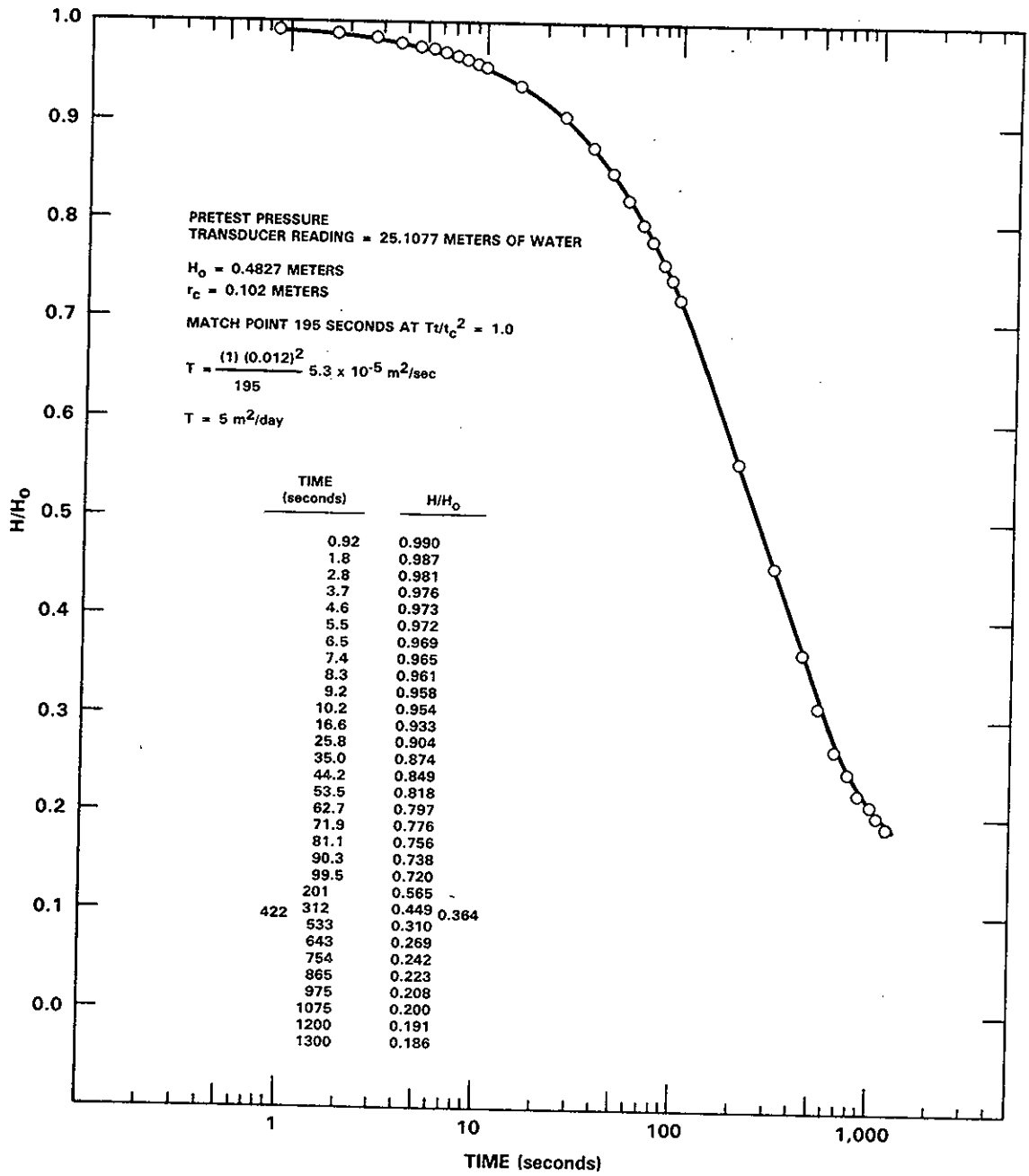
FIGURE D.20. Slug Withdrawal Test: 699-52-46, 11/16/82, Rattlesnake Ridge

RCP8302-14



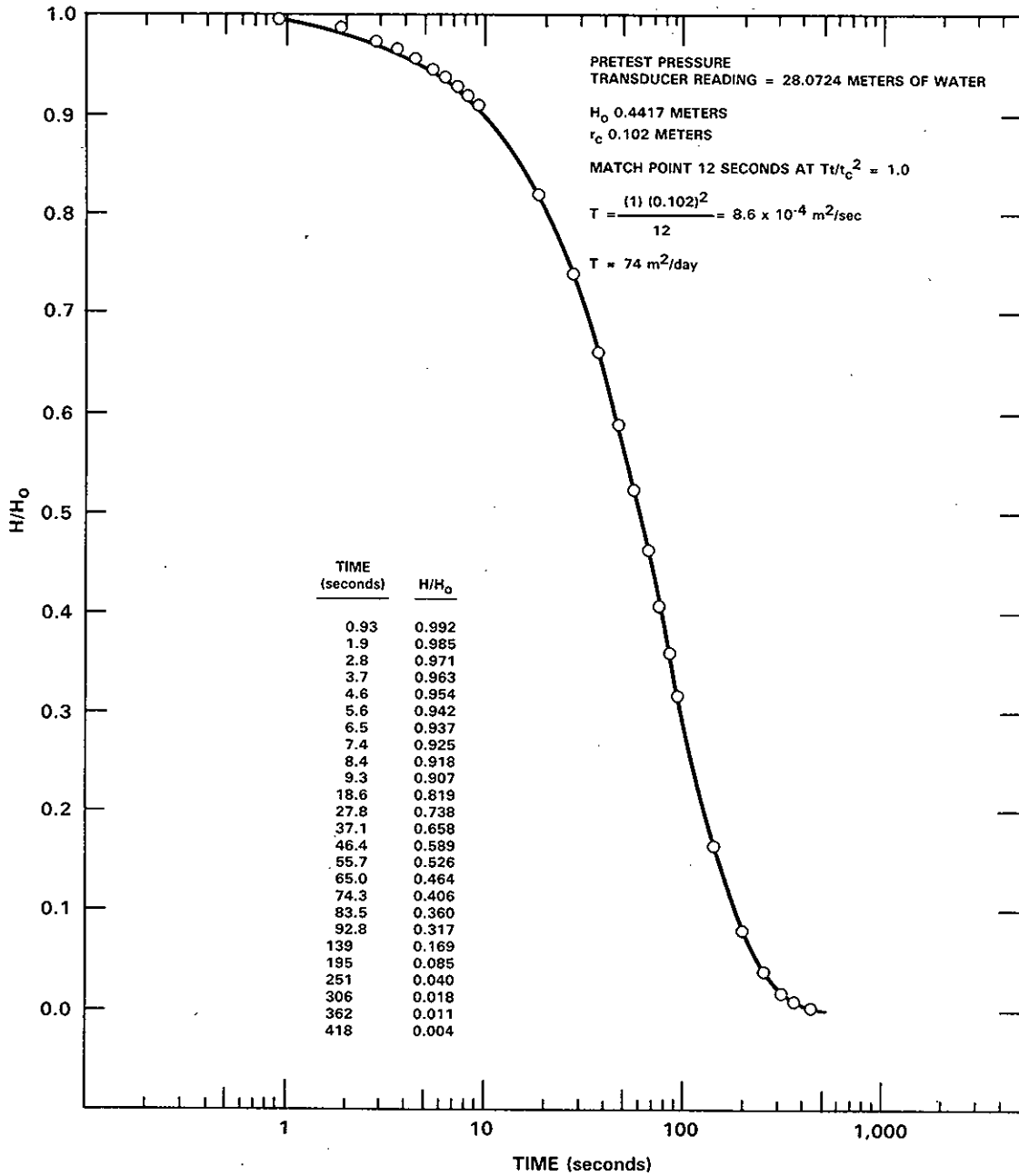
RCP8302-1

FIGURE D.21. Slug Injection Test: 699-52-48, 11/22/82, Rattlesnake Ridge



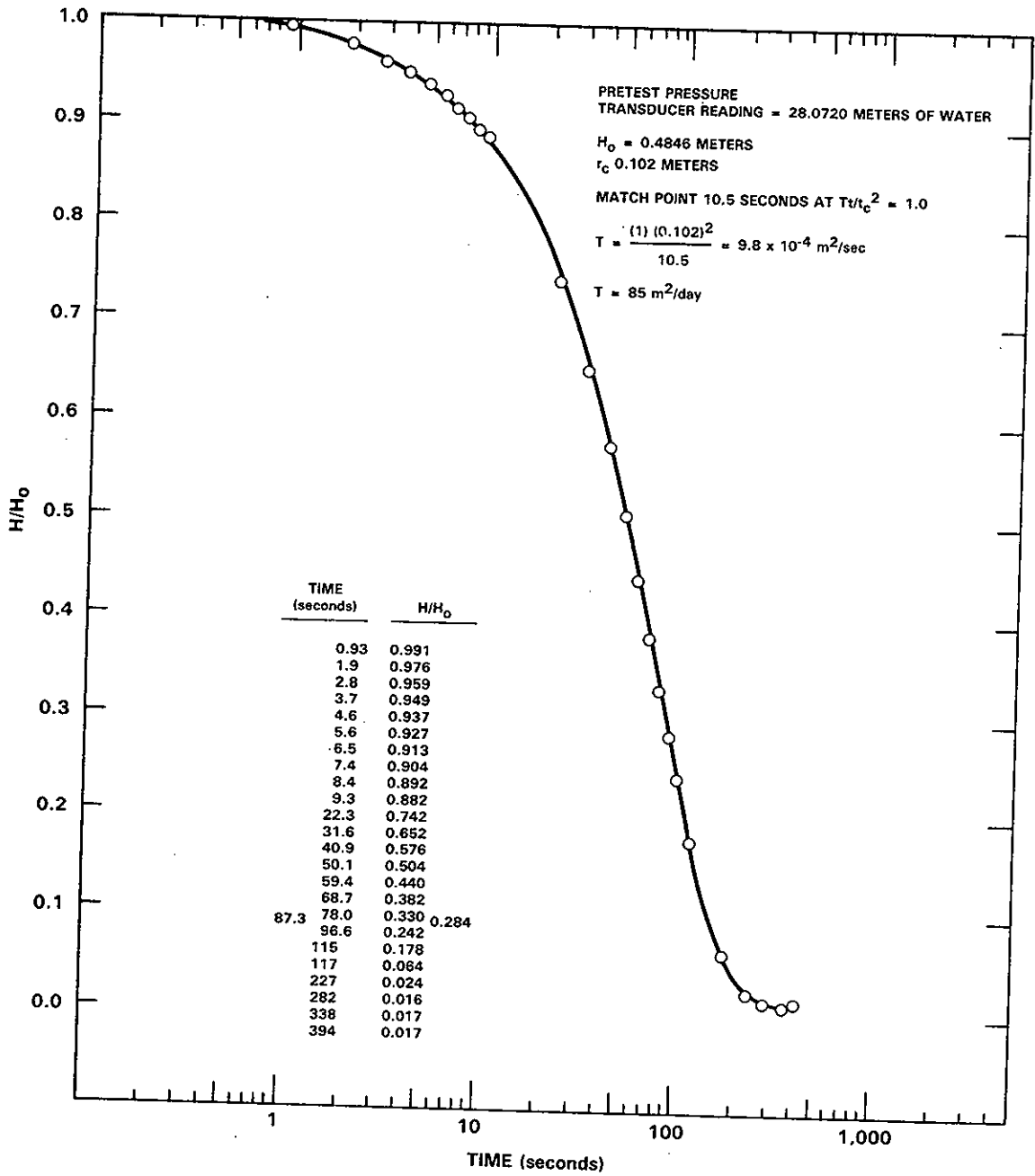
RCP8302-16

FIGURE D.22. Slug Withdrawal Test: 699-52-48, 11/22/82, Rattlesnake Ridge



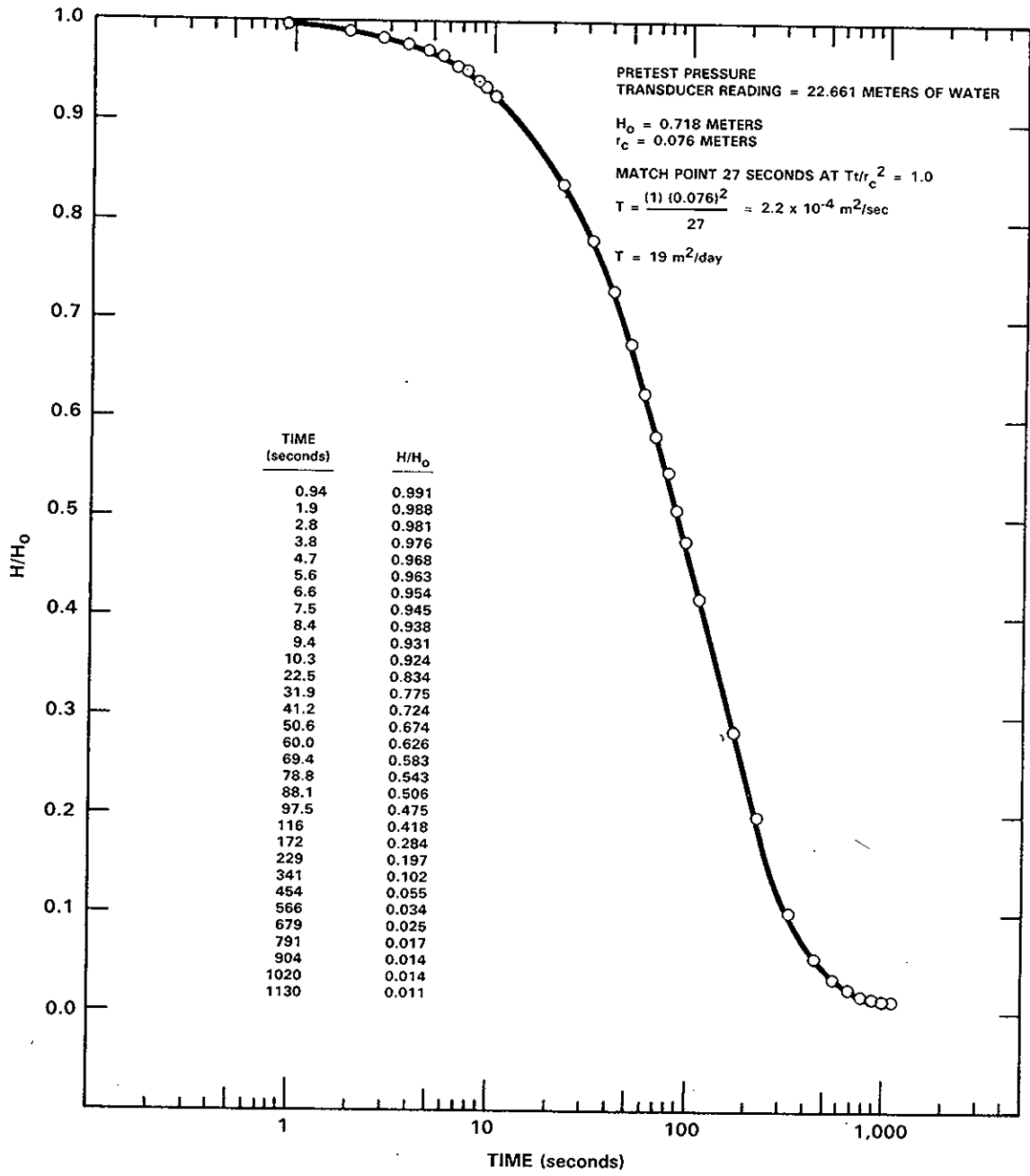
RCP8302-5

FIGURE D.23. Slug Injection Test: 699-53-50, 11/23/82, Rattlesnake Ridge



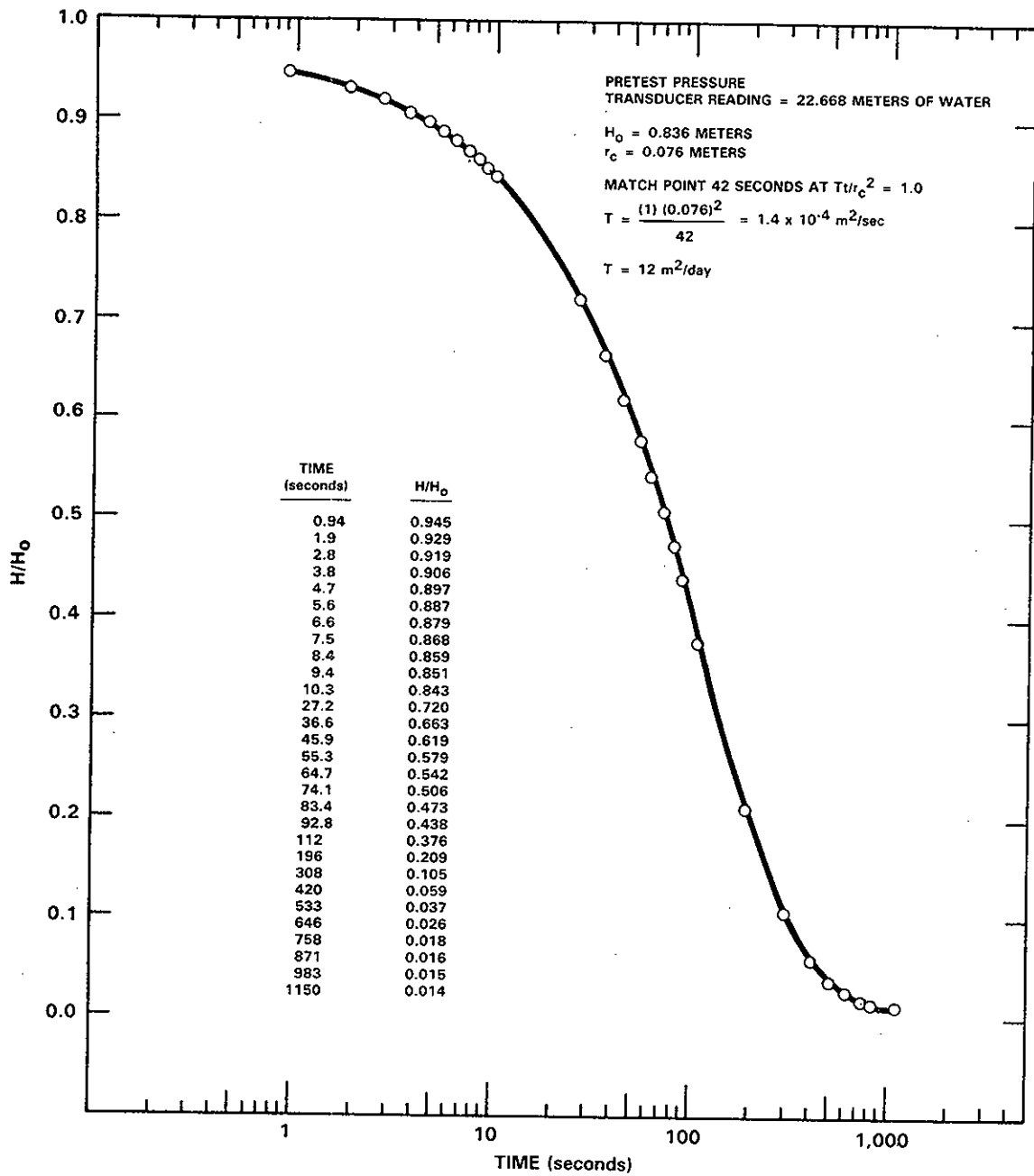
RCP8302-10

FIGURE D.24. Slug Withdrawal Test: 699-53-50, 11/23/82, Rattlesnake Ridge



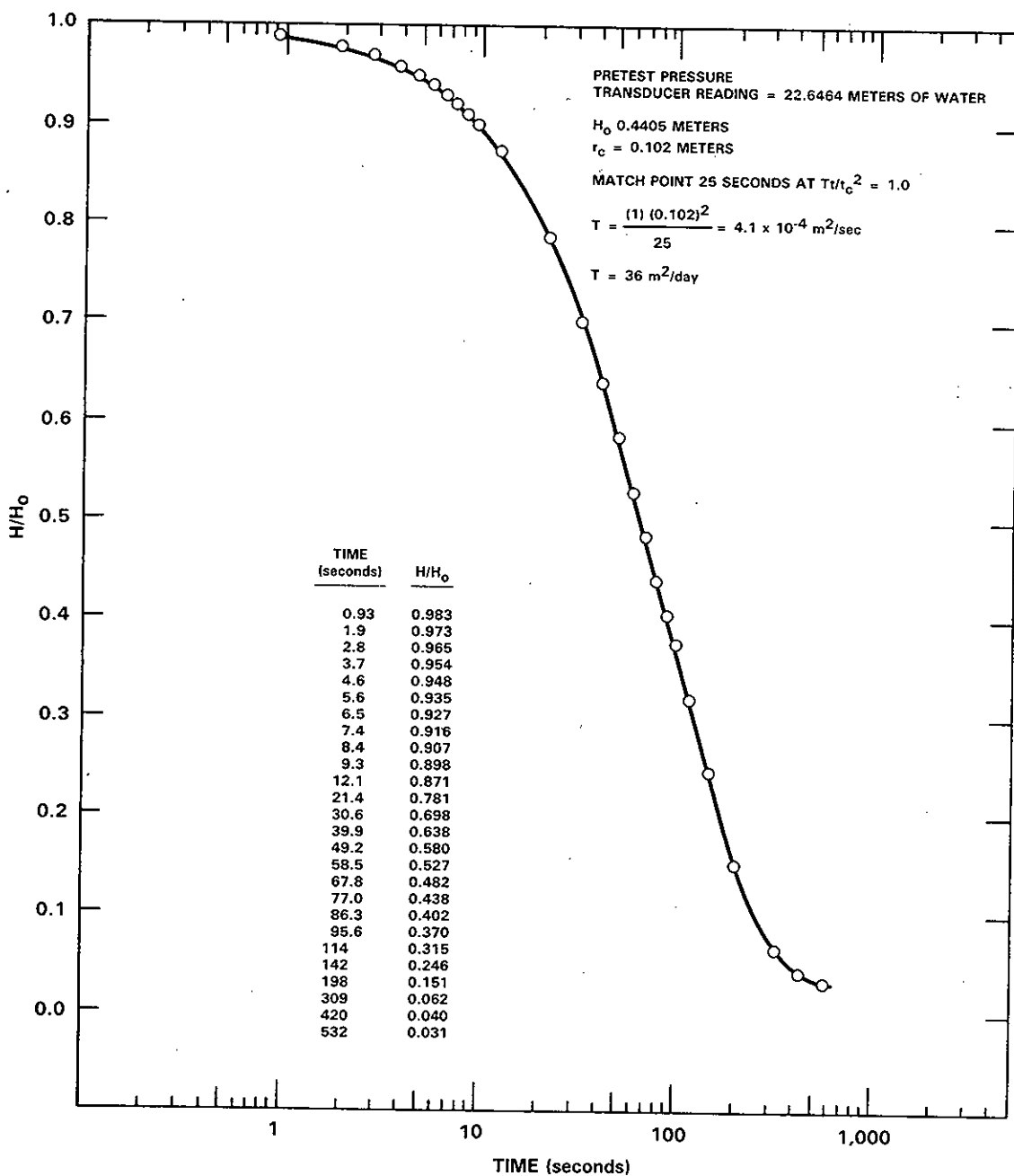
RCP8211-112

FIGURE D.25. Slug Injection Test: 699-54-57, 11/11/82, Rattlesnake Ridge



RCP8211-113

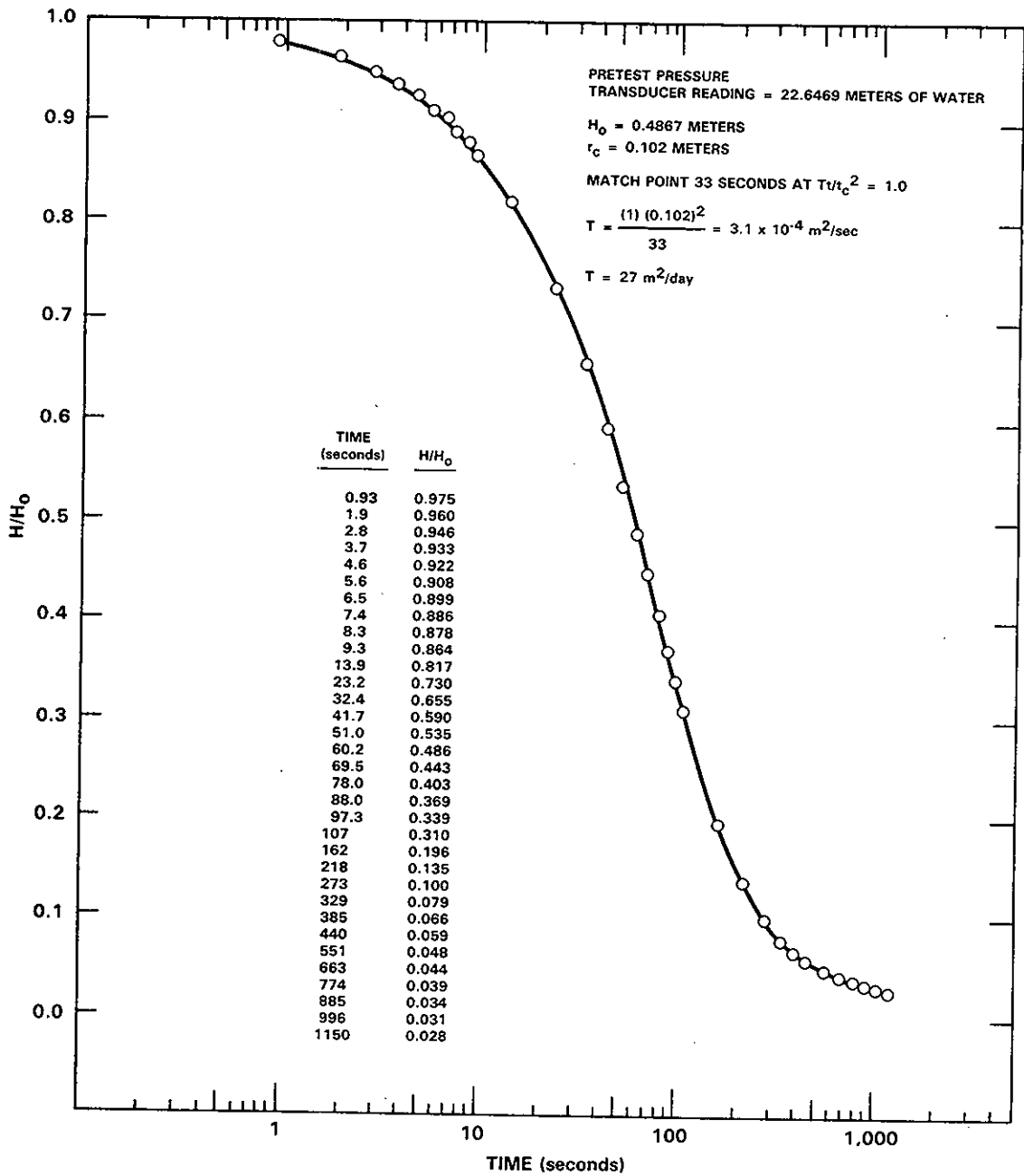
FIGURE D.26. Slug Withdrawal Test: 699-54-57, 11/11/82, Rattlesnake Ridge



RCP8302-8

FIGURE D.27. Slug Injection Test: 699-56-53, 11/22/82, Rattlesnake Ridge

RHO-RE-ST-12



RCP8302-6

FIGURE D.28. Slug Withdrawal Test: 699-56-53, 11/22/82, Rattlesnake Ridge

APPENDIX E

AQUIFER WATER-LEVEL MEASUREMENTS
AND WELL ELEVATIONS

TABLE E.1. Confined Aquifer Water-Level Measurements

Well Number	Date	Elevation, m	Date	Elevation, m	Date	Elevation, m	Date	Elevation, m	Date	Elevation, m	Date	Elevation, m	Date	Elevation, m	Date	Elevation, m	Date	Elevation, m	Date	Elevation, m																		
299-E16-1	6/14/82	123.20	7/12/82	123.62	9/15/82	123.35	10/08/82	123.41	10/13/82	123.47	10/15/82	123.46	10/20/82	123.15	10/27/82	123.42	11/02/82	123.43	11/09/82	123.47	11/15/82	123.50	11/16/82	123.54	12/15/82	123.52	1/18/83	123.54	2/15/83	123.55	3/21/82	123.50	4/19/83	123.51	5/20/83	123.52	6/15/83	123.50
299-E26-8	6/14/82	122.59	7/30/82	122.72	8/07/82	122.75	9/14/82	122.73	9/15/82	122.78	9/21/82	122.75	10/15/82	122.81	11/04/82	122.84	11/12/82	122.83	11/19/82	122.77	12/15/82	122.82	1/16/83	122.87	1/29/82	122.87	1/18/83	122.90	2/15/83	122.89	3/21/83	122.87	4/19/83	122.85	5/20/83	122.86	6/15/83	122.88
299-E33-12	6/14/82	122.80	8/25/82	122.85	8/31/82	122.79	9/07/82	122.84	9/14/82	122.80	9/15/82	122.76	9/21/82	122.83	10/15/82	122.87	11/16/82	122.83	12/15/82	122.94	1/16/83	122.97	1/18/83	122.95	1/29/82	122.95	2/15/83	122.96	3/21/83	122.96	4/19/83	122.96	5/20/83	123.06	6/15/83	122.97		
699-42-40C	5/19/82	124.75	8/24/82	124.69	8/31/82	124.81	9/07/82	124.79	9/14/82	124.82	9/15/82	124.78	9/21/82	124.83	10/15/82	124.85	11/16/82	124.93	12/15/82	124.91	1/16/83	124.90	1/18/83	124.84	1/29/82	124.84	2/15/83	124.86	3/21/83	124.82	4/19/83	124.84	5/20/83	124.86	6/15/83	124.84		
699-47-50	6/14/82	123.29	8/24/82	123.30	9/15/82	123.32	9/21/82	123.32	9/28/82	123.32	10/05/82	123.32	10/11/82	123.32	10/15/82	123.32	10/18/82	123.32	10/25/82	123.31	11/16/82	123.36	1/18/83	123.39	1/29/82	123.40	2/15/83	123.40	3/21/83	123.40	4/19/83	123.40	5/20/83	123.40	6/15/83	123.40		
699-49-55B	5/25/82	122.65	6/14/82	122.58	7/12/82	122.71	8/31/82	122.70	9/15/82	122.73	10/05/82	122.75	10/15/82	122.83	10/25/82	122.76	11/16/82	122.80	12/15/82	122.79	1/16/83	122.84	1/18/83	122.85	1/29/82	122.86	2/15/83	122.86	3/21/83	122.86	4/19/83	122.86	5/20/83	122.83	6/15/83	122.83		
699-50-45	6/14/82	124.04	6/22/82	124.05	7/12/82	124.05	8/31/82	124.00	9/15/82	124.03	10/05/82	124.00	10/15/82	124.10	10/25/82	124.08	11/16/82	124.13	12/15/82	124.10	1/16/83	124.14	1/18/83	124.15	1/29/82	124.10	2/15/83	124.12	3/21/83	124.12	4/19/83	124.12	5/20/83	124.12	6/15/83	124.12		
699-50-48	6/14/82	123.77	7/30/82	123.81	8/05/82	123.83	9/15/82	123.85	10/05/82	123.97	10/15/82	123.95	10/22/82	123.92	10/25/82	123.72	11/16/82	123.87	12/15/82	123.94	1/16/83	123.97	1/18/83	123.89	1/29/82	123.96	2/15/83	123.96	3/21/83	123.96	4/19/83	123.99	5/20/83	124.01	6/15/83	124.01		
699-51-46	6/14/82	123.96	6/18/82	123.86	7/15/82	123.85	8/31/82	123.87	9/15/82	123.89	10/05/82	123.93	10/15/82	123.93	10/22/82	123.97	11/16/82	123.93	12/15/82	123.95	1/16/83	123.97	1/18/83	123.96	1/29/82	123.97	2/15/83	123.97	3/21/83	123.97	4/19/83	123.97	5/20/83	123.97	6/15/83	123.97		
699-52-46	6/14/82	124.12	7/30/82	124.12	8/05/82	124.07	9/15/82	124.18	10/05/82	124.16	10/15/82	124.21	10/22/82	124.19	10/25/82	124.21	11/16/82	124.19	12/15/82	124.21	1/16/83	124.22	1/18/83	124.18	1/29/82	124.19	2/15/83	124.19	3/21/83	124.19	4/19/83	124.19	5/20/83	124.19	6/15/83	124.19		
699-52-48	6/14/82	123.72	6/21/82	123.72	7/22/82	123.72	8/31/82	123.73	9/15/82	123.72	10/05/82	123.73	10/15/82	123.73	10/22/82	123.77	11/16/82	123.82	12/15/82	123.83	1/16/83	123.83	1/18/83	123.84	1/29/82	123.86	2/15/83	123.86	3/21/83	123.86	4/19/83	123.86	5/20/83	123.86	6/15/83	123.86		
699-53-50	6/14/82	123.21	6/21/82	123.22	7/15/82	123.25	8/31/82	123.29	9/15/82	123.30	10/05/82	123.30	10/15/82	123.34	10/22/82	123.35	11/16/82	123.41	12/15/82	123.36	1/16/83	123.37	1/18/83	123.36	1/29/82	123.37	2/15/83	123.36	3/21/83	123.36	4/19/83	123.36	5/20/83	123.36	6/15/83	123.36		
699-54-57	5/17/82	122.67	6/14/82	122.87	7/22/82	122.58	8/31/82	122.58	9/15/82	122.65	10/05/82	122.65	10/15/82	122.68	10/22/82	122.67	11/16/82	122.66	12/15/82	122.70	1/16/83	122.71	1/18/83	122.78	1/29/82	122.78	2/15/83	122.78	3/21/83	122.74	4/19/83	122.74	5/20/83	122.74	6/15/83	122.77		
699-56-53	6/03/82	122.61	6/14/82	122.62	9/15/82	122.70	10/05/82	122.70	10/11/82	122.69	10/15/82	122.69	10/22/82	122.68	11/16/82	122.72	12/15/82	122.77	1/16/83	122.79	1/18/83	122.85	1/29/82	122.84	2/15/83	122.82	3/21/83	122.81	4/19/83	122.81	5/20/83	122.86	6/15/83	122.85				

RHO-RE-ST-12

TABLE E.2. Water-Table Elevations, June 1982 to June 1983

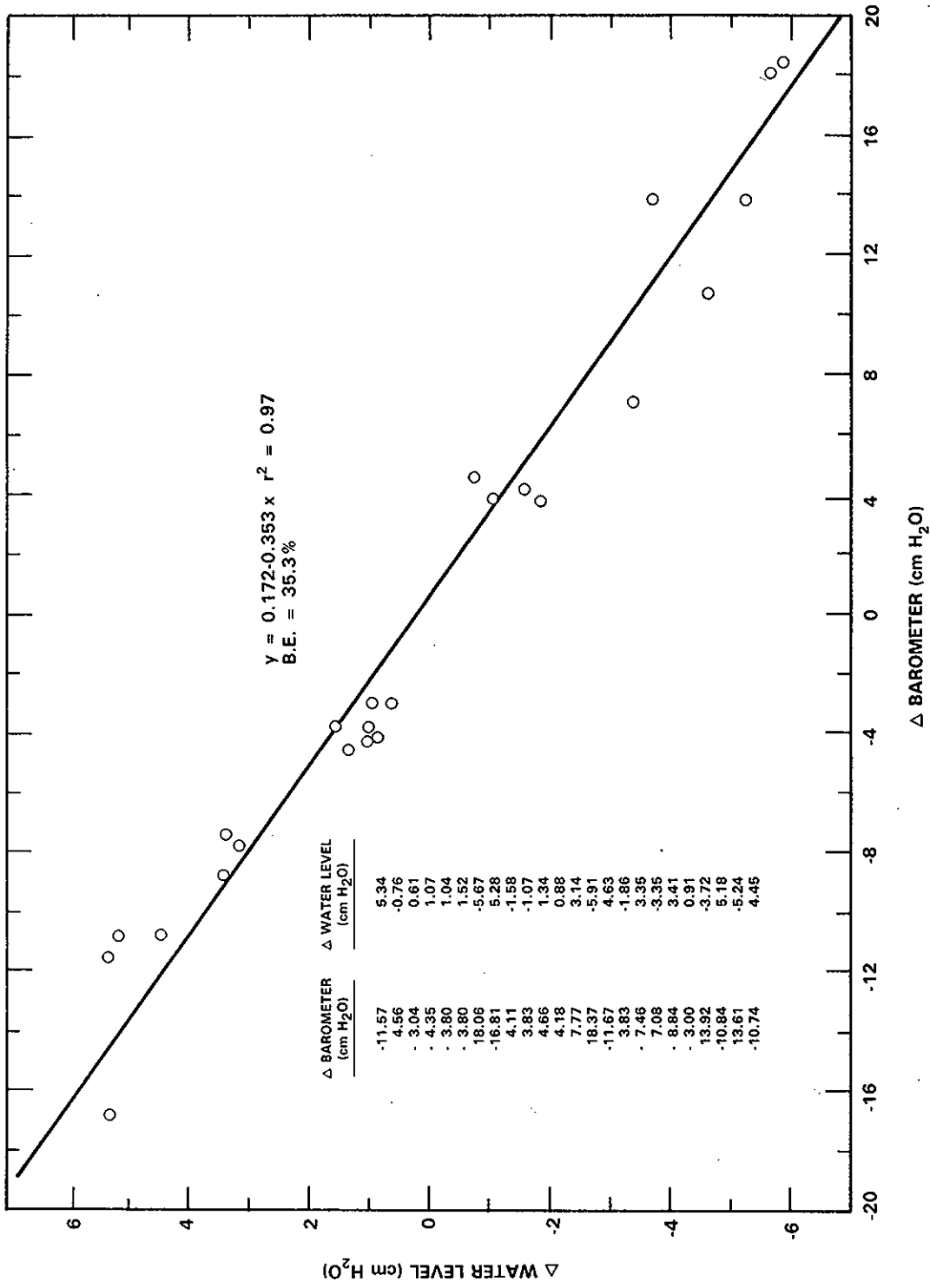
Well Number	Elevations, meters		
	June 1982	December 1982	June 1983
299-E16-2	122.27	122.74	---
299-E19-1	122.97	123.16	---
299-E23-1	122.60	122.75	122.76
299-E23-2(0)	122.61	122.69	122.72
299-24-4	122.62	122.73	122.77
299-E25-9	122.31	122.80	122.85
299-E25-11	122.59	122.71	122.79
299-E26-1	122.69	122.88	---
299-E27-1	122.65	122.78	122.81
299-E27-3(0)	122.69	122.74	---
299-E28-7	122.39	122.51	122.54
299-E28-18	122.61	122.76	122.79
299-E32-1	122.62	122.75	122.82
299-E33-7	122.52	122.62	122.72
299-E33-14	122.64	123.31	123.40
299-E33-17	122.61	122.70	122.81
299-E34-1	122.68	122.76	122.84
699-33-56	122.86	---	---
699-34-39A	122.43	122.51	122.55
699-34-42	122.47	122.27	122.61
699-34-51	122.65	---	---
699-36-46R	122.55	122.38	122.70
699-36-61A	122.34	124.34	124.39
699-37-43	122.61	122.22	122.99
699-39-39	124.09	124.15	124.15
699-40-33	124.11	124.19	124.17
699-40-62	123.46	123.50	123.49
699-42-40A	---	---	129.83
699-42-40B	---	---	130.77
699-47-35B	124.48	124.48	124.44
699-47-46	122.87	123.00	123.04

TABLE E.2. (contd)

Well Number	Elevations, meters		
	June 1982	December 1982	June 1983
699-47-60	122.61	122.73	122.80
699-49-55A	122.60	122.73	122.77
699-49-57	113.46	113.57	113.65
699-50-42	124.40	124.34	124.44
699-50-53	122.58	---	122.76
699-51-63	123.32	123.05	123.43
699-53-35	120.27	120.27	120.36
699-53-47	125.48	125.32	125.63
699-53-55B	122.44	122.60	122.66
699-54-34	124.00	123.84	123.99
699-55-40	124.10	124.03	124.16
699-55-50C	122.66	122.90	124.99
699-55-60B	122.54	---	---
699-56-43	124.07	---	---
699-59-55	---	---	122.95
699-59-58	121.78	121.59	---
699-60-60	122.22	122.19	122.47
699-61-62	122.46	122.59	---
699-63-58	122.13	121.82	122.31
699-64-62	121.91	122.13	122.26

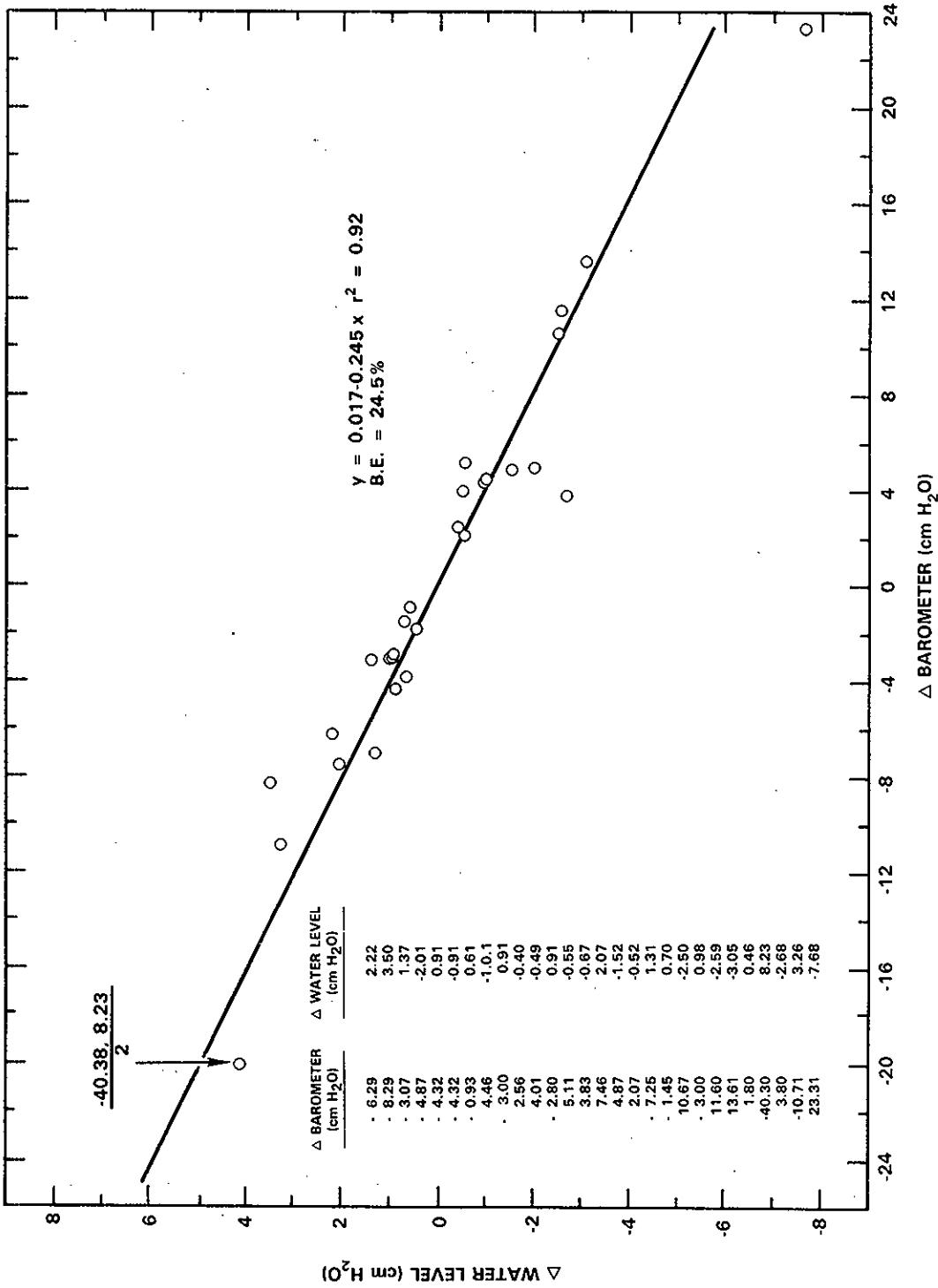
APPENDIX F

BAROMETRIC EFFICIENCY DATA
AND ANALYSES



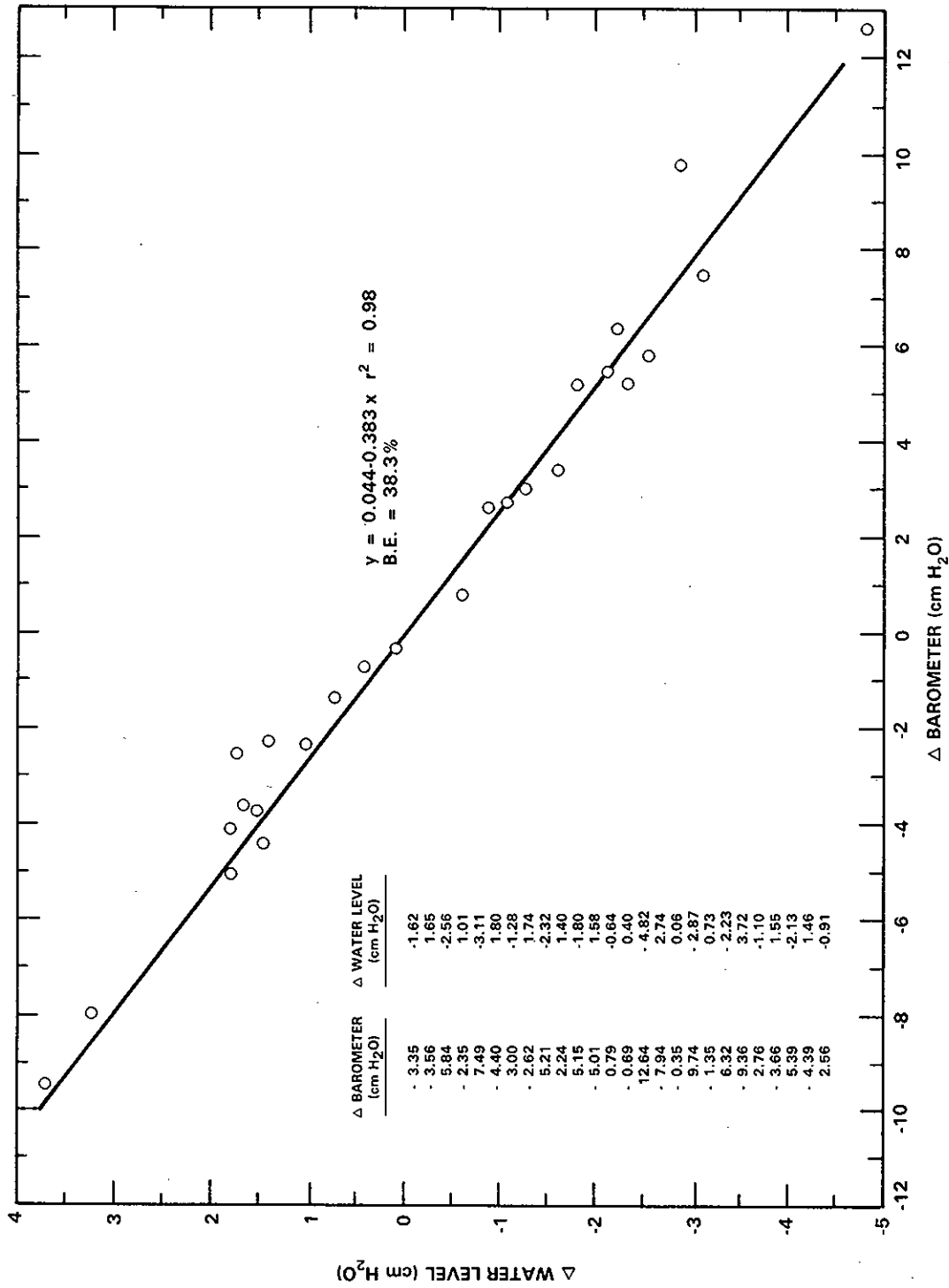
RCP8212-114

FIGURE F.1. Barometric Efficiency: 299-E16-1, Elephant Mountain Interflow



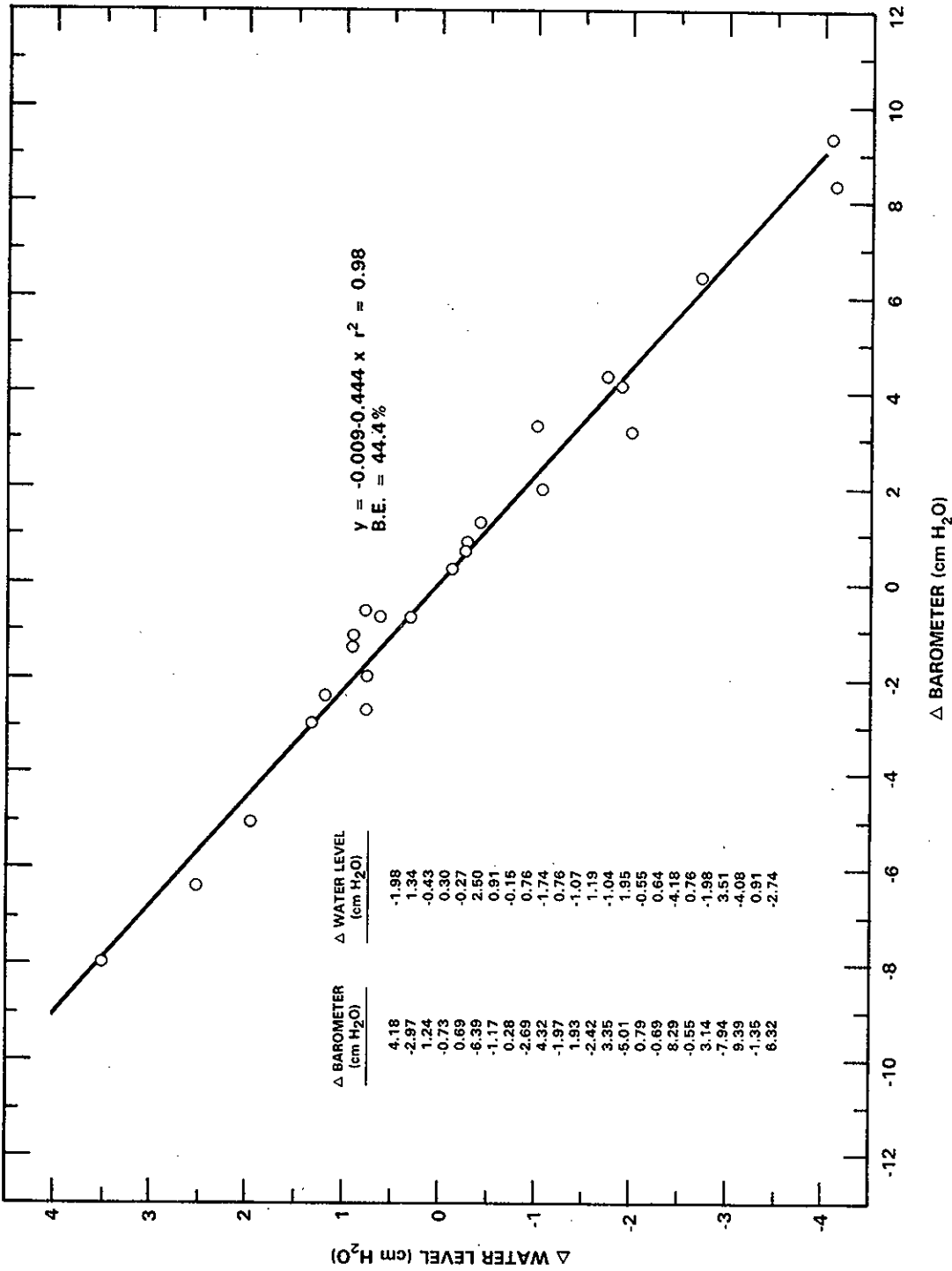
RCP8212-115

FIGURE F.2. Barometric Efficiency: 299-E26-8, Rattlesnake Ridge



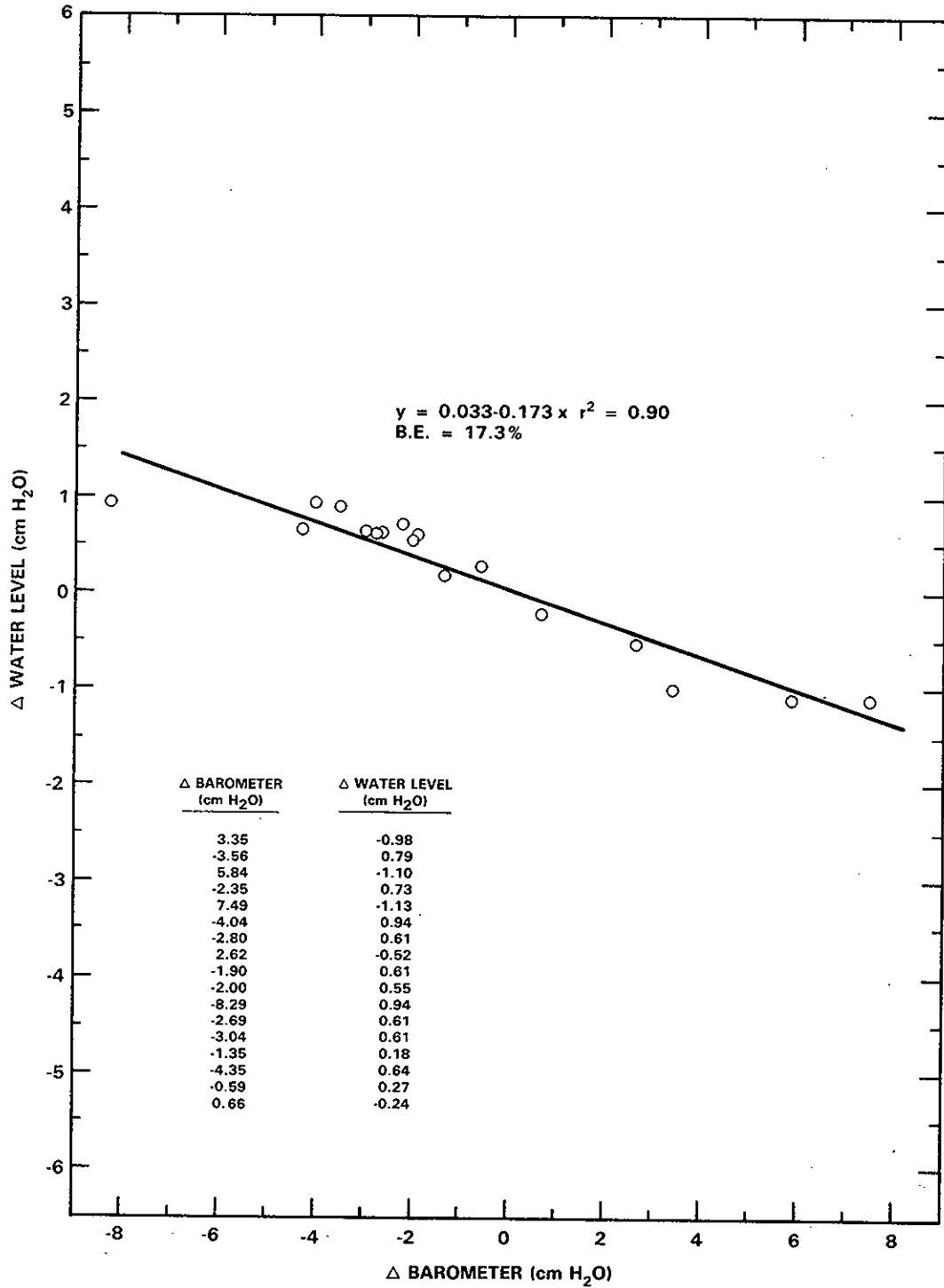
RCP8212-120

FIGURE F.3. Barometric Efficiency: 299-E33-12, Rattlesnake Ridge



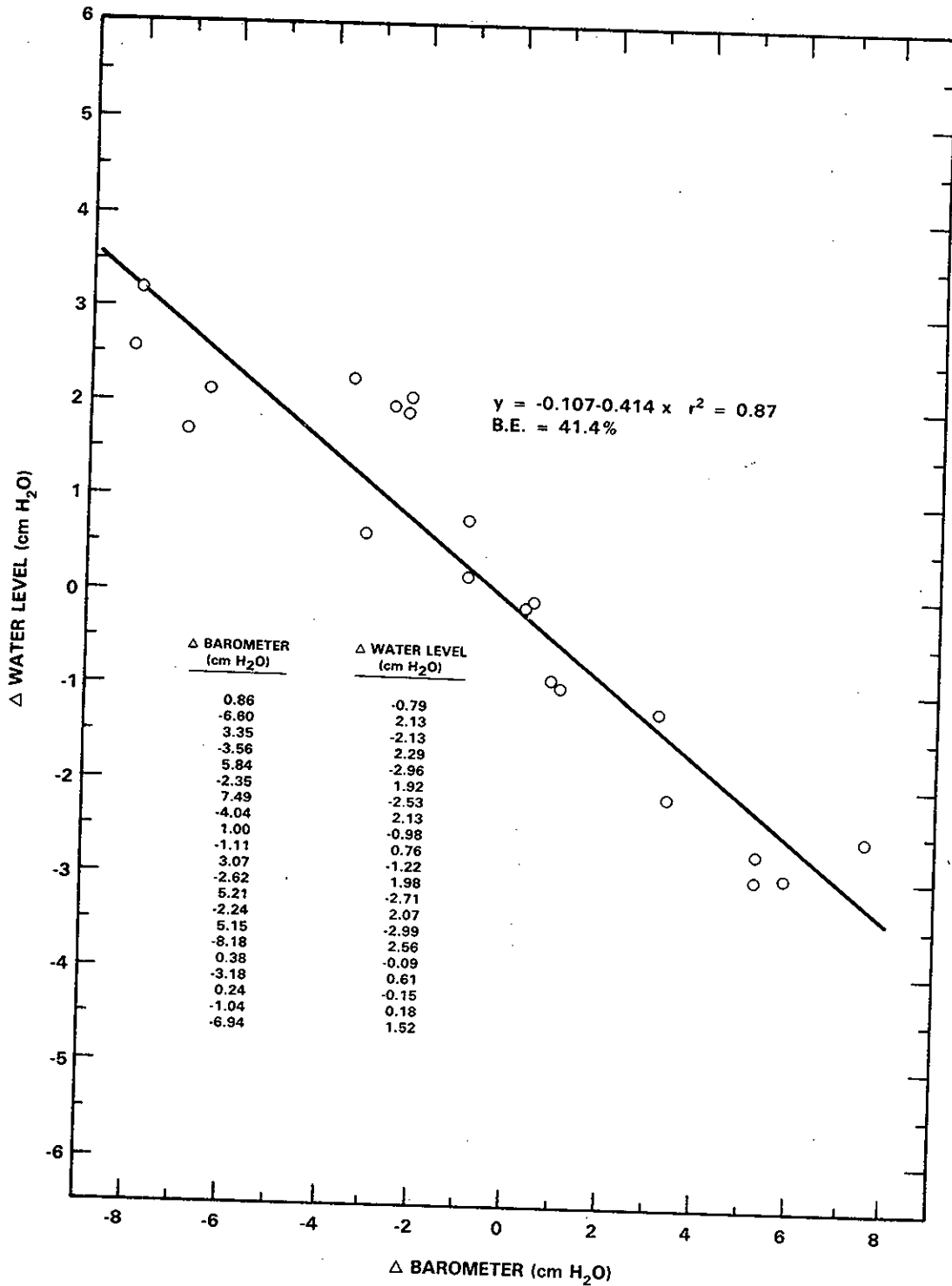
RCP8212-108

FIGURE F.4. Barometric Efficiency: 699-42-40C, Rattlesnake Ridge



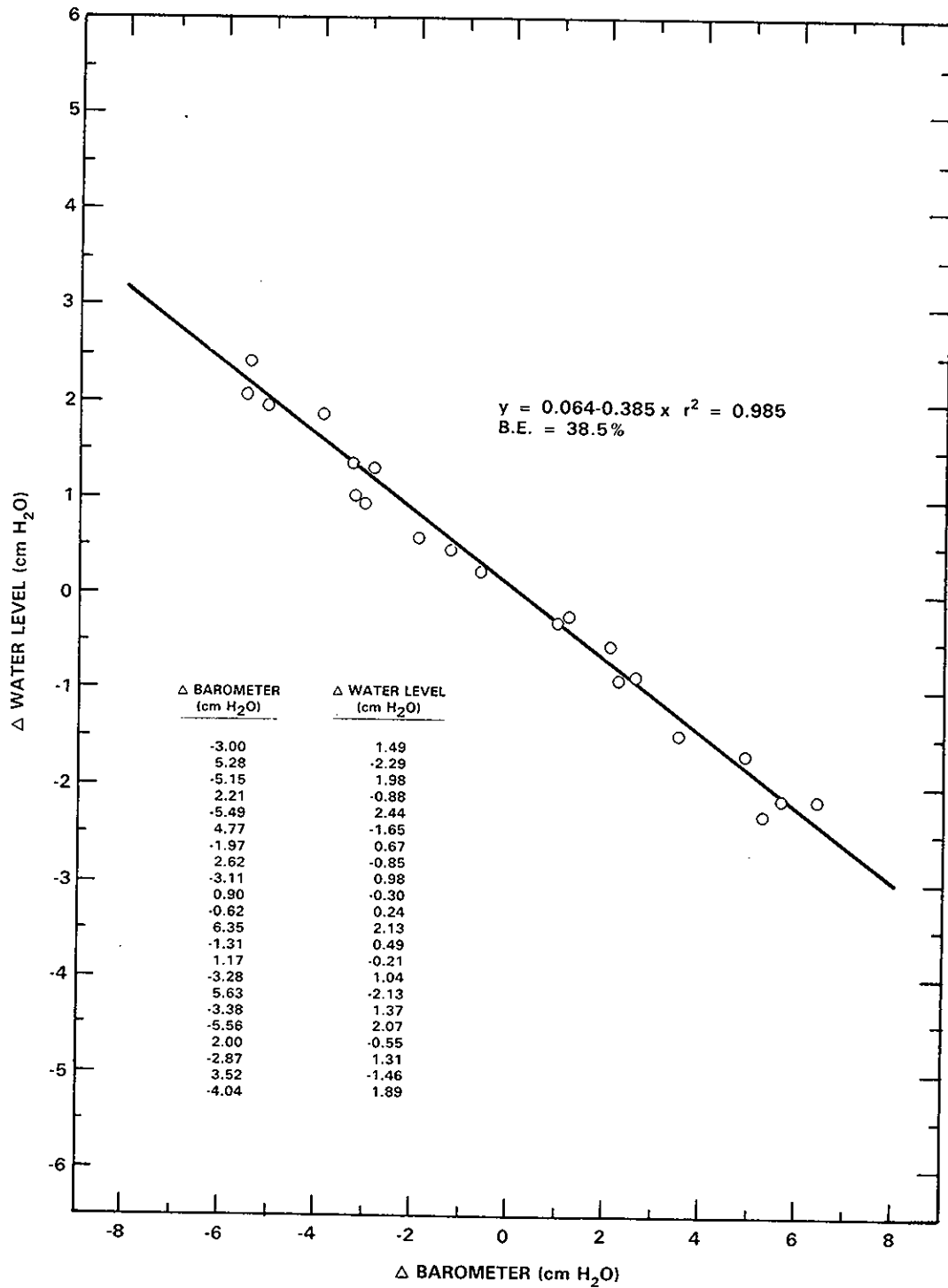
RCP8212-119

FIGURE F.5. Barometric Efficiency: 699-47-50, Rattlesnake Ridge



RCP8212-118

FIGURE F.6. Barometric Efficiency: 699-49-55B, Rattlesnake Ridge



RCP8212-117

FIGURE F.7. Barometric Efficiency: 699-50-45, Rattlesnake Ridge

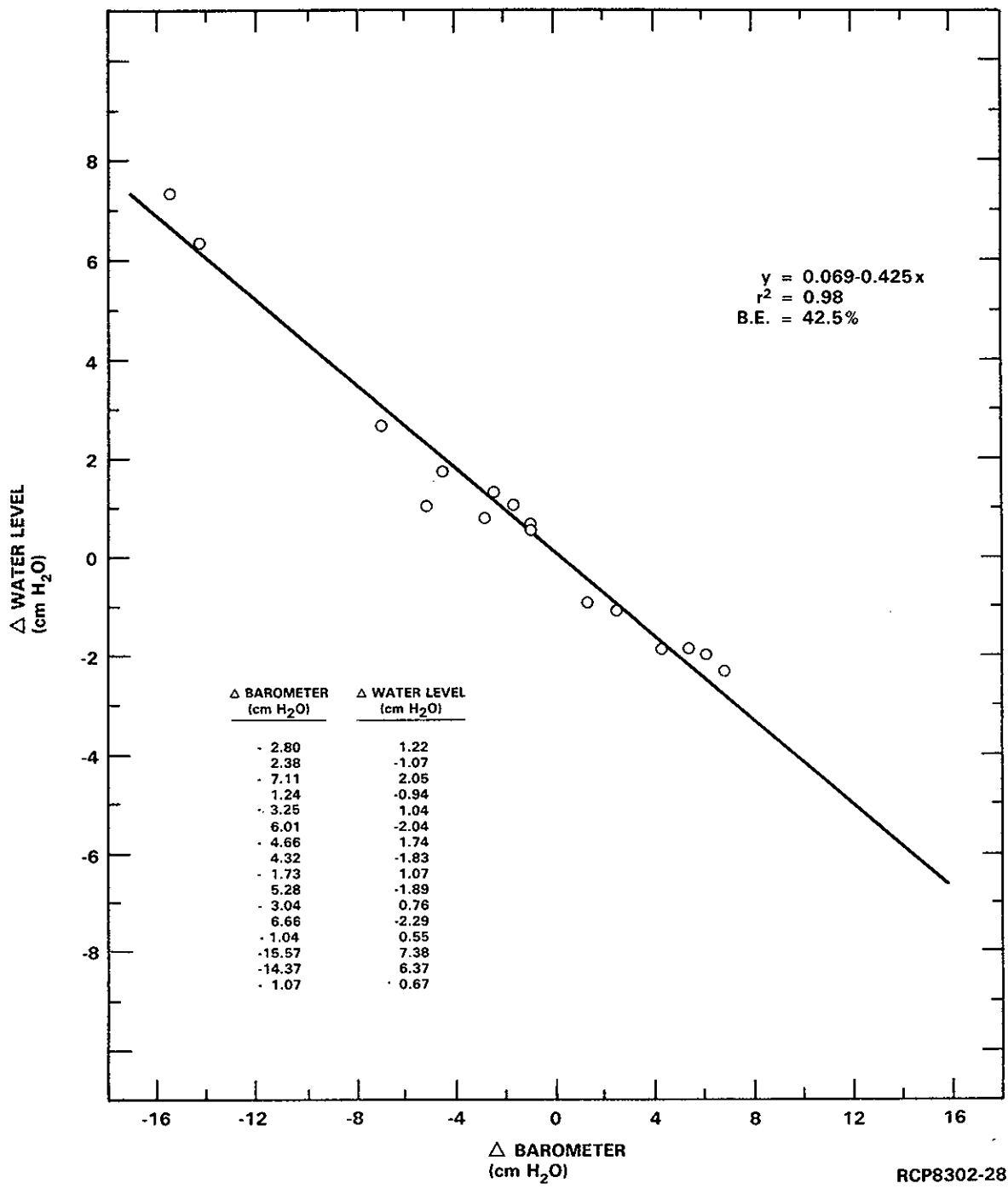
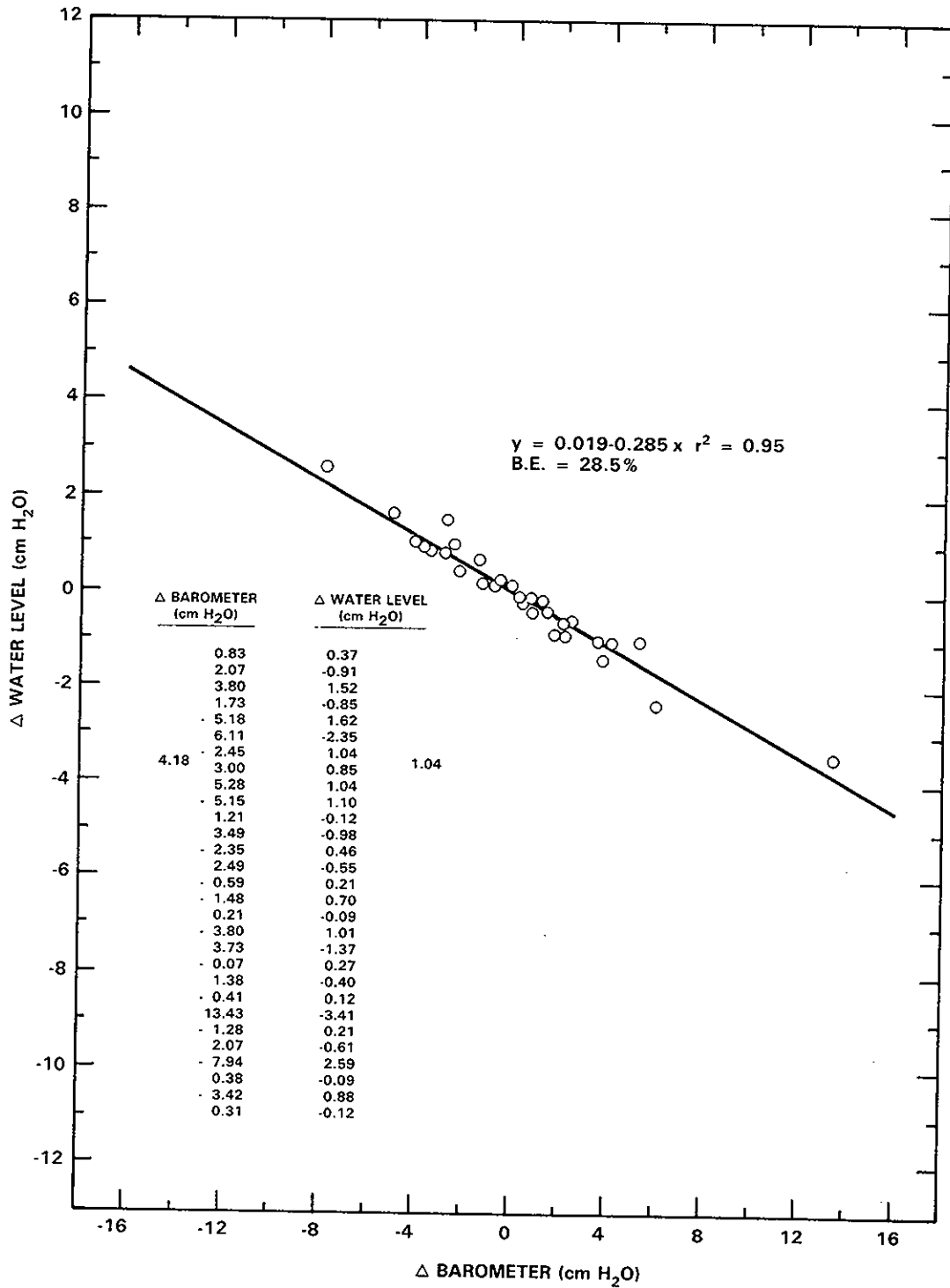
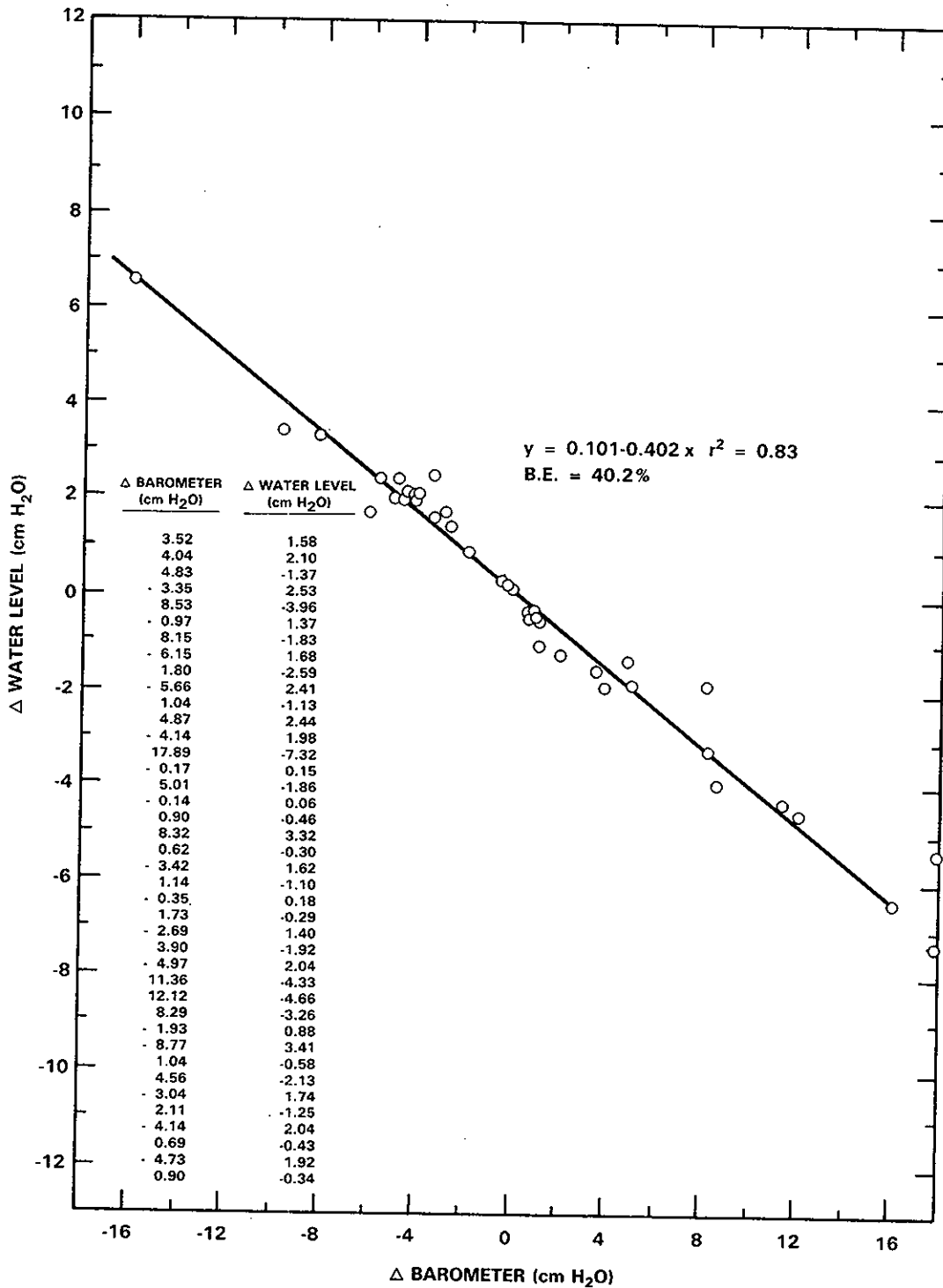


FIGURE F.8. Barometric Efficiency: 699-50-48, Rattlesnake Ridge



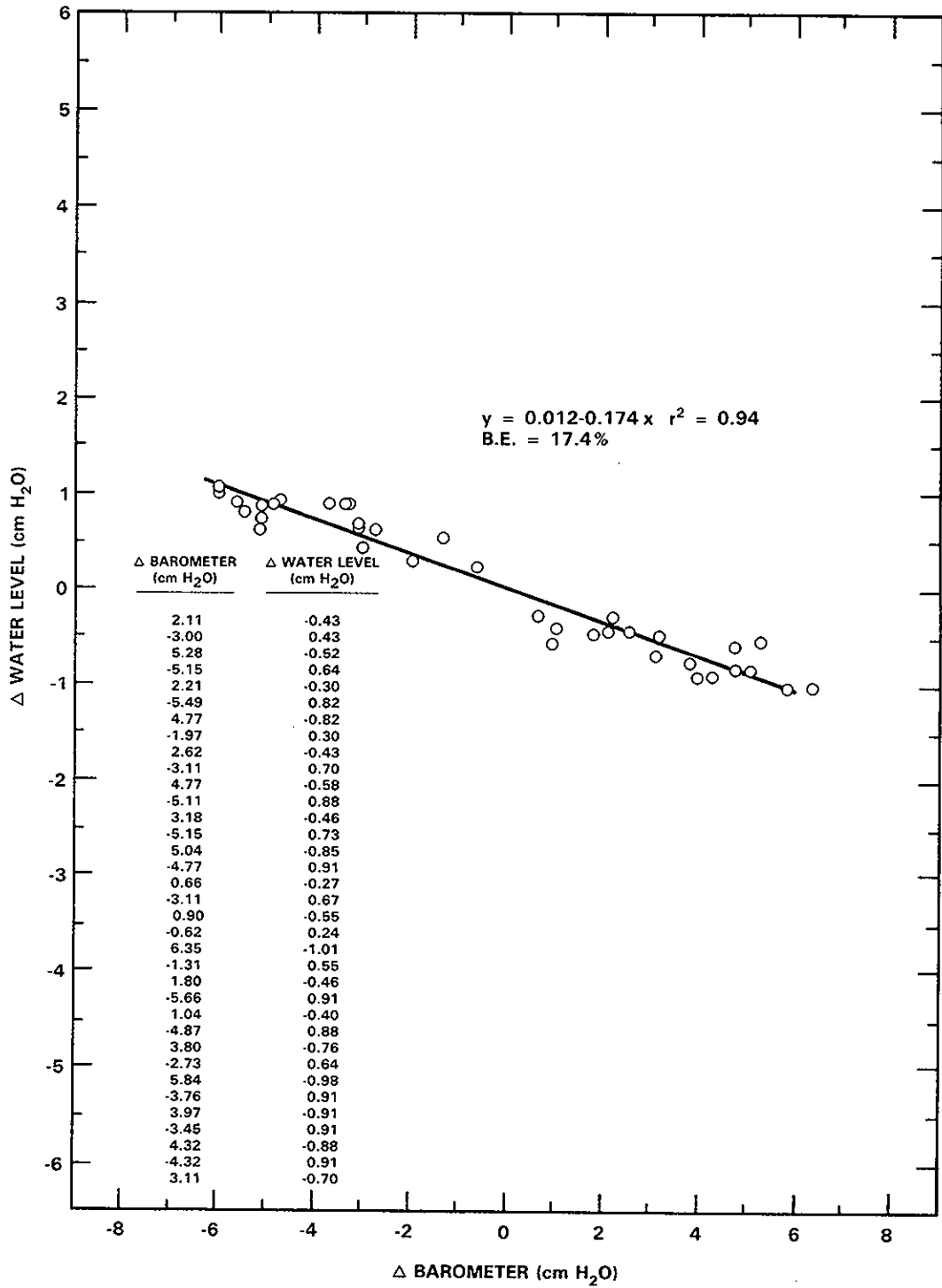
RCP8212-116

FIGURE F.9. Barometric Efficiency: 699-51-46, Rattlesnake Ridge



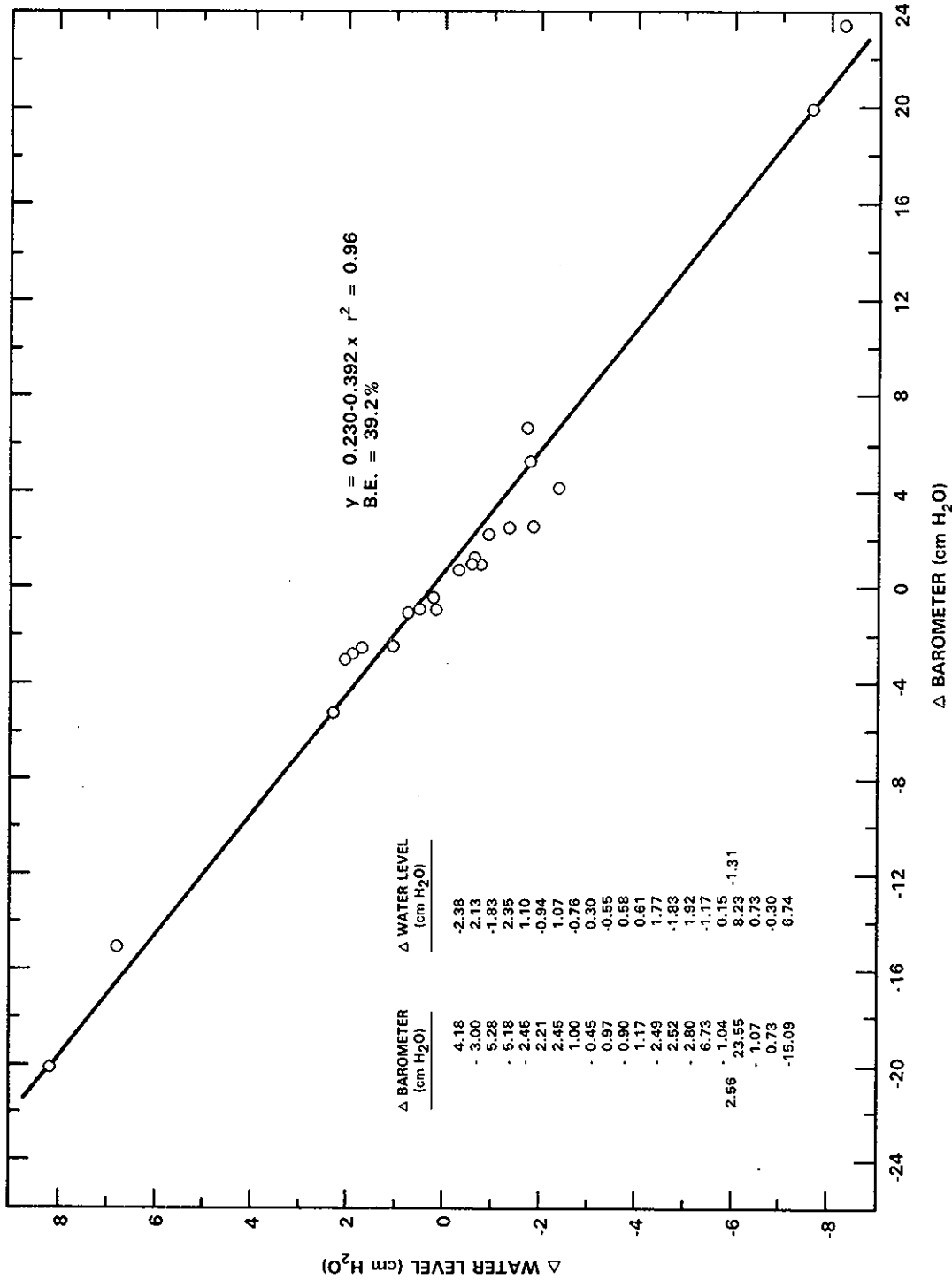
RCP8212-109

FIGURE F.10. Barometric Efficiency: 699-52-46, Rattlesnake Ridge



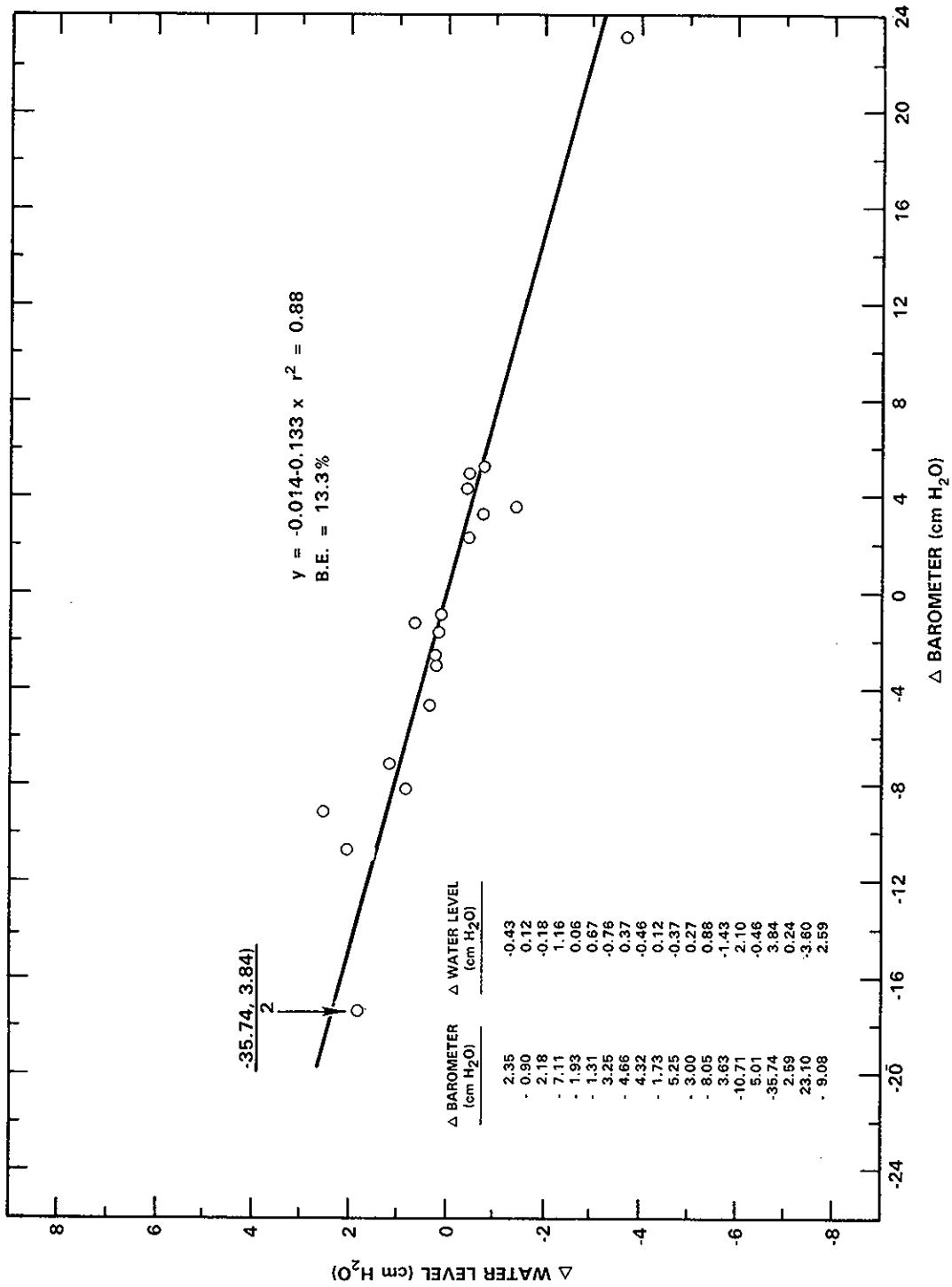
RCP8212-110

FIGURE F.11. Barometric Efficiency: 699-52-48, Rattlesnake Ridge



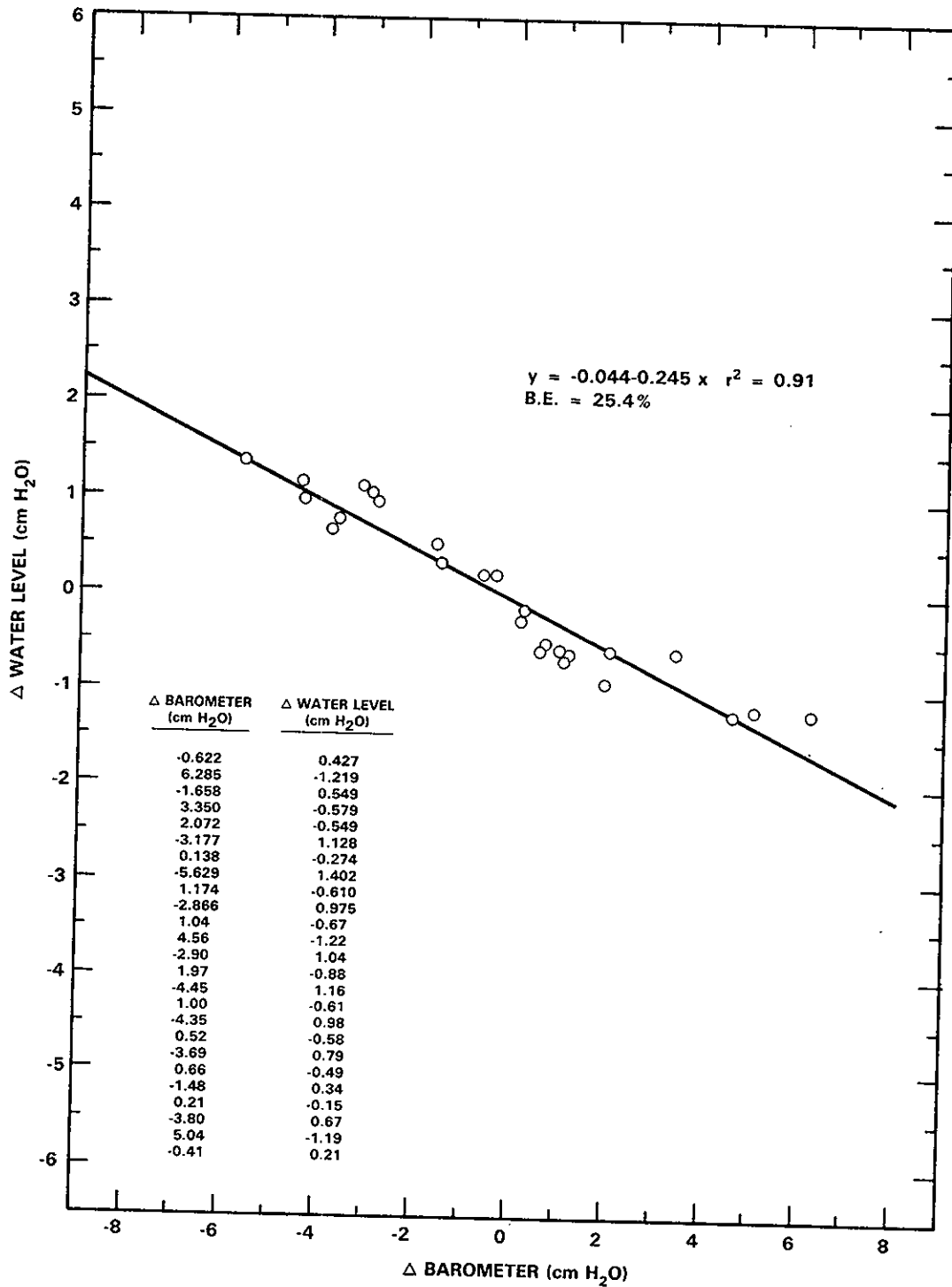
RCP8212-111

FIGURE F.12. Barometric Efficiency: 699-53-50, Rattlesnake Ridge



RCP8212-113

FIGURE F.13. Barometric Efficiency: 699-54-57, Rattlesnake Ridge



RCP8212-112

FIGURE F.14. Barometric Efficiency: 699-56-53, Rattlesnake Ridge

APPENDIX G

SINGLE-BOREHOLE TRACER TEST DATA

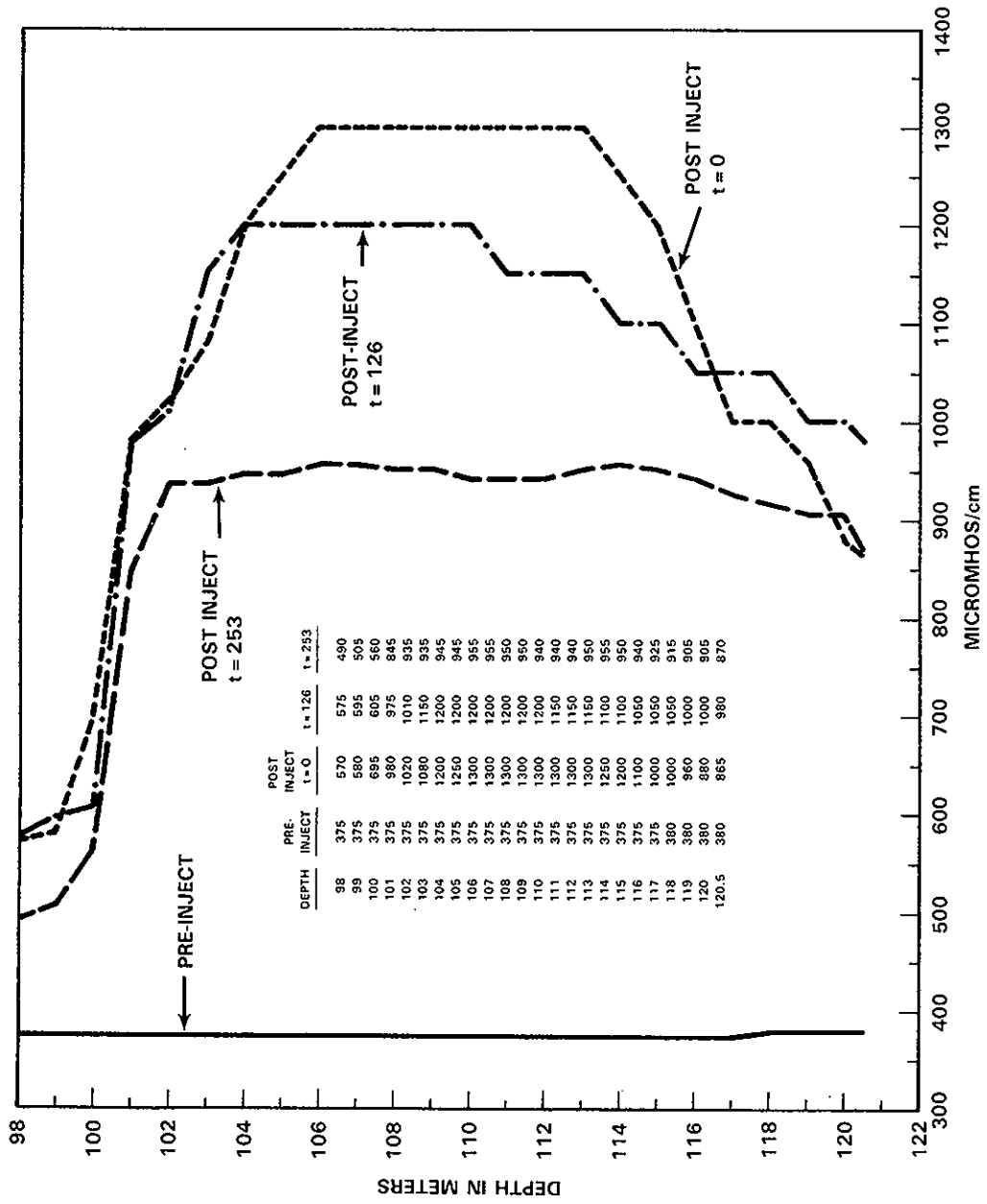


FIGURE G.1. Single Borehole Tracer Test: 299-E26-8, 2/25/83, Electrical Conductivity Profile

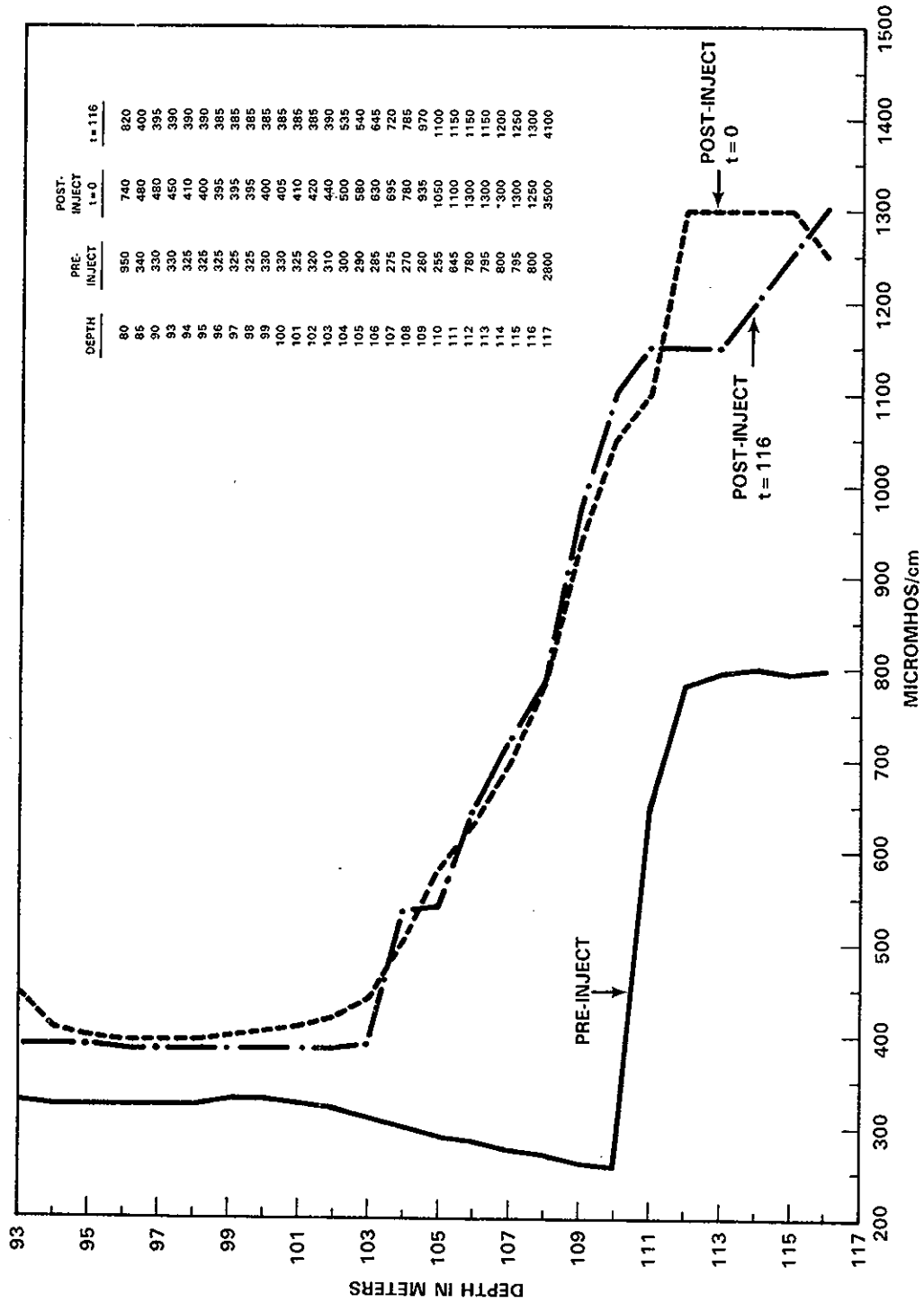


FIGURE G.2. Single Borehole Tracer Test: 299-E33-12, 3/30/83, Electrical Conductivity Profile

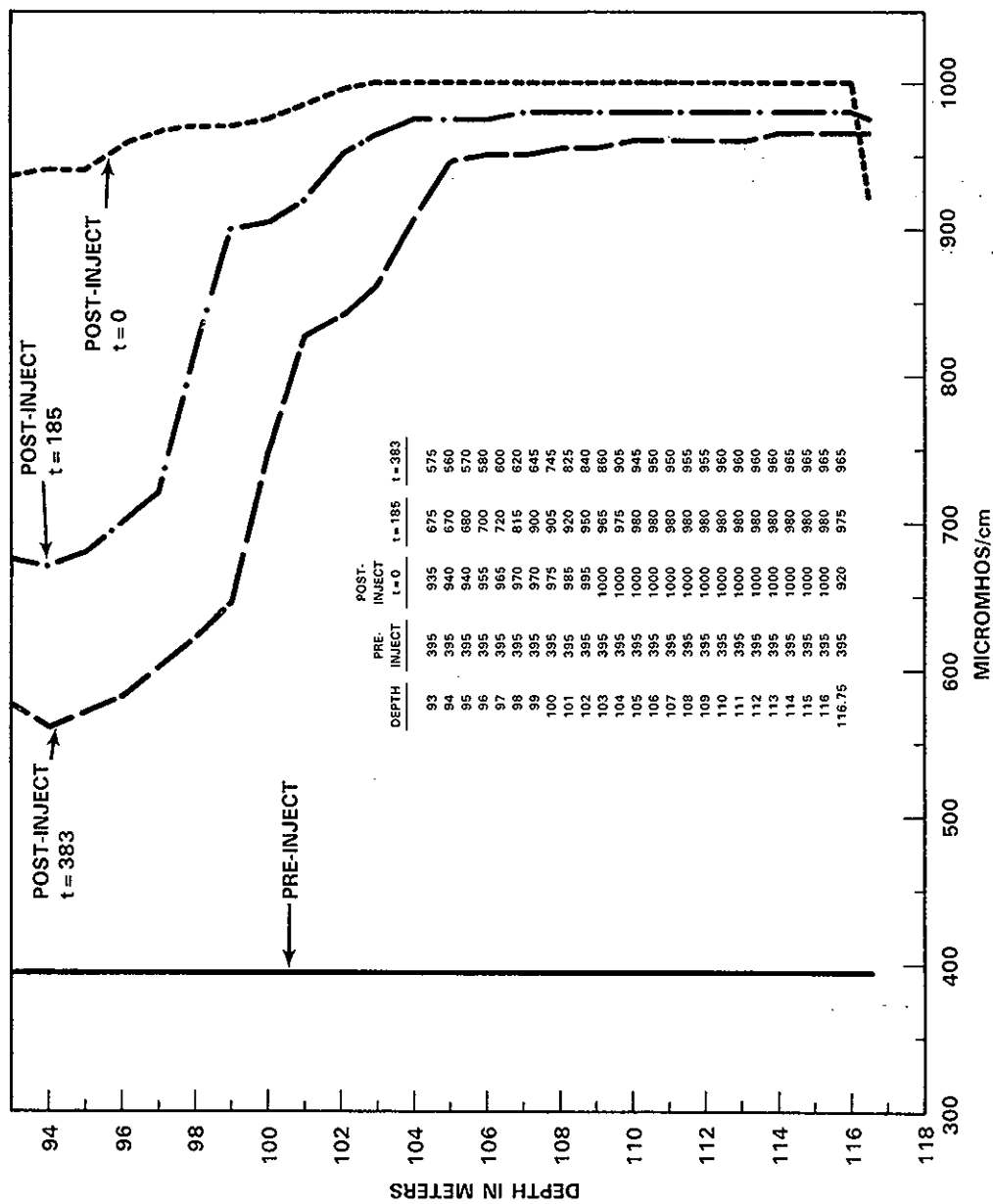


FIGURE G.3. Single Borehole Tracer Test: 699-42-40C, 2/19/83, Electrical Conductivity Profile

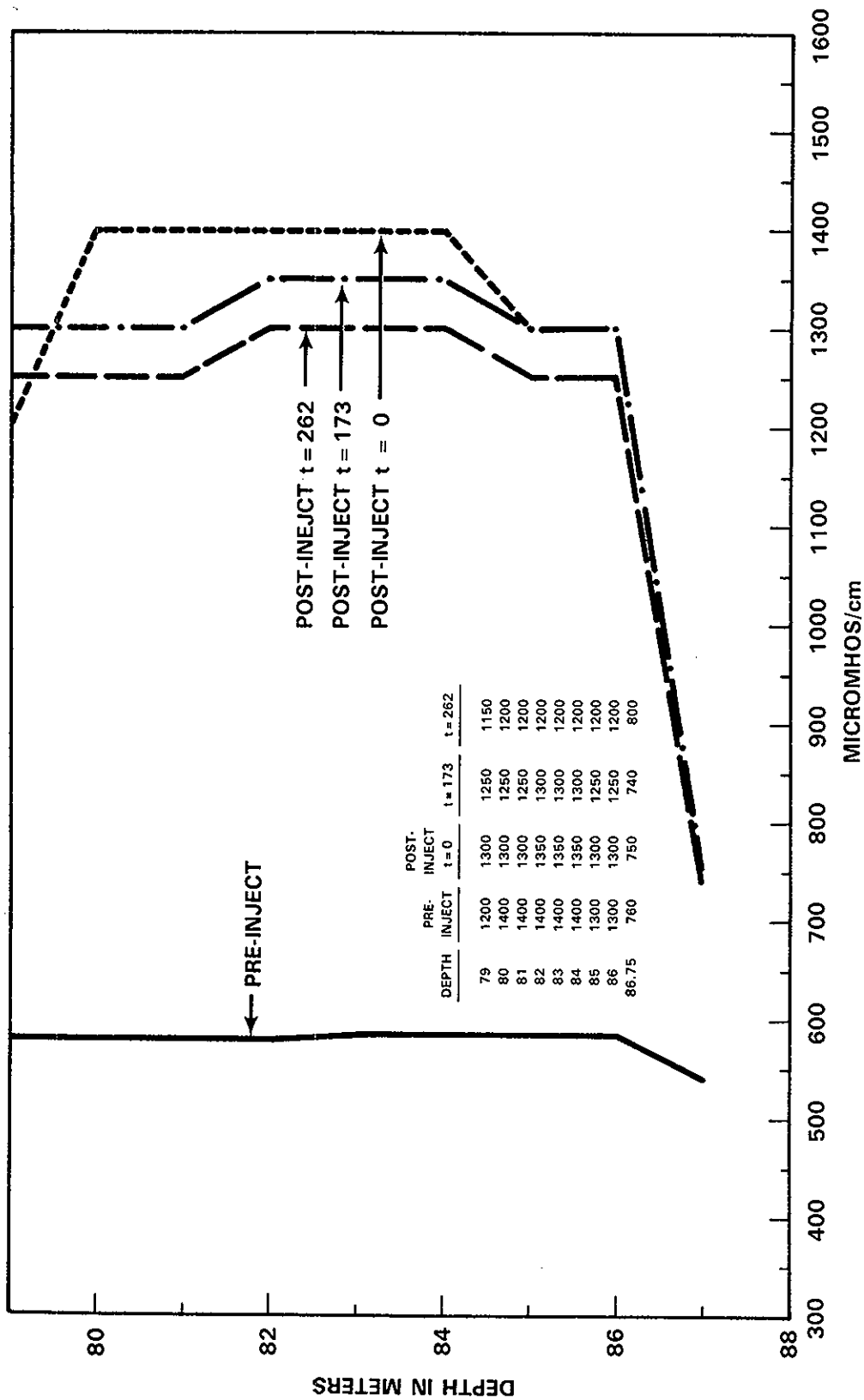


FIGURE G.4. Single Borehole Tracer Test: 699-47-50, 3/22/83, Electrical Conductivity Profile

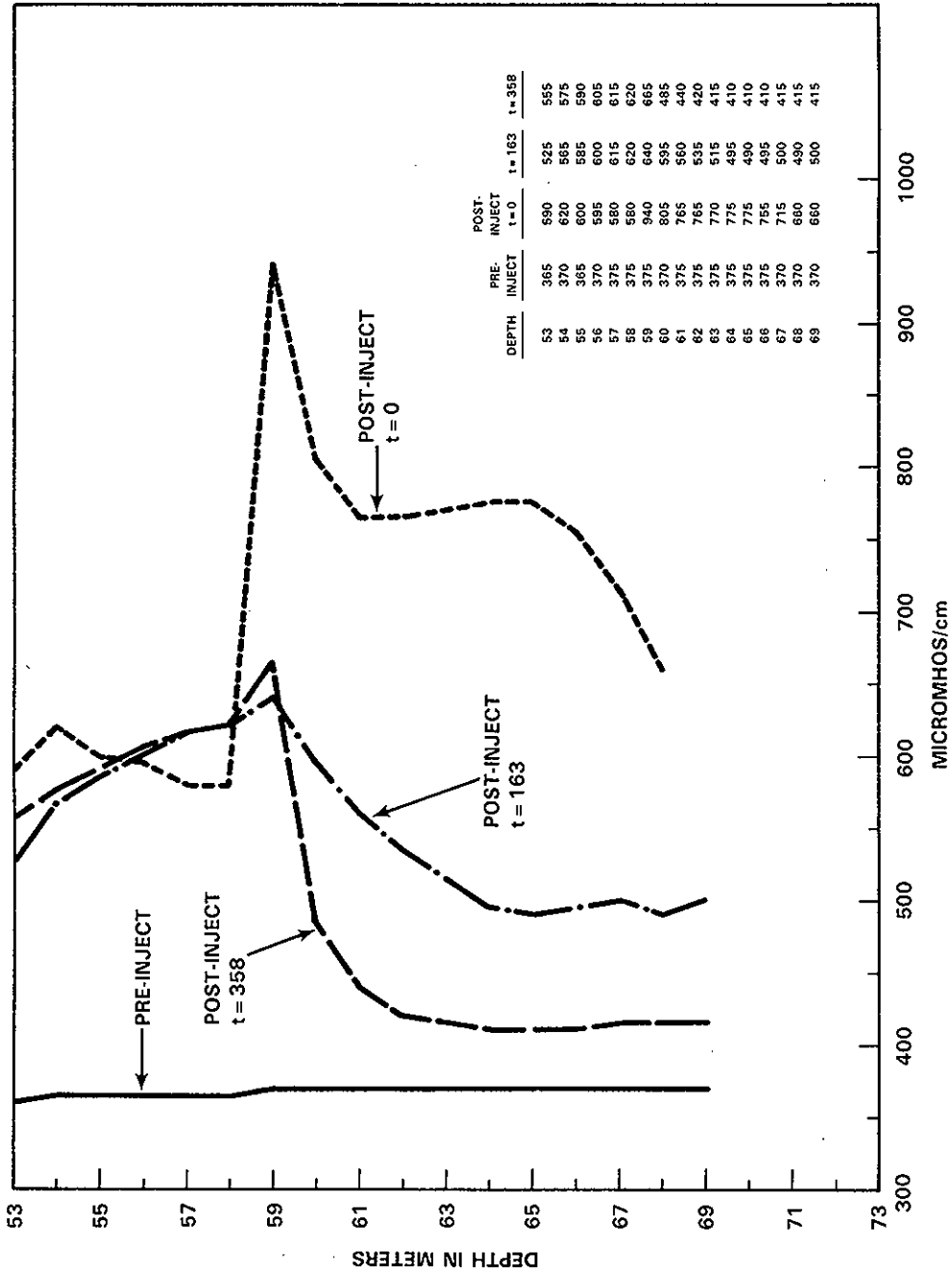


FIGURE G.5. Single Borehole Tracer Test: 699-49-55b, 2/16/83, Electrical Conductivity Profile

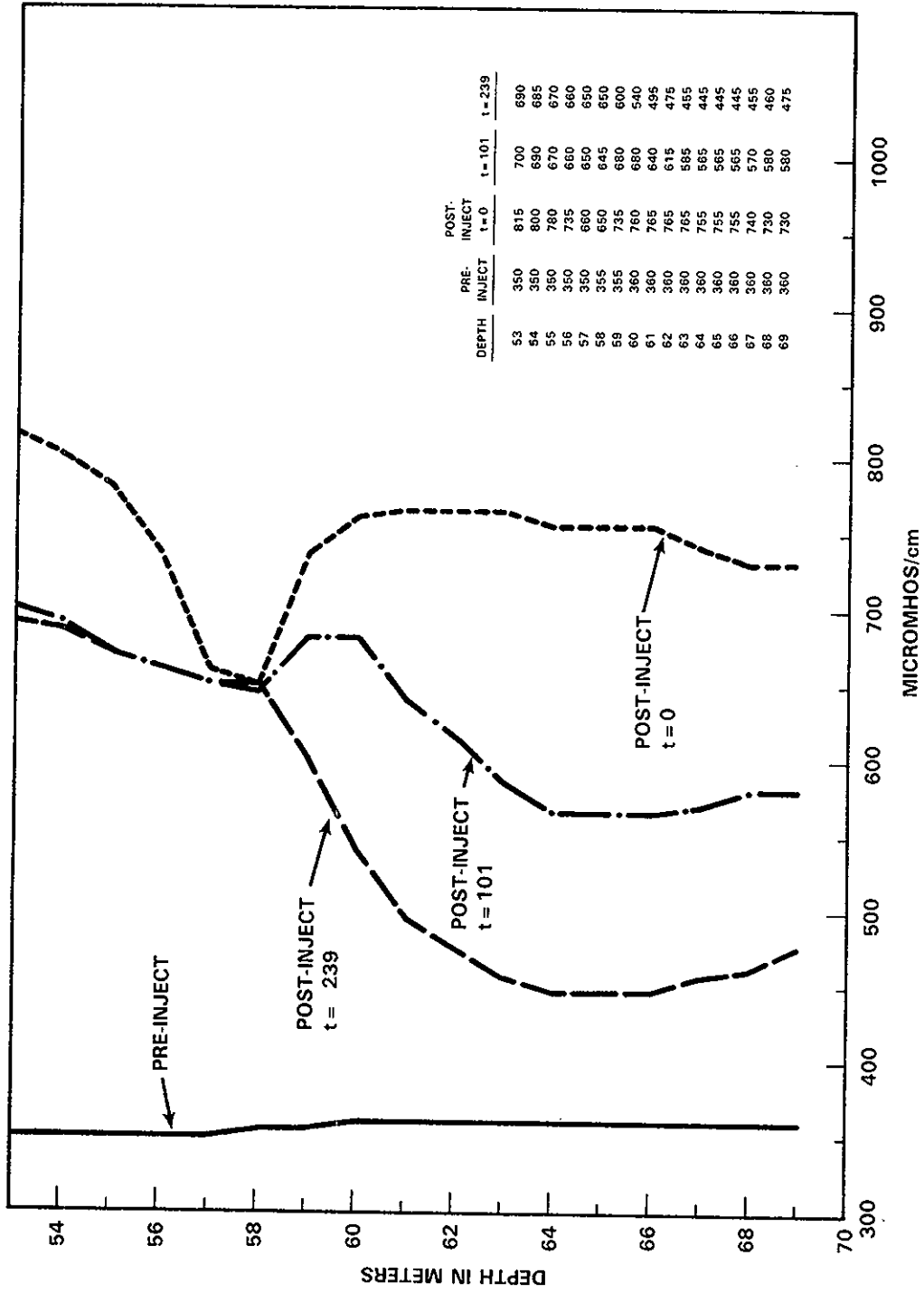


FIGURE G.6. Single Borehole Tracer Test: 699-49-55B, 3/23/83, Electrical Conductivity Profile

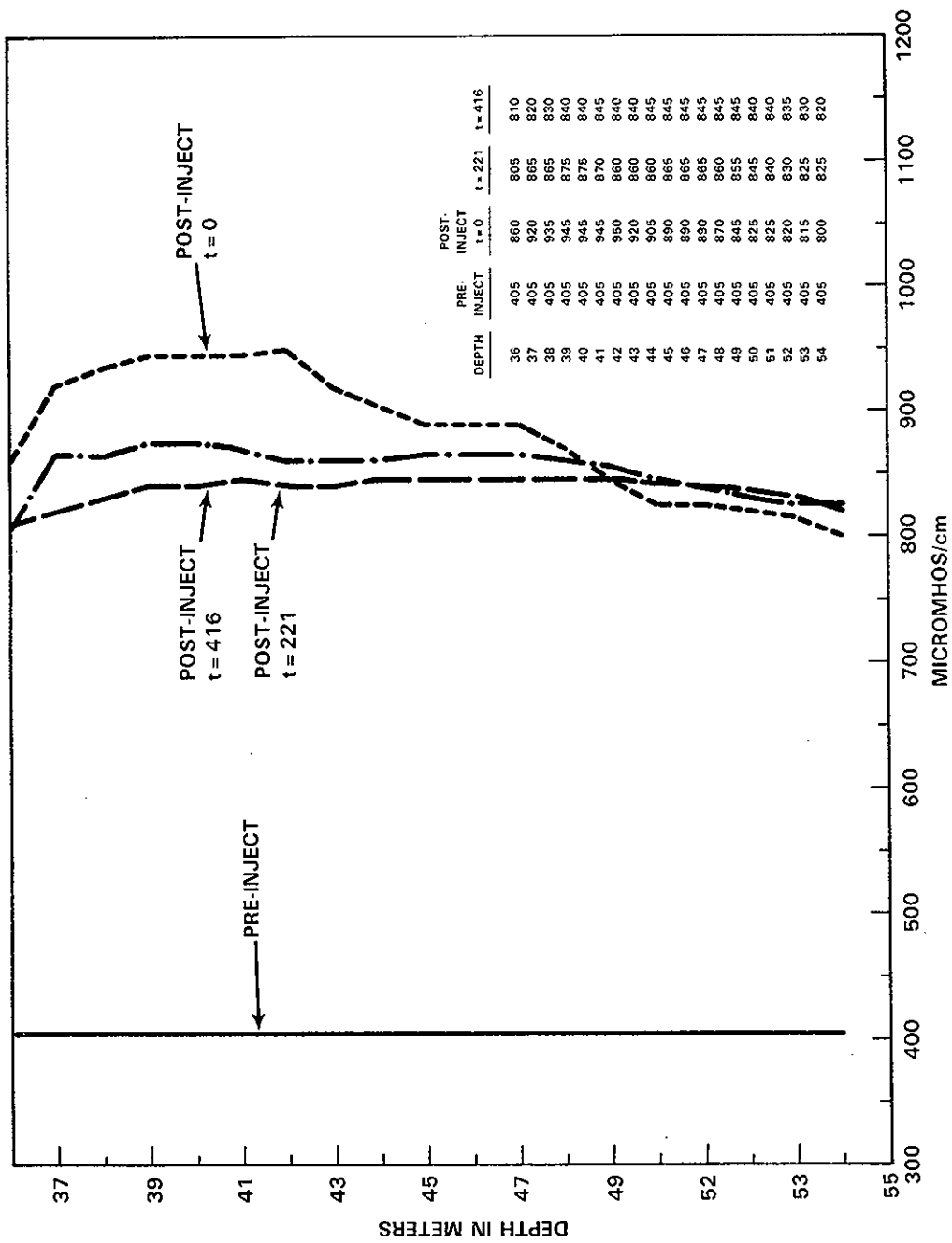


FIGURE G.7. Single Borehole Tracer Test: 699-50-45, 3/04/83, Electrical Conductivity Profile

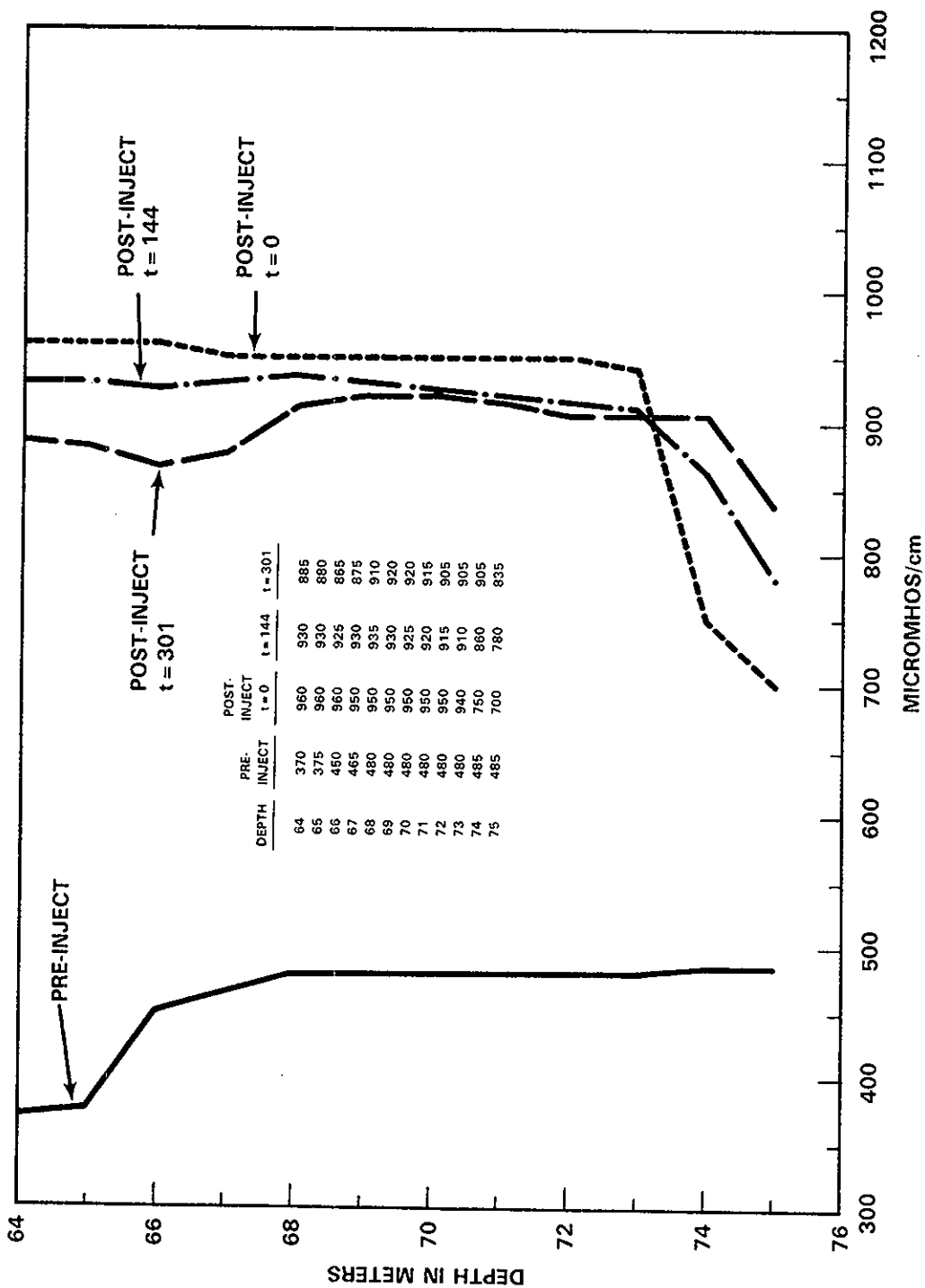


FIGURE G.8. Single Borehole Tracer Test: 699-50-48, 3/08/83, Electrical Conductivity Profile

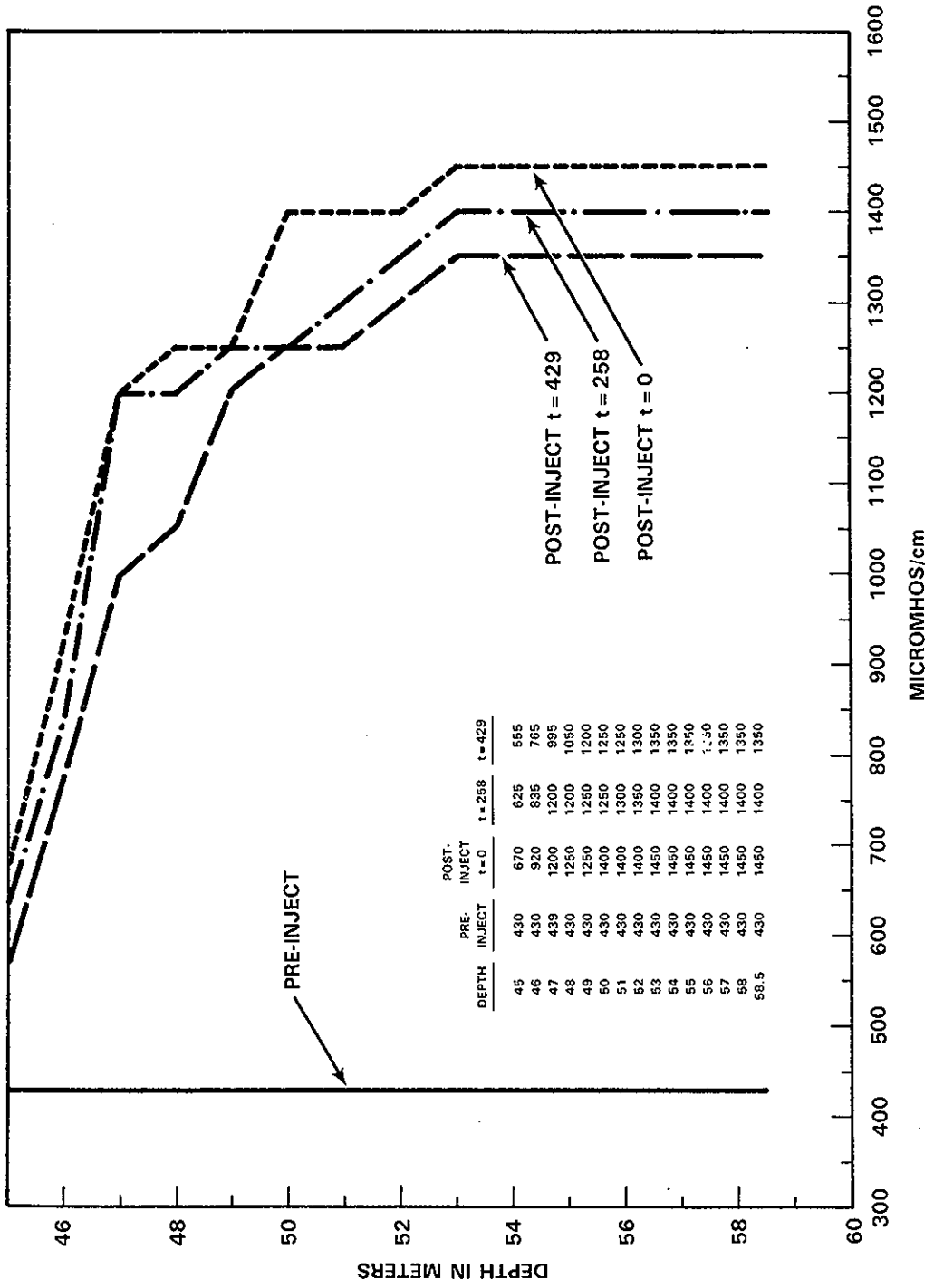


FIGURE G.9. Single Borehole Tracer Test: 699-52-48, 3/02/83, Electrical Conductivity Profile

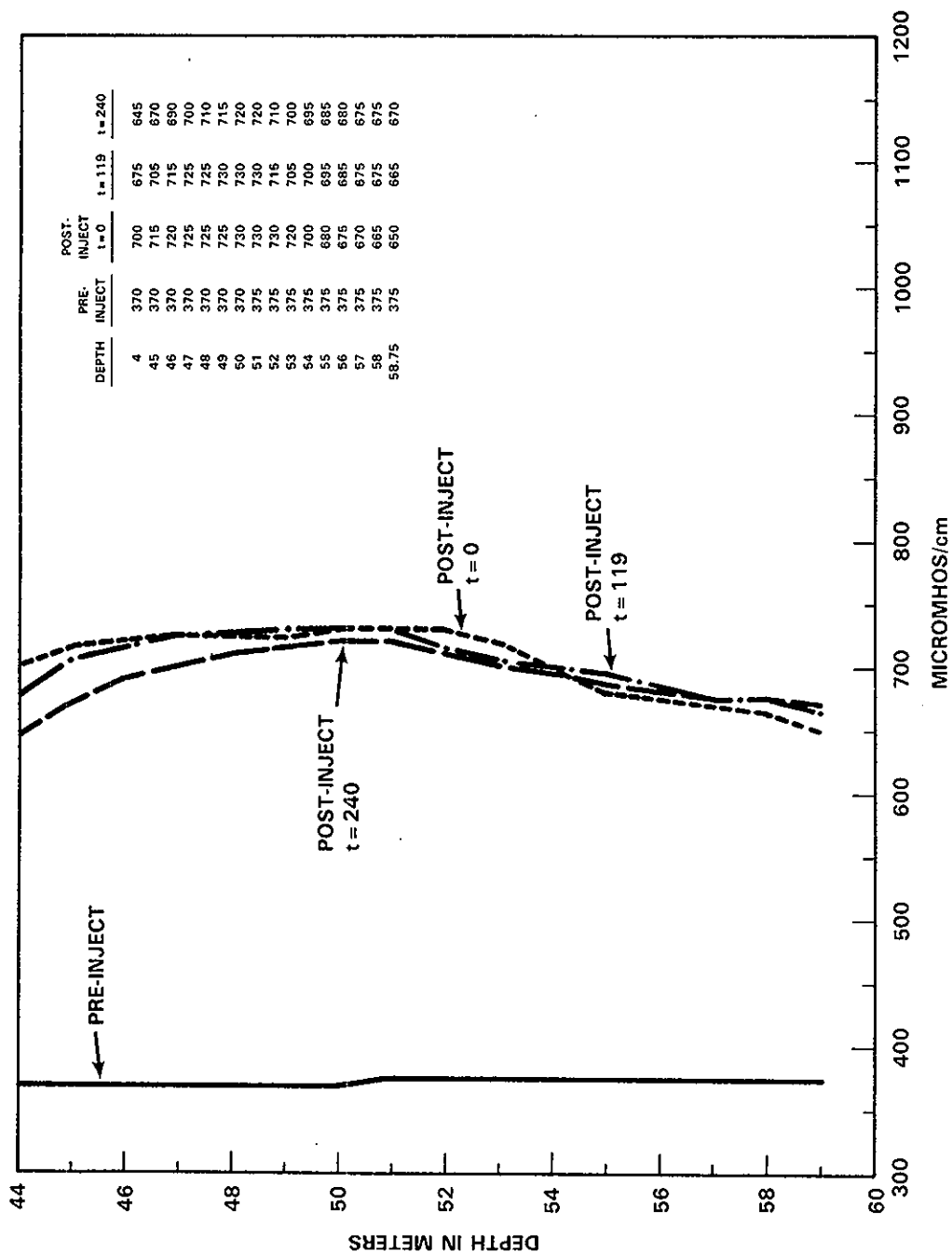


FIGURE G.10. Single Borehole Tracer Test: 699-53-50, 3/03/83, Electrical Conductivity Profile

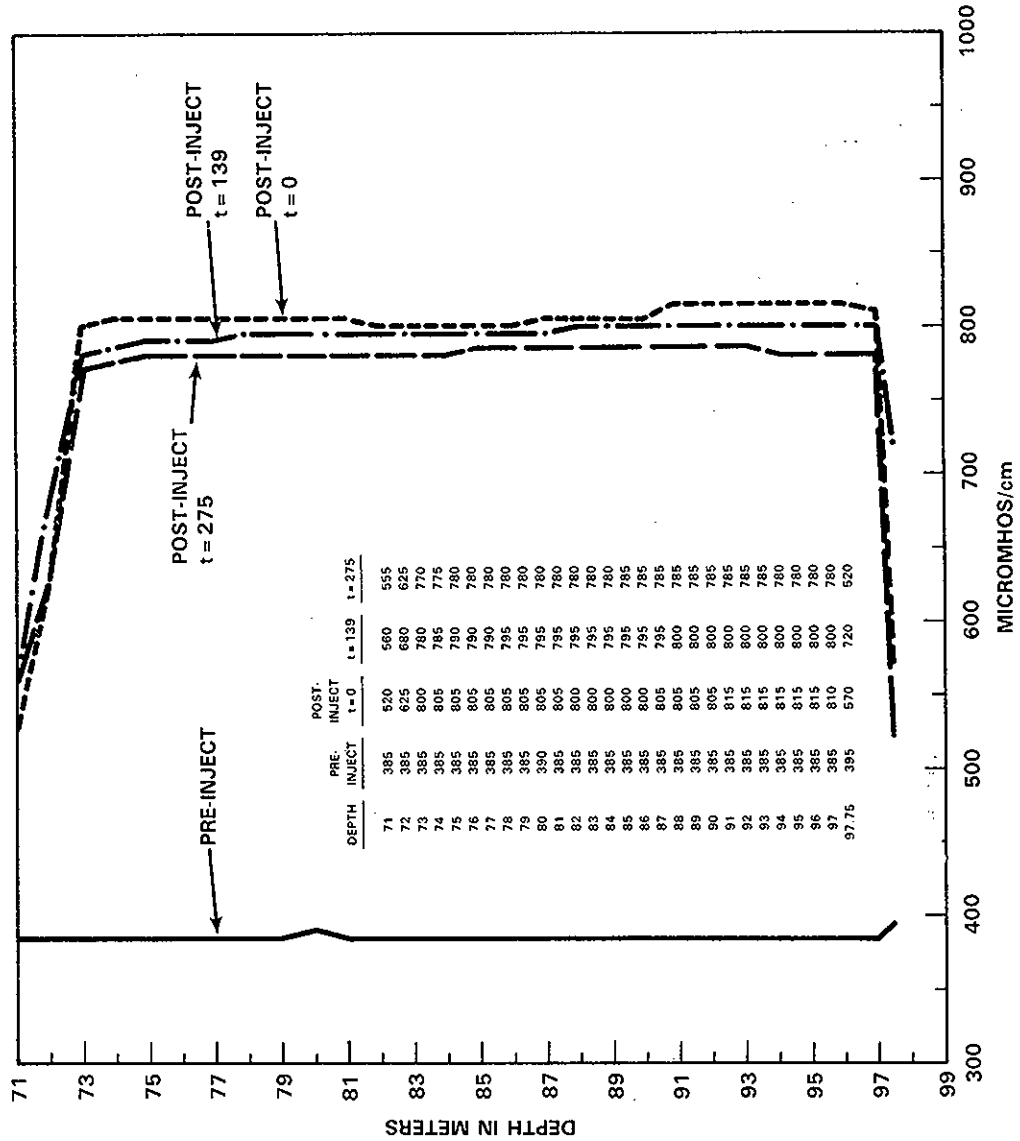


FIGURE G.11. Single Borehole Tracer Test: 699-54-57, 2/19/83, Electrical Conductivity Profile

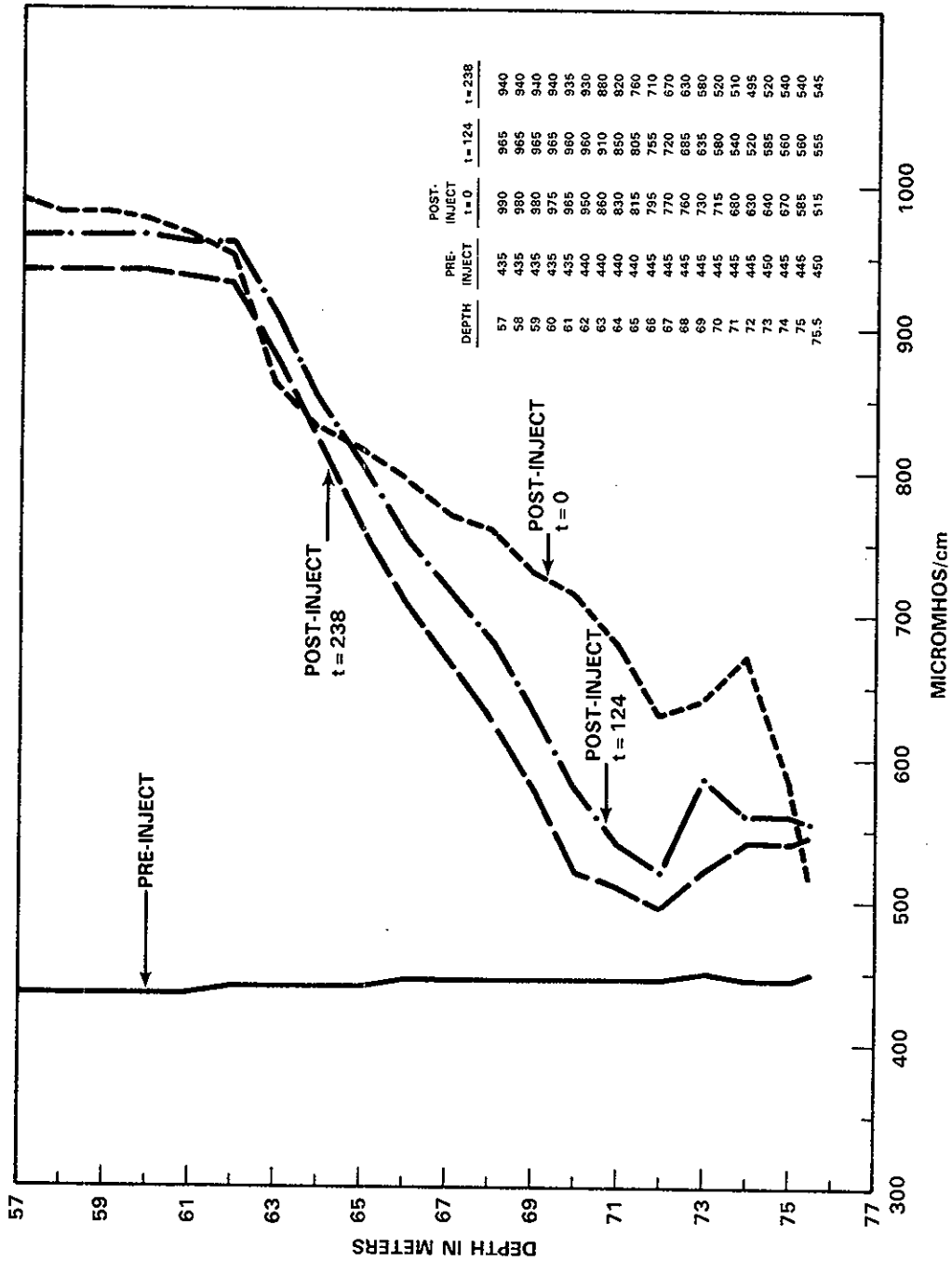


FIGURE G.12. Single Borehole Tracer Test: 699-56-53, 2/18/83, Electrical Conductivity Profile

APPENDIX H

X-RAY FLUORESCENCE ANALYSIS OF
BASALT CHIPS FROM TEST WELLS

TABLE H.1. X-Ray Fluorescence Analysis of Basalt Chips from Test Wells

SAMPLE NUMBER	BOREHOLE NUMBER	DEPTH (M)	CHEMICAL COMPOSITION (WT. %)													CHEMICAL TYPE
			SiO ₂	Al ₂ O ₃	TiO ₂	Fe ₂ O ₃	FeO	MnO	CaO	MgO	K ₂ O	Na ₂ O	P ₂ O ₅			
C6771	E16-1	147.8-150.6	50.28	14.38	3.60	2.00	12.39	0.20	8.68	4.35	1.12	2.	0.51-	ELEPHANT MOUNTAIN		
C6776	E16-1	153.9-155.4	49.87	13.94	3.63	2.00	12.99	0.22	8.55	4.49	1.39	2.39	0.54-	ELEPHANT MOUNTAIN		
C6772	E26-8	79.2- 80.8	49.86	14.16	3.46	2.00	12.44	0.21	9.08	4.38	1.35	2.53	0.52	ELEPHANT MOUNTAIN		
C6774	E26-8	121.90	53.26	16.55	1.72	2.00	9.10	0.17	8.64	5.58	0.44	2.29	0.25	POMONA		
C6777	42-40C	70.10	50.08	13.92	3.65	2.00	12.31	0.23	8.67	4.49	1.33	2.78	0.54	ELEPHANT MOUNTAIN		
C6778	42-40C	117.30	53.71	16.75	1.72	2.00	8.44	0.17	8.58	5.65	0.55	2.15	0.27	POMONA		
C6775	49-55B	42.7- 44.2	48.42	13.80	3.48	2.00	13.04	0.21	10.21	4.37	1.16	2.81	0.50	ELEPHANT MOUNTAIN		
C6770	54-57	62.5- 64.0	49.93	13.96	3.50	2.00	12.91	0.22	8.58	4.68	1.31	2.39	0.51	ELEPHANT MOUNTAIN		
C6779	54-57	97.50	51.72	16.41	1.84	2.00	8.76	0.16	10.45	5.79	0.34	2.25	0.27	POMONA		
C6769	56-53	32.00	49.85	14.40	3.63	2.00	12.94	0.22	8.29	4.28	1.19	2.64	0.55	ELEPHANT MOUNTAIN		
C6773	56-53	38.10	50.14	14.10	3.64	2.00	12.62	0.20	8.57	4.52	1.08	2.58	0.53	ELEPHANT MOUNTAIN		

*BOREHOLES PREFIXED BY 699- OR 299-

APPENDIX I

GROUND-WATER ANALYTICAL DATA

TABLE I.1. Major Cations and Anions and Field Measurements

Well Number	Zone Sampled	Date	Temp. Degrees Celsius	Field pH	Lab pH	Electrical Conductivity, $\mu\text{hos/cm}$	Total Dissolved Solids, mg/L	Calcium, mg/L	Magnesium, mg/L	Sodium, mg/L	Potassium, mg/L	Iron, mg/L	Silica, mg/L	HCO ₃ - Alkalinity, mg/L as CaCO ₃	Total Alkalinity, mg/L as CaCO ₃	Sulfate, mg/L	Chloride, mg/L	Nitrate, $\mu\text{S N}$	Fluoride, mg/L
299-E16-1	Elephant Mountain II	5/15/82	23.3	9.05	8.6	325	205	15	8.9	28	10.9	0.04	68	80	90	26	2.6	0.04	0.62
	Fracture zone	7/13/82	22.9	8.45	8.3	380	236	28	9.2	30	10.2	<0.03	68	134	143	36	1.4	<0.02	0.61
	Elephant Mountain	7/13/82	22.8	8.35	8.3	370	242	28	9.6	31	10.2	0.04	66	144	144	31	1.2	0.09	0.57
	Interflow zone	7/14/82	23.2	8.30	8.6	340	227	26	9.9	31	10.2	0.04	68	130	145	35	<1.0	<0.02	0.59
299-E26-8	Unconfined	3/23/82	21.3	7.70	8.2	395	171	25.8	10.7	15.6	5.5	<0.03	21	82	89	29	9.5	0.47	0.68
	Rattlesnake Ridge	5/18/82	19.5	8.50	8.4	360	248	19	8.2	20	10.4	<0.03	79	90	99	35	7.9	1.8	0.51
		5/19/82	20.6	8.35	8.3	370	249	21	9.2	18	9.9	<0.03	79	98	103	18	7.6	1.6	0.58
		5/19/82		8.3	8.3	375	249	19	9.2	19	9.9	<0.03	79	99	104	37	8.1	2.2	0.53
299-E33-12	Unconfined	5/11/82	20.3	7.10	7.6	630	486	34	13.1	74	7.0	0.05	46	100	109	70	5.8	36.0	2.6
	Rattlesnake Ridge	5/21/82	19.7	9.45	9.1	345	170	14	7.2	17	8.6	<0.03	60	34	39	28	6.6	4.0	0.23
		5/22/82	19.9	8.25	8.9	315	199	19	8.5	17	8.0	<0.03	72	56	64	25	6.1	6.0	0.17
699-37-43	Unconfined	8/13/82	21.0	7.75	7.8	1150	621	82	29	57	8.7	<0.03	44	90	106	305	19.0	3.6	0.46
699-42-40A	Unconfined	8/13/82	18.1	7.95	7.9	395	237	19	14	28	3.8	<0.03	44	95	114	37	7.0	4.4	0.70
699-42-40C	Unconfined	1/19/82	18.0	7.70	7.8	425	233	22	12.4	25	4.3	<0.05	--	99	106	29	6.7	3.6	--
	Elephant Mountain	4/16/82				425	172	26.6	11.8	24.6	6.4	2.72	49	122	128	18	5.1	0.24	0.85
	Interflow zone	5/20/82	18.4	8.75	9.0	365	229	10	3.7	35	14.4	<0.03	72	105	122	38	3.0	0.18	0.66
	Rattlesnake Ridge	5/21/82	19.8	8.3	8.2	280*	245	17	4.5	33	13.7	<0.03	72	114	123	17	4.0	0.10	0.96
		5/21/82	19.6	8.45	8.3	330	230	17.5	4.6	35	13.6	<0.03	72	115	125	16	4.0	0.11	0.84
		11/19/82				---	---	18.7	4.5	36	12.7	0.008	--	--	--	15.5	3.5	<0.02	0.70
699-47-50	Rattlesnake Ridge	7/15/82	19.4	7.80	7.8	560	362	46	18.5	22	7.2	0.06	51	84	95	100	31.0	2.3	0.66
699-49-58A	Unconfined	8/11/82	18.8	8.15	8.2	850	539	70	20	35	10.3	<0.03	39	85	104	209	21.0	2.8	0.54
699-49-58B	Rattlesnake Ridge	5/27/82	18.1	7.80	7.6	375	228	38	11.9	11	6.9	<0.03	73	112	120	20	16.7	0.33	0.37
		5/28/82	18.4	7.80	7.6	365	216	38	12.2	12	6.8	<0.03	73	114	122	21	9.6	0.35	0.26
		5/28/82	18.0	7.5	7.5	218	218	38	12.4	17	6.8	<0.03	71	109	117	17	10.6	0.32	0.23
699-50-45	Rattlesnake Ridge	8/06/82	17.6	7.60	8.2	410	256	92	15.7	12	6.0	0.04	58	105	114	18	22.0	0.71	0.60
699-50-48	Rattlesnake Ridge	8/07/82	19.8	7.60	8.2	470	291	19	6.2	33	11.0	<0.03	66	100	114	31	26.0	0.14	0.64
699-51-45	Rattlesnake Ridge	8/04/82	17.3	8.60	8.8	320	254	19	2.2	21	9.2	0.30	69	70	86	28	16.0	0.70	0.54
699-52-46	Rattlesnake Ridge	8/07/82	18.4	7.65	8.0	360	263	24	10.5	16	7.3	<0.03	79	100	117	19	25.0	0.30	0.47
699-53-50	Rattlesnake Ridge	8/10/83	17.9	8.05	8.0	400	249	6.2	1.9	50	6.4	<0.03	59	130	147	24	4.0	0.29	0.64
699-54-57	Rattlesnake Ridge	7/14/82	17.2	7.65	7.6	365	222	30	10.9	21	7.3	0.08	70	105	114	29	21.0	0.70	0.60
699-55-50C	Unconfined	5/17/82	18.7	7.80	7.6	350	217	25	11.6	2.3	7.2	<0.03	70	113	117	20	12.9	0.43	0.53
		8/09/82	16.5	7.65	8.0	220	478	19	9.2	4.7	4.1	<0.03	26	95	109	18	2.0	0.20	0.27
699-56-53	Unconfined	1/11/82	14.6	7.06	8.4	260	143	25	10.5	8.4	5.3	<0.05	--	95	95	8.4	3.7	0.23	--
	Unconfined	1/11/82	17.4	7.55	7.5	275	176	25	10.2	8.5	5.4	<0.05	--	106	107	8.4	3.7	0.23	--
	Rattlesnake Ridge	6/03/82	17.4	7.55	7.5	242	242	38	13.2	21	6.8	<0.03	43	124	130	<1	28.0	0.14	0.20
	Rattlesnake Ridge	6/03/82	19.4	7.85	7.6	229	229	38	13.5	21	6.6	<0.03	41	122	129	2	27.0	0.14	0.14
699-60-57	Unconfined	8/10/82	18.5	7.95	8.1	375	228	16	8.5	38	7.8	<0.03	44	135	155	1.8	13.0	0.50	1.60

NOTE: * = Battery problems.

TABLE I.2. Trace Metals Analyses

Weil Number	Zone Sampled	Date	Ag	Ba	Cd	Co	Cr	Cu	Mn	Ni	Pb	Zn
299-E16-1	Elephant Mountain II fraction zone	5/15/82	<2.6	59.9		<36	<30	<1		<12	<20	81
	Elephant Mountain Interflow zone	7/4/82	<3.0	92.2	<30	<11	<8	<1		<2	<28	119
299-E26-8	Unconfined Rattlesnake Ridge	3/23/82 5/19/82	<1.1 <3.7	30.7 92.2	<19 <33	<12	<12	49.3 <1	114	<3 <2	<17 <49	93 117
299-E33-12	Unconfined Rattlesnake Ridge	5/11/82 5/22/82	<4.2 <2.1	25.6 98.3	<22 <11	<18 <8.4	<9	<1 <1	<2	<5.2 <2	<24 <48	180 97
699-37-43	Unconfined	8/13/82	<3.0	58.7	<15		<18	<1	8.3	<3	<17	84
699-42-40A	Unconfined	8/13/82	<2.4	44.7			<31	<1	14.3	<3	<9	95
699-42-40C	Elephant Mountain Interflow zone	8/16/82	<3.3	108.0		<11	<8	<1	173	<3	<18	186
	Rattlesnake Ridge	5/21/82	<3.0	126.0		<17		<1	100	<2	<32	108
	Rattlesnake Ridge	11/19/82(a)	---	110.0	---	<10	<30	<6		<20	<150	20
699-47-50	Rattlesnake Ridge	7/15/82	<3.4	88.3		<18		<1		<2	<28	97
699-47-50A	Unconfined	8/11/82	<4.0	44.1	<14		<15	<1	13.8	<2	<25	97
699-49-55B	Rattlesnake Ridge	5/28/82	<4.3	105.0	<17	<14		<1	<3	<2	<16	140
699-50-45	Rattlesnake Ridge	8/06/82	<1.6	90.3	<13	<12	<10	<1		<6	<25	117
699-50-48	Rattlesnake Ridge	8/07/82	<2.9	44.3	<31	<37	<30	<1	33	<16	<13	85
699-51-46	Rattlesnake Ridge	8/04/82	<2.8	87.3		<16		<1		<3	<16	150
699-52-46	Rattlesnake Ridge	8/07/82	<2.2	58.7	<16	<5.1	<6.9	<1	<3	<3	<11	81
699-52-48	Rattlesnake Ridge	8/10/82	<2.2	64.3		<8	<7	<1	5.4	<3	<18	88
699-53-50	Rattlesnake Ridge	7/14/82	<1.5	52.8	<23	<10		<1		<14	<13	120
699-54-57	Rattlesnake Ridge	5/17/82	<2.5	129.0	<25			<1		<14	<16	226
699-54-50C	Unconfined	8/09/82	<2.6	14.7		<13	<13	<1	<1.1	<3	<23	101
699-56-53	Rattlesnake Ridge	6/03/82	<4.5	96.4		<12		<1		<14	<23	149
699-60-57	Unconfined	8/10/82	<4.2	28.8		<2.8	<2.5	<1	79.5	<3	<9	96

(a) Analysis performed by Basalt Waste Isolation Project

TABLE I.3. Stable Isotope Analyses

Well Number	Zone Sampled	Date	$\delta D\%$	$\delta^{18}O\%$	$\delta^{34}S\%$
299-E16-1	Elephant Mountain II fracture zone	5/15/82	-142	-16.6	
	Elephant Mountain interflow zone	7/13/82	-142	-16.8	
		7/13/82	-143	-16.9	
		7/14/82	-140	-16.2	7.4
299-E26-8	Unconfined Rattlesnake Ridge	3/23/82	-139	-16.9	2.2
		5/18/82	-141	-17.3	
		5/19/82	-142	-17.3	
		5/19/82	-142	-17.3	0.5
299-E33-12	Unconfined Rattlesnake Ridge	5/11/82	-139	-17.1	3.4
		5/21/82	-147	-18.4	
		5/22/82	-151	-18.3	
		5/22/82	-152	-18.3	6.2
		8/14/82			6.0
699-E33-12	Unconfined	8/13/82	-143	-17.0	-9.1
699-42-40A	Unconfined	8/13/82	-142	-16.7	3.0
699-42-40C	Elephant Mountain interflow zone Rattlesnake Ridge	4/16/82	-150	-18.5	2.7
		5/20/82	-156	-18.7	
		5/21/82	-156	-18.6	
		5/21/82	-156	-18.4	3.3
699-47-50	Rattlesnake Ridge	7/15/82	-142	-16.8	-1.4
699-49-55A	Unconfined	8/11/82	-144	-17.0	-1.5
699-49-55B	Rattlesnake Ridge	5/27/82	-148	-17.9	
		5/27/82	-148	-17.8	
		5/28/82	-145	-17.6	2.8
699-50-45	Rattlesnake Ridge	8/06/82	-146	-17.0	0.8
699-50-48	Rattlesnake Ridge	8/07/82	-144	-16.8	-1.2
699-51-46	Rattlesnake Ridge	8/04/82	-144	-16.5	1.5
699-52-46	Rattlesnake Ridge	8/07/82	-146	-16.9	0.5
699-52-48	Rattlesnake Ridge	8/10/82	-149	-17.8	-0.7
699-53-50	Rattlesnake Ridge	7/14/82	-147	-17.3	-0.1
699-54-57	Rattlesnake Ridge	5/17/82	-149	-17.8	
		8/14/82			4.0
699-55-50C	Unconfined	8/09/82	-138	-16.5	7.9
699-56-53	Rattlesnake Ridge	6/03/82	-148	-17.6	
	Rattlesnake Ridge	6/03/82	-148	-17.2	3.6
699-60-57	Unconfined	8/10/82	-143	-17.2	

TABLE I.4. Tritium Analyses

Well Number	Zone Sampled	Date	Tritium Units	Tritium Concentration, pci/L
299-E16-1	Elephant Mountain II fracture zone	5/15/82	5.25 ± 0.22	1.7E+1
	Elephant Mountain interflow zone	7/13/82	0.30 ± 0.07	9.7E-1
		7/13/82	-0.01 ± 0.07	0
		7/14/82	0.09 ± 0.06	2.9E-1
299-E26-8	Unconfined Rattlesnake Ridge	3/23/82	403 ± 7.0	1.3E+3
		5/18/82	-0.03 ± 0.06	0
		5/19/82	1.04 ± 0.11	3.36E+0
		5/19/82	1.82 ± 0.11	5.91E+0
299-E33-12	Unconfined Rattlesnake Ridge	5/11/82	426 ± 8.0	1.38E+3
		5/21/82	84.5 ± 1.8	2.73E+2
		5/22/82	90.0 ± 2.1	2.9E+2
		5/22/82	103 ± 2.0	3.33E+2
699-E37-43	Unconfined	8/13/82	28900 ± 500	9.3E+4
699-42-40A	Unconfined	1/19/82		3E+5 ^(a)
		8/13/82	80200 ± 1000	2.6E+5
699-42-40B	Unconfined	1/19/82		3.5+5 ^(a)
699-42-40C	Unconfined Elephant Mountain interflow zone Rattlesnake Ridge	1/19/82		2.5E+5 ^(a)
		4/16/82	374 ± 7.0	1.21E+3
		5/20/82	12 ± 0.4	3.9E+1
		5/21/82	5.98 ± 0.22	1.93E+1
		5/21/82	3.78 ± 0.13	1.22E+1
		11/19/82	4.18 ± 0.13	1.35E+1
699-47-50	Rattlesnake Ridge	7/15/82	97 ± 3.1	3.1E+2
699-49-55A	Unconfined	8/11/82	0.26 ± 0.08	8.4E-1
699-49-55B	Rattlesnake Ridge	5/27/82	0.24 ± 0.09	7.8E-1
		5/27/82	0.25 ± 0.08	8.1E-1
		5/28/82	0.22 ± 0.08	7.1E-1
699-50-45	Rattlesnake Ridge	8/06/82	0.36 ± 0.07	1.16E+0
699-50-48	Rattlesnake Ridge	8/07/82	4.1 ± 0.22	1.32E+1
699-51-46	Rattlesnake Ridge	8/04/82	0.57 ± 0.09	1.84E+0
699-52-46	Rattlesnake Ridge	8/07/82	0.09 ± 0.08	2.91E-1
699-52-48	Rattlesnake Ridge	8/10/82	0.28 ± 0.08	9E-1
699-53-50	Rattlesnake Ridge	7/14/82	0.45 ± 0.08	1.44E+0
699-54-57	Rattlesnake Ridge	5/17/82	0.02 ± 0.09	0
699-55-50C	Unconfined	8/09/82	46.2 ± 1.6	1.49E+2
699-56-53	Unconfined	11/11/82	54.1 ± 25.2	1.74E+2 ^(a)
		11/11/82	85.9 ± 28.3	2.76E+2 ^(a)
	Rattlesnake Ridge	6/03/82	0.42 ± 0.08	1.35E+0
		6/03/82	-0.02 ± 0.06	0
699-60-57	Unconfined	8/10/82	214 ± 6.0	6.9E+2

(a) Analyses performed by U.S. Testing Company.

TABLE I.5. Iodine-129 and Gamma Scan Data

Well Number	Zone Sampled	Date	^{129}I , pci/L	% Error	^{127}I , g/L	% Error	^{60}Co , pci/L	% Error	^{106}Ru , pci/L
299-E16-1	Elephant Mountain interflow zone	8/13/82	2.9E-5	5	6.0	2	6.4E-4	471	-9.6E-3
299-E26-8	Rattlesnake Ridge	8/12/82	7.9E-6	6	1.2	3	1.8E-3	111	3.9E-2
299-E33-12	Rattlesnake Ridge	8/14/82	3.8E-2	4	1.1	4	5.4E+1	6	-1.4E-1
699-37-43	Unconfined	8/13/82	1.1E+0	4	1.1	4	4.3E-3	64	-8.5E-3
699-42-40A	Unconfined	8/13/82	2.5E+0	4	1.6	3	-1.7E-3	-121	9.1E-3
699-42-40C	Rattlesnake Ridge	8/13/82	8.5E-3	4	9.3	2	3.2E-4	902	-5.1E-3
699-42-40C	Rattlesnake Ridge	11/19/82	1.4E-2						
699-47-50	Rattlesnake Ridge	8/11/82	2.2E-3	5	1.9	2	3.0E-3	95	-1.9E-2
699-49-55A	Unconfined	8/11/82	3.5E-5	10	3.1	3	8.8E-3	62	3.4E-2
699-49-55B	Rattlesnake Ridge	8/11/82	5.6E-6	6	2.9	3	3.2E-4	802	-4.9E-3
699-50-45	Rattlesnake Ridge	8/06/82	3.4E-4	3	11.0	1	2.0E-3	118	-4.0E-2
699-50-48	Rattlesnake Ridge	8/07/82	3.7E-3	4	8.1	2	7.7E-3	55	-2.0E-2
699-51-46	Rattlesnake Ridge	8/10/82	1.1E-5	5	6.8	2	3.4E-3	88	-2.8E-2
699-52-46	Rattlesnake Ridge	8/07/82	4.9E-5	4	2.6	3	-1.8E-3	-302	-5.3E-2
699-52-48	Rattlesnake Ridge	8/10/82	3.4E-6	7	4.8	2	-2.6E-3	-213	-6.3E-3
699-53-50	Rattlesnake Ridge	8/07/82	6.4E-5	4	4.7	2	6.2E-3	66	-5.8E-3
699-54-57	Rattlesnake Ridge	8/14/82	1.5E-5	3	3.9	2	-2.7E-3	-80	-1.5E-2
699-55-50C	Unconfined	8/09/82	5.2E-2	4	0.96	7	-2.5E-3	-160	6.1E-2
699-56-53	Rattlesnake Ridge	8/14/82	3.1E-5	3	8.5	1	7.6E-3	72	1.6E-2

APPENDIX J

VELOCITY PROFILES

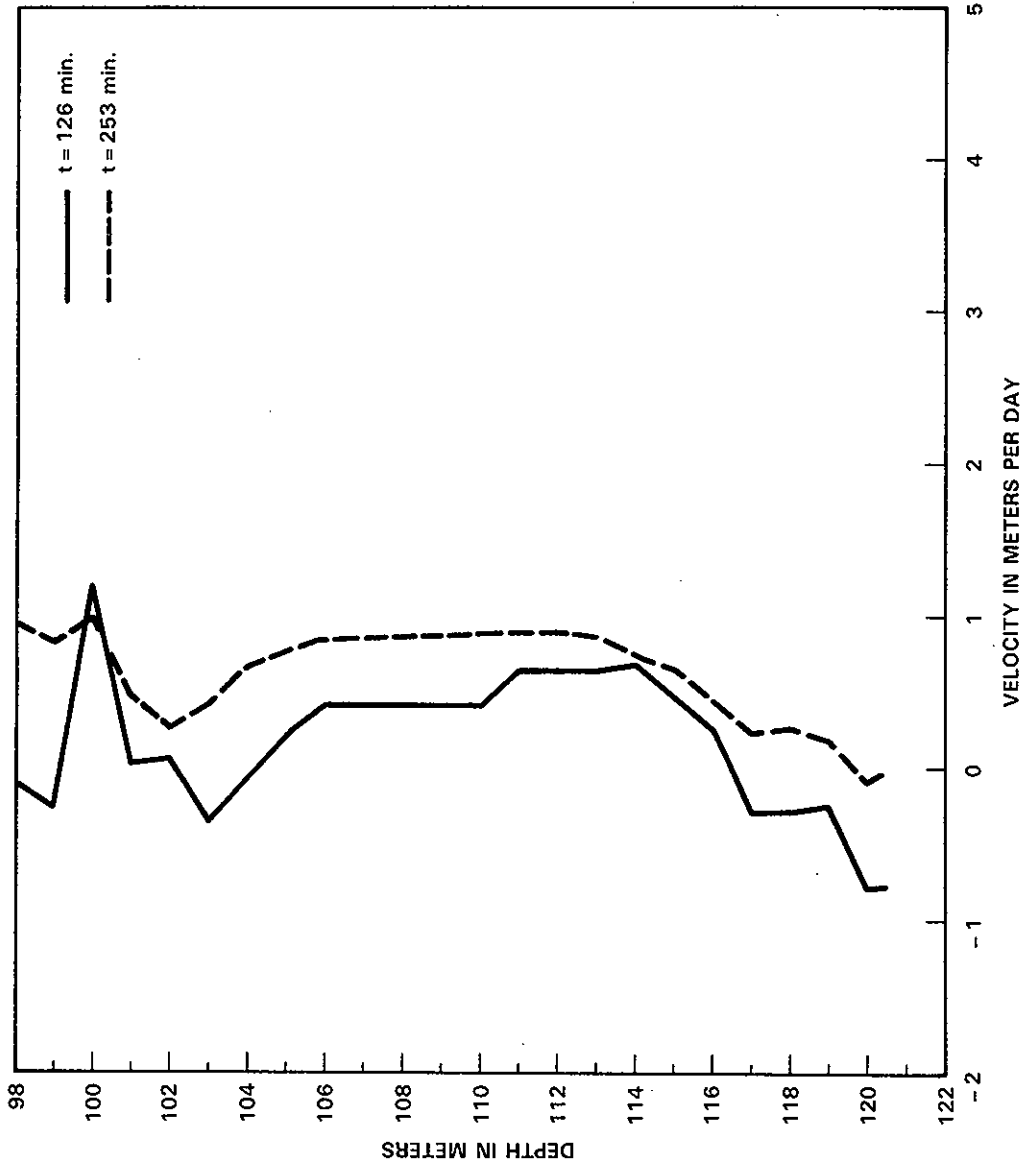


FIGURE J.1. Velocity Profile: 299-E26-8, 2/25/83, Rattlesnake Ridge Interbed

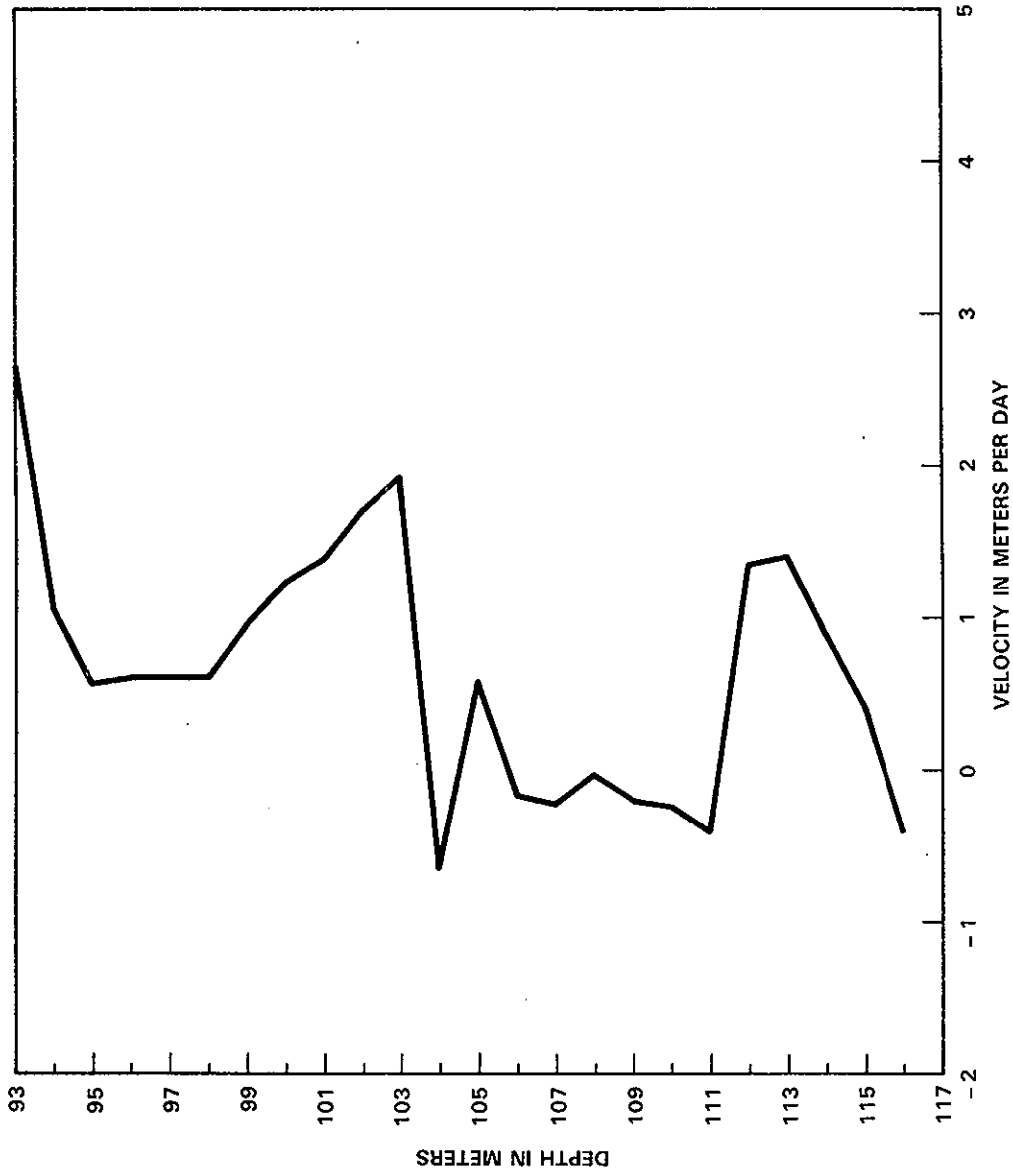


FIGURE J.2. Velocity Profile: 299-E33-12, 3/30/83, Rattlesnake Ridge

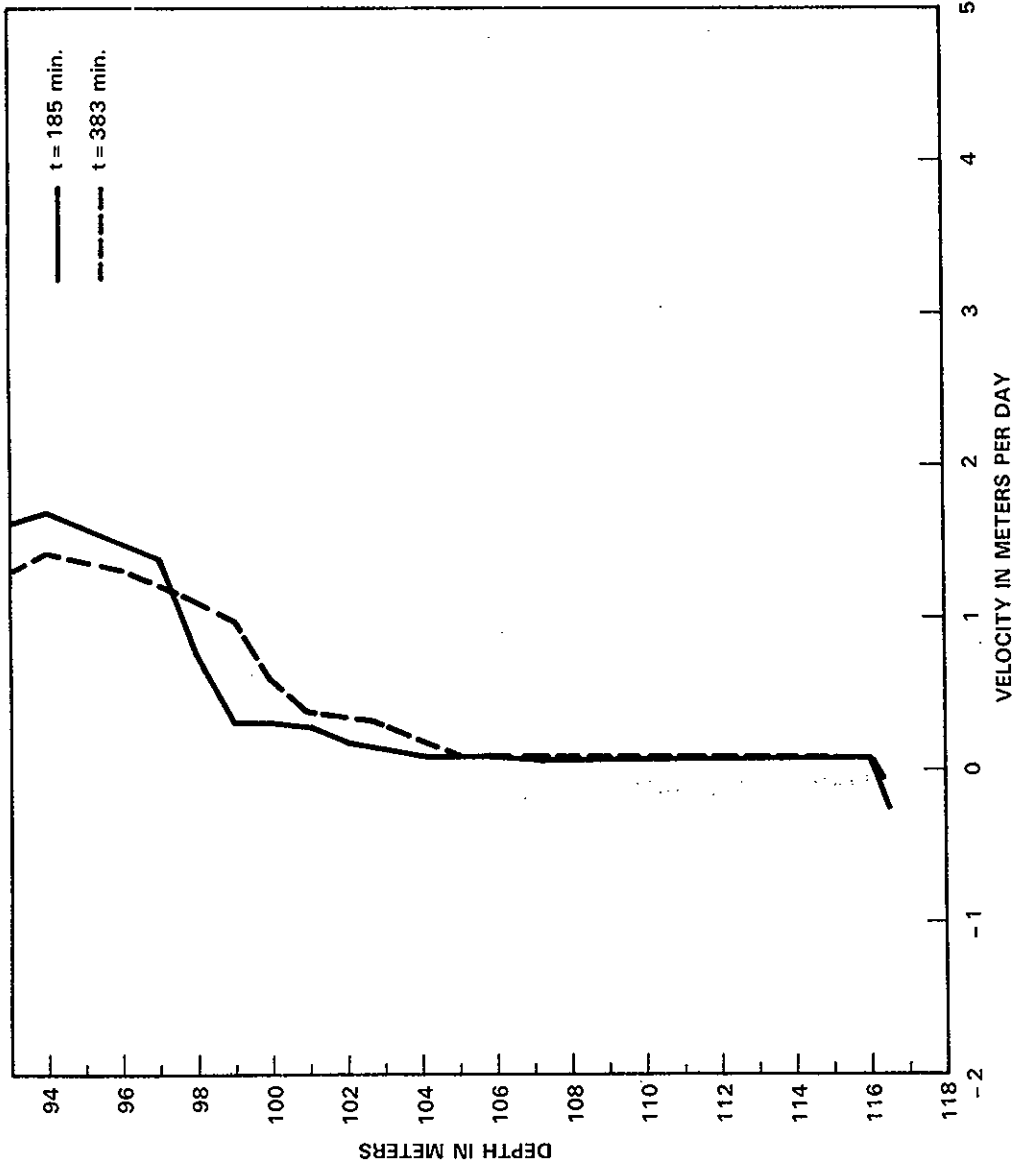


FIGURE J.3. Velocity Profile: 699-42-40c, 2/19/83, Rattlesnake Ridge Interbed

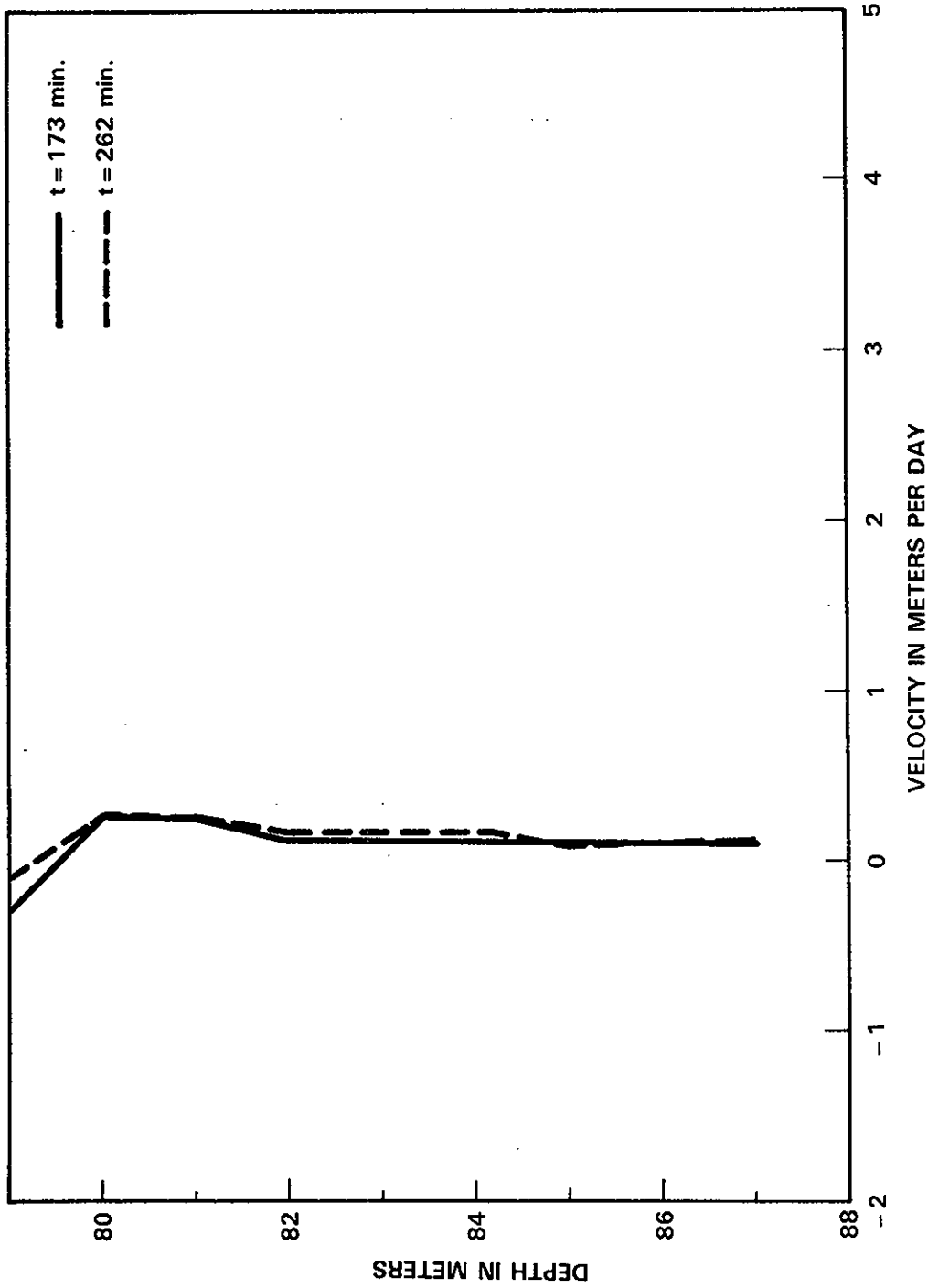


FIGURE J.4. Velocity Profile: 699-47-50, 3/22/83, Rattlesnake Ridge Interbed

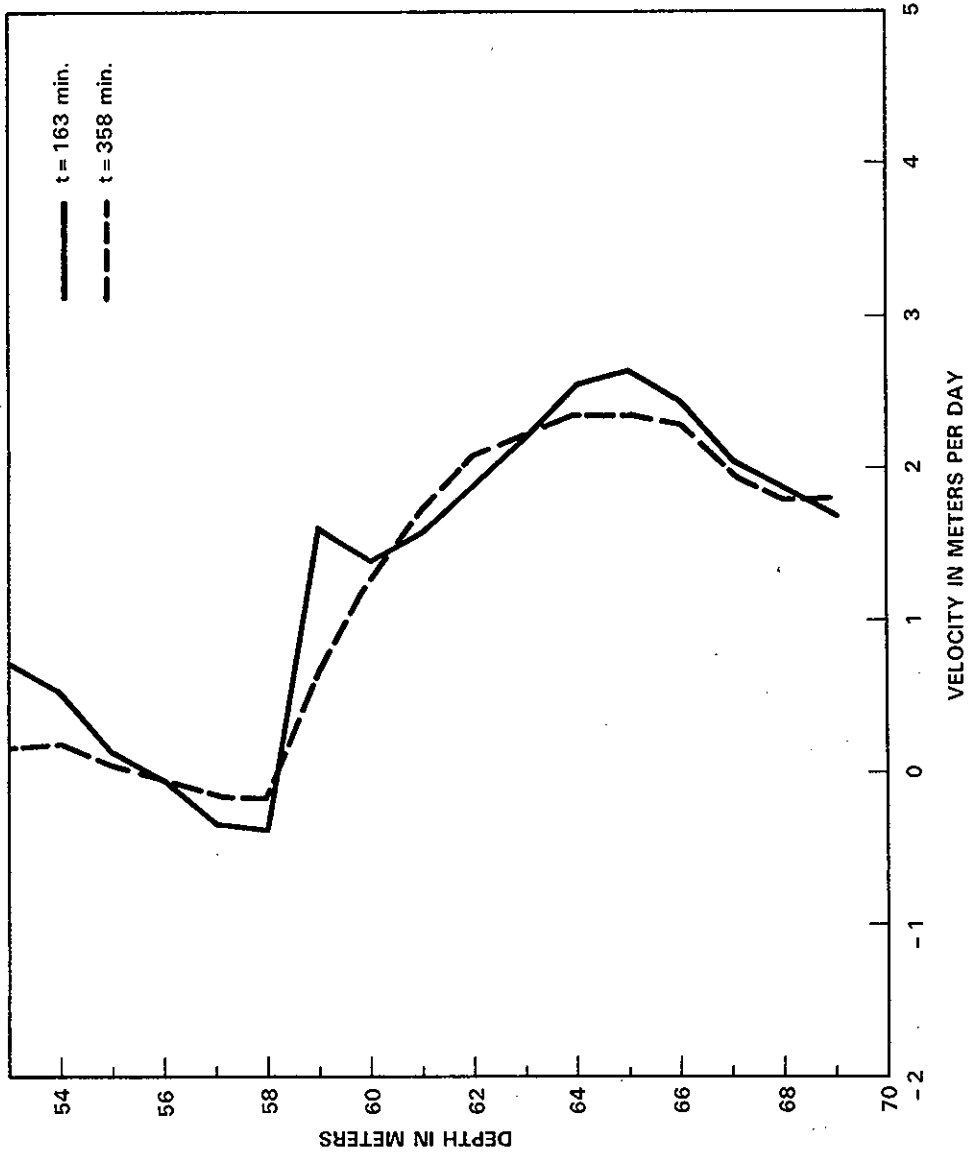


FIGURE J.5. Velocity Profile: 699-49-55b, 2/16/83, Rattlesnake Ridge Interbed

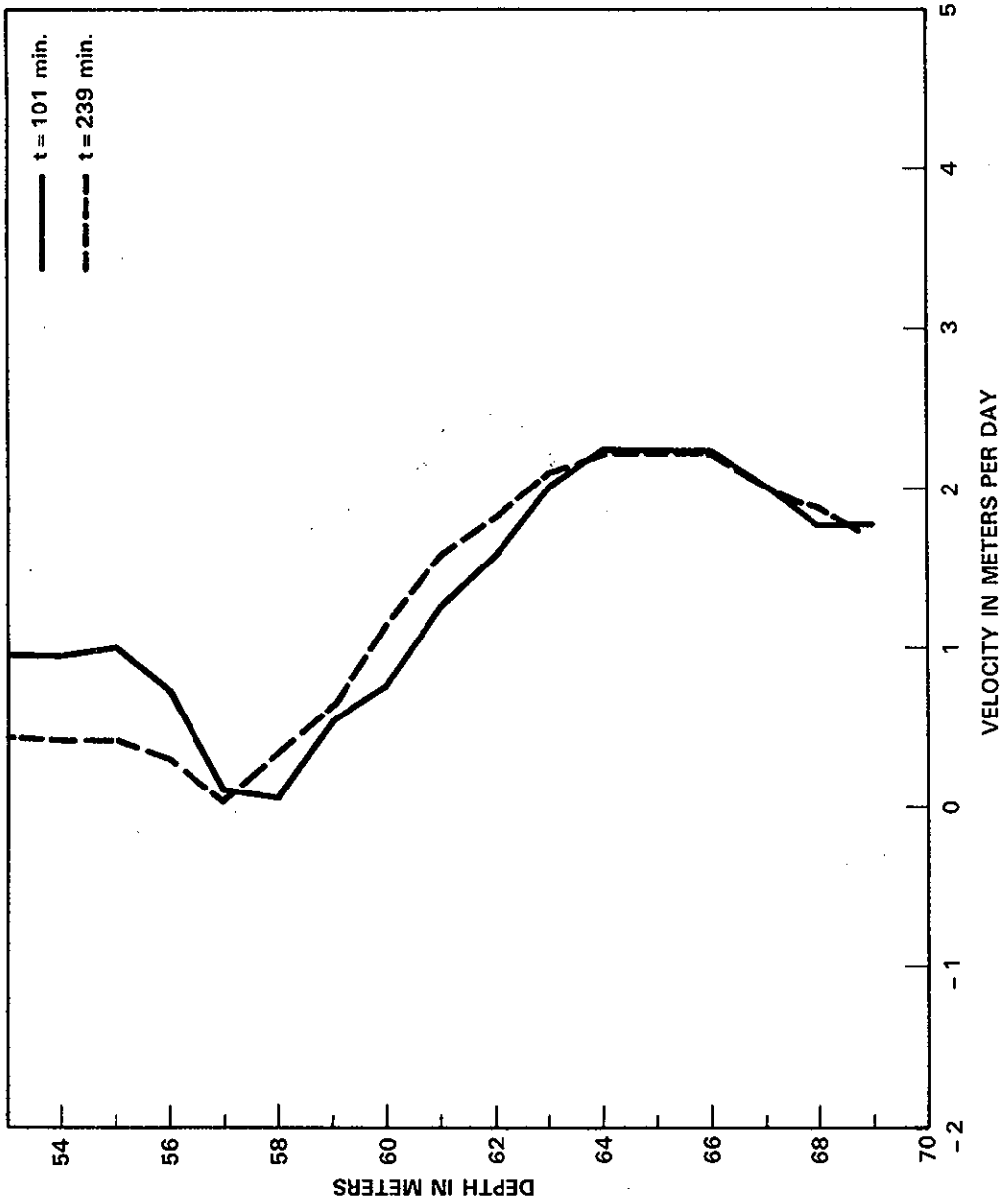


FIGURE J.6. Velocity Profile: 699-49-55b, 3/23/83, Rattlesnake Ridge Interbed

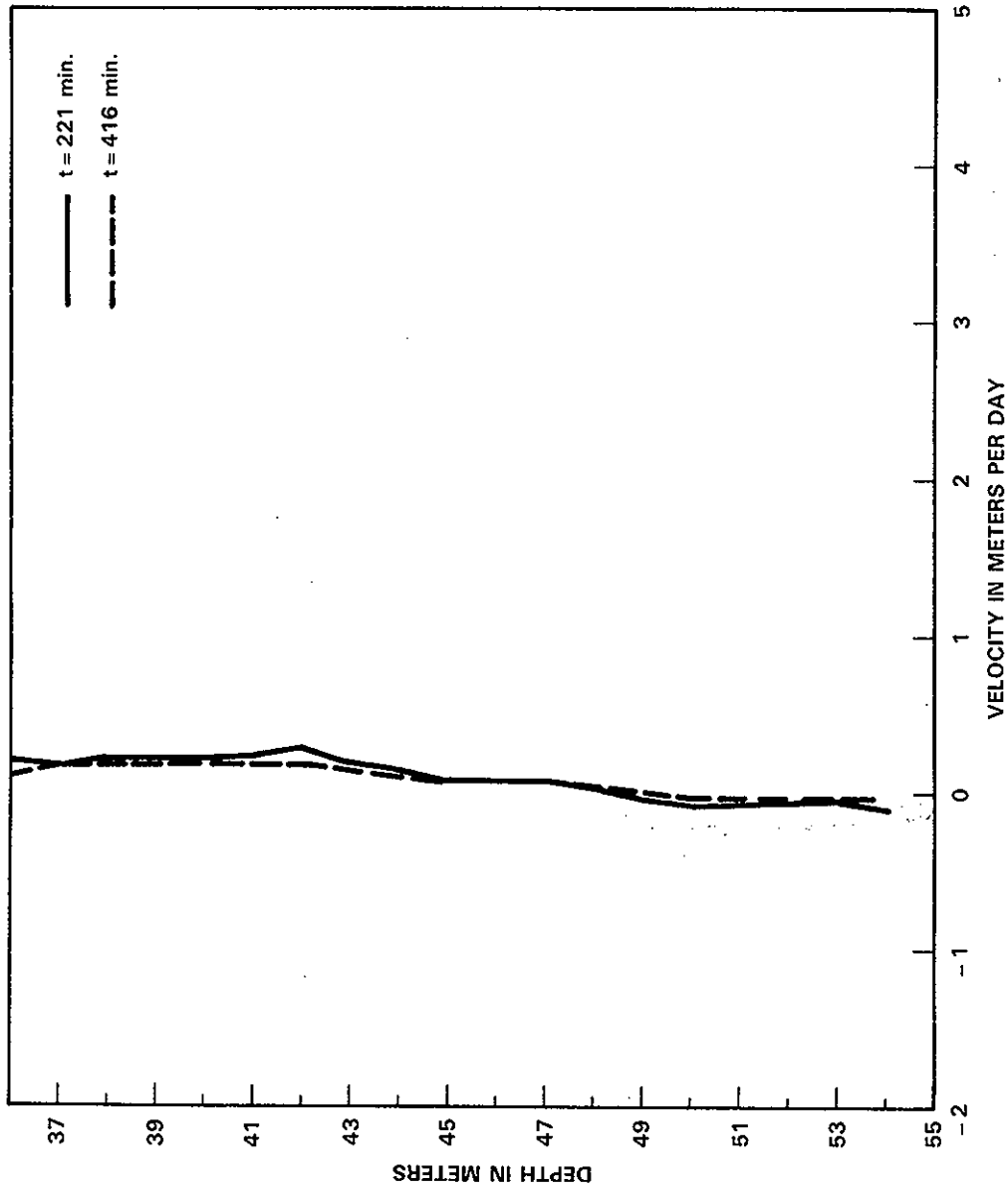


FIGURE J.7. Velocity Profile: 699-50-45, 3/04/83, Rattlesnake Ridge Interbed

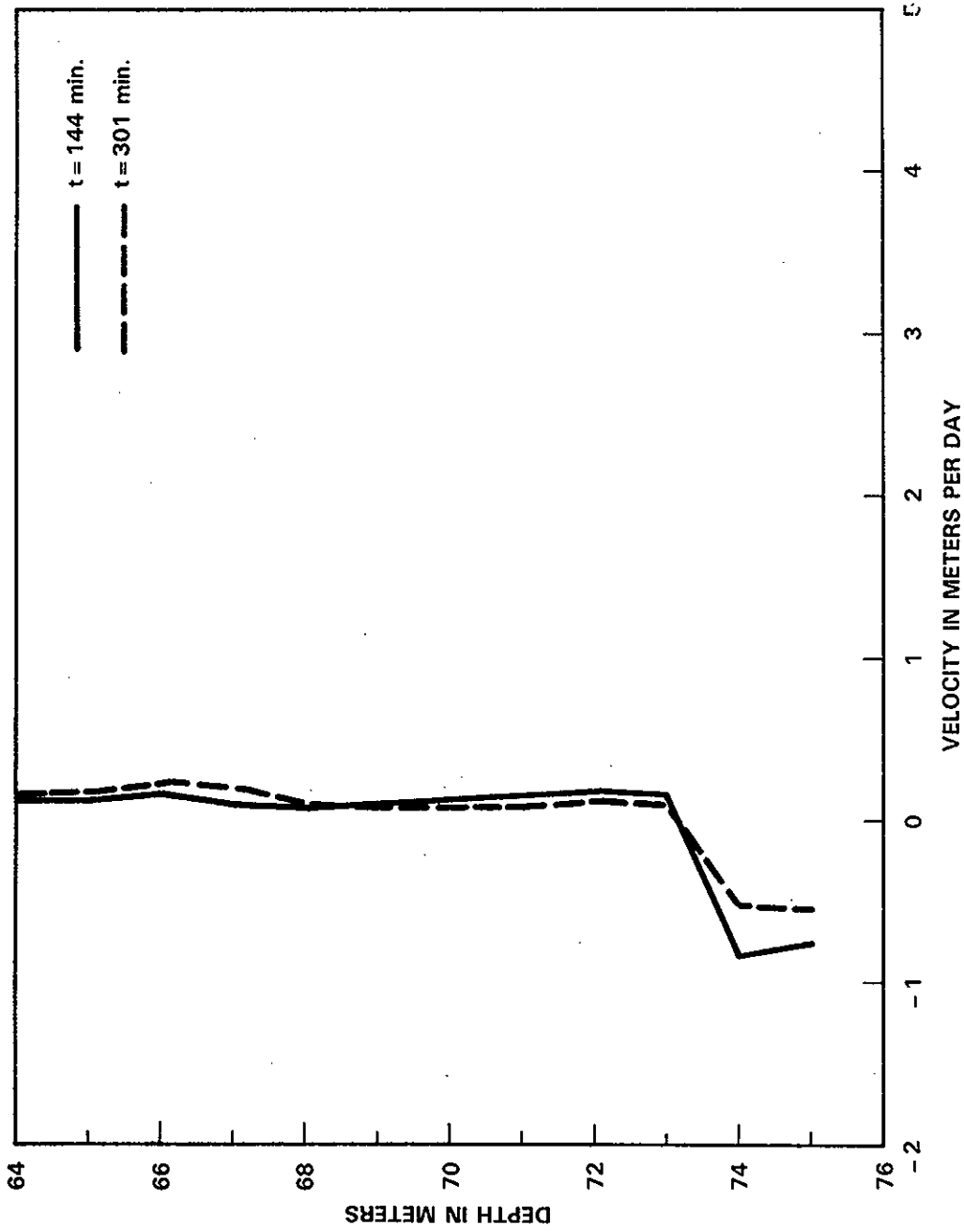


FIGURE J.8. Velocity Profile: 699-50-48, 3/08/83, Rattlesnake Ridge Interbed

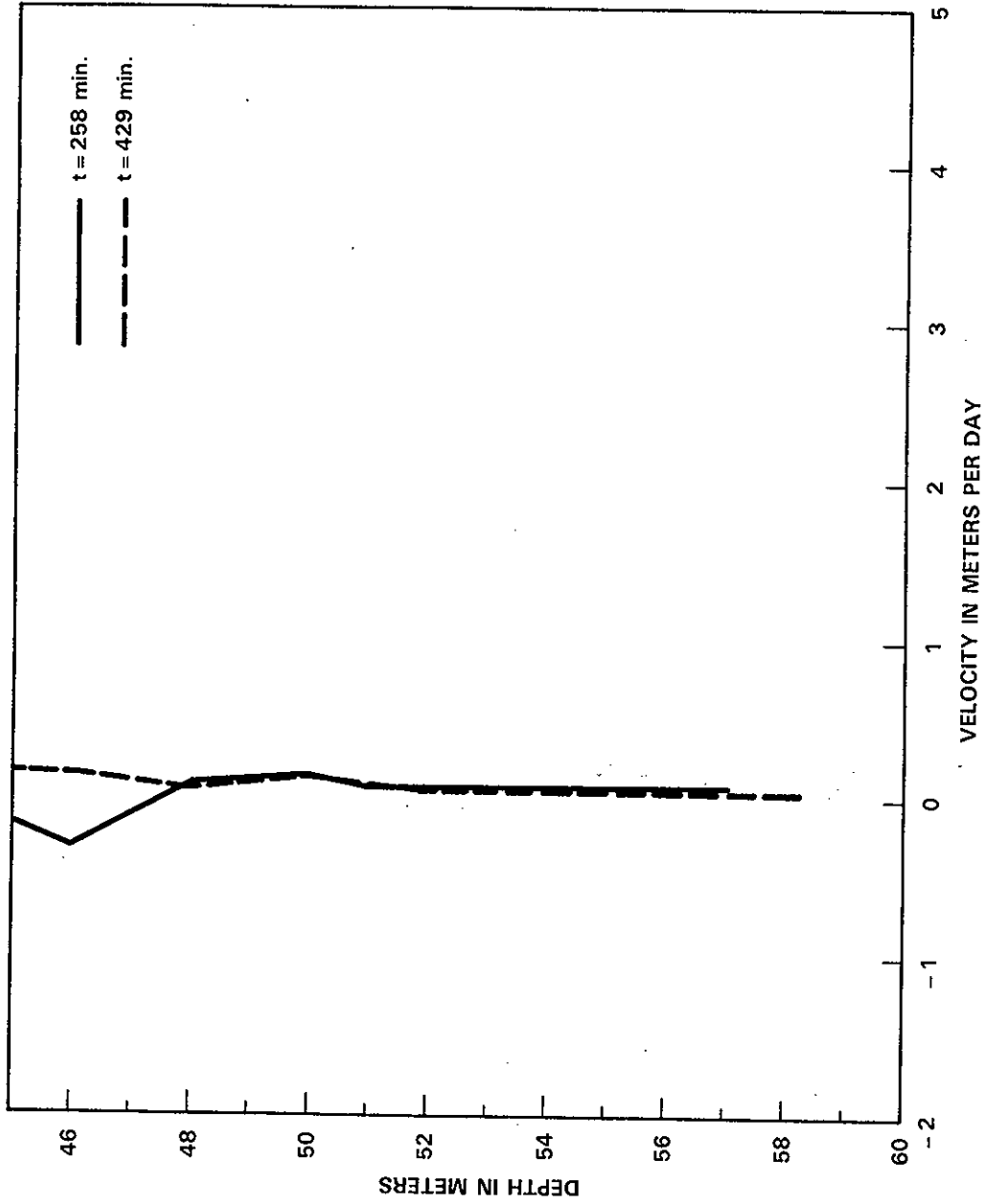


FIGURE J.9. Velocity Profile: 699-52-48, 3/02/83, Rattlesnake Ridge Interbed

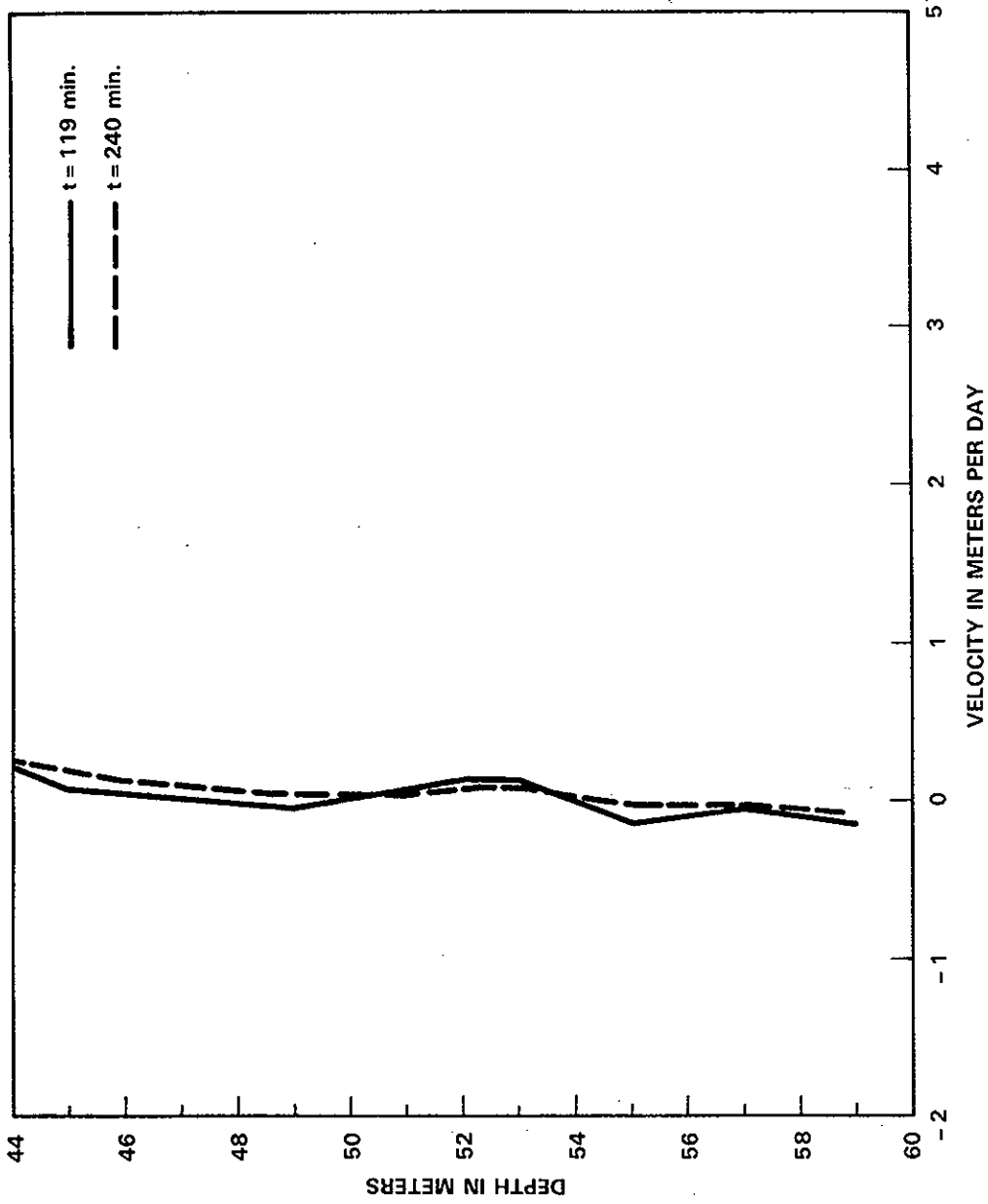


FIGURE J.10. Velocity Profile: 699-53-50, 3/03/83, Rattlesnake Ridge Interbed

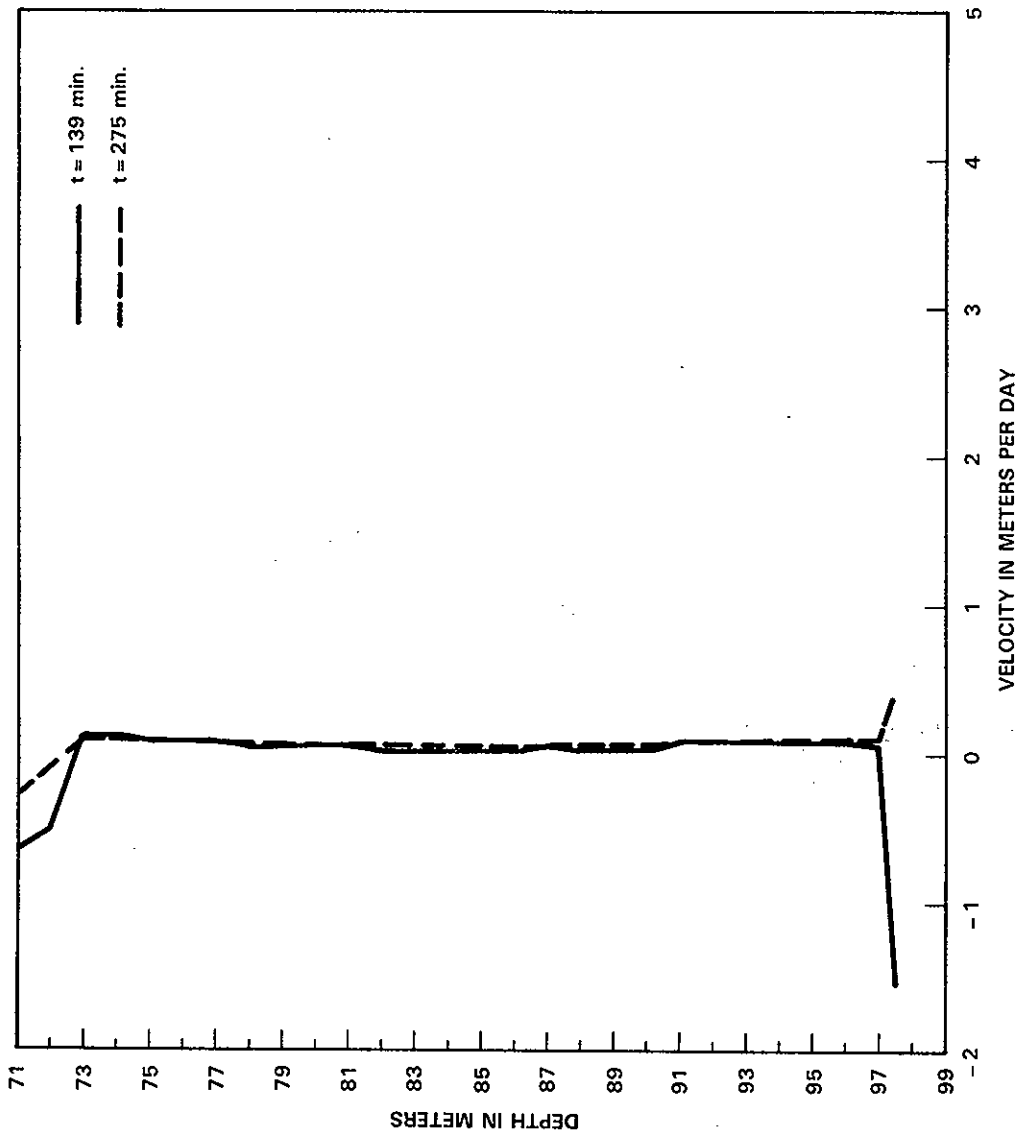


FIGURE J.11. Velocity Profile: 699-54-57, 2/19/83, Rattlesnake Ridge Interbed

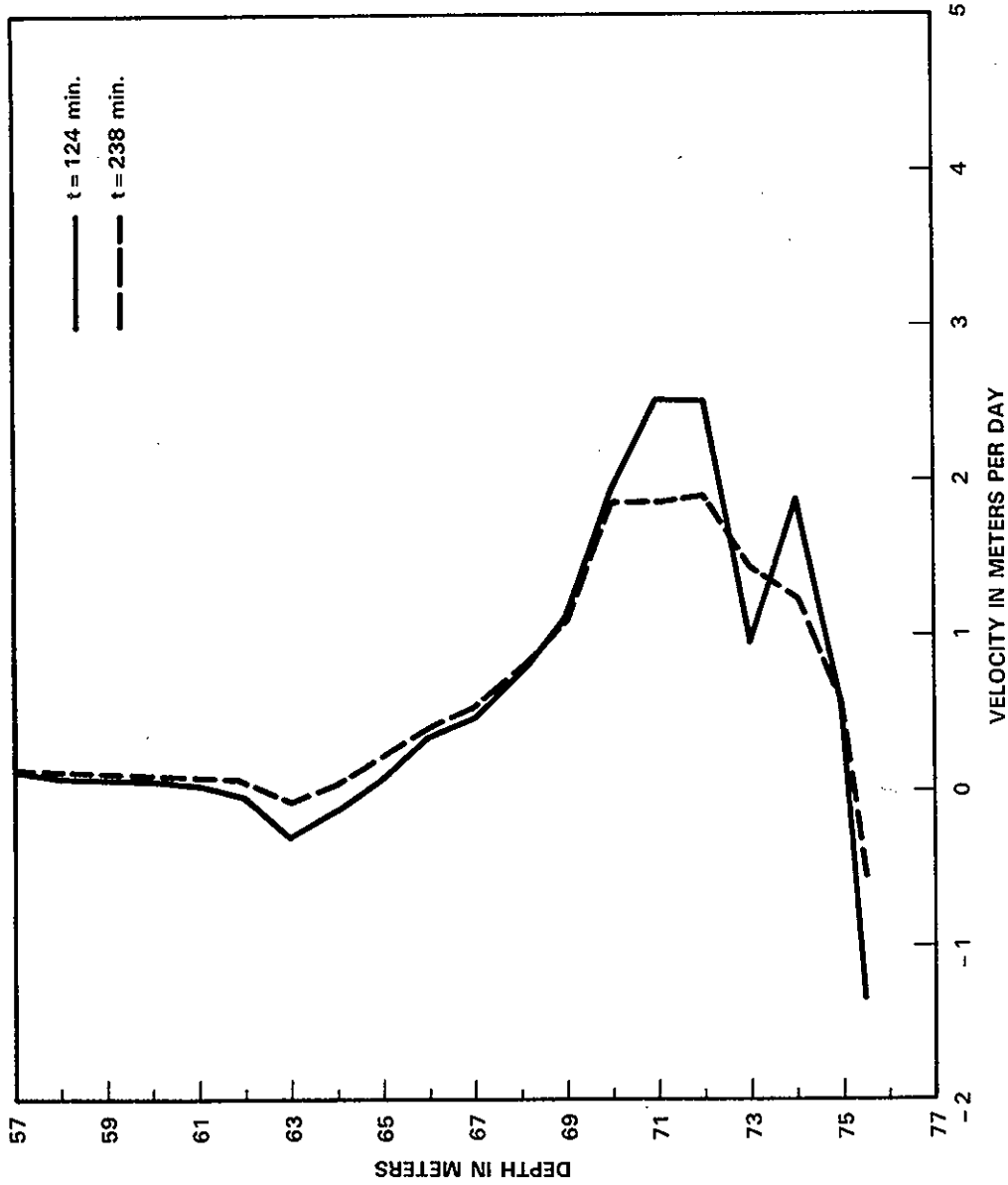


FIGURE J.12. Velocity Profile: 699-56-53, 2/18/83, Rattlesnake Ridge Interbed

APPENDIX K

CROSS SECTIONS OF STUDY AREA

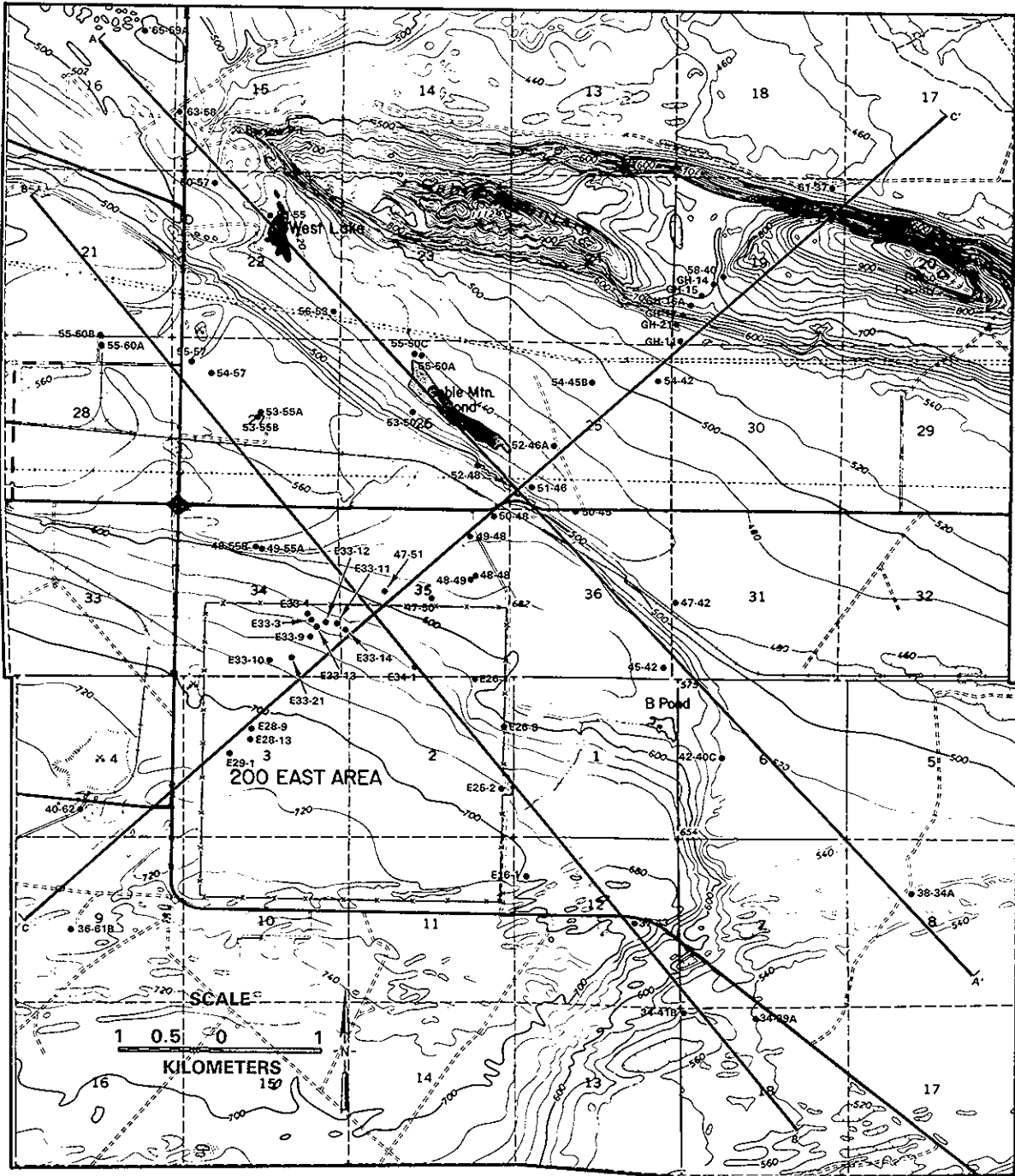


FIGURE K.1. Cross-Section Location Map

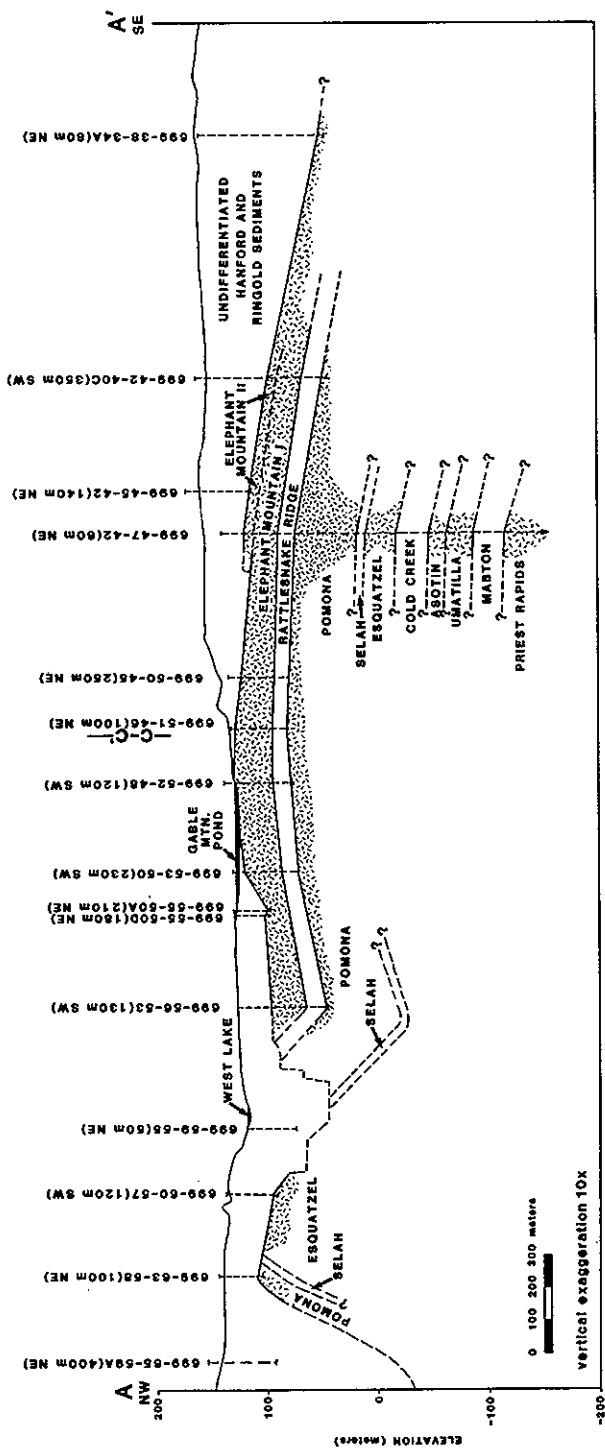


FIGURE K.2. Cross-Section A - A'

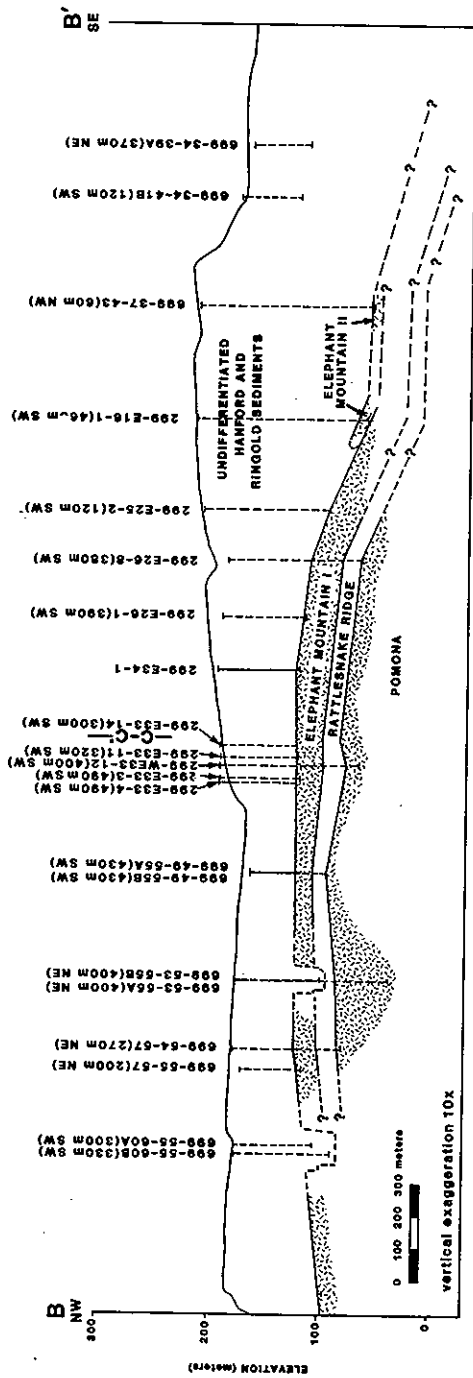


FIGURE K.3. Cross Section B - B'

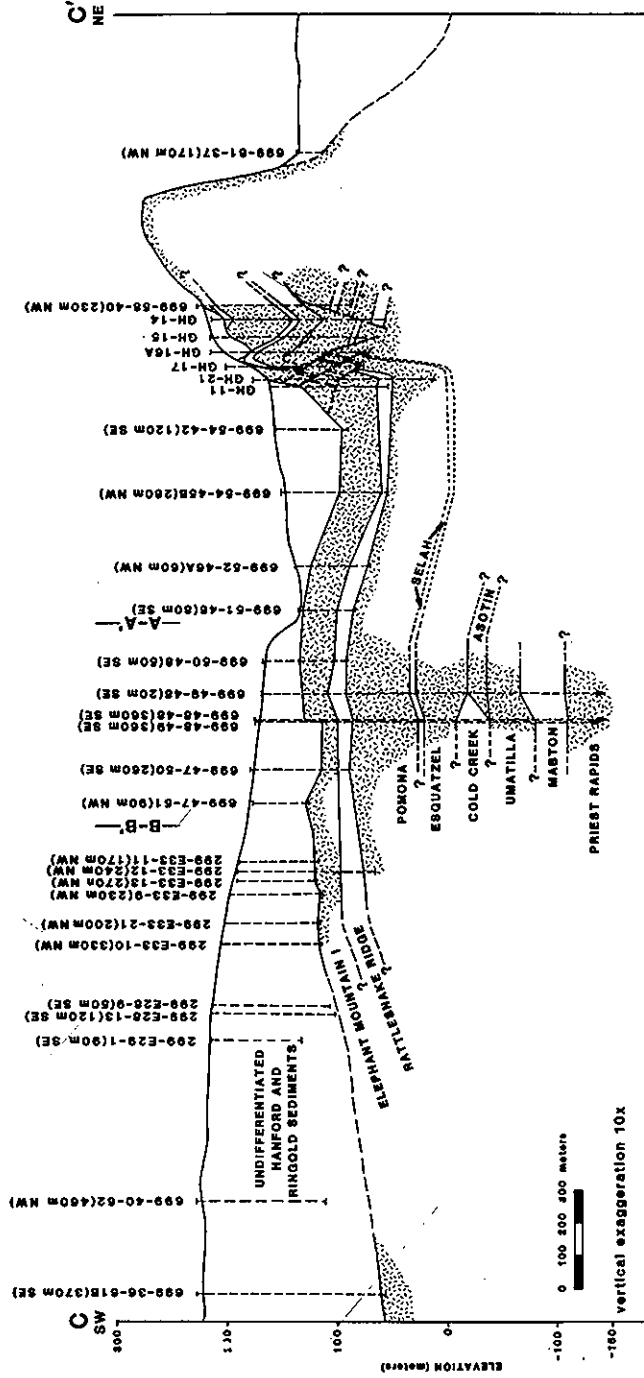


FIGURE K.4. Cross-Section C - C'

RHO-RE-ST-12

DISTRIBUTION

No. of
Copies

No. of
Copies

OFFSITE

56 Rockwell Hanford Operations

27 U.S. Department of Energy
Technical Information Center
Oak Ridge, Tennessee

M. R. Adams
S. M. Baker
W. H. Chapman-Riggsbee (5)
G. F. Boothe
D. J. Brown
W. R. Bwown

ONSITE

23 Pacific Northwest Laboratory

P. A. Eddy (2)
M. J. Graham (5)
E. A. Jenne
G. V. Last (10)
D. A. Myers
R. J. Serne
J. L. Swanson
R. E. Wildung
M. A. McKinney

A. C. Crawford
K. L. Dillon
K. R. Fecht (5)
M. R. Fuchs
D. L. Graham
H. A. Haerer
A. R. Hawkins
W. M. Hayward
W. F. Heine (2)
R. E. Isaacson
R. J. Jensen
A. G. Law
P. G. Lorenzini
A. H. Lu
H. E. McGuire
S. M. Price
R. D. Prosser
J. H. Roecker
R. C. Routson
R. M. Smith
S. R. Strait
R. E. Wheeler
D. E. Wood
D. D. Wodrich
BWIP Library (2)
Document Control (2)
Environmental Library (10)
Publications Services Dept. (3)

10 U.S. Department of Energy

Richland Operations Office
Richland, Washington 99352
Attn: R. E. Austin
D. R. Elie
T. R. Fitzsimmons
R. E. Gerton
J. J. Krupar
P. J. Krupin
J. L. Rhoades
A. R. Schwankorf
M. W. Tiernan
J. D. White